

MIXED VALENCE CHEMISTRY—A SURVEY AND CLASSIFICATION

Melvin B. Robin

Bell Telephone Laboratories, Inc., Murray Hill, New Jersey

and

Peter Day

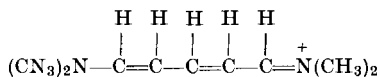
Inorganic Chemistry Laboratory, University of Oxford, Oxford, England

I. Introduction	248
II. Theory of Mixed Valence Effects	253
A. The Wave Functions and Mixed Valence Classification	254
B. Mixed Valence Spectra	258
C. Magnetism and Electron Transport	263
D. Molecular Geometry	269
III. Survey of the Elements	270
A. Titanium	271
B. Vanadium	275
C. Chromium	282
D. Manganese	288
E. Iron	291
F. Cobalt	305
G. Nickel	310
H. Copper	312
I. Zirconium and Hafnium	321
J. Niobium and Tantalum	321
K. Molybdenum and Tungsten	335
L. Technetium and Rhenium	344
M. Ruthenium and Osmium	345
N. Rhodium and Iridium	347
O. Palladium and Platinum	348
P. Silver	355
Q. Gold	361
R. Gallium	366
S. Indium	369
T. Thallium	371
U. Tin	374
V. Lead	375
W. Phosphorus and Arsenic	381
X. Antimony	382
Y. Bismuth	393
Z. Lanthanides	394
AA. Actinides	397
BB. Miscellaneous	401
IV. Conclusions	402
References	403

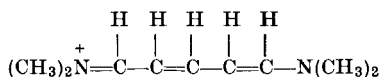
I. Introduction

This review is concerned with the neglected class of inorganic compounds which contain ions of the same element in two different formal states of oxidation. Although the number of references cited in our review shows that many individual examples of this class have been studied, yet they have very rarely been treated as a class, and there has never before, to our knowledge, been a systematic attempt to classify their properties in terms of their electronic and molecular structures. In the past, systems containing an element in two different states of oxidation have gone by various names, the terms "mixed valence," "nonintegral valence," "mixed oxidation," "oscillating valency," and "controlled valency" being used interchangeably. Actually, none of these is completely accurate or all-embracing, but in our hope to avoid the introduction of yet another definition we have somewhat arbitrarily adopted the phrase "mixed valence" for the description of these systems.

The concept of resonance among various valence bond structures is one of the cornerstones of modern organic chemistry. The most important feature of resonance among degenerate or near-degenerate structures is that the states resulting from the resonance have properties quite different from those expected of any one of the structures taken separately. Thus, for example, the pentamethinium ion requires the two degenerate structures



and



for an adequate description of its ground state, and, as a consequence of the resonance interaction between them, has a deep green color. On the other hand, either of the structures taken alone would be expected to have the color of 1,3,5-hexatriene, i.e., would be colorless. In this example, the resonance and the consequent green color spring from the fact that the nitrogen atoms can assume two valencies, 3+ and 4+, and are in equivalent positions in the ion so that on interchanging the nitrogen valencies, an equivalent structure results. There is ample reason to believe that exactly similar results would follow if a molecule could be synthesized in which the nitrogens were replaced by, say, Fe(II) and Fe(III). Thus it seems clear from the dramatic effects of resonance in organic chemistry that one can expect unusual properties in inorganic materials

possessing the same metal ion in different oxidation states, properties not to be found in the salts of either oxidation state taken separately.

Occasionally one finds examples of mixed valence among the inorganic nonmetals (the triiodide ion contains iodine atoms with formal valence zero and minus one). However, it is easily understood that by far the largest number and greatest variety of such compounds to be encountered in chemistry involve the transition and B subgroup metal elements, since many of these elements can exist in a variety of oxidation states. It is paradoxical, then, that the revitalization of transition metal chemistry brought about by the successes of the crystal field and ligand field theories has not been extended to the area of mixed valence compounds and their properties. It is the aim of this article to carry the renaissance of inorganic chemistry into this neglected area.

Mixed valence systems are, or should be, of great interest because their properties are rarely just the sum of the properties of the two metal ions taken separately; as with resonating organic molecules, there frequently is an "interaction" between the metal ions which results in the most dramatic changes in the physical properties of the system. Thus, as examples, $W^{VI}O_3$ and LiW^{VO}_3 ¹ are insulators whereas the mixed valence compound $Li_xW^VW_{1-x}^{VI}O_3$ is a conductor, the crystals $K_4Fe^{II}(CN)_6$ and $Fe_2^{III}(SO_4)_3$ are pale yellow whereas $KFe^{III}Fe^{II}(CN)_6$ is deep blue, and paramagnetic substances may become ferromagnetic or diamagnetic, all by changing the oxidation state of a part of the metal ions in the system by one or more units. Thus, for those interested in the interrelationships between electronic structure, molecular structure, electronic spectra, electronic conduction, and molecular magnetism, the mixed valence systems offer a class of compounds unique in chemistry. As would be expected, a study of such mixed valence systems suggests a close correlation between their color, crystal structure, magnetism, and electronic conductivity, which hopefully will allow one to predict aspects of all the above properties, after determining any one of them.

The most obvious and striking feature of many mixed valence compounds is the presence of intense absorption in the visible region of the spectrum, not present in compounds containing either valence state alone. Thus, whereas the colors of almost all $Fe(III)$ and $Fe(II)$ compounds are colorless, pale orange, or pale green, the color of almost all mixed valence systems simultaneously containing $Fe(III)$ and $Fe(II)$ is deep blue to black. And there is another paradox here, for although the blue-black systems are being actively ignored today in the midst of a

¹ In this work, the Roman numeral which follows an atomic symbol refers to the formal oxidation state of the metal ion, and is not to be confused with similar numerals used differently by atomic spectroscopists for the same purpose.

flurry of quantum mechanical activity on the pale orange ones, in the dark ages of the prequantum mechanical days, when no one could guess the explanation for the color of the Fe(III) ion, there was presented a very reasonable rationale for the deep blue color of Prussian blue, $\text{KFe}^{\text{III}}\text{Fe}^{\text{II}}(\text{CN})_6$. Because the deep colors of mixed valence systems were so unexpected, they could not be ignored for long, with the result that an explanation of the effect was presented with which we today can find little fault.

Thus, Wells (759), describing with great insight the very dark colors of various Au(I), Au(III), Sb(III), Sb(V), Fe(II), Fe(III), and Cu(I), Cu(II) chromophoric groupings, wrote:

"The chromophore grouping that has been presented here is a very curious thing. In the cases of Au(I)–Au(III) and Sb(III)–Sb(V) there is a difference of two units of valency, while with Fe(II)–Fe(III) and Cu(I)–Cu(II) there is a difference of only one unit, and, furthermore, these four pairs of valencies are all different. It is particularly remarkable that the three chlorides, CsCl, SbCl₃, and SbCl₅, which constitute one of the examples of the chromophore grouping, are all of them colorless compounds.

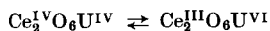
It seems possible that the action of this chromophore may be explained by exchanges of negative electrons between the atoms that differ in valency. It is supposed that in passing from one valency to another an atom gives up or takes on one or more electrons, and, if it is assumed that the atoms of a metal in two states of valency in the same molecule, instead of retaining fixed individual valencies, continually make these exchanges of electrons, it may be supposed that light, passing through such molecules, is in some way affected, so that colors or opacity are produced."

As the reader will find on reading ahead, in a good many systems so little work has been done on this phenomenon that we can add little today to what Wells wrote over 45 years ago. It is interesting to note that Wells' idea predates the pioneering work of Bury (116) on resonance in organic dyes by over 10 years.

The history of mixed valence chemistry goes far beyond the work of the twentieth century chemists, beginning with the synthesis in 1704 of one of the first coordination compounds, Prussian blue (572). The early history of the mixed valence phenomenon can be clearly seen as consisting of two phases. In the first earlier phase, we have the slow recognition of the mixed valence color phenomenon and an appreciation of the conditions which must prevail for its appearance. Thus, as early as 1847, Berzelius (63) described the blue-black ink derived from tannin-containing gall nuts as a double salt of Fe(II) and Fe(III) ions, similar to the other blue iron salts then known to contain these ions simultaneously. Werner (764) also commented on the extraordinary colors and metallic sheen of certain Pt(II), Pt(IV) oxalate complexes he newly synthesized, comparing their colors to that of the tungsten bronzes and

hydroquinone, the common denominator in all these systems being the simultaneous presence of oxidizing and reducing species. Hofmann (365) followed shortly thereafter with convincing evidence that the blue color of Prussian blue and other iron cyanide complexes was due to the presence of iron in two different oxidation states in the molecule. The significance of the mixed valence phenomenon to the colors of certain iron-containing minerals was later elucidated by MacCarthy (470), who explained that the presence of Fe(II) and Fe(III) in minerals leads to deep colors, black if the mineral is anhydrous, blue if it is hydrated. In addition to these few examples, a long list of citations can be made of the appearance of transient dark colors in the course of oxidation and/or reduction of many transition metal compounds.

In the historical second phase, the seemingly logical inferences are drawn that in fact the different valences are not uniquely fixed, one to each ion, but oscillate rapidly in a mixed valence system, and that the result of this unique valence oscillation is a unique absorption of light, i.e., color. Thus, in 1915 Hofmann and Hörschle (366) suggested that the blue color of "cerium-uranium blue," a mixed oxide of UO_2 and CeO_2 , was the result of the valence oscillation,

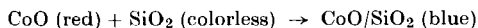


and coined the phrase "constitutive coloration" to describe this and other systems having colors which are not the sum of the colors of their components, but unexpectedly appear only on the union of these components:

"It is necessary that the distribution of oxidation states within the molecule can exchange under the influence of light so as to produce the light absorption and hence the color. This situation occurs most frequently in inorganic chemistry when the same element is present in different valence states in the same molecule."

Wells (759) shortly after, and without reference to the work of the Germans, came to the same conclusion quoted above, proposing in addition that the "spontaneous electronic activity" present in mixed valence compounds must also result in enhanced electrical conductivity. This latter conclusion of Wells made understandable the earlier work of Streintz (688), who found that white, yellow, red, and gray powders do not conduct electricity, whereas the deeply colored ones may show metallic conduction. Biltz (69) soon followed with an article outlining the origins of the colors of various inorganic materials, giving space to mixed valence colors and many examples of compounds wherein the same element occurs in two different oxidation states, and also to the situation wherein two different elements are present in different oxidation states.

This latter collection of examples is complicated by the possibility that the color change on mixing arises not from an oscillation of valence between different metal ions, but instead from a change in the ligand field about one of the components on going into the mixed crystal. Thus, the combination



is given as an example of the formation of a mixed valence, constitutive coloration. However, the red-to-blue color change given above could reasonably be interpreted as that expected for Co(II) in an octahedral site of CoO going into a tetrahedral site of SiO₂. The question raised here can obviously be settled by a study of the electronic spectrum, but until this is done there remains an ambiguity, which we take as an example of the fact that not *every* color change observed on mixing can be attributed to the mixed valence phenomenon.

Finally, the work of Stieglitz (687) must be mentioned as being of historical importance, for he expressed the thought that the deep color of many inorganic substances was intimately connected with the interatomic oxidation-reduction tendency of the compound. Thus, in mixed valence systems, he pointed out that intense colors can result from photochemical oxidation-reduction, the electrode potentials permitting, and that there is no compelling need to introduce an oscillation of the valences. As we shall see later, these two views are simply the extreme solutions of the same general problem, and many mixed valence systems can be found which support each of the two seemingly opposite positions.

Up to the present time, mixed valence phenomena have not very often been considered in the wider context of theories of spectroscopy and the solid state, but rather as peculiar occurrences occasionally met with here and there, their consequences here having no relationship to their consequences there. In fact, as we shall illustrate, mixed valence is found in a tremendous number of places, and it is hoped that a systematic study of the electronic phenomena related to its occurrence will serve to unite many seemingly unrelated facts. In Table I we list a number of the scientific areas in which mixed valence is encountered, together with examples. In a great many cases, the mixed valence introduces profoundly new effects.

Our first task is to cast the older, qualitative description of the mixed valence phenomena into a more modern, qualitative quantum mechanical one, relying heavily on ligand field theory. The accent here will be on the relationship between electronic spectra, electronic structure, and molecular structure. Following this, we will consider the experimental results at hand and attempt to apply our quantum

theoretical generalizations to them. Hopefully, by proceeding in this way, with all the data gathered in one place, we will uncover unexpected relationships and generalities, and, by pointing out where more work is needed, stimulate the completion of this work.

TABLE I
AREAS IN WHICH EXAMPLES OF MIXED VALENCE CAN BE FOUND

Area	Example
(1) Metal-metal bonding	$[\text{Ta}_6\text{Cl}_{12}]^{2+}$
(2) Nonstoichiometry	UO_{2-x}
(3) Coloration of glasses	Blue color of silicate glasses containing iron
(4) Biology	Hemocyanin
(5) Reaction intermediates	$\text{Fe}(\text{OH})_2$ (colorless) $\xrightarrow{\text{air}}$ (blue) $\xrightarrow{\text{air}}$ $\text{Fe}(\text{OH})_3$ (brown)
(6) Spot tests, qualitative analysis	$\text{Fe}^{\text{II}} + \text{Fe}^{\text{III}}(\text{CN})_6 \rightarrow$ blue solution
(7) Solid state	Self trapping, color centers, Na in NaCl (?)
(8) Electronic conduction	Controlled valency spinels
(9) Magnetic interactions	Ferromagnetic double exchange (LaMnO_3)
(10) Minerals	Biotite, Fe_3O_4
(11) Photochemistry, photography	Iron oxalate blueprint reaction, phosphotungstous acid images
(12) Metals in molten salts	Bi in BiI_3
(13) Intermetallics	$\text{In}^{\text{I}}\text{In}^{\text{III}}\text{Te}_2$
(14) Polyhalides	I_3^-
(15) Unusual oxidation states	Cs_2SbCl_6 , GaCl_2 , Pb_2O_3
(16) Statistical mechanics	Entropy-induced defect structures and shear phases
(17) Electrochemistry	AgO electrodes, Pb_2O_3
(18) Superconductivity	Tungsten bronze, Ag_2F
(19) Dyes, pigments, inks	Mo_3O_8 , W_3O_8 , Prussian blue
(20) Valence isomerization	$\text{Cu}^{\text{II}}\text{Ta}^{\text{IV}}\text{O}_3 = \text{Cu}^{\text{I}}\text{Ta}^{\text{V}}\text{O}_3$

II. Theory of Mixed Valence Effects

Our theory of mixed valence effects begins with a simple one-electron theory of the electronic structure of mixed valence systems, and then goes on to discussions of the electronic spectra, resistivity, and magnetic

interactions in such systems, followed by a few words about geometry and valence. The theory of mixed valence will use the concepts of ligand field theory as a basis, and is phrased in very broad and general terms. This is because there are very little quantitative data available on mixed valence compounds, and consequently very little need as yet for a detailed theory. The theory as outlined, however, is sufficient for drawing important preliminary qualitative conclusions about the electronic structures of these materials, and offers a foundation for a valuable classification scheme.

A. THE WAVE FUNCTIONS AND MIXED VALENCE CLASSIFICATION

Our initial concern is with the delineation of the mixed valence wave functions, the prime value of which is as a qualitative measure of the extent of delocalization of the valence shell electrons. Although these

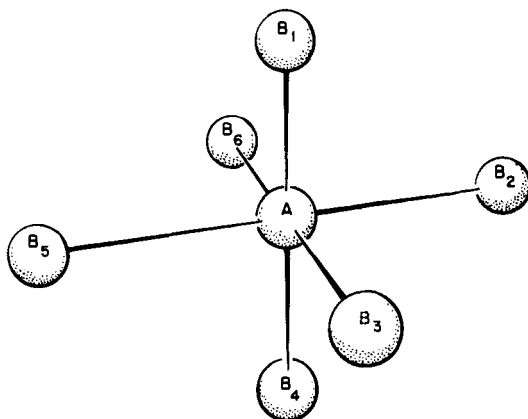


FIG. 1. A hypothetical mixed valence system consisting of the reduced metal ion at A, and six oxidized metal ions at the equivalent B sites. The ligands are not shown.

wave functions will not actually be used in a direct calculation of excitation energies, they can be of use in estimating other spectral properties, such as relative excitation energies, the number of excited states and their ordering, and spectral intensities. The extent of delocalization also correlates with the resistivity of mixed valence solids and their magnetic properties.

Consider the set of seven metal ions having the geometrical arrangement shown in Fig. 1. The metal ion in site A differs from those in the B sites not because of their relative geometrical arrangement, but because

the fields of the ligands, not shown, are supposed to be of different strengths and/or symmetries at the two sites. All the B sites are equivalent. Let us also suppose that the ion in the A site is of formal valence III [Ti(III), say] and that the ions in the B sites are all of formal valence IV [Ti(IV), say].

Neglecting explicit mention of the ligand wave functions, the ground state wave function of the system in *zeroth* order may be taken as

$$\Psi'_0 = \psi_A^{III} \psi_{B_1}^{IV} \psi_{B_2}^{IV} \cdots \psi_{B_s}^{IV} \quad (1)$$

where ψ_A^{III} is the wave function of the trivalent ion in the A site, and the $\psi_{B_i}^{IV}$ are the wave functions of the quadrivalent ions in the B sites. On transferring one electron from the A site to the B site, the A site and B site wave functions will change their oxidation state labels by + (I) and - (I), respectively, yielding excited state wave functions, which may be written as:

$$\Psi_k = \psi_A^{IV} \sum_j C_{kj} \psi_{B_1}^{IV} \psi_{B_2}^{IV} \cdots \psi_{B_j}^{III} \cdots \psi_{B_s}^{IV} \quad (2)$$

There will be six Ψ_k 's, each with numerical coefficients C_{kj} chosen to normalize Ψ_k and chosen to guarantee that Ψ_k will transform according to one of the representations of the appropriate symmetry point group.

Suppose also that one of the Ψ_k 's, say Ψ_l , has a symmetry appropriate for mixing with Ψ'_0 , i.e., Ψ'_0 and Ψ_l belong to the same representation. The ground state, Ψ_0 , will then be taken as the linear combination

$$\begin{aligned} \Psi_0 &= \sqrt{1 - \alpha^2} \Psi'_0 + \alpha \Psi_l \\ &= \sqrt{1 - \alpha^2} \psi_A^{III} \psi_{B_1}^{IV} \psi_{B_2}^{IV} \cdots \psi_{B_s}^{IV} + \alpha \psi_A^{IV} \sum_j C_{lj} \psi_{B_1}^{IV} \psi_{B_2}^{IV} \cdots \psi_{B_j}^{III} \cdots \psi_{B_s}^{IV} \\ &= \sum_j \frac{\sqrt{1 - \alpha^2}}{6} \psi_A^{III} \pi_{B_j} \psi_{B_j}^{IV} + C_{lj} \alpha \psi_A^{IV} \pi_{B_j} \psi_{B_j}^{III} \end{aligned} \quad (3)$$

where π_{B_3} is defined as

$$\pi_{B_3} = \psi_{B_1}^{IV} \psi_{B_2}^{IV} \psi_{B_4}^{IV} \psi_{B_5}^{IV} \psi_{B_6}^{IV}, \quad (4)$$

and similarly for the other π_{B_j} 's. Thus,

$$\Psi_0 = \frac{1}{N} \sum_j \pi_{B_j} \left\{ \frac{\sqrt{1 - \alpha^2}}{6} \psi_A^{III} \psi_{B_j}^{IV} + C_{lj} \alpha \psi_A^{IV} \psi_{B_j}^{III} \right\} \quad (5)$$

where $1/N$ is a normalization factor.

At this point let us presume for simplicity that the reduced species in any site consists of one electron outside of a closed shell, so that we may take

$$\begin{aligned} \psi_A^{IV} &= \phi_A^C; & \psi_{B_j}^{IV} &= \phi_{B_j}^C \\ \psi_A^{III} &= \phi_A^C \phi_A^*; & \psi_{B_j}^{III} &= \phi_{B_j}^C \phi_{B_j}^* \end{aligned} \quad (6)$$

where ϕ^C represents the wave function for the closed-shell core, and ϕ^* is the only orbital outside the core. Using the above relations, one finds

$$\begin{aligned}\Psi_0 &= \frac{1}{N} \sum_j \pi_{B_j} \left\{ \frac{\sqrt{1-\alpha^2}}{6} \phi_A^C \phi_A^* \phi_{B_j}^C + \alpha C_{lj} \phi_A^C \phi_{B_j}^C \phi_{B_j}^* \right\} \\ &= \frac{1}{N} \sum_j \phi_A^C \phi_{B_j}^C \pi_{B_j} \left\{ \frac{\sqrt{1-\alpha^2}}{6} \phi_A^* + C_{lj} \alpha \phi_{B_j}^* \right\}\end{aligned}\quad (7)$$

The prefactor $\phi_A^C \phi_{B_j}^C \pi_{B_j}$ is simply the product of all the closed-shell core functions, κ , and can be carried along from this point onward without further comment. Thus,

$$\Psi_0 = \frac{\kappa}{N} \left[\sqrt{1-\alpha^2} \phi_A^* + \alpha \sum_j C_{lj} \phi_{B_j}^* \right] \quad (8)$$

We recognize the wave function in Eq. (8) as describing the optical electron in a *molecular orbital* written as a sum of atomic orbitals spanning both A and B positions. Notice that, since the A and B sites are distinguishably different and no symmetry operation will take a wave function centered on A into one centered on B, the two fragments ϕ_A^* and $\sum_j C_{lj} \phi_{B_j}^*$ must have the same symmetry if they are to be mixed. That is, the only Ψ_l which will be mixed in with Ψ'_0 must have its sum of $\phi_{B_j}^*$ orbitals transform like the ϕ_A^* orbital. Thus the electron will be delocalized from A onto the B sites only if the orbitals on A and B have the same point group symmetry, a result already well known in molecular orbital theory.

For normalized wave functions, the value of α^2 can be derived to be

$$\alpha^2 = N^2 \left[1 - \left\{ 1 + \frac{2E_l^2 - 2E_l \sqrt{E_l^2 + 4V^2} + 4V^2}{4V^2} \right\}^{-1} \right] \quad (9)$$

from the solution of the secular equation which expresses the mixing between Ψ'_0 and Ψ_l . In this equation, V is the mixing matrix element $\langle \Psi'_0 | V | \Psi_l \rangle$ and E_l is the energy of Ψ_l above Ψ'_0 . With an appropriate change of the zero of energy, the energies E_0 and E_l may be taken as approximately the valence state ionization potentials of the reduced ion at A and the reduced ion at B, respectively.

One sees from Eq. (9) that, as E_l approaches zero, both α and $\sqrt{1-\alpha^2}$ approach $(N\sqrt{2})/2$, whereas, for very large E_l , α tends to zero and $\sqrt{1-\alpha^2}$ to one. Thus if E_l is large, then α is small, and Eq. (8) reduces to the *zeroth order* Eq. (1) for the wave function of the system in the ground state, but Eq. (8) becomes more appropriate the smaller is E_l and the larger is α . A large value of E_l may come about either because the ions in

the two sites are of different elements, or because the sites differ in ligand field strength or ligand field symmetry. Inasmuch as this review considers only mixed valence compounds in which the oxidation states involved are those of the same element, nonzero values of E_i will be associated only with differences in ligand field strength and/or ligand field symmetry.

We now propose a mixed valence classification scheme which is based essentially upon the strength and symmetry of the ligand fields about the metal ions, and their relationship to the value of α appropriate to a particular system. By definition, in a class I system, the ions of differing valence are in sites of very different symmetry and ligand field strength, so that E_i is large and α approaches zero. In a class I system the simple product function of Eq. (1) is used to describe the ground state. An example of a class I system would be a mixed valence cobalt compound in which the Co(III) ions were in octahedral ligand fields with low-spin configurations, and the Co(II) ions were in tetrahedral ligand fields with high-spin configurations.

On the other hand, if the Co(II) and Co(III) ions are in exactly equivalent sites, so that E_i is zero and $\alpha = (N\sqrt{2})/2$, then the system is class III, and the molecular orbital description, Eq. (8), is needed for the ground state of the system. Class III mixed valence systems can be further subdivided into classes III-A and III-B, depending upon whether or not discrete polynuclear ions can be distinguished in the crystal. An intermediate classification, class II, is defined for cases in which delocalization does take place ($\alpha > 0$), but the two types of site are still distinguishable, and so the optical electron does not spend equal times on them. As an example, a class II system might have both oxidized and reduced cations in octahedral sites, but with the metal-ligand distances shorter at one site than at the other. It is not easy to draw a precise demarcation between classes I and II, but, in the vast majority of cases, class II systems have at least one ligand which bridges the two ions of differing valency, whereas in class I systems the metal ions are either removed from one another by two or more ligands which are relatively non-interacting, or have very different coordinations.

A further point arising from Eq. (9), and relevant to our selection of compounds as examples of mixed valence, is that α can become large not only when E_i is small, but also when V becomes large. It is for this reason that we have, with very few exceptions, excluded sulfides, arsenides, and all other compounds in which there is likely to be extreme metal-ligand covalency. In many single valence examples of this type, electron delocalization can occur with such a small expenditure of energy that the resulting low-frequency absorption bands and high

electronic conductivity would be difficult to distinguish from that to be ascribed to mixed valence interaction. Our approach to mixed valence systems is thus predominantly an ionic one, in which electron delocalization, if it occurs, involves primarily the metal ions whose valences are under discussion, and the ligands to a much smaller extent.

The motivation for the classification scheme outlined above sprang from our observation that each of the classes as defined exhibits certain easily recognized physical properties which are characteristic of that class. Thus, by a measurement of a single property which is characteristic of one of the four classes, many of the other physical properties of the system can be guessed, or become understandable. Because compounds with properties common to more than one class are rare, the classification scheme is of rather greater utility and has been used extensively in the discussion of the mixed valence compounds (Section III).

B. MIXED VALENCE SPECTRA

Since we are neither capable nor desirous of calculating spectra in a review of this kind, our goal is to present some generalizations which, although they are phrased in the form of a theory, in fact were arrived at by a study of the experimental results reported in the literature. Thus our effort here is to rationalize "the truth" in terms of a simple model which, by its generality, will be of use in the discussion of the spectra of a wide variety of mixed valence compounds.

Our fundamental concern in this section is with the mixed valence electronic transition,

$$\frac{\kappa}{N} \left[\sqrt{1 - \alpha^2} \phi_A^* + \alpha \sum_j C_{ij} \phi_{B_j}^* \right] \rightarrow \frac{\kappa}{N'} \left[\beta \phi_A^* - \sqrt{1 - \beta^2} \sum_j C_{mj} \phi_{B_j}^* \right] \quad (10)$$

where β plays the same role for the excited state that α does for the ground state. It is electronic transitions of this sort that comprise the mixed valence absorption spectrum in all three classes. Because the classification scheme is based essentially on geometry, and since the nuclei in the excited state will be considered as fixed in the ground state configuration, the ground and excited states of mixed valence transitions are assumed to belong to the same mixed valence class.

A study of the literature shows that in systems which are known by their crystal structures to be mixed valence class I ($\alpha = \beta = 0$), the mixed valence absorption bands fall at frequencies higher than $27,000 \text{ cm}^{-1}$, for they are almost all colorless. Those class I systems that do show absorption in the visible invariably contain a colored ion as a constituent, their

visible spectra being merely sums of the spectra of the constituent ions, and nothing more. Virtually all the colorless class I systems involve nontransition metal ions, which are quite stable in the ground state as M^n and M^{n+2} , but which are relatively unstable in the M^{n+1}, M^{n+1} configuration of the mixed valence upper state. Actually, a mixed valence absorption has never been observed in a class I system, so there is no evidence as to where in the spectrum it might be found.

In contrast, the class II mixed valence systems are characterized by an absorption band in the visible region of the spectrum (14,000–27,000 cm^{-1}) which is absent in the spectra of the constituent ions taken separately. In the simplest approximation, the energy of this transition is

$$h\nu = E_A + E_B + E_{mad} \quad (11)$$

where E_A and E_B are the changes in internal energy at sites A and B, respectively, on transferring an electron from A to B, and E_{mad} is the Madelung energy expended in moving the optical electron from A to B in the electrostatic field of all the other charges in the crystal. This last term can be calculated from a cycle in which adjacent ions are removed from the crystal to infinity, an electron transferred adiabatically between them, and the ions then returned to their sites in the crystal. The two internal energy terms in Eq. (11), however, correspond to the ionization potential and electron affinity of sites A and B, respectively, and as yet cannot be estimated or measured for inorganic complexes. Inasmuch as a class II mixed valence transition is a photochemical oxidation-reduction, the possibility of somehow adapting half-cell potentials to the estimation of the internal energy terms is attractive. However, it should be mentioned that the only application of such potentials to mixed valence systems resulted in the incorrect valence assignment for the ground state of Prussian blue (754).

Although the various contributions to the energy of the lowest-frequency mixed valence absorption band in class II compounds cannot yet be interpreted in detail, certain other features of the spectrum are more readily understood. It seems clear that in class II compounds, even though α and β are nonzero, the perturbation of the wave function can be sufficiently small so that constituent ion absorptions can still be recognized, albeit not at exactly their normal frequencies. Thus the 29,000 cm^{-1} transition characteristic of the $\text{Sb}^{\text{III}}\text{Cl}_6$ group is identified at 31,000 cm^{-1} in the blue class II compound $\text{Cs}_4\text{Sb}^{\text{III}}\text{Sb}^{\text{V}}\text{Cl}_{12}$, and the 50,000 cm^{-1} charge transfer bands of the $[\text{Fe}^{\text{II}}(\text{CN})_6]^{4-}$ ion are observed at this frequency in the class II compound $\text{KFe}^{\text{III}}\text{Fe}^{\text{II}}(\text{CN})_6$. Because of this, the electronic spectrum holds promise for resolving ambiguities in the ground state valence configurations of many class II mixed valence

compounds. Similar constituent ion absorptions can be found in the infrared and Mössbauer spectra of class II compounds. For example, the ν_3 stretching frequency of the $[\text{Sb}^{\text{V}}\text{Cl}_6]^-$ ion in $\text{Cs}_4\text{Sb}^{\text{III}}\text{Sb}^{\text{V}}\text{Cl}_{12}$ is shifted only 5 cm^{-1} from its position in $\text{RbSb}^{\text{V}}\text{Cl}_6$.

A second interesting point, which also follows from the slight perturbation of the constituent ion levels in class II systems, involves the remaining mixed valence spectrum. For illustration, consider the d -orbital pattern of a hypothetical class II $\text{Cu}(\text{I}), \text{Cu}(\text{II})$ complex in which

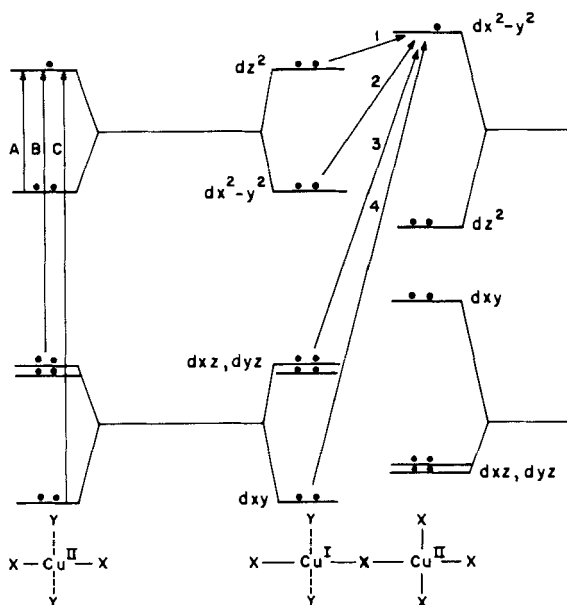


FIG. 2. The molecular orbital scheme for the hypothetical class II mixed valence system $\text{Cu}^{\text{I}}\text{Y}_2\text{X}_2\text{Cu}^{\text{II}}\text{X}_3$, showing how the energy difference between the two mixed valence transitions 2 and 1 is equal to the crystal field transition A in $\text{Cu}^{\text{II}}\text{X}_2\text{Y}_2$, etc.

the $\text{Cu}(\text{I})$ is in square coordination with two X and two Y ligands, and $\text{Cu}(\text{II})$ is in square coordination with four X ligands (Fig. 2). In such a simple system there will be four mixed valence absorption bands, labeled 1, 2, 3, and 4. The point of interest here is that the energy difference between mixed valence transitions 1 and 2 will be equal to the first crystal field excitation energy of the $\text{Cu}(\text{II})$ ion in the $\text{Cu}(\text{I})$ ion site, i.e., transition A ($dx^2 - y^2 \rightarrow dz^2$) in the oxidized ion. Similarly, mixed valence transition 3 will appear displaced from transition 1 by the $\text{Cu}(\text{II})$ crystal field excitation B ($dxz, dyz \rightarrow dz^2$). Thus in this case, the entire crystal field spectrum of the oxidized ion, $\text{Cu}(\text{II})$, in the reduced

ion site (A) appears in the mixed valence spectrum, shifted from where it ordinarily would appear by the energy of the lowest mixed valence transition. Other samples exist where the mixed valence spectrum consists of the crystal field spectrum of the reduced ion in the oxidized ion site, or of combinations of both kinds of spectrum. However, not all crystal field states will necessarily appear in the mixed valence spectrum, since many of the excited crystal field configurations require two-electron excitation when attained from the mixed valence ground state. Only one example of the shifting of the crystal field spectrum by the mixed valence excitation energy has so far been reported (591).

The intensities of electronically allowed transitions in class II systems are another interesting aspect of mixed valence spectra. In an electronically allowed transition, the orbital $\sum_j C_{mj} \phi_{B_j}^*$ of the upper state must transform differently under the operations of the symmetry point group than does $\sum_j C_{lj} \phi_{B_j}^*$, so that $\sum_j C_{mj} \phi_{B_j}^*$ cannot mix with ϕ_A^* , and thus β is zero. The intensity of such an electronically allowed mixed valence transition is proportional to the square of the transition moment integral,

$$\mu = \frac{g^{1/2}}{NN'} \int \left[\sqrt{1 - \alpha^2} \phi_A^* + \alpha \sum_j C_{lj} \phi_{B_j}^* \right] \mathbf{M} \sum_j C_{mj} \phi_{B_j}^* d\tau \quad (12)$$

where g is the orbital degeneracy of the transition, and \mathbf{M} is the electric moment operator. By neglecting overlap distributions between the A and B sites, the x component of Eq. (12) can be reduced to

$$\mu_x = \frac{\alpha g^{1/2}}{NN'} \int \sum_j C_{lj} \phi_{B_j}^* \epsilon x \sum_j C_{mj} \phi_{B_j}^* d\tau \quad (13)$$

$$= \frac{e \alpha g^{1/2}}{NN'} \sum_j C_{lj} C_{mj} x_j \quad (14)$$

in which x_j is the x coordinate of the j th site. Exactly similar equations hold for the y and z moments. The utility of Eq. (14) lies in the fact that, if the system is sufficiently regular geometrically so that the C_{lj} 's and C_{mj} 's are determined by symmetry, and the x_j 's are known from a crystal structure determination, α can be obtained from a measurement of μ ; μ is calculated from the equation

$$\mu^2 = 9.17 \times 10^{-4} \int \epsilon d \log \lambda \quad (15)$$

in which ϵ is the molar extinction coefficient of the mixed valence absorption band at wavelength λ , and μ^2 is measured in cm^2 .

There is one complication worth considering here, and that is the case where there are two types of orbital at each B site, call them

$\phi(z^2)_j^*$ and $\phi(x^2 - y^2)_j^*$, say. The possibility then arises for a transition involving the two types of orbital, leading to the transition moment :

$$\mu = \frac{\alpha g^{1/2}}{NN'} \int \sum_j C_{lj} \phi(z^2)_j^* \mathbf{M} \sum_j C_{mj} \phi(x^2 - y^2)_j^* d\tau \quad (16)$$

$$\mu = \frac{\alpha g^{1/2}}{NN'} \sum_j C_{lj} C_{mj} \int \phi(z^2)_j^* \mathbf{M} \phi(x^2 - y^2)_j^* d\tau \quad (17)$$

The transition moment integral in Eq. (17) is one between atomic orbitals on the same atom, and can be zero even though the selection rules predict an allowed transition between Ψ_0 and Ψ_m . This is possible because the selection rule allowing a transition between Ψ_0 and Ψ_m guarantees that the intensity generated in one part of the molecular system is not canceled by that in another part, but by itself does not guarantee that the intensity within this part of the molecular system is not itself zero. Inasmuch as the intensity of an electronically allowed mixed valence transition does depend upon α , it can readily be appreciated that there can be no *intense* ($\epsilon \geq 4000$) mixed valence absorption unless ϕ_A^* and some ϕ_B^* have a nonzero overlap.

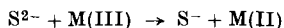
That highly hydrated mixed valence compounds have only the pale color of their constituent ions, but become more deeply colored as the water is removed, is one of the mixed valence facts of life. This is understandable, since water is not a bridging ligand and would promote the formation of a class I system when present in large proportions. However, as the water is removed, the empty sites must be filled by ligand anions which can bridge two metal ions and thereby turn the compound into a more deeply colored class II system.

Polynuclear mixed valence anions, cations, and neutral species in which the sites of all metal ions are equivalent are classified as III-A. The interpretation of the spectral properties of class III-A systems differs from that of class II systems, for in class III-A the distinction between A and B sites is lost completely, so that $E_A = -E_B$, and E_{mad} is zero. The excitation energies in class III-A are instead dependent upon ligand field splittings and molecular orbital resonance integrals, just as they are in an ordinary polynuclear complex having metal-metal bonds. Also, unlike class II, there will be no recognizable constituent ion spectra in class III-A compounds.

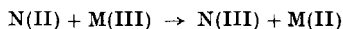
Class III-B systems are metals and as such show an absorption edge, usually in the infrared, and are opaque with a metallic reflex in the visible region.

In a broader sense, there is really nothing unique about mixed valence systems, for mixed valence properties are to be expected in any

system containing simultaneously an oxidizable and a reducible species in close contact. Thus, transition metal sulfides may have many properties in common with class II mixed valence systems, for the excitation



may be thought analogous to the excitation



in a mixed valence system. The difference between these two examples is one of degree only, for if the N and M ions are of the same element and are in identical ligand fields, then the energy difference between $N(II) + M(III)$ and $N(III) + M(II)$ will be as small as zero, whereas no such statement can be made for $S^{2-} + M(III)$ versus $S^{-} + M(II)$.

The relationship of inorganic mixed valence systems to the organic charge transfer complexes is also a close one. In fact, the charge transfer complex quinhydrone is mentioned in Biltz's early article on inorganic mixed valence systems (69). The unexpected deep black color of quinhydrone was correctly seen by Biltz to be a consequence of having formed a crystal containing an intimate mixture of the oxidized material (benzoquinone) and the corresponding reduced material (hydroquinone), in every way equivalent to the formation of a deep blue color in crystals which contain $Fe(III)$ (an oxidized material) and $Fe^{II}(CN)_6$ (a reduced material).

C. MAGNETISM AND ELECTRON TRANSPORT

The magnetic and electron transport properties of mixed valence compounds are closely related to one another, and the wide variations observed in their behavior give further weight to our proposed classification scheme. In particular, we can make operational distinctions between class I and class II compounds on the basis of these properties in a way not possible from a knowledge of the crystal structure alone.

In a class I mixed valence material, the electrons which distinguish the valence of one ion from another are so firmly trapped that virtually no magnetic coupling between partly filled shells on adjacent metal ions is possible, and these substances are paramagnetic down to very low temperatures. Thus a class I compound such as $Co^{II}Co_2^{III}O_4$ will have a molar magnetic susceptibility precisely that expected for a mixture of one mole of $Co(II)$ in tetrahedral coordination and two moles of $Co(III)$ in octahedral coordination. That electron transfer can occur only at the expense of a large amount of energy also means that class I materials are electrical insulators.

At the opposite extreme, when α in Eq. (9) has its maximum value, the odd electrons responsible for the mixed valence occupy a band spanning the entire cation sublattice (we are ignoring the possibility that they have any appreciable density on the anion sublattice, as mentioned above). In such a case, two electrons occupy each state of the energy band up to the Fermi surface so that, with completely filled inner shells and in the absence of a magnetic field, each atom has no net spin, and atomic moments exist only through induction by an applied field. By Lenz's law, such moments give a diamagnetic susceptibility, but for collective electrons there is a further possibility that an applied field might alter the populations of the electron states, producing what is known as temperature-independent Pauli paramagnetism. If each cation contributes either zero or two electrons to a band, then the band will be either completely empty or completely filled, and in either case the material will be an insulator. However, by their very nature of being mixed valence, the cations in class III-B materials will contribute, on the average, an intermediate number of electrons to the band, filling it only partially. Thus class III-B mixed valence materials will show metallic conductivity. The class III-B tungsten bronzes are good examples of these mixed valence effects, for they have temperature-independent paramagnetic susceptibilities and metallic conductivities. A second type of magnetic behavior in class III-B systems is described below.

The possibility of ferromagnetic ordering between the local magnetic moments in transition metals was first considered by Zener (812), who proposed that, in the metallic state, it was the conduction electrons which coupled the d -shell moments together. Since, according to Hund's rule, the lowest energy configuration within each d -shell has the spins of all of the unpaired electrons parallel, if the conduction electrons are to carry their spins unchanged from atom to atom, they must move in an environment of parallel spins, i.e., the moments of all the atoms must point in the same direction. Contrasting the Heusler alloys, which are conducting and ferromagnetic, with MnF_2 , which is an antiferromagnetic insulator, Zener concluded that ferromagnetism would never occur in the absence of conduction electrons (812). Shortly afterwards, the properties of a series of metallic mixed valence manganites, $\text{La}_{1-x}\text{Sr}_x\text{Mn}_{1-x}^{\text{III}}\text{Mn}_x^{\text{IV}}\text{O}_3$, were investigated by Jonker and van Santen (392, 393), and these have since become the classic examples of Zener's "double exchange" phenomenon. The relationship between ferromagnetism and conductivity is brought out most clearly by a simple example. In contrast to the metals described above, between each manganese ion in the perovskite structure of $\text{La}_{1-x}\text{Sr}_x\text{Mn}_{1-x}^{\text{III}}\text{Mn}_x^{\text{IV}}\text{O}_3$

there is an oxide ion, through which any electron transport must occur, although, as we have noted several times, the initial and final states of electron transfer are assumed to have very little unpaired spin density on any intervening ions. This is equivalent to saying that we could write wave functions for systems such as those described by Eqs. (1) and (2) as if their metal-ligand electronic configurations were $\text{Mn}_A^{\text{III}}\text{O}^{2-}\text{Mn}_B^{\text{IV}}$ and $\text{Mn}_A^{\text{IV}}\text{O}^{2-}\text{Mn}_B^{\text{III}}$. The magnetic exchange energy of such a system is given by

$$E_m = \int \psi_A^{\text{III}} \psi_O \psi_B^{\text{IV}} (H - E_0) \psi_A^{\text{IV}} \psi_O \psi_B^{\text{III}} d\tau \quad (18)$$

where H is the Hamiltonian for the entire system, and E_0 is the energy associated with the initial states, assumed degenerate. The dominant term of the exchange integral contains a product of wave functions $\psi_A(1)\psi_O(1)\psi_O(2)\psi_B(2)$, suggesting that one visualize the electron transfer from one manganese to the next as a transfer of electron (2) from the oxygen to the Mn_B^{IV} ion with a simultaneous transfer of electron (1) from Mn_A^{III} to the oxygen; a connection between ferromagnetic coupling and electronic conductivity is thus apparent. That the interaction in a mixed valence compound is ferromagnetic arises in the following way. Of the two antiparallel electron spins on the oxide ion, Hund's rule predicts that the oxide ion electron with spin parallel to those of the $3d^3$ Mn(IV) ion will be transferred the more readily, leaving behind the electron of opposite spin. Similarly, the $3d^4$ Mn(III) ion will transfer an electron to the O^- ion which has a spin opposite to that remaining on O^- . The net result is that the manganese ions are coupled via the oxide ligand only if the spins on the two metal ions are parallel, i.e., in ferromagnetic alignment.

If the magnetic exchange energy in the system discussed above is E_m , the "extra" electron, when placed on one of the manganese atoms, will oscillate between them with a frequency

$$\nu = 2E_m/\hbar \quad (19)$$

and will have a diffusion coefficient

$$D = a^2 E_m / \hbar \quad (20)$$

where a is the cation-cation separation. Using the Einstein relation between electrical conductivity, σ , diffusion coefficient, and the number of ions per unit volume, n ,

$$\sigma = ne^2 D / kT \quad (21)$$

one then finds that

$$\sigma = ne^2 a^2 E_m / \hbar kT \quad (22)$$

If we further assume, along with Zener and Heikes (814), that $E_m \simeq kT_c$, where T_c is the ferromagnetic Curie temperature, then the resistivity at this temperature for a typical cation-cation separation of 3 Å is approximately 10^{-3} ohm cm. As we shall see, the resistivities of a number of class III-B mixed valence materials at room temperature are in order of magnitude agreement with this estimate. The number of charge carriers/cc in a class III-B metal is estimated simply from the density of the material and the difference in the formal oxidation states of the cations involved in the mixed valence.

We now want to consider the magnetic and electrical properties of the intermediate, mixed valence class II materials. Mott (519) was the first to point out that there should exist some critical interatomic separation at which the types of molecular orbital (or band, in the limit of an infinitely extended lattice), which we have set up, are no longer the best approximation for treating the interactions between cations. For large interatomic separations, a Heitler-London approach, which assigns a fixed integral number of electrons to each cation and does not permit polar states as does the molecular orbital model, would have to be used. This argument was originally proposed to account for the fact that transition metal oxides like NiO, with incompletely filled *d*-shells and bridging anions separating the cations, are not metals but insulators. As will be discussed below, it is this model which is most appropriate to class II materials.

Zener assumed that the two configurations $\text{Mn}^{\text{III}}\text{O}^2-\text{Mn}^{\text{IV}}$ and $\text{Mn}^{\text{IV}}\text{O}^2-\text{Mn}^{\text{III}}$ were indistinguishable, which is equivalent to setting $E_t = 0$ in Eq. (9), so that the system belongs to class III-B. If this were not the case and the "extra" electron were trapped by lattice polarization ($\text{Mn}^{\text{III}}-\text{O}$ and $\text{Mn}^{\text{IV}}-\text{O}$ bond lengths different), further work must be spent in rendering the bond lengths equal so that electron migration can occur. This activation energy corresponds to ΔG , the change in Gibbs free energy of the system, and the diffusion coefficient would then be:

$$D = a^2\nu_0 e^{-\Delta G/kT} \quad (23)$$

Heikes and Johnston (351), who first derived expressions for the so-called "hopping model," identified ν_0 with the lattice vibration frequency, and values obtained from their work on lithium-doped mixed valence transition metal oxides are of the expected magnitude (about 10^{13} sec $^{-1}$).

The temperature dependence of conductivity implied by Eq. (23) is that of a semiconductor, and we thus expect this type of electronic activity in class II substances. Inasmuch as class II compounds have relatively low conductivities as compared with class III-B compounds, according to Eq. (22), they will have correspondingly weaker ferro-

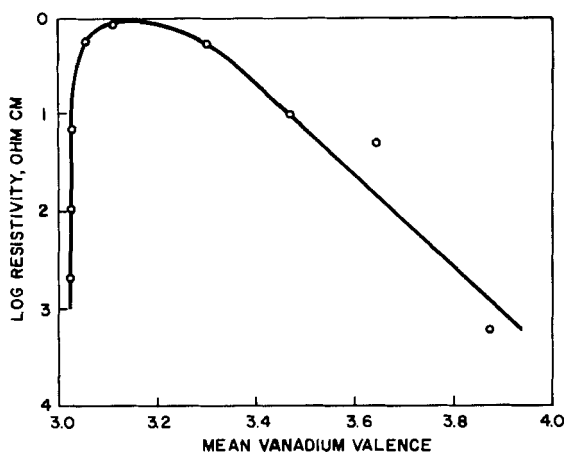


FIG. 3. The resistivity of mixed crystals of $\text{MgV}_2^{\text{III}}\text{O}_4$ and $\text{Mg}_2\text{V}^{\text{IV}}\text{O}_4$ as a function of the mean valence of the vanadium ions (581).

magnetic interactions. Thus they will remain paramagnetic down to much lower temperatures than will class III-B materials, and at low temperatures may go either ferromagnetic or antiferromagnetic, depending upon the relative strengths of the interactions between like and unlike valences.

TABLE II
CONTROLLED VALENCY SEMICONDUCTORS

Host	Dopant ^a	Valence introduced	Crystal lattice
$\text{Ni}^{\text{II}}\text{O}$	Li_2O	Ni^{III}	Rock salt
$\text{Mn}^{\text{II}}\text{S}$	Li_2O	Mn^{III}	Rock salt
$\text{CaTi}^{\text{IV}}\text{O}_3$	La_2O_3	Ti^{III}	Perovskite
$\text{BaTi}^{\text{IV}}\text{O}_3$	La_2O_3	Ti^{III}	Perovskite
$\text{CaMn}^{\text{IV}}\text{O}_3$	La_2O_3	Mn^{III}	Perovskite
$\text{LaMn}^{\text{III}}\text{O}_3$	CaO	Mn^{IV}	Perovskite
$\text{LaFe}^{\text{III}}\text{O}_3$	SrO	Fe^{IV}	Perovskite
$\text{Fe}_2^{\text{III}}\text{ZnO}_4$	TiO_2	Fe^{II}	Spinel
$\text{Fe}_2^{\text{II}}\text{O}_3$	SnO_2	Fe^{III}	Hematite
$\text{Ti}^{\text{IV}}\text{O}_2$	Ta_2O_5	Ti^{III}	Rutile
$\text{MgW}^{\text{VI}}\text{O}_4$	Cr_2O_3	W^{V}	Wolframite

^a In each of these systems, the dopant cation is thought to replace the cation listed first in the formula of the host crystal.

TABLE III
CHARACTERISTICS OF THE FOUR CLASSES OF MIXED VALENCE COMPOUNDS

Class I	Class II	Class III-A	Class III-B
(1) Metal ions in ligand fields of very different symmetry and/or strength, i.e., tetrahedral vs. octahedral	(1) Metal ions in ligand fields of nearly identical symmetry, differing from one another by distortions of only a few tenths Å	(1) Metal ions indistinguishable but grouped into polynuclear clusters	(1) All metal ions indistinguishable
(2) $\alpha = 0$; valences very firmly trapped	(2) $\alpha > 0$; valences distinguishable, but with slight delocalization	(2) α maximal locally	(2) α maximal; complete delocalization over the cation sublattice
(3) Insulator; resistivity of 10^{10} ohm cm or greater	(3) Semiconductor; resistivity in the range 10 – 10^7 ohm cm	(3) Probably insulating	(3) Metallic conductivity; resistivity in the range 10^{-2} – 10^{-6} ohm cm
(4) No mixed valence transitions in the visible region	(4) One or more mixed valence transitions in the visible region	(4) One or more mixed valence transitions in the visible region	(4) Absorption edge in the infrared, opaque with metallic reflectivity in the visible region
(5) Clearly shows spectra of constituent ions, IR, UV, Mössbauer	(5) Shows spectra of constituent ions at very nearly their normal frequencies	(5) Spectra of constituent ions not discernible	(5) Spectra of constituent ions not discernible
(6) Magnetically dilute, paramagnetic or diamagnetic to very low temperatures	(6) Magnetically dilute, with both ferromagnetic and antiferromagnetic interactions at low temperatures	(6) Magnetically dilute	(6) Either ferromagnetic with a high Curie temperature or diamagnetic, depending upon the presence or absence of local moments

Among the mixed valence manganites (392, 393), the connection between composition, Curie temperature, and resistivity is well established, and, in other systems in which the concentrations of two valence states can be varied, the conductivity also varies strongly (Fig. 3). Verwey and co-workers (730) have successfully altered these concentrations in a great many oxides, producing what are known as "controlled valency semiconductors." As illustrated in Table II, the addition of an insulating dopant to an insulating host crystal can alter the mean valency of the host's cations so as to render the system class II mixed valence and semiconducting.

The characteristics of the four classes of mixed valence compounds are compared in Table III.

D. MOLECULAR GEOMETRY

Inasmuch as the class of a mixed valence compound is intimately related to its crystal structure, the a priori prediction of the class of a mixed valence compound is equivalent to the a priori prediction of its crystal structure, a feat to which we can only aspire. The only mixed valence species upon which one can readily perform a calculation is the H_3^+ molecule-ion, which, from very complete calculations (147), would appear to be class III-A. A simple calculation on this molecule-ion reveals the two factors of importance in determining whether any mixed valence system will belong to class III or to a class of lower symmetry.

The total energy of the ground state of H_3^+ in various configurations was calculated, using as a basis nine *s*-type Gaussian orbitals on each proton, scaled to reproduce a Slater orbital with an effective nuclear charge of 1.414. In the first configuration (Fig. 4), the proton is situated 0.89 Å from each of the protons in H_2 (internuclear separation, 0.74 Å) and the two electrons are localized within the H_2 molecule. With the electrons still localized, the H_2 molecule is then stretched from 0.74 Å to 0.89 Å internuclear separation, raising the total energy by 24 kcal/mole and making all three protons equivalent. In the third configuration, the valence oscillates with the electrons moving over all three nuclei, and the total energy is then lowered by 135 kcal/mole.

This example of the H_3^+ molecule-ion illustrates the two opposing factors which must be considered in any problem of mixed valence geometry: (a) the reorganization energy which must be expended to stretch and/or compress certain bonds so as to make all the sites equivalent, and (b) the resonance energy stabilization which accrues from the oscillation of valence. If the second factor is larger than the first, then the system will belong to class III-A or III-B, whereas, if it is smaller than

the first, then the system will belong to class II or I. As explained in the previous section, if the reorganization energy is of the order of thermal energies, then the valence may oscillate via a hopping process.

Other attempts to predict which class a pair of mixed valence metal ions might prefer are frustrated by the fact that unusual coordinations can result in mixed valence compounds. Thus, for example one would ordinarily guess that Cu(I),Cu(II) systems would be class I or II, for

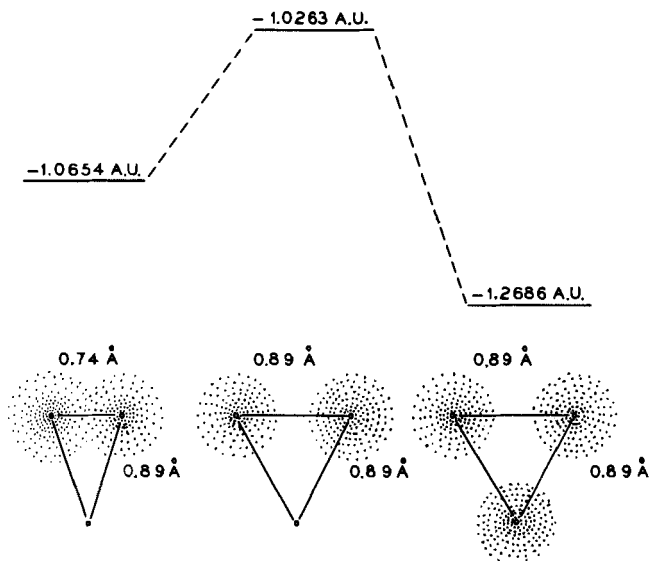


FIG. 4. The relative effects of reorganization and resonance on the total energy and geometry of the H_3^+ mixed valence molecule-ion.

these ions in general have very different coordination symmetries. However, in $KCu_3Cu^{II}S_3$, all the copper ions are in identical regular tetrahedral sites, a geometry never found for Cu(II) salts. There are other examples of unexpected geometries in class III systems.

III. Survey of the Elements

An indiscriminate study of mixed valence chemistry rapidly takes one from the simple salts and oxides into the realm of sulfides, tellurides, arsenides, and a vast array of other intermetallics. In an effort to keep this review of manageable length, we have arbitrarily ignored all but a very few compounds of this latter group, concentrating instead on the mixed valence oxides, halides, cyanides, and other simple salts, as well as coordination compounds. Many of the properties of mixed valence

compounds described in Section II can also be found in mixed metal complexes, such as $\text{KMn}^{\text{II}}\text{Fe}^{\text{III}}(\text{CN})_6$, which also have been ignored in this review. Similarly, we have neglected mention of all thermodynamic properties of mixed valence compounds, and have paid only slight attention to areas such as mixed valence kinetic and mechanism studies, fused salt chemistry, and the defect solid state.

In general, a mixed valence compound is most readily identified as such by its formula. However, there are certain difficulties in this, since in many cases the proposed formula is little more than a statement of analytical results, and a poor analysis might mistakenly turn a single valence material into a mixed valence one. A second problem, which arises most especially with oxides, is that of mixtures mistaken for pure mixed valence materials, and we mention this possibility wherever it seems advisable. Our emphasis throughout is first on structure, since this enables one to make a preliminary estimate of a compound's mixed valence class, and then on electronic properties as enumerated in Section II.

The order of presentation follows that of the Periodic Table, starting with the first-row transition elements, followed by the second- and third-row transition elements considered jointly, the groups III-A, IV-A, and V-A elements, and finally the lanthanide and actinide elements.

A. TITANIUM

The most extensively studied titanium mixed valence compounds are the oxides. That they provide a good example of the sensitivity of physical properties to stoichiometry is demonstrated by Verwey's early work on TiO_x (727), which has a resistivity of 10^{10} ohm cm when $x = 2.000$, decreasing to 10 when $x = 1.999$, and to 1.2 for $x = 1.995$. In addition to studies of the optical and electrical properties of $\text{Ti}^{\text{IV}}\text{O}_2$ containing small amounts of $\text{Ti}(\text{III})$, interest in the titanium mixed valence oxides has centered on the structures of the numerous oxides intermediate between Ti_2O_3 and TiO_2 , although it is unfortunate that rather less attention has been devoted to their physical properties.

The first X-ray phase analysis of the titanium-oxygen system, by Ehrlich (216), uncovered four phases with homogeneity ranges $\text{TiO}_{2.00}$ – $\text{TiO}_{1.90}$, $\text{TiO}_{1.80}$ – $\text{TiO}_{1.65}$, $\text{TiO}_{1.56}$ – $\text{TiO}_{1.46}$, and $\text{TiO}_{1.25}$ – $\text{TiO}_{0.6}$. After some disagreement (15, 349) as to whether the composition variation was due to random removal of some of the oxygen atoms or addition of extra titanium atoms to the parent TiO_2 rutile lattice, it is now recognized that in the $x = 1.65$ – 1.80 range there are at least seven stable

oxides, all with the general formula $\text{Ti}_n\text{O}_{2n-1}$, with $n = 4-10$ (18). Members of the series with $n = 1, 2$, and 3 are also known. The occurrence of such "homologous series" or Magneli phases (474) among mixed valence transition metal oxides is quite frequent, and further examples are described in the sections on vanadium, niobium, and molybdenum and tungsten. In each case, blocks of the parent lattice structure (here rutile) are interrupted by regions of higher cation concentration, which can be thought of as resulting from the "shearing" (738) of one block past another. In the present example, blocks of the rutile (MO_2) structure are interleaved with layers of corundum (M_2O_3) structure. In the rutile structure, TiO_6 octahedra are joined through their corners and edges, but, in an oxide such as Ti_5O_9 (18) (Fig. 5), every fifth TiO_6 in one

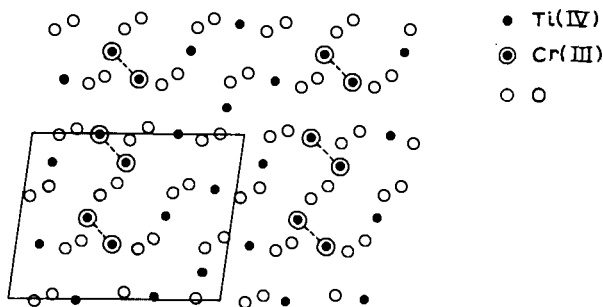


FIG. 5. The crystal structure of Ti_5O_9 and the isostructural compound $\text{Cr}_2\text{Ti}_3\text{O}_9$, viewed along $[100]$ (18).

direction is joined to one of its neighbors by sharing one of their octahedral faces. The distance between the face-sharing pairs of titanium atoms in Ti_5O_9 is 2.81 Å, compared with 2.56 Å for the closest metal-metal distance in Ti_2O_3 , which has a corundum structure in which the TiO_6 units share both faces and edges. While there is no conclusive evidence that this series of oxides could be described as class II mixed valence systems of the sort $\text{Ti}_{n-2}^{\text{IV}}\text{Ti}_2^{\text{III}}\text{O}_{2n-1}$, there are two pieces of evidence that make the suggestion plausible. First, it has proved possible to isolate several mixed oxides of Ti(IV) and Cr(III), isostructural with the above homologous series, which have the general formula $\text{Ti}_{n-2}^{\text{IV}}\text{Cr}_2^{\text{III}}\text{O}_{2n-1}$ (8). Thus each block of rutile lattice, regardless of its size, accommodates only two chromium ions, and the question is whether these are randomly distributed or, as seems more likely, located in the face-sharing pairs of octahedral sites at the ends of each rutile block (the circled atoms in Fig. 5). ESR or static susceptibility measurements would settle the question if they could show whether or not the Cr(III) ions were mag-

netically coupled in pairs. The second piece of evidence bearing on the pairing of Ti(III) ions in $\text{Ti}_n\text{O}_{2n-1}$ has to do with a set of magnetic susceptibilities determined by Ehrlich (216) on samples which, in the light of the more recent structural work, may have been phase mixtures. Measurements were made at -183°C and $+20^\circ\text{C}$ only, but the form of the plots of molar susceptibility against composition at the two temperatures suggests that, when $x = 1.95-2.00$, the Curie-Weiss law applies. When larger amounts of Ti(III) were incorporated in the TiO_2 lattice, the molar susceptibility fell rapidly, and Ehrlich calculated that, in the region of $\text{Ti}_n\text{O}_{2n-1}$ formation, the antiferromagnetic interaction between the Ti(III) ions was as marked at -183°C as in Ti_2O_3 , as might be expected if the magnetic Ti(III) ions were in face-sharing pairs. If we are right in regarding the shear structures of the $\text{Ti}_n\text{O}_{2n-1}$ compounds as sheets of corundum-like Ti_2O_3 separating blocks of rutile TiO_2 , the mixed valence interaction is between cations situated in octahedra which share edges rather than faces. Because all the metal ions, regardless of valence, are in octahedral sites, the $\text{Ti}_n\text{O}_{2n-1}$ compounds are catalogued as class II. However, more physical measurements will be needed before the picture can be made more precise. Although the $\text{Ti}_n\text{O}_{2n-1}$ oxides are all dark blue to black, the facts that Ti_2O_3 is violet because of the $d-d$ transitions of the octahedrally coordinated Ti(III) ion (16), and also that the $\text{Ti}_{n-2}^{\text{IV}}\text{Cr}_2^{\text{III}}\text{O}_{2n-1}$ compounds are "graphite gray" (16), mean that no simple conclusions about the interaction absorption in these compounds can be drawn from the qualitative reports of their colors.

Although its formula fits the $\text{Ti}_n\text{O}_{2n-1}$ sequence, Ti_3O_5 has a structure in which rutile and corundum fragments cannot be distinguished. Two forms of Ti_3O_5 exist, a high-temperature modification (anosovite), whose structure was determined by Zhdanov and Rusakov (815), and a black modification stable at room temperature, investigated by Asbrink and Magneli (26). These phases provide an interesting contrast, for anosovite appears to be a class III-B system with all the TiO_6 octahedra having somewhat similar distortions and all sharing six edges with their neighbors, whereas in the low-temperature phase there are three ways in which the octahedra, although similarly distorted, share edges with their neighbors. In anosovite there are no exceptionally close metal-metal contacts but, in low-temperature Ti_3O_5 , one pair of titanium atoms per unit cell is separated by only 2.61 Å, and other metal-metal distances are intermediate between this and 3.1 Å. Thus the system is class II, although the valence distribution cannot be unambiguously defined.

Since small deviations from stoichiometry in TiO_2 due to traces of Ti(III) darken the color of this white pigment, and are therefore extremely important to the paint industry, a number of optical studies

of reduced TiO_2 have been reported. Weyl (385) suggested that the discoloration of rutile on firing was due to reduction of some of the cations, and found that a similar result could be achieved by doping the rutile with pentavalent ions. Working with medium and strongly reduced rutile crystals, Cronmeyer (169) found a very broad absorption band near $10,000 \text{ cm}^{-1}$, whose intensity was proportional to the room temperature conductivity of the samples. An equally broad band also occurs at nearly the same frequency in samples containing only very small concentrations of Ti(III) (735). These results, as well as much of the earlier work on the optical and electrical properties of reduced TiO_2 (306), were interpreted on the assumption that the defect centers were oxygen vacancies acting as doubly charged donors. That the correct description involves interstitial Ti(III) ions is shown not only by the structural studies of the $\text{Ti}_n\text{O}_{2n-1}$ compounds, described above, but also by a good deal of ESR work (135, 136, 805). Reduced and niobium- and tantalum-doped samples of TiO_2 were studied, as well as centers produced by γ and ultraviolet irradiation, and in all cases the "extra" electrons were found trapped on titanium atoms, as shown also by the presence of weak hyperfine structure due to titanium nuclei with spins $5/2$ and $7/2$. To explain the results of his electrical conductivity, Hall effect, and thermoelectric power measurements on reduced rutile single crystals, Frederikse (260) therefore started from the assumption that, at very low temperatures, nearly all the electrons were self-trapped on cation sites by polarization of the surrounding lattice. The traps are sufficiently shallow to be thermally ionized, however, and so, at higher temperatures, conduction occurs in a narrow $3d$ band associated with the titanium ions, which is equivalent to a class III-B mixed valence system. This conclusion was broadly confirmed by recent high-temperature conductivity experiments over a wide range of oxygen pressure (76). If the energy required to discharge a trapped $3d$ electron into a conduction band is indeed within the range of thermal energies, there must be some doubt whether the system should be described as class II or III-B in our classification. Strictly speaking, therefore, the criteria of the classification ought to be applied at absolute zero.

Compounds which are more likely to belong in class III-B at all temperatures are the alkali metal (17, 739) and lanthanum (411) titanium bronzes, $\text{Na}_x\text{Ti}_4\text{O}_8$ and $\text{La}_{(2/3+x)}\text{TiO}_3$. Both series are said to form blue-black or black electrically conducting crystals with a metallic luster, but no detailed optical or conductivity experiments have been reported. A series of manganese titanates, $\text{Mn}_{(1+x)}^{\text{II}}\text{Ti}_{2(1-x)}^{\text{III}}\text{Ti}_x^{\text{IV}}\text{O}_4$, with spinel structures (459) might be class II or III-B mixed valence systems, according to the distribution of the cations. An X-ray study of the

$x = 0.48$ compound showed that the tetrahedral sites were exclusively occupied by Mn(II) (as indeed they are in MnTi_2O_4 and Mn_2TiO_4), suggesting that Ti(III) and Ti(IV) occupy the octahedral sites, but conductivity measurements have not been made on this apparently class III-B system.

In addition to the many Ti(III),Ti(IV) oxides, one oxide containing Ti(II) and Ti(III) has been reported. Both TiO and LiTiO_2 crystallize in rock salt lattices, and mixed crystals $\text{Li}_x\text{Ti}_{1-2x}^{\text{II}}\text{Ti}_x^{\text{III}}\text{O}$ can be prepared in which x lies between 0 and 0.5, and the cations are randomly distributed. The room temperature resistivity rises monotonically from 5×10^{-3} ohm cm for TiO, which is in any case a metal, up to 2 ohm cm for LiTiO_2 . Thus there appears to be no enhancement of conductivity over that of TiO due to the presence of the mixed valences.

Interaction absorption between Ti(III) and Ti(IV) has been detected in aqueous solutions as well as oxide lattices. Partial oxidation of sky blue Ti(III) solutions in 12 *M* HCl gives a deep purple coloration, which was studied by Jorgensen (395). The spectra of such solutions were said to be a superposition of the *d-d* bands of the Ti(III) ion (at 15,100 and 17,400 cm^{-1}) and an intense new absorption band at 20,200 cm^{-1} , which also had a shoulder at 16,100 cm^{-1} . Furthermore, absorption in the near-ultraviolet was very much intensified compared with single valence solutions. Arguing from the known formation constants of the Ti(III) and Ti(IV) chloro complexes, it was suggested that the interaction complex might be $[\text{Ti}^{\text{III}}\text{Cl}]^{2+}[\text{Ti}^{\text{IV}}\text{Cl}_6]^{2-}$, but there is no direct evidence that this is so. In 20 % sulfuric acid a 1:1 Ti(III),Ti(IV) interaction complex is also formed, with an absorption maximum at 21,200 cm^{-1} (298), but is destroyed by higher concentrations of acid.

B. VANADIUM

The vanadium mixed valence compounds whose structural and electronic properties have received the greatest attention are the oxides intermediate between V_2O_3 and V_2O_5 . Hoschek and Klemm (370), who were the first to make a systematic study of the system, identified three mixed valence phases, α ($\text{VO}_{1.80}\text{--VO}_2$), α' ($\text{VO}_2\text{--VO}_{2.2}$), and β ($\text{VO}_{1.65}\text{--VO}_{1.8}$), in addition to V_2O_3 , which has a structure similar to corundum, and V_2O_5 , whose structure is based on very distorted octahedral VO_6 units (36). It is not immediately obvious whether the intermediate phases should all be formulated as V(III),V(V) compounds or whether the mixture of valences is V(III),V(IV) for compounds in the range $\text{VO}_{1.5}\text{--VO}_2$, and V(IV),V(V) in the range $\text{VO}_2\text{--VO}_{2.5}$. This problem has

attracted the attention of a number of investigators (318, 370, 437), who have attempted to resolve the dilemma by performing magnetic susceptibility measurements. However, since many of the compounds are strongly antiferromagnetic, such measurements are not easy to interpret without a detailed knowledge of the signs and magnitudes of the magnetic interactions between ions of like and unlike valence states.

The VO_2 - V_2O_5 phase region was examined in greater detail by Aebi (3), who found evidence for only one intermediate compound, with a formula $\text{VO}_{2.17}$, i.e., V_6O_{13} , and a structure which was considered to be derived from that of V_2O_5 by the regular removal of one third of the planes consisting solely of oxygen atoms (276). It is interesting that, of all the vanadium oxides, only products with compositions between V_2O_5 and V_6O_{13} are good oxidation catalysts, a result which may be explicable in terms of the ease with which oxygen atoms can migrate through channels in the lattice of V_2O_5 (276). V_6O_{13} forms needles of the same blue-black color as VO_2 (3). It is antiferromagnetic, with a Neel temperature of 154°K (437), above which it behaves as a semiconductor having a conductivity and activation energy not very different from V_2O_5 (318). Below the Neel point, the conductivity increases approximately 10-fold, in contrast to VO_2 and V_2O_3 , which at their Neel points undergo a transition from the metallic to the semiconducting state, accompanied by a decrease in conductivity of about five orders of magnitude. Above the Neel point in V_6O_{13} , the effective magnetic moment per paramagnetic vanadium atom is either 2.13 B.M. (437) or 1.95 B.M. (318) compared with either 2.16 B.M. (437) or 3.10 B.M. (318) for VO_2 above its Neel point. The very large divergence between these results, not to mention the difficulty in interpreting effective magnetic moments for substances having very large Weiss constants, makes it unprofitable to consider their significance any further. That the phase is paramagnetic and the conductivity low seem to indicate that in the ground state the valences are trapped. Alternative valence structures, $\text{V}_4^{\text{V}}\text{V}_2^{\text{III}}\text{O}_{13}$ or $\text{V}_2^{\text{V}}\text{V}_4^{\text{IV}}\text{O}_{13}$, can be written, in both of which the two valence states are present in the stoichiometric ratio 2:1. A closer examination of Aebi's structure shows that there are indeed two types of metal ion sites present in this ratio, and Gillis' view (276) of the structural relationship with V_2O_5 leads to the conclusion that the minority sites are most likely to be occupied by the pentavalent ions. A neutron diffraction study of the magnetic ordering in this lattice would be of great value.

In the phase region labeled α by Klemm (370), a series of more accurate X-ray studies (13, 14, 18) has revealed the existence of a homologous series of Magneli shear phases, $\text{V}_n\text{O}_{2n-1}$, isostructural with the titanium-

(III,IV) series based on the rutile and corundum structures. Members of the series with $4 \leq n \leq 8$ have been identified. The two magnetic studies (318, 437) again disagree on the precise effective moments of these compounds, but agree that they lie in the range 2–3 B.M. and that all except V_6O_{11} and V_7O_{13} are antiferromagnetic, with Neel temperatures

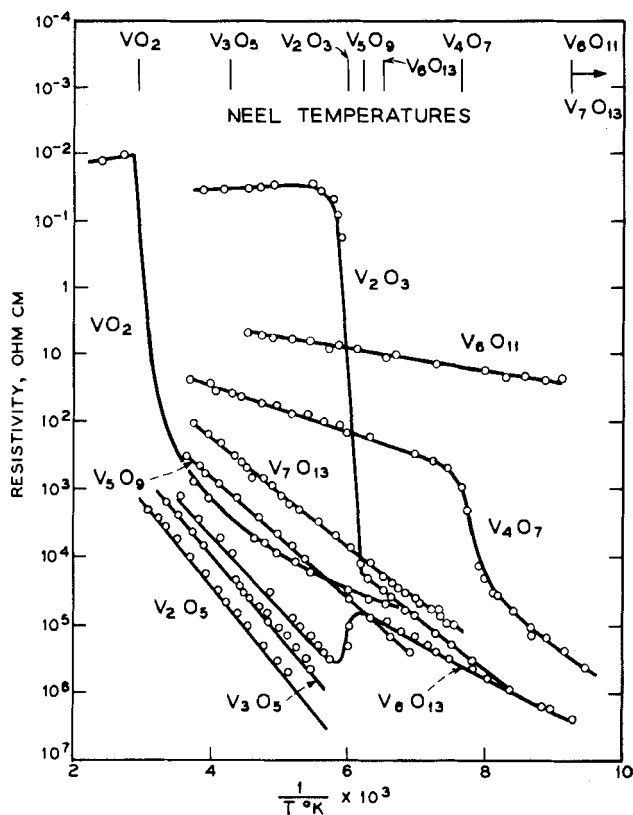
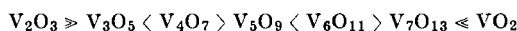


FIG. 6. The Neel temperatures and resistivity-temperature curves of various vanadium oxides (402).

somewhat lower than that of VO_2 . The two exceptions remained paramagnetic down to the lowest temperatures studied ($90^\circ K$). The compounds, which are all blue-black (13), behave as semiconductors, although with widely and apparently randomly varying resistivities and activation energies (402), as shown in Fig. 6. On feature apparent from this figure is that, among the mixed valence phases below their Neel temperatures, only V_4O_7 has a conductivity more than one order of magnitude greater than the single valence compounds V_2O_3 and VO_2 below their

Neel temperatures. Furthermore, at temperatures above their magnetic transitions, none of the mixed valence compounds conducts better than either V_2O_3 or VO_2 , although at all temperatures they all conduct better than V_2O_5 . It is therefore safe to say that, even when their spins are disordered, these remain class II systems. A further mysterious feature of the resistivity results is that, although one of the Magneli phases (V_4O_7) does undergo a discontinuous resistivity change at the Neel temperature, V_5O_9 shows no change in resistivity with magnetic ordering. Possibly this is connected with the fact that, for a given temperature above the Neel points of all the Magneli phases, there is a very marked alternation in conductivity with increasing size of the rutile-like slabs:



Clearly this interesting system deserves a very careful study.

There exist a number of V(IV), V(V) minerals, usually designated by the blanket term "vanadyl vanadates." The unit cell dimensions of several have been reported (601), but no other detailed structural or physical data are available.

The lower mixed valence oxides of vanadium have been of greater interest to metallurgists than to chemists. Oxygen dissolves interstitially in vanadium, yielding a number of different phases up to $VO_{0.57}$ (see Stringer (692) for a review). Vanadium monoxide is stable over a wide range of composition, since defects can occur at either cation or anion sites (13, 35, 641). Although stoichiometric VO has been shown to undergo a semiconductor-metal transition (35) at the Neel point, as do V_2O_3 and VO_2 , no physical properties of nonstoichiometric samples have been reported.

There exist two series of alkali metal vanadium bronzes with the general formulas $A_xV_2O_5$ and $A_xV_3O_8$, the structures of which have been determined by Wadsley (736, 737). Both contain double strings of octahedra sharing edges, and strings of octahedra distorted so much that they might almost be regarded as trigonal bipyramids. Since the formulas of the bronzes are continuously variable over wide limits, these two types of coordination can hardly correspond to the distribution of the valences in a class I or class II system, although in the compound LiV_2O_5 , where there are equal numbers of V(IV) and V(V) ions, this may well be the case. The latter compound contains two types of vanadium site (267), around one of which the oxygens approach more closely than around the other. LiV_2O_5 is also said to be blue, the characteristic color of V(IV) surrounded by oxygen atoms, so that there may be a smaller degree of mixed valence interaction in this class II compound than in the other bronzes. The first electrical measurements on the vanadium bronzes were made by

Flood (253), but more recently Ozerov (554) and Sienko (661) have studied these compounds. Ozerov found that, at room temperature, single crystals of $\text{Na}_{0.33}\text{V}_2\text{O}_5$ in the form of black needles showed very anisotropic resistivity, ρ being 0.046 ohm cm along and 20 ohm cm perpendicular to the needle axis. When measured between 400° and 600°C a compressed pellet of the same material behaved as a semiconductor, not a metal like the tungsten bronzes of comparable sodium content. Sienko also reports that $\text{Na}_{0.33}\text{V}_2\text{O}_5$ is a semiconductor, but with a room temperature resistivity and activation energy much lower than Ozerov's. The compound's magnetic susceptibility at room temperature is an order of magnitude higher than that of any sodium tungsten bronze, and actually agrees with expectation for a full spin-only contribution from the appropriate number of trapped V(IV), $3d^1$ ions. As in the tungsten bronzes, there is no detectable Knight shift in the ^7Li or ^{23}Na NMR spectra (273), so the mixed valence electrons are confined to the vanadium-oxygen framework. Since the observed g factors in the ESR spectra (1.96) are close to that reported for V(IV) in other compounds, we may confidently describe the vanadium bronzes as weakly trapped class II systems. Unfortunately, no hyperfine lines due to electron coupling with the ^{51}V nuclei could be detected in the ESR spectra.

The mixed valence vanadium oxide whose electronic structure is known in greatest detail is probably the black crystalline hydrate first prepared by Glemser (283) by reducing a suspension of V_2O_5 in concentrated ammonium chloride solution with zinc for several hours. Glemser gave the compound, which has an effective vanadium oxidation state of 4.66, the formula $\text{V}_3\text{O}_5(\text{OH})_4$, but a careful reexamination of the preparation under a variety of conditions suggested (59) that it should rather be written $\text{V}_6\text{O}_{20}\text{H}_{12}$. An X-ray powder photograph was compatible with a tetragonal unit cell. The electronic structure of this compound has recently been the subject of some magnetic studies (60, 701). First the intensity of the ESR spectrum of a powdered sample was measured as a function of temperature and shown to obey Curie's law between -150° and +300°C. Thus by comparison with a sample of diphenylpicrylhydrazyl, the concentration of paramagnetic centers could be calculated and compared with that expected from the formula if the compound contained two V(IV) ($3d^1$) and four V(V) ($3d^0$) ions per mole. The agreement was excellent ($n_{\text{obs}} = 1.4 \times 10^{18}$ spins/mg, $n_{\text{calc}} = 1.9 \times 10^{18}$ spins/mg). Assuming that the V(IV) ion lies in a field of tetragonal symmetry with $dx y(b_2)$ lowest in energy, the observed g values (1.970 and 1.920) could be fitted by excitation energies $E_e(dxzdyz) - E_{b_2}(dxy)$ and $E_{b_1}(dx^2 - y^2) - E_{b_2}(dxy)$ of 10,000 cm^{-1} and 15,000 cm^{-1} ,

respectively, if the vanadium spin-orbit coupling constant was taken as 150 cm^{-1} . Hence the relative ordering of the $3d$ orbitals of the V(IV) ions is $b_2 < e < b_1 < a_1$, suggesting a tetragonally compressed octahedral environment. The spin-spin and spin-lattice relaxation times (t_2 and t_1) of the ESR signal in Glemser's oxide were measured by two independent methods, one involving rapid modulation and the other progressive saturation of the signal. The two methods agreed that t_2 is virtually invariant with temperature, and that t_1 varies only a little, both being in the region of 10^{-7} sec. Theobald (701) assumed that exchange played the dominant part in the relaxation processes, and, from the line width of the signal, calculated that the exchange integral J was large enough (3000 MHz) to act as a thermostat so that t_1 did not vary with temperature, and was close to t_2 . As a result of these experiments we therefore have the beginnings of a very satisfying view of the class II mixed valence interaction in Glemser's hydrate, but without a complete structure determination there is little more to be said at this stage. One point of great interest in relation to the role of water in mixed valence interactions (see subsection E on iron) is Theobald's statement (701) that the exchange interaction in other anhydrous vanadium(IV,V) oxides is almost zero.

Glemser's compound is probably a hydrate of one of the reduced isopolyvanadic acids. Further examples were prepared and their formulas characterized by Ostrowetsky (549, 550) in a comprehensive survey of the mixed valence chemistry of V(IV) and V(V) in acid and alkaline solutions. Above pH 10, no mixed valence absorption could be detected but, between pH 7 and 10, spectrophotometry revealed the existence of a single polyanion which was isolated as a dark gray-green sodium salt, $\text{Na}_3[\text{V}_6\text{O}_{15}\text{H}]\cdot 6\text{H}_2\text{O}$. In weakly acid solutions, six polyanions corresponding to varying degrees of reduction of $[\text{V}_{10}^{\text{V}}\text{O}_{28}]^{6-}$ were identified, although only two, formulated by Ostrowetsky as $[\text{V}_7^{\text{V}}\text{V}_3^{\text{IV}}\text{O}_{26}\text{H}]^{4-}$ and $[\text{V}_3^{\text{V}}\text{V}_7^{\text{IV}}\text{O}_{24}\text{H}]^{4-}$, are at all stable. Since these anions almost certainly retain the $\text{V}_{10}\text{O}_{28}$ skeleton, whose structure was determined by Evans (227), they are probably better written as $[\text{V}_{10}\text{O}_{28}\text{H}_5]^{4-}$ and $[\text{V}_{10}\text{O}_{28}\text{H}_4]^{4-}$. The others, which have $\text{V(V)}/\text{V(IV)}$ ratios of 8/2, 6/4, 5/5, and 4/6, are formed only within very narrow ranges of pH, temperature, and concentration, and readily disproportionate into $[\text{V}_{10}^{\text{V}}\text{O}_{28}\text{H}_2]^{4-}$ and $[\text{V}^{\text{IV}}\text{O}]^{2+}$ or into mixtures of either of the latter and the 7/3 and 3/7 compound, according to their composition. The spectra of all these compounds, which vary in a most interesting way with degree of reduction, are collected in Fig. 7. Excepting the 5/5 and 4/6 compounds, they all have absorption maxima in the $13,000\text{--}20,000\text{ cm}^{-1}$ region. In energy and width, these bands resemble the ligand field bands of vanadium(IV),

but, because they are at least an order of magnitude more intense, should probably be assigned as mixed valence absorptions. Their significance is not likely to become apparent until more is known of the structures of

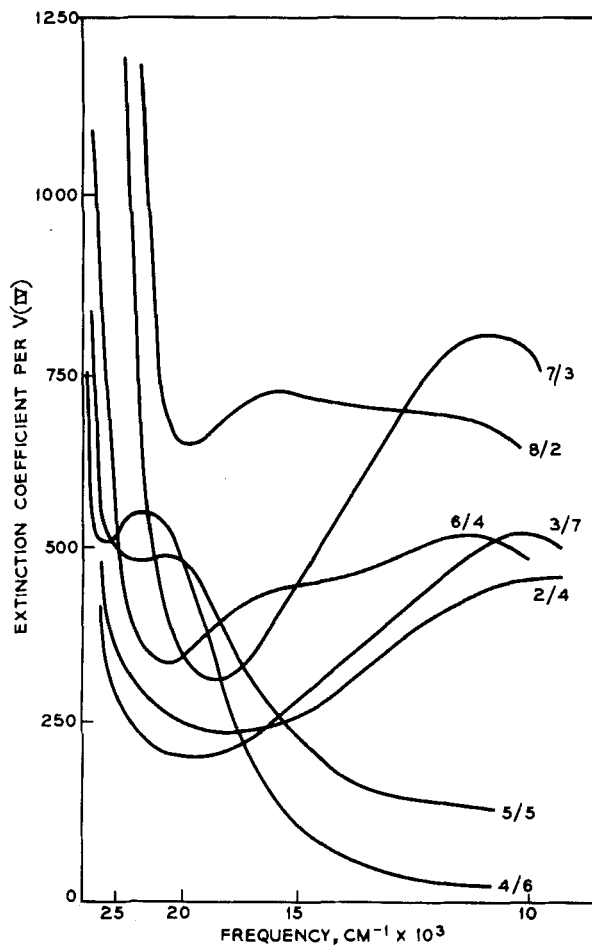


FIG. 7. Electronic spectra of the isopolyvanadate ions $[V_{10}O_{28}]^{n-}$ of various $V(V)/V(IV)$ ratios (550).

the polyanions. In particular, we have no information at this stage on whether the valences are trapped by distortion of the appropriate number of vanadium sites or, indeed, whether some are class II and others class III-A, except for the two compounds with no intense low-energy absorption, which must surely be class I. The low molar extinction coefficients of the mixed valence absorption bands in all cases indicate a

rather firm trapping of the valence. ESR measurements on glassy solutions would certainly help to decide the question. Another intriguing question is the exceptional stability of the 7/3 and 3/7 anions, for which the structure (227) of the parent ion $[V_{10}O_{28}]^{6-}$ suggests no obvious explanation.

The only other vanadium species detected in solution, which might be mixed valence, appears as an intermediate in the reaction between V(II) and V(IV) in acid perchlorate solutions (530). A dark color, which developed much more rapidly than the rate of the overall reaction to produce V(III), was shown to be due to the formation of the ion $[VOV]^{4+}$, identified by the author as a hydrolytic dimer of V(III). However, the intensity of the absorption (ϵ_{\max} calculated as 6800 at $23,200\text{ cm}^{-1}$) suggests that a V(II),V(IV) class II system is formed.

C. CHROMIUM

A discussion of the mixed valence compounds of chromium is hampered by the fact that this element can assume integral valences from 1+ to 6+. Thus, whereas Cr_3O_8 is clearly a mixed valence compound, the formula of KCr_3O_8 , for example, could be written as either $KCr_2^{VI}Cr^{III}O_8$, $KCr^{IV}Cr^VCr^{IV}O_8$, or $KCr_3^VO_8$, for all four oxidation states, 3+, 4+, 5+, and 6+, are known for chromium. Although there are experiments (optical absorption, magnetic susceptibility, X-ray structure analysis, etc.) which will distinguish between these alternatives, they have not always been performed as yet and hence limit our discussion to the more obvious mixed valence compounds.

In contrast to titanium and vanadium, chromium forms mixed valence halides as well as oxides, two types of mixed valence chromium halide (Cr_2X_3 and Cr_2X_5) having been reported. The halides Cr_2Br_3 and Cr_2I_3 are formed as brown-black solids in the thermal degradation of the appropriate tetraphenylchromium halides, $(C_6H_5)_4CrX$ (352). Cr_2F_5 is formed as green translucent crystals from both the oxidation of CrF_2 and the incomplete reduction of CrF_3 (693). Since CrF_3 is yellow-green and CrF_2 is blue-green, and since the refractive indices of Cr_2F_5 are intermediate between those of CrF_2 and CrF_3 , there appears to be no low-lying mixed valence transition in this material. As a class I substance, Cr_2F_5 should therefore be an insulator. The crystal structure of Cr_2F_5 (Fig. 8) shows the expected trapping of the chromium valences as Cr(II) and Cr(III), for one half of the chromium ions are found at the centers of almost regular fluoride ion octahedra with an average Cr—F distance of 1.89 \AA , whereas the other half occupy tetragonally distorted octahedral sites with four Cr—F distances at $1.96\text{--}2.01\text{ \AA}$ and the remaining two

at 2.57 Å (683). That these are to be identified with Cr(III) and Cr(II) ions, respectively, follows not only from the Cr—F distances but also from the structures of CrF_3 and CrF_2 themselves, which contain, respectively, octahedrally and tetragonally coordinated chromium ions. Steinfink and Burns (683) explain that the three 3*d* electrons in the Cr(III) ion occupy nonbonding t_{2g} orbitals, but Cr(II) must place its fourth 3*d* electron in an antibonding dz^2 orbital, thereby extending the octahedron in the *z*

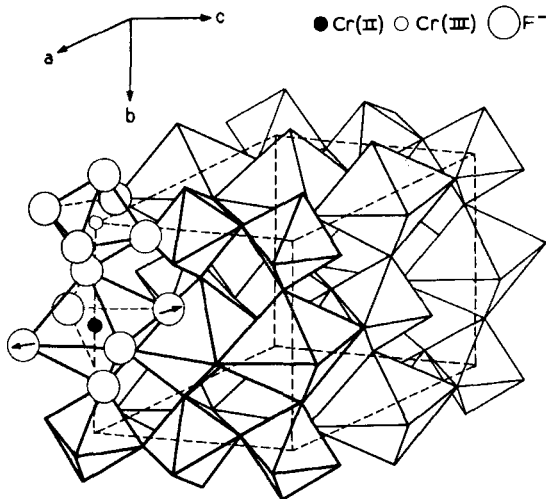


FIG. 8. The crystal structure of class I Cr_2F_5 . In this substance, the Cr(III)—F distances in a $\text{Cr}^{\text{III}}\text{F}_6$ octahedron average 1.89 ± 0.01 Å, whereas the neighboring $\text{Cr}^{\text{II}}\text{F}_6$ octahedron is distorted, as shown by the arrows, four of the Cr(II)—F distances being 1.98 Å and the other two being 2.572 Å (683).

direction. Osmond (546) suggests that, according to qualitative superexchange considerations, the chains of cations in Cr_2F_5 should be ferromagnetically aligned in the (001) direction with neighboring chains coupled antiferromagnetically, resulting in an overall antiferromagnetic ground state. There are no experimental data on this point.

The oxides of chromium present a bewildering array of possible mixed valence compounds. Extrapolating from what very little is known, one can say, in general, that the ions involved in mixed valence chromium oxides are almost always Cr(VI) and Cr(III) in appropriate ratios, and that, since Cr(VI) appears always as a tetrahedrally coordinated species whereas the $3d^3$ configuration of Cr(III) prefers octahedral coordination, the oxides will be class I systems. The discussion begins with the better known oxides and then proceeds to the more speculative materials. It should be mentioned that, although little is known of the intermediate

chromium oxides, they have a great commercial value as catalysts for the polymerization of olefins.

Suchow *et al.* (695) were the first to point out that, although the chromium in KCr_3O_8 has an average valence of 5+, their preliminary crystal structure suggests that two of the chromium ions are of one type and one of the chromiums of another, suggesting in turn the formulation of the compounds as $\text{KCr}_2^{\text{VI}}\text{Cr}^{\text{III}}\text{O}_8$ with the $\text{Cr}(\text{III})$ ions in octahedral coordination and the $\text{Cr}(\text{VI})$ in tetrahedral coordination. Wilhelmi (775, 777) confirmed this view, demonstrating that the $\text{Cr}(\text{III})$ ions are in very nearly octahedral coordination with $\text{Cr}-\text{O}$ distances averaging 1.97 Å,

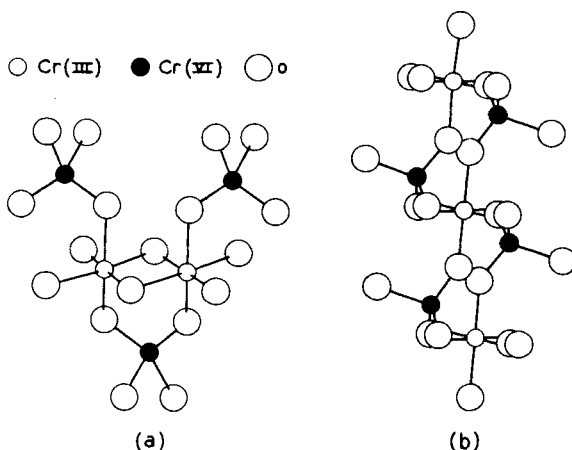


Fig. 9. The relative orientations of $\text{Cr}^{\text{VI}}\text{O}_4$ tetrahedra and $\text{Cr}^{\text{III}}\text{O}_6$ octahedra in the class I substances (a) Cr_5O_{12} , and (b) KCr_3O_8 (775, 778).

and that the $\text{Cr}(\text{VI})$ ions are surrounded tetrahedrally by oxide ions at an average distance of 1.60 Å, as in Fig. 9. Klemm (428) pointed out that the question of the chromium valences in KCr_3O_8 might also be answered by a measurement of the magnetic susceptibility, for magnetically dilute $\text{KCr}_3^{\text{VI}}\text{O}_8$ would have an effective moment of 3.00 B.M., whereas $\text{KCr}_2^{\text{VI}}\text{Cr}^{\text{III}}\text{O}_8$ would have an effective moment of 3.87 B.M. His measurements yield an effective magnetic moment for KCr_3O_8 which varies from 4.09 to 4.36 B.M. over the temperature range 90°–295°K. Applying a correction for temperature-independent paramagnetism gives an upper limit of 3.97–4.23 B.M., which does not disagree with that expected for the $\text{Cr}(\text{III}), \text{Cr}(\text{VI})$ mixed valence formulation of KCr_3O_8 . The material is black and said to have a very high electrical resistivity (777). Wilhelmi (779) reports that the lithium and cesium salts of HCr_3O_8 similarly

contain octahedral $\text{Cr}^{\text{III}}\text{O}_6$ and tetrahedral $\text{Cr}^{\text{VI}}\text{O}_4$ groups sharing corners.

The alkaline earth chromium oxides, $\text{M}_3^{\text{II}}\text{Cr}_2\text{O}_8$, form another class of compounds in which the chromium has an average valence of 5+. Alternatively, one can write a mixed valence formula for the compound, $\text{M}_3^{\text{II}}\text{Cr}_4^{\text{IV}}\text{Cr}_2^{\text{III}}\text{O}_{24}$, which has a Cr(VI)/Cr(III) ratio of 2, as in KCr_3O_8 . Surprisingly, the evidence seems to be in favor of the single valence formulation, for not only do Ford and co-workers (256–258) and others (278) point out that $\text{Ca}_3\text{Cr}_2\text{O}_8$ has a powder pattern very much like that of $\text{Ca}_3(\text{P}^{\text{VO}}_4)_2$, but Klemm (640) finds an effective moment of 1.7 B.M. per chromium ion in $\text{Ba}_3\text{Cr}_2\text{O}_8$, where the pentavalent formula requires 1.73 B.M. and the mixed valence formula requires 2.24 B.M. Ford *et al.* and Vasenin (723) also describe the preparation of the oxides $\text{Ca}_2\text{Cr}_2\text{O}_7$, CaCr_2O_5 , $\text{Ca}_4\text{Cr}_3\text{O}_{10}$, and $\text{Ca}_6\text{Cr}_4\text{O}_{15}$, the last three of which are green, as is also $\text{Ca}_3\text{Cr}_2\text{O}_8$. Only a combination of optical, magnetic, and X-ray studies can settle the question of the chromium valence in these compounds.

Bashilova's (45) thallium chromate $\text{Tl}_2\text{Cr}_2\text{O}_8$, if taken as a salt of $\text{Tl}(\text{III})$, is analogous to the calcium salt mentioned above, for it can be written as either $\text{Tl}_2^{\text{II}}\text{Cr}_2^{\text{V}}\text{O}_8$ or $\text{Tl}_6^{\text{I}}\text{Cr}_4^{\text{VI}}\text{Cr}_2^{\text{III}}\text{O}_{24}$. Bashilova, however, maintains that it is the thallium mixed valence oxide, $\text{Tl}^{\text{I}}\text{Tl}^{\text{III}}\text{Cr}_2^{\text{VI}}\text{O}_8$. The latter formulation would be diamagnetic, whereas the other two would have effective magnetic moments of 1.73 B.M. and 2.24 B.M., depending on whether the chromium is, respectively, Cr(V) or Cr(III), Cr(VI).

Because of the difficulty of preparing pure intermediate chromium oxides, it seems probable that, of the large number of different anhydrous chromium oxides reported in the literature, a significant fraction will prove to be mixtures, or are in fact the same compound masquerading under different stoichiometries. The list of intermediate chromium oxides encompasses the following: Cr_2O_5 , Cr_3O_4 , Cr_3O_5 , Cr_3O_8 , Cr_4O_9 , Cr_5O_9 , Cr_5O_{12} , Cr_5O_{13} , Cr_5O_{19} , Cr_6O_{15} , Cr_7O_{18} , Cr_8O_{15} , Cr_8O_{21} , and $\text{Cr}_{32}\text{O}_{93}$, in addition to many "nonstoichiometric" materials of the formula CrO_x , which are not easily expressed as small whole number ratios of chromium and oxygen.

The materials described by Schwartz *et al.* (647) as Cr_3O_8 , and by Simon and Schmidt (664) as Cr_5O_{13} , are crystallographically identical, according to later work by Glemser and co-workers (281, 282), who feel that the formula Cr_5O_{13} better fits their analytical data. Cr_5O_{13} , as prepared by the thermal decomposition of CrO_3 , is a black substance and has a magnetic susceptibility consonant with the mixed valence description $\text{Cr}_3^{\text{VI}}\text{Cr}_2^{\text{IV}}\text{O}_{13}$ (8), although it has been said that its ESR

spectrum is characteristic of the Cr(III) ion (596). Rode *et al.* (596) first proposed that Cr_5O_{13} was really Cr_8O_{21} , and later work by Lorthioir and Michel (468) has confirmed Cr_8O_{21} as a product of the thermal decomposition of CrO_3 . According to their study, Cr_8O_{21} in water gives Cr(III) and Cr(VI) ions in 1:3 ratio, and has a magnetic susceptibility compatible with its formation as $\text{Cr}_2^{III}\text{Cr}_6^{\text{VI}}\text{O}_{21}$.

Cr_5O_{12} , also reported as Cr_2O_5 (281), is one of the few chromium oxides for which a crystal structure has been determined. Wilhelmi (778) found that Cr_5O_{12} contains structural units much like those found in KCr_3O_8 , i.e., octahedrally coordinated Cr(III) ions sharing ligands with tetrahedrally coordinated Cr(VI) ions. The structure is built up of Cr_5O_{18} units (Fig. 9), in which the Cr(VI)—O distances in the tetrahedral sites are 1.65 Å on the average, and the Cr(III)—O distances in the octahedral sites average 1.97 Å, as was found in KCr_3O_8 . Although this oxide is black, possibly suggesting a class II spectrum, its electrical resistivity is reported to be 1.78×10^{10} ohm cm at 360°C and 72 atm oxygen (446), as expected from the class I crystal structure. Cr_5O_{12} is ferromagnetic, with a Curie point at about 80°C (597), above which it shows an ESR signal attributable to the Cr(III) ion (596). An apparently related hydrated oxide, $\text{Cr}_5\text{O}_{12} \cdot 3\text{H}_2\text{O}$, is formed as a brown precipitate on mixing a solution of $\text{Cr}^{\text{III}}\text{Cl}_3$ with $\text{Ag}_2\text{Cr}^{\text{VI}}\text{O}_4$ (292).

Chromium dioxide, CrO_2 , presents a rather curious picture of conflicting claims, for, although CrO_2 has been said not to have a homogeneity region and to be quite stoichiometric (22, 647), materials ranging from $\text{CrO}_{1.89}$ (133) to $\text{CrO}_{2.14}$ (776) have been described in the literature as " CrO_2 ." Moreover, whereas Chapin *et al.* (776) have studied the electrical conductivities of samples in the range $\text{CrO}_{1.89}$ – $\text{CrO}_{2.02}$ and explained their quasi-metallic nature (ρ is approximately 3×10^{-3} ohm cm) on the basis of a *d*-band model involving Cr(IV) ions, Kubota (446) claims that the extraordinary conductivity results from the presence of Cr(III) and Cr(IV) ions in the rutile crystal lattice. In support of the mixed valence formulation, Rode *et al.* (596) interpret the ESR spectrum of CrO_2 above its Curie point (119°C) as showing that the oxide is a Cr(III),Cr(VI) compound. The saturation magnetization of CrO_2 at 0°K yields an effective moment of 2.07 B.M. per chromium atom (325), whereas Cr(IV) is expected to have an effective moment of 2.83 B.M. The decision as to whether CrO_2 is a mixed valence oxide or simply contains Cr(IV) clearly cannot be made without further physical measurements.

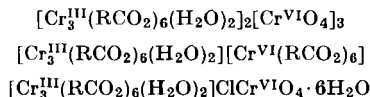
The hydrated material formed by mixing an aqueous solution containing Cr(III) with one containing $[\text{Cr}^{\text{VI}}\text{O}_4]^{2-}$ presents a situation related to that discussed above for CrO_2 . According to King and Neptune (423),

the mixing of Cr(III) and $[\text{Cr}^{\text{VI}}\text{O}_4]^{2-}$ in acidic solution leads to the formation of a 1 : 1 complex ion, $[\text{Cr}^{\text{II}}\text{Cr}^{\text{VI}}\text{O}_4]^+$, probably with sharing of oxo and/or hydroxyl ligands. Interestingly, the stoichiometry of this complex was determined, using its interaction absorption band at $14,300\text{ cm}^{-1}$, thereby showing that a class II absorption can occur in a Cr(III),Cr(VI) system. Krauss and Gnatz (440) confirmed the 1 : 1 nature of this complex by a conductivity titration, but also showed that the precipitate from the solution has the composition $\text{H}_4\text{Cr}_3\text{O}_8 \cdot x\text{H}_2\text{O}$ (x is continuously variable), which can be formulated as either $\text{H}_4\text{Cr}_3^{\text{IV}}\text{O}_8 \cdot x\text{H}_2\text{O}$ or $\text{H}_4\text{Cr}_2^{\text{III}}\text{Cr}^{\text{VI}}\text{O}_8 \cdot x\text{H}_2\text{O}$. Aten *et al.* (32) showed conclusively that the latter formulation is the proper one by mixing a solution of radioactive Cr(III) with inactive $[\text{Cr}^{\text{VI}}\text{O}_4]^{2-}$ ion, dissolving the $\text{H}_4\text{Cr}_3\text{O}_8$ so formed, and precipitating and counting the $[\text{CrO}_4]^{2-}$ as PbCrO_4 . As the PbCrO_4 showed less than 1 % of the original activity, it is clear that the two types of chromium in this substance at no time were equivalent as they would be if they were all Cr(IV). Formulations of $\text{H}_4\text{Cr}_3\text{O}_8 \cdot x\text{H}_2\text{O}$ as a compound of Cr(IV) also demands an effective magnetic moment of 2.83 B.M. per chromium, whereas the calculated effective moment of the mixed valence compound is 3.16 B.M., in excellent agreement with the experimental value of 3.15 B.M. (440). The same dark brown material forms at the cathode on electrolysis of a 25 % solution of CrO_3 in HClO_4 (450).

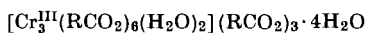
Sisler and co-workers (201, 669) have shown that liquid ammonia will partially reduce CrO_3 to a mixture containing, among other things, the brown polymeric materials $[\text{Cr}^{\text{III}}(\text{NH}_3)_3]_{2n}(\text{Cr}^{\text{VI}}\text{O}_4)_{3n}$ and $[\text{Cr}^{\text{III}}(\text{NH}_3)_3\text{NO}_2\text{Cr}^{\text{VI}}\text{O}_4]_n$, both of which are postulated to be class I systems with the Cr(III) ions in octahedral and the Cr(VI) ions in tetrahedral coordination, the two being joined by oxo bridges.

The thermal decomposition of chromyl chloride, $\text{Cr}^{\text{VI}}\text{O}_2\text{Cl}_2$, leads to the formation of a number of polychromyl chlorides having the general formula $(\text{CrO}_2)_n\text{Cl}_2$, where n is equal to 3, 4, 5, or 7 (479). Although a mixed valence formula for these substances can be written $(\text{Cr}^{\text{VI}}\text{Cr}_{n-1}^{\text{IV}}\text{O}_{2n}\text{Cl}_2)$, little is known of their physical properties, other than that they are brown-black in color and sensitive to moisture.

The formates and acetates of chromium offer further examples of class I mixed valence systems. Trivalent chromium forms a very stable trinuclear cationic species having the general formula $[\text{Cr}_3^{\text{III}}(\text{RCO}_2)_6(\text{H}_2\text{O})_2]^{3+}$, where RCO_2^- is an acetate or formate anion. Combinations of this trinuclear cation with chromium-containing anions yield salts (292), such as:



That the above are class I systems seems evident from the fact that they are all green, the color of the single valence compound:



Recoura (579) reports the preparation of the dark brown sulfates $\text{K}_{2n}\text{Cr}_2^{\text{III}}(\text{Cr}^{\text{VI}}\text{O}_4)_n(\text{SO}_4)_3$, where $n = 1, 2$, and 3 . They are also most likely class I systems.

D. MANGANESE

As with most of the other elements of the first transition series, the most important examples of mixed valence in manganese compounds involve oxide lattices. At one time it was suggested (208a) that there existed a continuous series of oxides with formulas intermediate between MnO and MnO_2 , of which no less than eleven had been reported between 1862 and 1907! Very few of these nonstoichiometric oxides have survived the passage of time and closer scrutiny, and we shall therefore concentrate attention only on those based on stoichiometric phases. Of the latter, Mn_3O_4 , the mineral haussmannite, is the best known. When heated in air to 1000°C , all manganese oxides and hydroxides are converted to Mn_3O_4 , which forms as black crystals with a metallic sheen, or as a dark red powder when finally divided. Its electrical conductivity was studied many years ago (181, 731), using compressed pellets. Although behaving as a semiconductor, the fact that it is much less conducting than Fe_3O_4 at room temperature led de Boer and Verwey (181) to suggest that it was a normal spinel, $^2\text{Mn}^{\text{IV}}\text{Mn}_2^{\text{II}}\text{O}_4$ or $\text{Mn}^{\text{II}}\text{Mn}_2^{\text{III}}\text{O}_4$, and not of the inverse type $\text{Mn}^{\text{II}}(\text{Mn}^{\text{II}}, \text{Mn}^{\text{IV}})\text{O}_4$ or $\text{Mn}^{\text{III}}(\text{Mn}^{\text{II}}, \text{Mn}^{\text{III}})\text{O}_4$. This conclusion has been confirmed, but disagreement continues as to the valence structure of the compound. A recent magnetic susceptibility study (569) showed that, between 90° and 800°C , the susceptibility followed a Neel hyperbola, but below the Curie point it was consistent with a ferromagnetic model for an $\text{Mn}(\text{II}), \text{Mn}(\text{IV})$ normal spinel. On the other hand, the observed intensities of neutrons diffracted by powdered specimens at 4.2° , 77° , and 298°K (404) agree very well with those calculated for a model based on $\text{Mn}^{\text{II}}\text{Mn}_2^{\text{III}}\text{O}_4$. The latter results are probably the more reliable.

² A spinel compound has the formula AB_2O_4 and a lattice containing octahedral and tetrahedral cation sites in the ratio 2:1. In a normal spinel the B cations occupy the octahedral sites and the A the tetrahedral, whereas in an inverted spinel the tetrahedral sites are exclusively occupied by B cations so that the octahedral sites are occupied by equal numbers of A and B cations (see Fig. 16).

In a number of other instances, different methods of estimating the valence distributions in manganese oxides also appear to yield differing results. For example, X-ray analysis showed that the structure of manganite (γ - MnOOH) was based on sheets of O^{2-} and OH^- ions enclosing trivalent manganese ions (112, 237), but measurements of magnetic anisotropy appear to suggest that half of the manganese is divalent and half quadrivalent. Also the crystal structure of the mineral bixbyite (α - Mn_2O_3) agrees with a trivalent formulation (563), but it has been stated that chemical decomposition leads to divalent and quadrivalent ions (264). The latter result is of doubtful importance, however, when one considers the ease with which Mn(III) disproportionates in aqueous solution.

Another stoichiometric manganese oxide phase, which seems to have been fully characterized, has the formula Mn_5O_8 . The X-ray diagram of the black powder indexes as monoclinic (551) with unit cell dimensions very similar to those of $\text{Cd}_2\text{Mn}_3\text{O}_8$, and approximate structure factor calculations show that the two compounds are isotypic. Thus the valence structure of Mn_5O_8 is clearly $\text{Mn}_2^{\text{II}}\text{Mn}_3^{\text{IV}}\text{O}_8$, and the compound belongs to either class I or class II.

In common with a number of other first series transition metals, mixed valence manganese oxide systems based on perovskite lattices may be prepared with formulas intermediate between $\text{M}^{\text{III}}\text{Mn}^{\text{III}}\text{O}_3$ and $\text{M}^{\text{II}}\text{Mn}^{\text{IV}}\text{O}_3$, where the trivalent metal is commonly lanthanum and the divalent metal is one of the alkaline earths. The magnetic (392) and electrical (722) properties of these compounds have been the subject of extensive study over the past 15 years. They are all ferromagnetic, but their Curie temperatures are very strongly dependent on composition, with maxima in the region 25–40% M(II) (392). Values of the saturation magnetization as a function of composition also showed that, over the same region of composition, all the $3d$ electrons contribute their full spin moments, although without appreciable orbital contribution. The form of the relationship between magnetization and composition can be understood qualitatively if one assumes that the $\text{Mn(III)}\text{--Mn(III)}$ interaction is almost zero (very low Curie temperature), and that there is a very strong $\text{Mn(III)}\text{--Mn(IV)}$ magnetic interaction with a positive exchange integral raising the Curie temperature with increasing Mn(IV) concentration. Finally, to explain the asymmetrical position of the maximum magnetization with respect to composition, it is necessary to assume a somewhat weaker negative interaction between Mn(IV) and Mn(IV) . Elegant confirmation of this picture was obtained by Wollan and Koehler (791) from neutron diffraction experiments on $(\text{La}_{1-x}\text{Ca}_x)\text{MnO}_3$. They found that the phase is purely ferromagnetic only over a small range of

composition near $x = 0.35$, and that, from 0 to 0.25 and from 0.40 to 0.50, ferromagnetic and antiferromagnetic interactions were simultaneously present. Thus LaMnO_3 is ferromagnetic along all three axes. In the mixed valence phases many different kinds of spin superlattice are built up, according to the distribution of manganese valence in the lattice. Some of the possibilities are shown in Fig. 10. To explain the occurrence of these superlattices, Goodenough (295) used a valence bond model in which the Mn(III) ions have dsp^2 (square) and the Mn(IV) ions have

LABEL	ONE OCTANT OF MAGNETIC UNIT CELL	IONS PER UNIT CELL				
		$\text{Mn}^{+3} \rightarrow 8$	6	4	2	0
		$\text{Mn}^{+4} \rightarrow 0$	2	4	6	8
A						
B						
F						

FIG. 10. Some of the possible spin superlattices in mixed valence calcium lanthanum manganese perovskites (791).

d^2sp^3 (octahedral) hybridization, and invoked a concept called "semi-covalence." This is equivalent to saying that electron transfer from a filled anion p orbital to an unfilled cation d orbital occurs with greater probability for an electron having the same spin as those already occupying the d -shell of the cation. Similarly, electron transfer from the lower-valent cation to the oxidized anion will align their spins, thus resulting in a net coupling of the spins of the two mixed valence cations, as described more fully in Section II.

Since all the manganese ions of $(\text{La}_{1-x}\text{Ca}_x)\text{MnO}_3$ are in equivalent sites in the perovskite lattice, the series of compounds is class III-B and should have metallic resistivities. This is confirmed by the work of van Santen and Jonker (722), who found a minimal resistivity of 3×10^{-2} ohm cm at 100°K for samples of $(\text{La}_{1-x}\text{Sr}_x)\text{MnO}_3$ having x between 0.2 and 0.4.

It has been suggested (667) that CuMn_2O_4 has a normal rather than an inverse spinel structure, because the valence distribution is $\text{Cu}^{\text{I}}(\text{Mn}^{\text{III}}, \text{Mn}^{\text{IV}})\text{O}$ rather than $\text{Cu}^{\text{II}}\text{Mn}_2^{\text{III}}\text{O}_4$, which requires that $\text{Cu}(\text{II})$ occupy a tetrahedral site in preference to $\text{Mn}(\text{III})$. In the absence of resistivity measurements, which would readily distinguish between the two valence distributions, it is not possible to comment further on this interesting suggestion. The structure of another $\text{Mn}(\text{III}), \text{Mn}(\text{IV})$ oxide, $\text{DyMn}^{\text{III}}\text{Mn}^{\text{IV}}\text{O}_5$, has been deduced by Abrahams and Bernstein (1a) as being class I, with $\text{Mn}(\text{III})$ in penta-coordination and $\text{Mn}(\text{IV})$ in octahedral coordination. As expected from its class I structure, $\text{DyMn}^{\text{III}}\text{Mn}^{\text{IV}}\text{O}_5$ has a resistivity of 10^{10} ohm cm at room temperature.

Unlike the $\text{Mn}(\text{III}), \text{Mn}(\text{IV})$ perovskites, the $\text{Mn}(\text{II}), \text{Mn}(\text{III})$ lattice in the compounds $\text{Li}_x\text{Mn}_{1-x}\text{O}$ does not show ferromagnetic ordering (386). As the lithium content is increased, the susceptibility curves change from a typically antiferromagnetic to a paramagnetic form, merely as a result of diluting the magnetic cations.

The naturally occurring minerals braunite, $\text{Mn}_7\text{SiO}_{12}$ (119), and pinakiolite, $\text{Mg}_3\text{Mn}^{\text{II}}\text{Mn}_2^{\text{III}}\text{B}_2\text{O}_{10}$ (698), are other $\text{Mn}(\text{II}), \text{Mn}(\text{III})$ compounds whose structures have been solved. The unit cell of braunite contains 48 octahedrally coordinated $\text{Mn}(\text{III})$ ions with average $\text{Mn}-\text{O}$ distances of 2.09 Å, and eight octa-coordinated $\text{Mn}(\text{II})$ ions with $\text{Mn}-\text{O}$ equal to 2.16 Å. Evidently the system is class I. Although all the manganese ions in pinakiolite are in octahedral sites, the distortions of the sites are sufficient to render the system class II.

While studying the reduction of transition metal cyanide complexes by sodium in liquid ammonia, Kleinberg and co-workers (142, 175) isolated the only mixed valence manganese compound not containing oxide as a ligand. The dark brown product of the reduction had an empirical formula $\text{K}_{11}\text{Mn}_2(\text{CN})_{12} \cdot 2\text{NH}_3$, and was thought to contain equimolar proportions of $\text{Mn}(0)$ and $\text{Mn}(\text{I})$. It was paramagnetic, with a room temperature magnetic moment of 1.25 B.M., but no further experiments were carried out on it.

E. IRON

The mixed valence compounds of iron form by far the largest group presently known for any element. This group of compounds is exceptional not only for its size, but also for its variety, for it contains oxides, hydroxides, halides, sulfates, cyanides, phosphates, carbonates, acetates, silicates, borates, and sulfites. There is also no small historical interest here, for the mixed valence iron cyanides were among the earliest

coordination compounds investigated, and a large number of the qualitative ideas presently used in thinking about mixed valence chemistry arose first in consideration of mixed valence iron compounds.

The study of mixed valence iron chemistry has recently received impetus from the discovery of the Mössbauer effect. Because the Mössbauer spectrum is potentially capable of indicating the valences of the iron ions in a solid, as well as their amounts and their coordination, its use can take one a long way towards understanding the structural elements of an iron compound [see, for example, Fluck *et al.* (254)].

The preparations of the mixed valence fluorides $\text{Fe}_2\text{F}_5 \cdot 7\text{H}_2\text{O}$, $\text{Fe}_2\text{F}_5 \cdot 3\text{H}_2\text{O}$, and the anhydrous material Fe_2F_5 have recently been reported (93). The first of these compounds, $\text{Fe}^{\text{II}}\text{Fe}^{\text{III}}\text{F}_5 \cdot 7\text{H}_2\text{O}$, is but one member of a large class of compounds of general formula $\text{M}^{\text{II}}\text{Fe}^{\text{III}}\text{F}_5 \cdot 7\text{H}_2\text{O}$. Because the Fe(II) in this compound can be replaced readily by other M(II) ions and also because of its yellow color, it appears that $\text{Fe}_2\text{F}_5 \cdot 7\text{H}_2\text{O}$ is a class I crystal which, consequently, does not involve sharing of ligands, there being just six ligands per metal ion. Because water inhibits the formation of a deep mixed valence color, it is not surprising that dehydrating the yellow heptahydrate to the trihydrate yields crystals which are deep red. Further dehydration to Fe_2F_5 yields a steel-blue compound, which by its color and stoichiometry is at least class II, and may even be class III and metallic.

Deussen (192) first showed that the colorless iron fluoride thought to be $\text{FeF}_3 \cdot 4\frac{1}{2}\text{H}_2\text{O}$ in reality was the mixed valence salt $\text{Fe}^{\text{II}}\text{Fe}_2^{\text{III}}\text{F}_8 \cdot 10\text{H}_2\text{O}$. The chlorides (451) and bromides (288) of the $\text{Fe}^{\text{II}}\text{Fe}_2^{\text{III}}\text{X}_8 \cdot 10\text{H}_2\text{O}$ systems are also known and, as expected from the large amount of water in them, are yellow in color. There also exists a reduced chloride $\text{Fe}_2^{\text{II}}\text{Fe}^{\text{III}}\text{Cl}_7 \cdot 10\text{H}_2\text{O}$ with the expected yellow color (288). In the bromide series, dehydration of $\text{Fe}_3\text{Br}_8 \cdot 10\text{H}_2\text{O}$ to the hexahydrate changes its color from yellow to black (542), indicating a transformation from class I to class II. The mixed valence bromide Fe_3Br_8 forms a number of other interesting adducts; thus, $\text{Fe}_3\text{Br}_8 \cdot (\text{CN})_2 \cdot 3\text{BrCN}$ (brown-black), $\text{Fe}_3\text{Br}_8 \cdot 4\text{BrCN}$ (dark brown), $\text{Fe}_3\text{Br}_8 \cdot 5\text{HCN}$ (black-brown), and $\text{Fe}_3\text{Br}_8 \cdot [(\text{CN})_2]_x$ are all known (542). However, since $\text{Fe}^{\text{II}}\text{Br}_3 \cdot 4\text{BrCN}$ is itself almost black, nothing can yet be said of the colors of the mixed valence adducts.

The large number of $\text{Fe}_3\text{X}_8 \cdot \text{Y}$ compounds so far described (and others, see below) at first suggests the presence of a trinuclear Fe_3X_8 species. Such a polynuclear species would necessarily be at least class II because of the shared ligands, and should have the deep color characteristic of this class. That there are no polynuclear species involved here follows from the pale colors of several of the Fe_3X_8 hydrates, and also

from the crystal structure of $\text{Fe}_3\text{Br}_8 \cdot 16\text{H}_2\text{O}$ published by Zvonkova (820). In this substance, the bromide ions and water molecules form chains of octahedra ($2\text{Br}^-, 4\text{H}_2\text{O}$) sharing corners. Three fourths of these octahedral sites are filled statistically with iron, the average Fe—Br distance being 2.60 Å and the average Fe—O distance being 2.01 Å. Although Zvonkova extrapolates from this *average* structure to the conclusion that $\text{Fe}_3\text{Br}_8 \cdot 16\text{H}_2\text{O}$ is a mixed valence class III-B system much as Fe_3O_4 (see below), more careful work will probably show that in fact the ligand-metal distances about the Fe(II) and Fe(III) ions in this compound are quite different, and that the valences are firmly trapped.

Walden (742) reports the preparation of the triple bromides $\text{KFe}_3\text{Br}_9 \cdot 3\text{H}_2\text{O}$ and $\text{RbFe}_3\text{Br}_9 \cdot 3\text{H}_2\text{O}$. As one can guess by the high proportion of iron to water in these substances, the crystals are deeply colored. Although rather unstable, the crystals of these iron bromides are deep green and opaque.

McConnell and Davidson (497) have investigated the mixed valence absorption of HCl solutions containing the Fe(II) and Fe(III) ions. As with antimony, tin, and copper, the mixtures of $\text{Fe}^{\text{II}}\text{Cl}_2$ and $\text{Fe}^{\text{III}}\text{Cl}_3$ in concentrated HCl showed an absorbance in the region 11,000–22,000 cm^{-1} , which was much greater than that measured for the sum of the FeCl_2 and FeCl_3 solutions taken separately. This enhancement of absorption was found to decrease on lowering the HCl concentration, so that, in aqueous solutions of $\text{Fe}^{\text{II}}(\text{ClO}_4)_2$ and $\text{Fe}^{\text{III}}(\text{ClO}_4)_3$, there is no noticeable mixed valence absorption. It was concluded that the mixed valence chromophore involves a chloride-containing species having equal numbers of Fe(II) and Fe(III) ions. There is a suggestive relationship between this work and electron exchange kinetic studies, in which it was found that the thermal electron transfer between Fe(II) and Fe(III) is accelerated by the presence of Cl^- ions (129). In fact, Weiss (755) quotes several such catalyzed reactions: the Cl^- -catalyzed exchange between Eu(II) and Eu(III), and the F^- -catalyzed exchange between Ce(III) and Ce(IV). It would be interesting to see if these systems show mixed valence absorption bands in solution analogous to that shown by HCl solutions of Fe(II) and Fe(III).

Hathaway and Holah (347) have found that the oxidation of elemental iron by halogens in various solvents leads to the formation of mixed valence compounds formulated as $[\text{Fe}^{\text{II}}(\text{Sol})_6][\text{Fe}^{\text{III}}\text{X}_4]_2$, where Sol is a solvent molecule and X is a halide ion. As expected from the class I geometry and the lack of shared ligands in these materials, the spectra show only the absorptions of the component ions.

The low ratio of ligand to iron in the mixed valence alkali iron carbonates $\text{M}^{\text{I}}\text{Fe}_2^{\text{II}}\text{Fe}^{\text{III}}(\text{CO}_3)_3(\text{OH})_2 \cdot \text{H}_2\text{O}$ (47, 288) demands a rather

intimate association of the ferric and ferrous ions. In accord with this, the crystals are green and their solutions in water test negative for free Fe(III).

A mixed valence iron acetate has been reported, which may be related to the carbonate described above. The acetate,

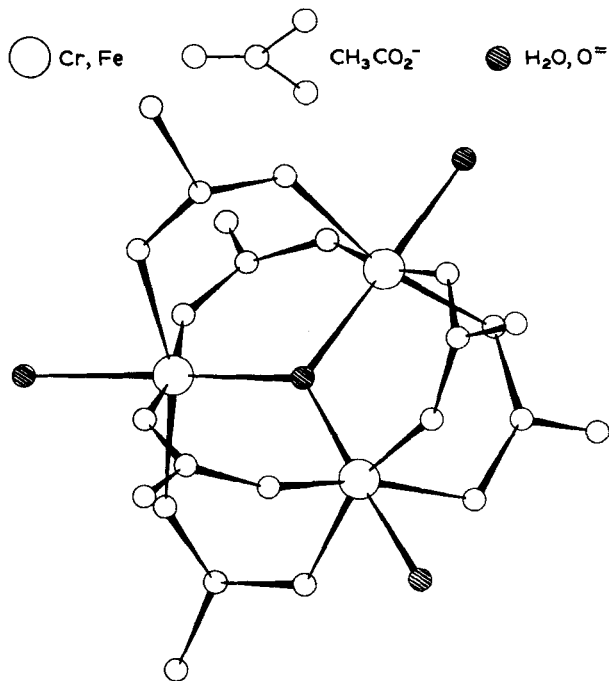
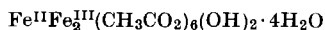
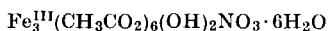


Fig. 11. The structure of the $[\text{M}_3(\text{CH}_3\text{CO}_2)_6\text{O} \cdot 3\text{H}_2\text{O}]^{n+}$ trinuclear ion.

is described as dark brown and, like the carbonate, yields a polynuclear ion in solution (141). There also exists here a possible connection with the ferric acetate with formula



which is known to involve a triangular array of Fe(III) ions in a cluster complex (Fig. 11) (251).

The mixed valence iron cyanides have been the object of constant study for over 250 years (572), a large part of their allure springing no doubt from their deep blue colors. Although it was long held that Prussian blue, made by adding Fe(III) to $[\text{Fe}^{\text{II}}(\text{CN})_6]^{4-}$, and Turnbull's

blue, made by adding Fe(II) to $[\text{Fe}^{\text{III}}(\text{CN})_6]^{3-}$, were distinct compounds, an overwhelming amount of evidence has since accumulated demonstrating that they are identical materials (66–68, 209, 225, 254, 753). We shall call this material Prussian blue. There are two kinds of Prussian blue, the first of which, soluble Prussian blue, is generally taken to be $\text{M}^{\text{I}}\text{Fe}_2(\text{CN})_6$, whereas insoluble Prussian blue is $\text{Fe}_4[\text{Fe}(\text{CN})_6]_3$. The earlier history of these “iron blues” has been reviewed by Holtzman (368).

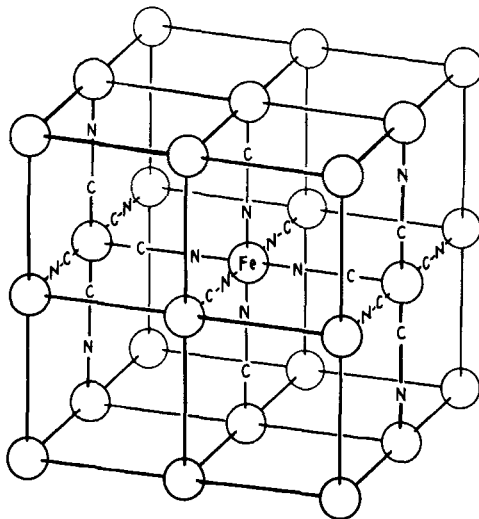


FIG. 12. The unit cell of Prussian blue-type crystals. In “soluble” Prussian blue ($\text{KFe}^{\text{III}}[\text{Fe}^{\text{II}}(\text{CN})_6]$), four potassium ions occupy octant sites and surround the body-centered ion tetrahedrally, whereas, in “insoluble” Prussian blue ($\text{Fe}_4^{\text{III}}[\text{Fe}^{\text{II}}(\text{CN})_6]_3$), hydrated Fe(III) ions are thought to occupy octant sites.

The crystal structures of soluble and insoluble Prussian blue are closely related to one another (409, 754), and to a large number of other heavy metal ferrieyanides and ferrocyanides (588, 718) having face-centered cubic lattices with iron ions at the corners of a cube and cyanide ions bridging the irons along the cube edges. The centers of the cubes are filled with charge-compensating cations, if necessary, and/or water (Fig. 12). The iron-iron distance in Prussian blue is 5.1 Å as deduced from X-ray powder pattern data, which, however, were inadequate for determining the Fe—C, C—N, or N—Fe distances. Due to the roomy caverns at the cube centers, Prussian blue-type crystals are zeolitic and act as molecular sieves with channel diameters of ca. 3.2 Å (650). This is consistent with dehydration isotherm studies, which showed that Prussian blue is not a definite hydrate (753). Since the differentiation

between the Prussian blues as "soluble" and "insoluble" stems not from any real solubility of the "soluble" material, but instead from the ease with which it can be peptized to form a colloidal dispersion, knowledge of the crystal structure of soluble Prussian blue is essential to understanding the properties of its "solutions."

Both Thompson (703) and Korshunov and Lebedeva (436) have shown that, when Prussian blue is formed from inactive Fe(III) and radioactive $[\text{Fe}^{\text{II}}(\text{CN})_6]^{4-}$ and then decomposed by base, the resulting $\text{Fe}^{\text{III}}(\text{OH})_3$ is completely inactive. This demonstrates first that the Prussian blue crystal is not class III-B, as suggested indirectly by Emeleus and Anderson (221), and also that the cyanide ions do not rotate in the crystal or become carbon-bonded to the Fe(III) ions on forming the crystal. Thus, as can be readily seen from Fig. 12, there are two varieties of octahedral site in the class II Prussian blue crystal: those coordinated by the carbon ends of the cyanide ligands, and those coordinated by the nitrogen ends of these same ligands. It has been a problem of great interest to demonstrate which iron ion valence resides in which site, i.e., are the valences in Prussian blue trapped as ferric ferrocyanide or ferrous ferricyanide?

The magnetic susceptibility of Prussian blue, as measured by Davidson and Welo (176) and by Cambi (128), is consistent with either high-spin, $3d^5$ Fe(III) ions in the nitrogen sites and low-spin, $3d^6$ Fe(II) ions in the carbon sites, or high-spin, $3d^6$ Fe(II) ions in the nitrogen sites and low-spin, $3d^5$ Fe(III) ions in the carbon sites. On the basis of oxidation-reduction potentials in aqueous solutions, Weiser *et al.* (754) argue for the latter, claiming that Prussian blue is the ferrous salt of ferricyanic acid. A flood of more direct evidence has recently shown that, in fact, Prussian blue is better considered as the ferric salt of ferrocyanic acid. Thus, for example, on the basis of the fact that the C—N stretching frequencies of various ferrocyanides fall at 2090 cm^{-1} and below, whereas the C—N stretches in ferricyanides are found at 2150 cm^{-1} and above, Emschwiller (222) demonstrated that Prussian blue contained ferrocyanide ions since the C—N stretch in this compound lies at 2080 cm^{-1} . Again, Robin (591) has interpreted the first two bands at $14,700\text{ cm}^{-1}$ and $25,000\text{ cm}^{-1}$ in the electronic spectrum of Prussian blue as being associated with the transfer of an electron from a low-spin, $3d^6$ ferrocyanide ion to a high-spin, $3d^5$ ferric ion. The most compelling evidence for the formulation of Prussian blue as ferric ferrocyanide rests on the results of the many Mössbauer spectral studies of this material. As shown in Fig. 13, the Mössbauer spectrum of soluble Prussian blue consists of a pair of lines, 2 and 3, which are identified as the quadrupole split components of the high-spin Fe(III) ion in octahedral coordination,

and the single line, 1, due to the $[\text{Fe}^{\text{II}}(\text{CN})_6]^{4-}$ ion. The ratio of the intensities of lines 2 plus 3 to line 1 is 1.0 in soluble Prussian blue and almost 4/3 in insoluble Prussian blue (209, 225, 254, 410, 591).

Because the valences are firmly trapped, one can draw an orbital diagram for Prussian blue, using the orbitals of the $\text{Fe}^{\text{II}}(\text{CN})_6$ and $\text{Fe}^{\text{III}}(\text{NC})_6$ ions taken separately (591). This is shown in Fig. 14, where the mixed valence transition responsible for the blue color of Prussian blue ($14,700\text{ cm}^{-1}$, Fig. 15) is depicted by the arrow labeled 1. According to this assignment, the ground state of Prussian blue is $\text{KFe}^{\text{III}}\text{Fe}^{\text{II}}(\text{CN})_6$,

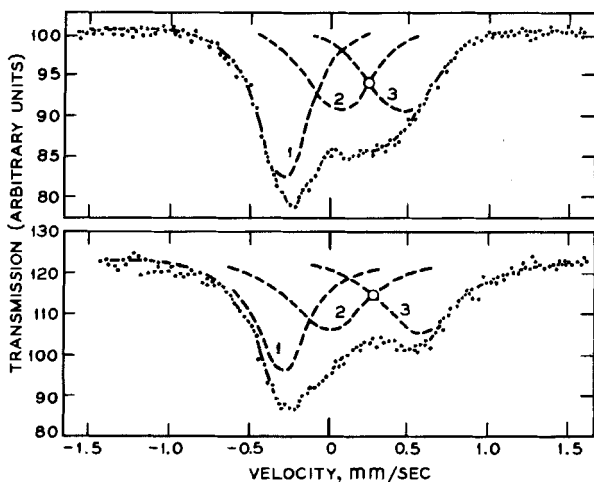


Fig. 13. The Mössbauer spectra of soluble Prussian blue ($\text{KFe}^{\text{III}}[\text{Fe}^{\text{II}}(\text{CN})_6]$), upper, and insoluble Prussian blue ($\text{Fe}_4^{\text{III}}[\text{Fe}^{\text{II}}(\text{CN})_6]_3$), lower, both at 143°K (254).

and the Turnbull's blue formulation, $\text{KFe}^{\text{II}}\text{Fe}^{\text{III}}(\text{CN})_6$, is more appropriate to the first excited state. Actually, because of configuration interaction, the system in the ground state is a mixture of the Prussian blue and Turnbull's blue configurations, in a proportion which can be estimated from the mixed valence absorption intensity. Application of Eq. (14) to the $14,700\text{ cm}^{-1}$ band of Prussian blue ($\epsilon = 9800$; $\mu = 1.23\text{ eÅ}$) yields a value of α^2 equal to 0.01, showing that the optical electron spends 99 % of its time in a carbon hole and 1 % in a nitrogen hole in the ground state.

Because Prussian blue is a class II crystal, with distinguishable oxidation states, its spectrum should contain not only the first mixed valence absorption (arrow 1), but a second band related to the first by a spectral interval in the high-spin $\text{Fe}(\text{II})$ ion, and also bands due to the $\text{Fe}(\text{III})$ and $[\text{Fe}^{\text{II}}(\text{CN})_6]^{4-}$ ions. The transition labeled 2 is assigned as the

band observed at $25,000\text{ cm}^{-1}$, for it is weak and separated from transition 1 by the $t_{2g} \rightarrow e_g$ separation ($10,000\text{ cm}^{-1}$) in the high-spin Fe(II) ion, as predicted for a class II system. The low intensity of this band follows from the fact that it is a transition between t orbitals on one center and e orbitals on another, and, according to Eq. (17), this is forbidden. The strong band in the $45,000\text{--}50,000\text{ cm}^{-1}$ region of the

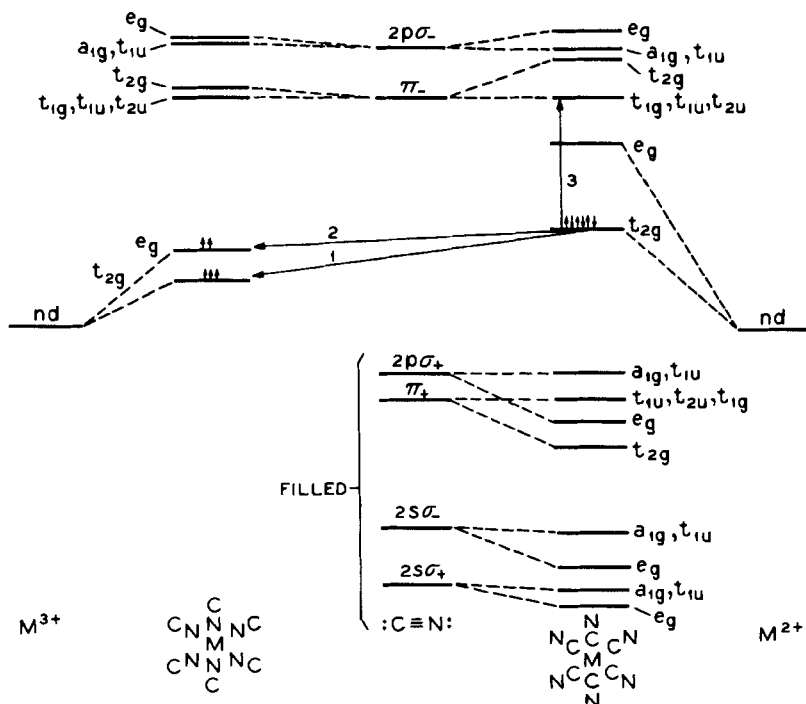


FIG. 14. A molecular orbital scheme for class II Prussian blue. The symmetry labels on any column of levels are appropriate only to the molecule listed at the foot of that column, and the transitions labeled 1, 2, and 3 correspond to the bands of Fig. 15 labeled in the same way (591).

Prussian blue spectrum is readily assignable as the intramolecular charge transfer excitation of the ferrocyanide ion (arrow 3 in Fig. 14). The bands at $35,000\text{--}40,000\text{ cm}^{-1}$ are tentatively assigned as transitions from a CN π -bonding orbital to the t_{2g} orbital of the Fe(III) ion. Braterman (85) has generalized the Prussian blue assignment scheme to include complexes in which the ions in the two holes are of different metals.

Also in accord with its class II assignment, Prussian blue has a room temperature resistivity of about 10^7 ohm cm , and is an intrinsic semi-

conductor with a negative temperature coefficient of resistance (250). Although ferromagnetic with a Curie temperature of 3.5°K (367), Prussian blue is not an example of mixed valence, Zener-type double exchange, for the Fe(II) ions in the ground state are diamagnetic.

There are numerous composition variations that can be made in the iron blues. A reduced form of Prussian blue, $\text{Fe}_2^{\text{II}}\text{Fe}^{\text{II}}(\text{CN})_6$, is colorless as one might expect, but the oxidized form, $\text{Fe}^{\text{III}}\text{Fe}^{\text{III}}(\text{CN})_6$, is green instead of the expected orange-brown color of $[\text{Fe}^{\text{III}}(\text{CN})_6]^{3-}$. Ibers and Davidson (373) present their spectrum of $\text{Fe}^{\text{III}}\text{Fe}^{\text{III}}(\text{CN})_6$ as well as those of Fe(III) and $[\text{Fe}^{\text{III}}(\text{CN})_6]^{3-}$, from which one sees clearly an "extraneous" absorption in $\text{Fe}^{\text{III}}\text{Fe}^{\text{III}}(\text{CN})_6$ centered at 20,000 cm^{-1} . DeWet and

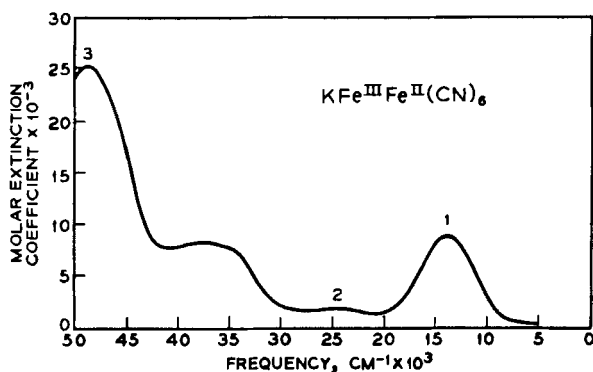


FIG. 15. The electronic spectrum of soluble Prussian blue as a colloidal dispersion in water (591).

Rolle (193), however, have demonstrated that $\text{Fe}^{\text{II}}\text{Fe}^{\text{III}}(\text{CN})_6$ is very readily reduced by water to a mixed valence Prussian blue-type compound, which no doubt is the cause of the 20,000 cm^{-1} band of " $\text{Fe}^{\text{III}}\text{Fe}^{\text{III}}(\text{CN})_6$." Both the oxidized and reduced compounds have the face-centered cubic lattice of Prussian blue (409).

Although Ibers and Davidson (373) were able to demonstrate a mixed valence absorption in solutions containing Fe(II) and Fe(III) ions, mixtures of the corresponding hexacyanides gave no such absorption. The lack of mixed valence absorption here is due in part to the impossibility of sharing ligands between these ions, and in part to the difficulty of forming pairs between ions of the same charge. However, they do exchange electrons rapidly in solution (703).

There are a large number of pentacyanide ions of the formula $[\text{Fe}^{\text{II}}(\text{CN})_5\text{X}]^{y-}$, where X is H_2O , NH_3 , AsO_2^- , SO_3^{2-} , NH_2NH_2 , or CO , all of which form deep blue precipitates with Fe(III) ion. On combining

the salts of $[\text{Ru}^{\text{II}}(\text{CN})_6]^{4-}$ or $[\text{Os}^{\text{II}}(\text{CN})_6]^{4-}$ with $\text{Fe}(\text{III})$ ion, blue to purple sols are formed which have electronic spectra virtually identical to that of Prussian blue (591).

As one might expect from the ubiquitous distribution of iron in nature, there are great numbers of naturally occurring minerals containing $\text{Fe}(\text{II})$ and $\text{Fe}(\text{III})$, both as major constituents and as impurities. As with the other iron compounds, the combination of X-ray crystallography and Mössbauer spectroscopy can be a great aid in determining the amounts, valencies, and coordinations of the iron ions in mixed valence minerals. From this information one can proceed to a qualitative understanding of their electronic structures. In this section, mixed valence iron minerals will be considered for which structures have been determined, together with only a few of the many other minerals which suggest themselves for future mixed valence study.

MacCarthy (470) many years ago presented the results of a study aimed at correlating the colors of a large number of iron-containing minerals with the oxidation state of the iron. Iron minerals as found in nature span the color spectrum, being colorless, yellow, red, brown, green, blue, purple, or black. MacCarthy showed that, in general, the colorless minerals contained only $\text{Fe}(\text{II})$, that the yellow, orange, and red ones were totally $\text{Fe}(\text{III})$, but that mixtures of these valence states led to blue materials if hydrated, black if anhydrous. The greens and purples were accounted for as physical mixtures of the other, more basic pigments. However, before one adjudges a naturally occurring mineral to be mixed valence on the basis of its unusual color, the possible contamination of the sample by colored impurities must be ruled out.

Both the partial reduction of colorless $\text{Fe}^{\text{III}}\text{PO}_4$ and partial oxidation of colorless $\text{Fe}_2^{\text{II}}(\text{PO}_4)_2$ lead to the formation of deeply colored $\text{Fe}(\text{II}), \text{Fe}(\text{III})$ phosphates (699). Thus, depending upon conditions, the reduction of slurried FePO_4 in H_2O with H_2 under pressure leads to green, blue, or black crystals (374). Vivianite, a naturally occurring mineral with composition $\text{Fe}_3^{\text{II}}(\text{PO}_4)_2 \cdot 8\text{H}_2\text{O}$, presents a dramatic example of the development of a deep color on attaining mixed valence, for the mineral is colorless until cleaved and exposed to the air, whereupon it oxidizes and develops a dark blue color. Since the reduced mineral contains pairs of ferrous ions in oxygen octahedra sharing an edge (514), it is clear how a chromophoric grouping can result on partial oxidation. A similar situation holds for iron in silicate and borate glasses (767) in which, for example, ferrous iron is colorless and ferric iron is brown, but glasses of intermediate oxidation are blue. The blue-color centers in these glasses must be "dimers" in the sense that no mixed valence color can develop if the $\text{Fe}(\text{II})$ and $\text{Fe}(\text{III})$ ions are too far separated.

Iron lazulite is another basic iron phosphate mineral. It is described as being "shiny, jewel-like black in color," and contains Fe(II) and Fe(III) in face-sharing octahedral coordination (407). The close approach of the Fe(II) and Fe(III) ions to class III geometry suggests that iron lazulite will have a low electrical resistivity, a quantity which is unmeasured as yet. A similar situation holds for barbosolite (462), $\text{Fe}_2^{\text{II}}\text{Fe}_4^{\text{III}}(\text{PO}_4)_4(\text{OH})_4$, a material in which the oxygen octahedra surrounding the Fe(II) and Fe(III) ions share faces and corners.

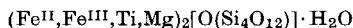
There are a great many silicate minerals containing iron in two valence states. Crocidolite is a bright blue, fibrous silicate containing Fe(II) and Fe(III) in octahedral coordination. The Mössbauer spectrum of crocidolite shows the presence of discrete Fe(II) and Fe(III) ions, as expected for a class II mixed valence system (275). That its blue color is due to a mixed valence interaction is apparent both from the fact that when the Fe(II) fraction is oxidized to Fe(III) the band responsible for the blue color at $16,000\text{ cm}^{-1}$ disappears, and from the fact that this band is polarized along the fiber axis, which is also the direction of shortest Fe(II)–Fe(III) separation (465). Crocidolite is a semiconductor along the fiber axis, but has a very high resistivity perpendicular to this axis.

Biotite is a micaceous mineral in which variable amounts of Al(III) and Mg(II) have been replaced by Fe(III) and Fe(II). As a result of this substitution into the layered mica structure, biotite appears quite black in light polarized with its electric vector within the layers but is colorless perpendicular thereto. Because of the mixed valence aspect of this material and the obvious related electronic conduction mechanism, it is clear why the best insulating micas are lowest in iron. Because the Mössbauer spectrum of biotite shows absorption due to clearly defined Fe(II) and Fe(III) ions, the system is mixed valence class II, as is also clear from its crystal structure (83).

Lievrite is a black mineral having the composition

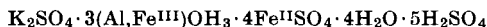


with both the Fe(II) and Fe(III) ions in distorted octahedra sharing edges (53). Taramellite, another iron-containing silicate, also contains chains of octahedral Fe(II) and Fe(III) ions sharing edges, and has the overall formula (490):



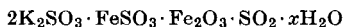
Cronstedtite is a layered mineral, $\text{Fe}_2^{\text{II}}\text{Fe}_2^{\text{III}}\text{SiO}_5(\text{OH})_4$, which has both Fe(II) and Fe(III) ions in octahedral coordination as well as Fe(III) in tetrahedral sites (354). The mineral is black in thick sections and emerald green in thinner ones.

Voltaite is an interesting mixed valence iron sulfate mineral with the composition



which is easily synthesized in the laboratory (300). Consistent with a class II mixed valence formulation, voltaite has a deep black color in massive form, but is green when viewed by transmission in thin sections. Synthesis of the corresponding material having $\text{Cd}^{\text{II}}\text{SO}_4$ replacing $\text{Fe}^{\text{II}}\text{SO}_4$ results in an almost colorless solid, as expected. In contrast to the black color of voltaite, the mixed valence iron sulfate mineral romerite ($\text{Fe}^{\text{II}}\text{Fe}_2^{\text{III}}(\text{SO}_4)_4 \cdot 14\text{H}_2\text{O}$) has only a reddish brown color (634, 635). However, dehydration of romerite to the dihydrate yields a blue-black material, just as in the case of the ferrous-ferric fluorides mentioned above. Pending a report of the structures of these minerals, one might guess that in voltaite the Fe(II) and Fe(III) ions are in rather close association with their octahedra probably sharing ligands, whereas in hydrated romerite these ions are effectively separated by "insulating" water molecules.

Gmelin (288) lists a number of synthetic mixed valence iron sulfates of rather similar composition: $\text{FeSO}_4 \cdot \text{Fe}_2(\text{SO}_4)_3 \cdot 2\text{H}_2\text{SO}_4$ (rose colored), $4\text{FeSO}_4 \cdot \text{Fe}_2(\text{SO}_4)_3 \cdot 12\text{H}_2\text{O}$ (yellow-green), $6\text{FeSO}_4 \cdot \text{Fe}_2(\text{SO}_4)_3 \cdot 10\text{H}_2\text{O}$ (pale green), and $3\text{FeSO}_4 \cdot 2\text{Fe}_2(\text{SO}_4)_3 \cdot 3\text{H}_2\text{O}$ (colorless). There is also an Fe(II), Fe(III) sulfite (57a),



which is a colorless material.

A cursory look through a modern book of mineralogy (172) will reveal a large number of other iron-containing substances of potential mixed valence interest. For example, the ferrous minerals augite (black, distinctly dichroic), riebeckite (dark blue, dichroic), glaucophane (blue, dichroic), hornblende (dark green to black), tourmaline (all colors, strongly dichroic), ludwigite (black, dichroic), and osumilite are all thought to contain ferrous and ferric ions.

The mineral magnetite, Fe_3O_4 , offers many illustrative examples of mixed valence effects. On the basis of its stoichiometry, Gay-Lussac first described Fe_3O_4 as involving a "special" valence state of iron. Shortly thereafter, Dalton and Berzelius proposed instead that Fe_3O_4 was a compound of $\text{Fe}^{\text{II}}\text{O}$ and $\text{Fe}_2^{\text{III}}\text{O}_3$ in 1 : 1 ratio. As we shall see, there is a certain amount of truth in both of these ideas. Fe_3O_4 is a cubic spinel, consisting of a cubic close-packed arrangement of oxide ions which define both octahedral and tetrahedral sites (Fig. 16). In a normal spinel with eight molecules per unit cell, eight of the tetrahedral holes are filled by M(II) metal ions, while sixteen of the octahedral holes are filled by

M(III) metal ions. In magnetite, however, because of the propensity of Fe(III) for tetrahedral coordination, all eight tetrahedral sites are filled by Fe(III) and the remaining sixteen edge-sharing octahedral sites are filled by eight Fe(II) ions and eight Fe(III) ions (726, 728). Thus if it were a normal spinel, magnetite clearly would be a class I mixed valence system, but the inverse spinel structure described above results in class III-B behavior within the octahedral sites and class I behavior between octahedral and tetrahedral sites.

Verwey *et al.* (729) felt that the rapid electron exchange implied by the mixed valence occupation of the octahedral sites in magnetite was

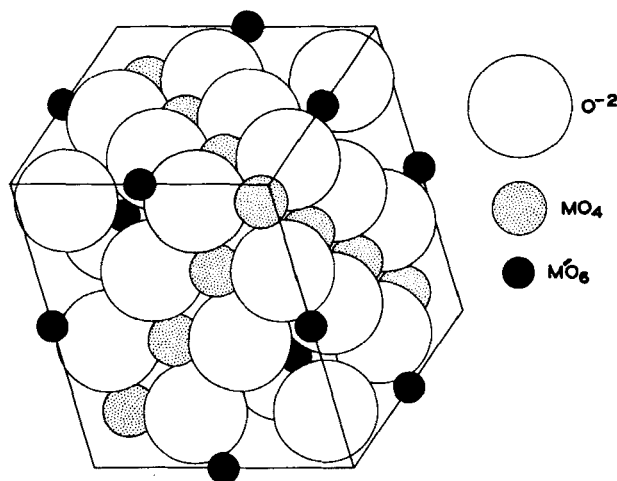


FIG. 16. The unit cell of the spinel MM_2O_4 , in which the M cations are in tetrahedral and the M' in octahedral sites.

responsible for its unusually low resistivity (4×10^{-3} ohm cm at 300°K). Unlike many oxides which show maximal resistance when stoichiometric and a decreasing resistance as the composition departs from stoichiometry, Fe_3O_4 is just the opposite, for the addition of defects and other valences of iron only act to trap the valence locally and thereby increase the activation energy for conduction (726).

Fe_3O_4 is ferrimagnetic with a Curie point at 500°–600°C. Neutron diffraction experiments (660) show that the Fe(II) in the tetrahedral sites is antiferromagnetically coupled to the ferromagnetically coupled Fe(II), Fe(III) ions in the octahedral sites, the net ferrimagnetism resulting from the larger numbers of octahedral sites.

Verwey *et al.* (729) reported that, on cooling Fe_3O_4 below 120°K, the resistivity rose abruptly by two orders of magnitude and became

distinctly anisotropic whereas above 120°K it is isotropic. They suggested that above 120°K the Fe(II) and Fe(III) in the octahedral sites are in "dynamic disorder," but that below this temperature the crystal is orthorhombic and the Fe(II) and Fe(III) ions become ordered, occupying perpendicular rows of octahedral sites. We can paraphrase Verwey and presume that the octahedral Fe—O distances alter abruptly at 120°K so as to trap the Fe(II) and Fe(III) valences, thereby making the octahedral system more class II, i.e., insulating. If the valences are partly trapped at room temperature through the introduction of Fe₂O₃ into the crystal, then the 120°K transition is absent. Careful neutron diffraction work by Hamilton (335) fully confirmed Verwey's conjectures, for Hamilton showed not only that the low temperature form of Fe₃O₄ was orthorhombic but that, whereas the Fe—O distance in the octahedral sites at 300°K is uniformly 2.0590 ± 0.0016 Å, in the low temperature phase there are two octahedral sites, one having Fe(III)—O equal to 2.00 Å, and one having Fe(II)—O equal to 2.123 Å. These Fe(II) and Fe(III) ions are in perpendicular rows, as predicted. Calhoun's resistivity measurements show that the anisotropy increases with decreasing temperature, indicating a firmer trapping at lower temperatures (126).

The Mössbauer spectra of Fe₃O₄ at 300°K and 85°K offer striking confirmation for the views expressed above (49). At room temperature, the Mössbauer spectrum of Fe₃O₄ shows that the magnetic fields at the octahedral sites are indistinguishable, indicating an oscillation of valence more rapid than 10^8 /sec. On the other hand, at 85°K, the Fe(II) and Fe(III) ions in the octahedral holes can be distinguished as expected for a class II system.

Magnetite can be brominated to yield a dark brown material of the composition (Fe₃O₄)₃Br₂ (360). This bromide still possesses a spinel lattice like Fe₃O₄ and although ferromagnetic, is less so than Fe₃O₄.

The binary oxides of barium and iron contain, among their number, two mixed valence materials. Derbyshire *et al.* (190) and Fraker (259) have shown that the barium iron oxide thought to be BaFeO₃ really contains only 76 % of its iron as Fe(IV), the remainder being Fe(III). This leads to a probable formula Ba(Fe^{III},Fe^{IV})O_{2.9}. A second oxide, BaFe^{II}₂Fe^{III}₁₆O₂₇, has a spinel-type structure (95) and, like magnetite, is an electrical conductor and ferromagnet (763).

We will present here only one of many examples of the dramatic effects that low-level doping can produce through mixed valence. In yttrium iron garnet, 3Y₂O₃·5Fe₂O₃, three fifths of the Fe(III) ions are found in tetrahedral sites and two fifths in octahedral sites, the stoichiometric crystal being an insulator with a resistivity of about 10^{11} ohm cm.

On doping such crystals with approximately 0.02 atom of silicon per formula weight, an equivalent amount of Fe(III) is reduced to Fe(II) and the resistivity decreases by seven orders of magnitude (792). It is not yet known whether the Fe(II) ions reside in the tetrahedral or the octahedral sites of the garnet.

The process of iron corrosion has been shown to proceed through an intermediate "green rust" of composition $2\text{FeO} \cdot \text{Fe}_2\text{O}_3 \cdot \text{H}_2\text{O}$, which precedes the formation of brown rust, $\gamma\text{-Fe}_2\text{O}_3 \cdot \text{H}_2\text{O}$ (1, 174, 803). Abe (1) showed that $2\text{FeO} \cdot \text{Fe}_2\text{O}_3 \cdot \text{H}_2\text{O}$, when made by the combination of $\gamma\text{-Fe}_2\text{O}_3 \cdot \text{H}_2\text{O}$ and $\text{Fe}(\text{OH})_2$, is really a blue material, and that "green rust" is probably a mixture of this blue compound and the brown rust. Shively and Weyl (659) also report that the partial oxidation of $\text{Fe}(\text{OH})_2\text{-Al}(\text{OH})_3$ coprecipitates yields dark blue materials. In a more detailed study, Feitknecht and Keller (238) report that the air oxidation of colorless $\text{Fe}(\text{OH})_2$ leads to the formation of a deep green material, which has the crystal structure of $\text{Fe}(\text{OH})_2$ although containing up to 10% Fe(III). Air oxidation of buffered FeCl_2 solutions yields a dark green mixed valence oxychloride of ideal composition $\text{Fe}_4^{\text{II}}\text{Fe}^{\text{III}}\text{Cl}(\text{OH})_{10} \cdot x\text{H}_2\text{O}$, which, however, can have appreciable amounts of its Fe(II) replaced by Fe(III) (238). Selwood (652) mentions that ferromagnetic gels can be formed by addition of base to solutions containing mixtures of ferric and ferrous ions.

There are two biologically important iron-containing materials of potential interest to our study. The first, photosynthetic pyridine nucleotide reductase, contains two nonheme Fe(III) ions per molecule. On photoreduction, one of the two Fe(III) ions is reduced to Fe(II) and the protein *decolorizes* (263). This fact suggests strongly that the two iron ions are not closely associated in the photoreduced protein. Ferredoxin contains seven iron ions per molecule, all of which appear to be Fe(III) (74). However, it is postulated that these ions are involved in electron transport, and that some of the Fe(III) is reduced on reduction of the protein.

F. COBALT

Like manganese and iron, cobalt forms a mixed valence oxide with a spinel structure, Co_3O_4 , and, as with the other two oxides, there has been a good deal of discussion about the distribution of the valency in it. In principle, four possibilities exist: normal or inverse $\text{Co}(\text{II}), \text{Co}(\text{III})$ spinels and normal or inverse $\text{Co}(\text{II}), \text{Co}(\text{IV})$ spinels. In common with Mn_3O_4 and in contrast to Fe_3O_4 , Co_3O_4 has a high resistivity (458, 741),

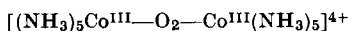
suggesting that the manganese and cobalt compounds are normal spinels (725). Cossee (158) measured the magnetic susceptibilities of tetrahedral Co(II) in $(\text{Co}^{\text{II}}, \text{Zn})\text{O}$, of Co(III) octahedrally coordinated in the spinel $\text{ZnCo}_2^{\text{III}}\text{O}_4$, and of Co_3O_4 from 77° to 1000°K and found that the effective magnetic moment per Co(II) in ZnO was 4.05 B.M., but that the moment of Co(III) in ZnCo_2O_4 was zero, as expected for a low-spin $3d^6$ configuration. The effective magnetic moment per mole of Co_3O_4 , 4.14 B.M., can then be interpreted in terms of the structure $\text{Co}^{\text{II}}\text{Co}_2^{\text{III}}\text{O}_4$ with Co(II) in tetrahedral and Co(III) in octahedral coordination. At 40°K, Co_3O_4 becomes antiferromagnetic (602), and the spin interaction between the Co(II) ions is an order of magnitude stronger than in the spinel CoAl_2O_4 , possibly as a result of indirect exchange involving the empty e_g orbitals of the Co(III) ions. The nuclear magnetic resonance chemical shift of ^{59}Co in Co_3O_4 (403, 509) contains a temperature-independent contribution due to mixing of the low-lying excited configuration $t_{2g}^5 e_g^1$ with the t_{2g}^6 ground state, and a temperature-dependent part attributed to hyperfine coupling between the nuclear spins of the diamagnetic Co(III) ions and the electron spins of the Co(II) ions at the tetrahedral sites.

Cobalt(III,IV) perovskites can be prepared with formulas intermediate between $\text{LaCo}^{\text{III}}\text{O}_3$ and $\text{SrCo}^{\text{IV}}\text{O}_3$, just as was found for the Mn(III),Mn(IV) manganites (394). In contrast to the octahedrally coordinated, low-spin Co(III) in Co_3O_4 , that in LaCoO_3 is high-spin, and all the mixed valence phases are ferromagnetic, with Curie temperatures that rise sharply with increasing Co(IV) concentration. LaCoO_3 behaves as a semiconductor, but when doped with strontium the room temperature resistivity drops sharply and the temperature coefficient of resistivity finally becomes positive. As in the case of the Mn(III),Mn(IV) manganites, the ferromagnetism of the mixed valence cobaltites is attributed to a strong positive Co(III)–Co(IV) interaction. As described in Section II, Zener (813) showed that the resonance energy between the canonical structures $\text{Co}^{3+}\text{—O}^{2-}\text{—Co}^{4+}$ and $\text{Co}^{4+}\text{—O}^{2-}\text{—Co}^{3+}$ is larger if the electron spins on the metal atoms are parallel. Since the integrals determining the interaction in Zener's model are those involving simultaneous electron transfer from O^{2-} to Co^{4+} and Co^{3+} to O^- , the spin correlation and electrical resistivity would both be accounted for by mixed valence interaction, were it not for the fact that there is no anomaly in the resistivity at the Curie temperature. This observation has not yet been satisfactorily explained.

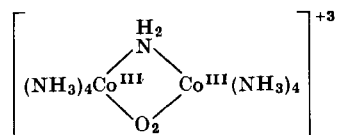
A further interesting example of a Co(II),Co(III) system with oxide ligands occurs among the class of heteropolytungstates. Powerful oxidizing agents, such as hot persulfate solution, oxidize the emerald

green anion $[\text{Co}_2^{\text{II}}\text{W}_{12}\text{O}_{42}]^{8-}$ to a mixed valence anion, the alkali metal salts of which form very dark brown to black cubic crystals. The anion was at first (37) formulated as $[\text{Co}^{\text{II}}\text{Co}^{\text{III}}\text{W}_{12}\text{O}_{42}]^{7-}$, with an "extra" $\text{Co}(\text{II})$ attached to the outside of the Keggin structure (408) characteristic of polytungstates. Very recently, however, the evidence for this formula has been reexamined (38) and the anion is now considered to be $[\text{Co}^{\text{II}}\text{Co}^{\text{III}}\text{W}_{11}\text{O}_{40}]^{9-}$, in which $\text{Co}(\text{II})$ replaces one of the tungsten atoms of the $\text{W}_{12}\text{O}_{40}$ framework, and is thus octahedrally coordinated by oxygen. The paramagnetic susceptibility of the potassium salt of this anion exhibits a most curious dependence on temperature, changing only 13% between -143° and 23°C , so that, although the two cobalt ions are in octahedral and tetrahedral coordinations and the system belongs to class I, there appears to be appreciable intraionic interaction. An ESR study would be rewarding.

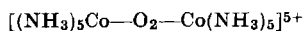
Peroxo-bridged binuclear cobalt complexes have been known for over 100 years (262) and were systematically investigated by Werner (765, 766). Diamagnetic cations such as



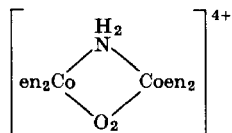
and



undergo one-electron oxidations (702), forming paramagnetic species, and the question is whether Werner's formulation with one $\text{Co}(\text{III})$ and one $\text{Co}(\text{IV})$ is correct, or whether the electron has been removed from the bridging peroxo group, i.e., is the oxidized cation a mixed valence species belonging to class II or III-A, or a single valence species containing the radical ligand O_2^- ? A number of workers established that the complexes



and



had magnetic moments corresponding to one unpaired spin (287, 480), but were unable to distinguish between the alternative formulations and, indeed, Malatesta (480) envisaged a resonance between them.

In 1938 Mathieu (488) measured the rotatory dispersion and circular

dichroism of the optically active ethylenediamine compounds of the peroxo-bridged cobalt complexes, but, in the absence of a quantum mechanical theory of rotational strengths in metal complexes, was unable to interpret them. Mathieu (488) and Ohyagi (544) reported some solution absorption spectra, but the most reliable available appears to

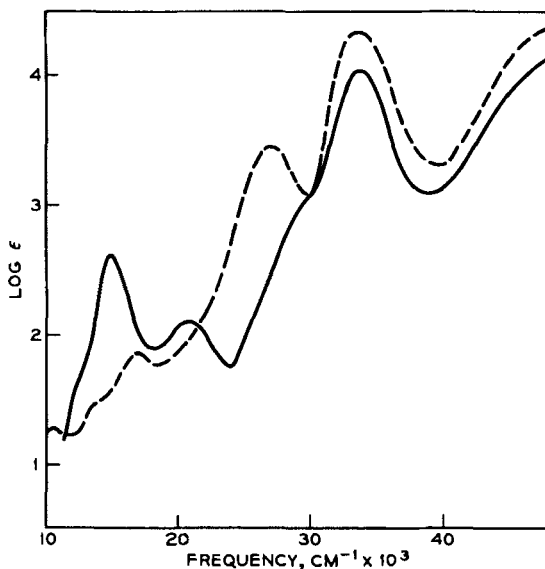
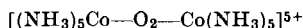
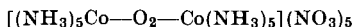


FIG. 17. The electronic absorption spectra of the $[(\text{NH}_3)_5\text{UO}_2\text{Co}(\text{NH}_3)_5]^{5+}$ (—) and $[\text{Co}(\text{NH}_3)_5\text{I}]^{2+}$ (---) ions in aqueous solution (463, 464).

be that of Linhard and Weigel (463, 464) (Fig. 17), who also were the first to note that the spectrum of

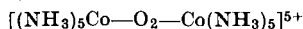


resembled the ligand field spectrum of an octahedral Co(III) complex, $\text{Co}^{\text{III}}(\text{NH}_3)_5\text{X}$, in which the ligand field strength of X was very different from that of NH_3 . Yamada *et al.* (797) had previously measured the polarized crystal spectrum of

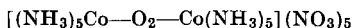


and concluded that the first absorption band was polarized parallel to what they call the $\text{Co}-\text{O}-\text{O}-\text{Co}$ direction, but, as the crystal structure of the compound had not been determined at that time, it is difficult to see how they arrived at this conclusion.

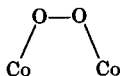
Dunitz and Orgel (210) attempted to rationalize the electronic structure of



using qualitative arguments based on π -bonding between t_{2g} orbitals on the cobalt atoms and $2p$ orbitals on the oxygens, with the assumption that the Co—O—O—Co unit was linear. Unfortunately, the first crystal structure determination (721) revealed that the O—O bond was at right angles to the metal-metal line. In either case, the two cobalt atoms would be equivalent, and the complex would be a class III-A system. That the two cobalt atoms are magnetically equivalent was clearly shown by the ESR spectrum of the cation in concentrated sulfuric acid solution (58). The fifteen observed hyperfine lines result from the interaction of the single unpaired electron with both cobalt nuclei ($I = 7/2$). The spectra of both peroxo- and peroxo-imino-bridged complexes were asymmetrical and varied with the acidity, viscosity, and temperature of the solvent in a manner which could be explained by a relaxation effect depending on protonation of the oxygen atoms (214). A further relaxation mechanism might come from rotation or torsional oscillations about the O—O bond, an effect made more likely by the fact that unpublished crystallographic work by Okaya, cited in (214), showed that in



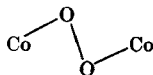
the two cobalts are cis to one another:



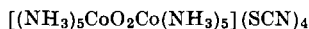
The crystal structure determination of Vannerberg and Brosset (721), in which both oxygen atoms were equidistant from the two cobalts, has been criticized recently by Schaefer and Marsh (623), who pointed out that it was based on only 234 reflections and refined to an R factor of only 19%, even after assuming that there was disorder in the lattice. Schaefer and Marsh measured 1458 reflections from



and refined their proposed structure to an R value of 7.7%. In this crystal, each oxygen is bonded to one cobalt as in Okaya's structure but in a trans



rather than a cis arrangement, which parallels that found in the diamagnetic compound (720):



The cobalt and oxygen atoms all lie in a plane, the Co—O—O angles are almost 120° , and the O—O bond length (1.31 ± 0.02 Å) is close to what one would expect for the O_2^- superoxide ion. The Schaefer and Marsh structure appears to be well substantiated, but without further details of Okaya's work it is not possible to state for certain whether there are two geometrical isomers of this cation. One can say that it is in fact not a class II or class III-A mixed valence system at all, but rather an example of the extremely small group of metal complexes which have a radical ligand. Polarographic reduction studies have been reported for the various peroxo and peroxo-imino complexes (302, 415), but the reduction reactions are complicated and difficult to interpret. The complexes have also been considered as potential semiconductors (249) on the basis of the ease of transferring electrons to or from them, but it is clear from dielectric constant measurements that they are not.

A binuclear cyanide complex $[(CN)_5CoO_2Co(CN)_5]^{5-}$ has also been prepared (333) as a deep red potassium salt. The intense absorption band at $32,000\text{ cm}^{-1}$ ($\epsilon = 6800$) probably corresponds to the band at $33,800\text{ cm}^{-1}$ ($\epsilon = 10,000$) in $[(NH_3)_5CoO_2Co(NH_3)_5]^{5+}$, although, because of the higher position of cyanide in the spectrochemical series, no ligand field bands like those of the amine complex are seen.

By the action of HCN on Co(II) solution in an inert atmosphere, one obtains a rose-colored precipitate with a Co:CN ratio of 1:2.4 and an effective magnetic moment of 3.2–3.6 B.M. per cobalt atom (127, 555, 584). Numerous crystallographic studies of this (716, 717) and a related hydrate (247) have led to the conclusion that the compound is cobaltous cobalticyanide, i.e., that the valences are firmly trapped and the system is class II. $Co_3^{II}[Co^{III}(CN)_6]_2$ has a cubic lattice isomorphous with the cobalticyanides of other divalent first transition metals and closely resembles that of Prussian blue. The diffuse reflectance spectrum of the compound (85) has been interpreted as a simple superposition of the ligand field bands of $[Co^{III}(CN)_6]^{3-}$ and Co(III) octahedrally coordinated by the nitrogen ends of the cyanides. That there is no mixed valence absorption like that found in Prussian blue (591) indicates the greater difficulty of reducing a low-spin, $3d^6$ Co(III) ion than a high-spin, $3d^5$ Fe(III) ion.

G. NICKEL

Being almost the only mixed valence compound of nickel, the lithium-doped nickel oxide system has played a central role in our understanding of the electrical properties of mixed valence solids (described in Section

II). Pure, stoichiometric NiO is a green compound with a room temperature resistivity greater than 5×10^{14} ohm cm and an absorption spectrum in the visible region closely resembling that of $\text{Ni}(\text{H}_2\text{O})_6^{2+}$. When heated with lithium carbonate at 800°C , however, Li^+ ions replace a variable number of Ni(II) ions in the rock salt lattice, and a corresponding number of Ni(II) ions are oxidized to Ni(III). The solids so produced range from gray to black and are semiconductors with activation energies and room temperature resistivities which decrease sharply with increasing lithium content. Thus, the presence of 2% lithium in NiO lowers the room temperature resistivity of a pressed pellet to only 10^2 ohm cm (719). De Boer and Verwey (182) first suggested that such enhanced conductivity would arise only when ions of differing valency were present at crystallographically indistinguishable sites, and since then many others have applied this idea, both to Ni_{1-x}O (348, 351, 730) and to many other systems (see subsections D and F on manganese and cobalt, for example).

As regards the mixed valence classification of Ni_{1-x}O , the question is whether, in the ground state at absolute zero, the Ni(II) and Ni(III) ions can be distinguished, in which case the system belongs to class II, or whether it would be more appropriate to speak of holes in a conduction band consisting of $3d$ orbitals on the metal ions (class III-B). There have been several magnetic studies of lithium-doped nickel oxides (239, 378, 566), but the observed ferromagnetism of some samples (378, 566), which might have been correlated with coupling between the bound $3d$ electrons and the conduction electrons (813), most probably results from impurities. The most comprehensive study to date (296) reveals that, when less than 30% of the nickel has been replaced by lithium, the lattice is antiferromagnetic and cubic above the Curie temperature; but when the lithium content is higher, the lattice is rhombohedral and ferrimagnetic, probably because the lithium and nickel ions are partly ordered in alternate (111) planes. The moments within each plane are either ferromagnetically coupled or paramagnetic. On the assumption that all Ni—O—Ni interactions are antiferromagnetic, the variation in magnetization per molecule with composition is explained much better by assuming that the Ni(III) ions are low-spin, with the $t_{2g}^6 e_g^1$ configuration. Such a configuration, however, having only one electron in the e_g orbitals, will promote a tetragonal elongation (see the earlier example in Cr_2F_5), which will trap the valence and make the system class II. Thus, even though the presence of Ni(III) results in a vast decrease in resistivity, the indirect exchange mechanisms providing antiferromagnetic coupling between near neighbors appear to be of lower energy than Zener-type double exchange.

Although the ground state electronic structure of these oxides places them firmly in class II, there remains the question of the conduction mechanism. Verwey *et al.* (730) thought that conduction arose by the motion of a positive hole from Ni(III) to Ni(II), the activation energy being that required to ionize the hole on Ni(III) from neighboring lithium ions. That this is not the case follows from the fact (351) that, at very high lithium concentrations, the activation energy, although decreasing, does not tend to zero. Heikes and Johnston (351) later proposed that conduction should be regarded as a thermally activated diffusion process, in which the activation energy comes from the self-trapping of the hole by its polarization field (802) (described in Section II). Extensive series of conductivity and Seebeck effect measurements as a function of temperature and lithium content (719) were held to confirm Heikes and Johnston's view, but all these considerations have recently been placed in question by measurements of the Hall effect (816), which show it to be much larger than those calculated using the thermal diffusion (hopping) model. Further, and more damaging, the Hall mobility does not increase exponentially with temperature as the hopping model requires. A reconsideration of the previous Seebeck measurements, which were carried out on heavily lithium-doped samples, and new measurements on very lightly doped samples (80), have also led to the same conclusion. Whether these observations spell the demise of the hopping model altogether, or only for this system, remains very much to be seen. There is the possibility that a model similar to the one proposed by Frederikse (260) for slightly reduced rutile (see Section III,A on titanium) may prove appropriate, but a further factor that has to be kept in mind is the possibility of compound formation in the lightly doped nickel oxides. Thus semiconductivity plots have been published (433) for pellets of Ni_{1-x}O , with x as large as 0.12, giving room temperature resistivities as low as 10^2 ohm cm. However, a study (77) of the nickel-oxygen phase diagram does not reveal the existence of stoichiometric higher oxides, such as Ni_3O_4 .

In addition to the Ni(II),Ni(III) oxides, one Ni(III),Ni(IV) system is known (453). The compounds $\text{BaNi}^{\text{IV}}\text{O}_3$ and $\text{Ba}_2\text{Ni}_2^{\text{III}}\text{O}_5$ are both black materials having low resistivities and magnetic moments, so the properties of the intermediate mixed valence phase $\text{Ba}_3\text{Ni}_2^{\text{III}}\text{Ni}^{\text{IV}}\text{O}_8$ will not be a clear guide to its classification.

H. COPPER

A wide variety of mixed valence copper compounds have been described, the majority containing halide ligands, although examples

with oxygen, nitrogen, and sulfur donors exist. Of the halides, a large number appear to fall into class I, in which the environments of the metal ions in the two oxidation states are very different and there are no bridging ligands. Thus, salts with empirical formulas $\text{Cu}_3\text{Br}_4(\text{pyr})_2$ and $\text{Cu}_3\text{Br}_4(\text{ant})_5(\text{H}_2\text{O})_6$ [pyr = dipyramidon, ant = antipyrine] were prepared some time ago by Souhay (672), who measured the conductivities of their solutions in acetone and concluded that they contained, for example, $[\text{Cu}^{\text{II}}(\text{pyr})_2]^{2+}$ and $[\text{Cu}^{\text{I}}\text{Br}_2]^-$. The colors of the solids (reported as dark green and yellow-green, respectively) are what one would expect for such a formulation. More recently, a large number of similar complexes were prepared (341–343) with simpler ligands, such as ammonia and ethylenediamine, which have the general formula $[\text{Cu}^{\text{II}}\text{A}_4][\text{Cu}^{\text{I}}\text{X}_2]_2$ or $[\text{Cu}^{\text{II}}\text{A}_4][\text{Cu}^{\text{I}}\text{X}_3]$. Compounds with similar formulas and presumably similar structures can also be prepared containing Cu(II) and Ag(I) (344–346), which, when vigorously shaken with water, decompose to AgX leaving $[\text{CuA}_4]^{2+}$ in solution. The chlorides and bromides were reported as deep blue or violet, but the iodides were all brown or black. Further compounds of the same type were prepared by Brauer and Eichner (90). Compounds in which X is CN^- have also been recognized for many years (513, 706) and other examples have been added more recently (506). Their colors suggest that they are all class I systems, with formulas analogous to those of the halides. Another class I cyanide containing one Cu(II) and two Cu(I) ions per mole has been reported by Cooper and Plane (146).

Attempts to prepare cupric complexes of methyldiphenylarsine (AsPh_2Me) always result in reduction of the copper to Cu(I), but Burrows and Sandford (115) isolated two compounds from the reaction, one blue and one brown, both of which appeared to have the empirical formula $\text{Cu}_2\text{Cl}_3 \cdot 3\text{AsPh}_2\text{Me}$. The original explanation offered for the apparent isomerism was in terms of ionic structures such as

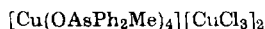


but, reinvestigating the reaction, Nyholm (540) found that the arsine had been oxidized, and that the analyses were much better described by the empirical formula $\text{Cu}_3\text{Cl}_4(\text{OAsPh}_2\text{Me})_4$. In nitrobenzene, the blue compound was an electrolyte, and the structural formula would appear to be



i.e., similar to the compounds containing ammonia and ethylenediamine discussed above. Because the blue compound became brown on storage, and also when exposed to chlorine gas, Nyholm concluded that the anion was oxidized to $[\text{Cu}^{\text{II}}\text{Cl}_3]^-$. Although the intensity of color of the brown

compound suggests that it may result from mixed valence absorption, this may perhaps be misleading, since on prolonged exposure to chlorine a red compound analyzing as



was isolated. Since all the copper in this compound is divalent, the color of this and possibly the other mixed valence compound may be related to that of red CsCuCl_3 .

A series of chlorocuprates (I,II) in which the color is clearly due to mixed valence absorption was first prepared by Mori (516). When hexaminecobalt(III) chloride solution is added to an aqueous solution of either CuCl or CuCl_2 containing excess chloride ions, orange-yellow crystals are obtained, but if the solution contains both CuCl and CuCl_2 the resulting crystals are brown or black, depending on the mole fraction of each valence state present. By measuring diffuse reflectance spectra, Mori found the new absorption band in the mixed valence material to be near $17,000\text{ cm}^{-1}$ (518), and its intensity was shown by the same method to be proportional to the product of the mole fractions of the two valence states (171). The crystal structures of the two single valence compounds are closely related, so that both valence states may be present in a crystal in any proportion with only minor structural variations. The chlorocuprate(II) has the formula $\text{Co}(\text{NH}_3)_6\text{CuCl}_5$, with a structure based on a cubic rock salt lattice of $[\text{Co}(\text{NH}_3)_6]^{3+}$ and $[\text{Cu}^{\text{II}}\text{Cl}_5]^{3-}$ ions (517), but the cuprous salt has the much more complicated formula, $[\text{Co}(\text{NH}_3)_6]_4\text{Cu}_5\text{Cl}_{17}$. Its crystal structure, however, is also cubic with $[\text{Co}(\text{NH}_3)_6]^{3+}$ and $\text{Cu}(\text{I})$ ions forming a rock salt lattice. Each $\text{Cu}(\text{I})$ is surrounded by four chloride ions, one of which forms a bridge to a $\text{Cu}(\text{I})$ at the body center of the cubic unit cell (522) (Fig. 18). Thus, the anion is a pentamer, $[\text{Cu}_5\text{Cl}_{16}]^{11-}$, considered as derived formally from condensation of four $[\text{CuCl}_4]^{3-}$ anions through addition of a fifth $\text{Cu}(\text{I})$. When compounds are formed containing only a small mole fraction of $\text{Cu}(\text{I})$, it may be presumed that it enters the $[\text{Cu}^{\text{II}}\text{Cl}_5]^{3-}$ lattice as $[\text{Cu}^{\text{II}}\text{Cl}_4]^{3-}$, but at higher mole fractions of $\text{Cu}(\text{I})$ there is an increased probability of finding four $[\text{CuCl}_4]^{3-}$ ions on adjacent, tetrahedrally related sites, and then $[\text{Cu}_5\text{Cl}_{16}]^{11-}$ may be formed by incorporating an extra $\text{Cu}(\text{I})$ and a chloride ion at another site (Fig. 19). The formula variation with mixed valence composition which this model suggests is substantiated by chemical analyses (179). It is worth noting that, apart from nonstoichiometric and doped oxides, these class II chlorocuprates(I, II) are among the very small number of systems in which the proportions of two valence states may be varied over the whole range of composition from 100% of one to 100% of the other.

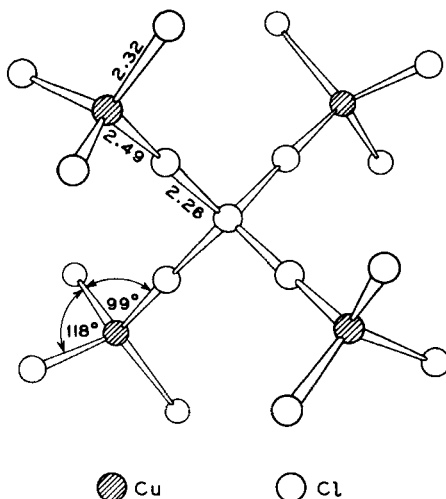


FIG. 18. Bond distances (Å) and angles in the $[\text{Cu}_5\text{Cl}_{16}]^{11-}$ ion (522).

The electrical resistivities of the chlorocuprates(I,II) have also been investigated (171). They are high resistance semiconductors, and at room temperature the specific conductivities, like the interaction absorption intensities, were proportional to the product of the mole fractions

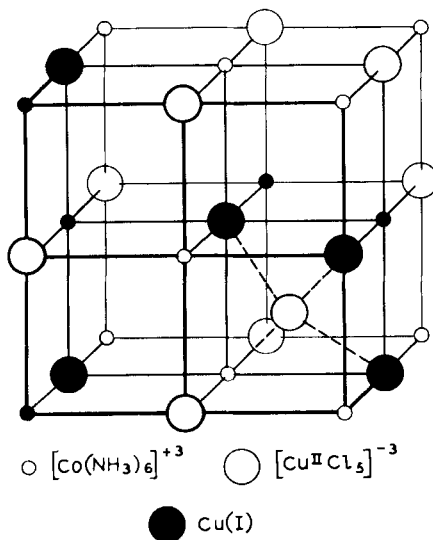


FIG. 19. The distribution of metal atoms in the mixed valence hexamminecobalt chlorocuprate(I,II) crystal.

of the two valence states. Plots of the mixed valence absorption intensity and room temperature resistivity as a function of the mole fraction of Cu(I) are shown in Fig. 20. As was also found with the interaction absorption energy, the semiconduction activation energy did not vary with mixed valence composition, although the value obtained was different from that for either of the single valence chlorocuprates. It was also reported that, unlike either single valence salt, all the mixed valence chlorocuprate salts obeyed Ohm's law quite accurately.

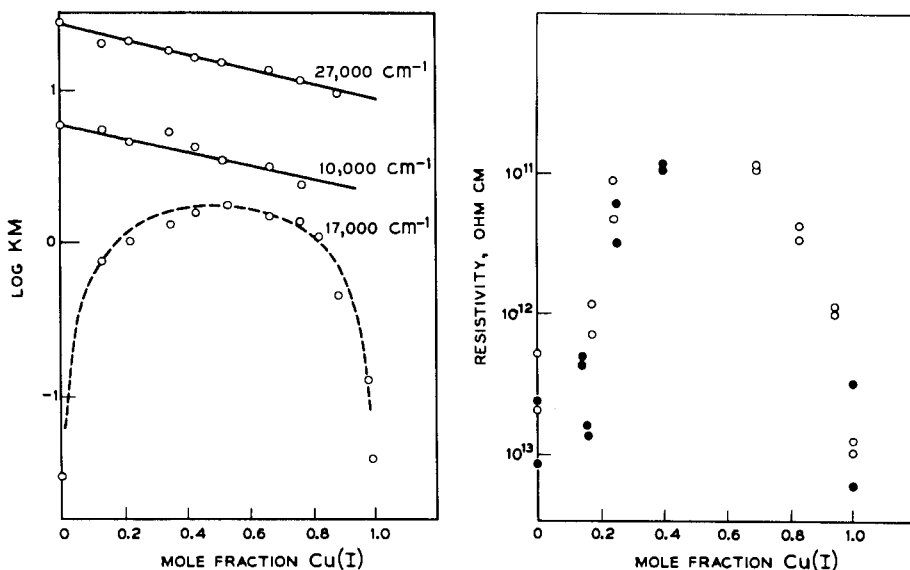
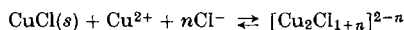


FIG. 20. The intensity of reflected light at three frequencies, and the room temperature resistivity of solid hexamminecobalt(III) chlorocuprates(I,II) as a function of the mole fraction of copper as Cu(I) in the sample (171).

Mixed valence copper chloro complexes have also been extensively studied in aqueous solution. Doehlemann and Fromherz (200) were the first to show that addition of CuCl to a solution of CuCl₂ in 10 M HCl caused a marked increase in absorption in the visible region (Fig. 21). It is of interest that the difference in the spectra of a mixed valence solution and two single valence solutions of equivalent concentration has a maximum at 18,000 cm⁻¹, close to that of the solid chlorocuprates(I,II) discussed above. It is clear from this figure and from Fig. 20 that the bands at 10,000 cm⁻¹ and 27,000 cm⁻¹ are Cu(II) constituent ion absorptions. Diehl *et al.* (195) demonstrated that the interaction complex contained equal amounts of Cu(I) and Cu(II). In an effort to determine the formula and association constant of the species responsible

for the mixed valence light absorption, McConnell and Davidson (496) worked at higher dilutions so that they could make use of previously determined association constants for the single valence chloro complexes. For solutions saturated with CuCl, they assumed that the equilibrium was



and found that, in solutions containing up to 0.30 *M* Cu(II) and 0.40 *M* chloride ion, *n* was very close to 2. At higher copper and chloride concentrations, *n* began to increase, and it was noticeable that the difference

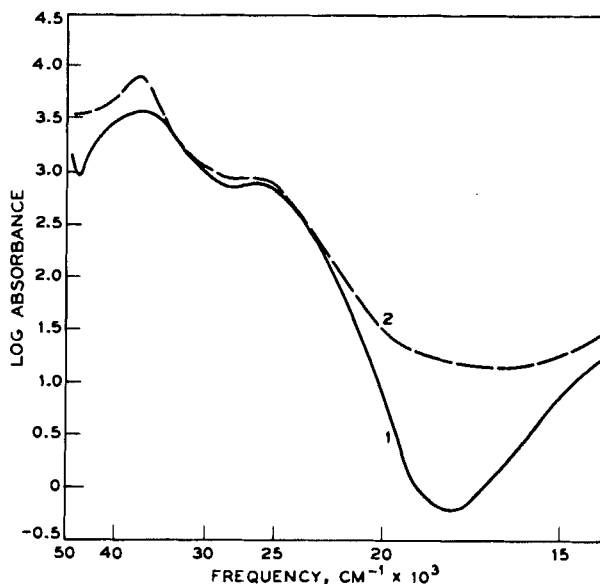


FIG. 21. The electronic spectra of 5.18 *M* solutions of CaCl_2 containing (1) 0.47 *M* Cu(II), and (2) 0.235 *M* Cu(II) and 0.273 *M* Cu(I) (200).

spectrum shifted to lower energy, approaching that found by Doehlemann and Fromherz. The formula of the interaction complex, Cu_2Cl_3 , alone does not permit a distinction between bridged or outer-sphere arrangements, since there is no indication of the manner in which the coordination spheres of the two metal ions are completed by water molecules. If the absorption band in the solid chlorocuprates(I, II) is due to an intermolecular (outer-sphere) charge transfer between $[\text{Cu}^{\text{II}}\text{Cl}_5]^{3-}$ and either $[\text{Cu}^{\text{I}}\text{Cl}_4]^{3-}$ or $[\text{Cu}_5^{\text{I}}\text{Cl}_{16}]^{11-}$, depending on the composition, then the fact that its energy is so similar to that of the mixed valence complex in solution suggests that the latter may also be an outer-sphere complex.

The rate of electron transfer between Cu(I) and Cu(II) in concentrated HCl solution was measured by McConnell and Weaver (498) in one of the first experiments to use NMR line broadening for this purpose. The ^{63}Cu resonance in a 1 *M* solution of CuCl in concentrated HCl was completely flattened by adding Cu(II) ions to a concentration of 10^{-2} *M*, which, using the theory worked out by McConnell and Berger (499), gave a bimolecular rate constant equal to 0.5×10^8 liter mole $^{-1}$ sec $^{-1}$, one of the highest ever measured up to that time. Unfortunately, however, it is not clear to which transition state this rate constant refers.

One of the first mixed valence copper compounds to be prepared was Chevreul's salt, $\text{Cu}_2\text{SO}_3 \cdot \text{CuSO}_3 \cdot 2\text{H}_2\text{O}$ (91a, 137). A recent determination of the crystal structure (418) places the compound in class I since the Cu(II) ions are surrounded by a distorted octahedron of oxygen atoms, two from water molecules at 1.92 Å and four from the sulfite ions, two at 2.03 Å and two at 2.47 Å, whereas the Cu(I) ions have a very different environment from the Cu(II) ions, being within a distorted tetrahedron consisting of three sulfite oxygen atoms (2.11–2.14 Å) and a sulfur atom (2.14 Å). The compound is reported to be red, but since the crystal structure shows it to be class I the color is most likely that of the constituent cupric sulfite. A related compound, Rogojski's salt, $\text{Cu}_2\text{SO}_3 \cdot \text{H}_2\text{O}$, was found by X-ray powder photography to be a mixture of Chevreul's salt and metallic copper (173).

A mixed valence copper thiosulfate salt, $\text{NaCu}^{\text{II}}\text{Cu}^{\text{I}}(\text{S}_2\text{O}_3)_2$, has been reported (663), but its blue-green color suggests that it belongs to class I, like the aminothiosulfate salt prepared by Ferrari *et al.* (243, 248). The structure of the latter, recently determined, contains well separated $[\text{Cu}^{\text{II}}(\text{NH}_3)_4]^{2+}$ square planar ions and $[\text{Cu}_n^{\text{I}}(\text{S}_2\text{O}_3)_{2n}]^{3n-}$ polyanions in which each Cu(I) is surrounded by four thiosulfate groups while each thiosulfate bonds two Cu(I) ions.

Because of their intense colors, a number of biological copper-containing compounds have been thought to contain the element in both valence states. Klotz *et al.* (429) investigated the reaction between thiomalic acid, $\text{HOOC}-\text{CH}_2-\text{CH}(\text{SH})-\text{COOH}$, and Cu(II) ions as a model system for hemocyanin, an oxygen-carrying protein. The intense violet color, similar to that of hemocyanin, appeared only when the Cu(II): thiomalate ratio reached 0.5, so assuming that the initial reaction was



the color could have been due to a mixed valence complex $\text{Cu}^{\text{II}}(\text{RSCu}^{\text{I}})_4$. About 20 % of the copper in the violet complex could be extracted with penten, following which the violet color was replaced by the blue color

of the Cu(II)-penten complex. The absorption spectrum of the violet complex has a single broad band at $19,200\text{ cm}^{-1}$ with an extinction coefficient of 6000 per $\text{Cu}_5(\text{SR})_4$ unit, indicating the presence of a class II species with appreciable delocalization, if indeed this band is a mixed valence absorption. From the violet solution a gray solid has been isolated (668), which is reported to have a Cu:SR ratio of 5:4, and a room temperature magnetic moment of 2.13 B.M. per Cu(II). Thio-glycolic acid and β -mercaptoethylamine both give similar violet colors, but β -mercaptopropionic acid and cysteine do not.

Ceruloplasmin, another intensely blue copper protein, contains eight copper atoms per molecule, of which approximately four could be exchanged with ionic Cu(II) and four reacted with biquinolyl, as is characteristic of Cu(I) (75). When all the copper is in the reduced state, the compound is colorless and diamagnetic, but in partially reduced samples the intensity of the visible absorption band at $16,400\text{ cm}^{-1}$ is proportional to that of the ESR absorption. The hyperfine splitting of the latter shows that the Cu(II) are magnetically dilute, but there remained the possibility that the color was due to mixed valence absorption, with the Cu(I) and Cu(II) in slightly different environments (class II) (75). However, a number of instances have since been discovered of copper proteins having optical and ESR properties similar to those of ceruloplasmin, but which contain only one copper atom per molecule (487). Thus, if ceruloplasmin is a mixed valence compound, the metal atoms of differing valence are sufficiently separated for there to be no detectable interaction between them in the ground or excited state, i.e., the system is class I.

For reasons set out at the beginning of this section, we have not generally included sulfides among the mixed valence systems reviewed here. Nevertheless, there are a number of copper sulfides whose mixed valence nature is clear enough to be worth mentioning. Of these, the most famous is probably the mineral covellite, CuS , the structure of which was investigated in some detail by Berry (61). This deep blue compound is not, as the formula implies, a simple Cu(II) salt, but contains both S^{2-} and S_2^{2-} ions as well as copper atoms in two distinctly different coordination sites, one planar triangular and the other tetrahedral. It appears from the crystal structure that the correct formulation is $\text{Cu}_4\text{Cu}_2^{\text{II}}(\text{S}_2)_2\text{S}_2$. The fact that covellite is a metal, and below 1.35°K a superconductor (111), shows either that covellite is an inverse structure (class III-B) with both Cu(I) and Cu(II) in the tetrahedral sites, or that one cannot draw firm conclusions about mixed valence class behavior from the crystal structures of highly covalent materials.

The series of dark blue mixed valence compounds $\text{Na}_2\text{Cu}_3\text{S}_3$,

$K_3Cu_3S_8$, KCu_4S_3 , and $RbCu_4S_3$ can be made by fusing copper metal, an alkali metal carbonate, and sulfur at various temperatures (605). Whereas the stoichiometries of these materials suggest that, of the m copper ions in each molecule, one is Cu(II) and $m-1$ are Cu(I), the crystal structures of isostructural KCu_4S_3 and $RbCu_4S_3$ (Fig. 22) show that all the copper atoms in these crystals are in equivalent ligand fields of sulfur atom tetrahedra, which form sheets separated by the alkali

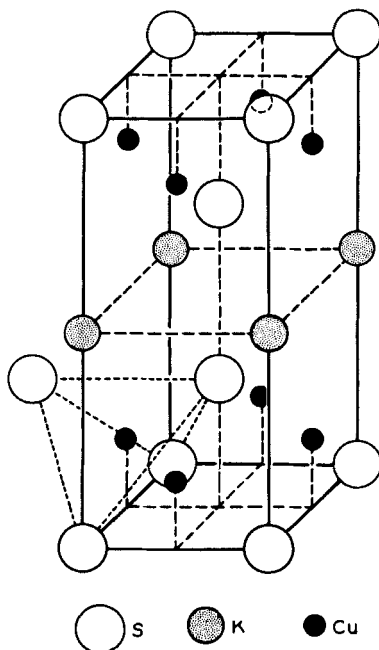


FIG. 22. The class III-B crystal structure of KCu_4S_3 , demonstrating the equivalence of the Cu(I,II) ions in the tetrahedral sites (605).

metal ions. Within the sheets, the copper-copper spacing is 2.76 Å, and not surprisingly these class III-B compounds are good conductors, with resistivities at 20°C of 2.5×10^{-2} and 1.7×10^{-2} ohm cm for KCu_4S_3 and $RbCu_4S_3$, respectively. Inasmuch as $Na_2Cu_3S_3$ and $K_3Cu_3S_8$ have resistivities comparable to those of KCu_4S_3 and $RbCu_4S_3$, these compounds may also have class III-B structures.

Gmelin's *Handbuch* lists many other supposed Cu(I),Cu(II) compounds, including sulfites and amino-cyanides, as well as more bizarre compounds such as $Cu_2Cl(VO_3)_2$, the majority of which were prepared over 50 years ago, and have not been investigated since. A random example is $Cu_4^I Cu_2^{II} Fe_3(CN)_{14} \cdot 2H_2O$ (?) (*sic*), prepared (645) as a black

shiny mass in 1856! We are unable to pass judgement on the status of these substances.

I. ZIRCONIUM AND HAFNIUM

Doubtless as a result of the extremely reducing character of the lower oxidation states of these two elements, there are no compounds of either which have ever been considered as possible mixed valence systems.

J. NIOBIUM AND TANTALUM

The mixed valence halides of niobium and tantalum, numbering over twenty with many as yet only briefly investigated, offer an interesting area for the experimental and theoretical study of mixed valence chemistry. It has become apparent during the last 5-10 years that a remarkable number of these compounds have in common a structural unit of high stability and most interesting electronic structure. It is with the properties of this structural unit that we will be almost totally occupied in dealing with the halides.

The first of the niobium and tantalum mixed valence halides synthesized have since proved to have the composition $M_6X_{14} \cdot 7H_2O$. The fact that the niobium and tantalum compounds of this composition yield only one seventh of their halide ions to aqueous silver nitrate (134, 340) was an early indication that these solutions contain the $[M_6X_{12}]^{2+}$ complex ion. In support of this conclusion, Vaughan, Sturdivant, and Pauling (724) later found that the X-ray diffraction patterns obtained from alcoholic solutions of $Nb_6Cl_{14} \cdot 7H_2O$, $Ta_6Cl_{14} \cdot 7H_2O$, and $Ta_6Br_{14} \cdot 7H_2O$ were interpretable as due to scattering by a polynuclear ion, the idealized structure of which has six metal ions at the face centers of a cube and twelve halide ions at the midpoints of the cube edges (Fig. 23). Single crystal X-ray work has since confirmed this structure of the $[M_6X_{12}]^{2+}$ ion and proved its presence in a number of other niobium and tantalum subhalides. Most recently it has been found that many of the $[M_6X_{12}]^{2+}$ ions can be oxidized to net charge 3+, 4+, and, in one case, a reported 5+, without change of the basic geometry, thereby increasing considerably the number of compounds containing the mixed valence M_6X_{12} structural unit. Many of these mixed valence niobium and tantalum subhalides are discussed in the recent metal-metal bonding review of Schäfer and Schnering (627).

According to the X-ray scattering data (724), the $[\text{Nb}_6\text{Cl}_{12}]^{2+}$ ion in solution has cis Nb—Nb distances of 2.85 Å and Nb—Cl distances of 2.41 Å, the former indicating appreciable metal-metal interaction in view of the 2.86-Å Nb—Nb distance in niobium metal. The authors admit, however, that there is little evidence that the symmetry of the complex ion is as high as they describe it. Indeed, the single crystal study of the anhydrous salt $\text{Nb}_6\text{Cl}_{14}$ (665) shows that in this material the $[\text{Nb}_6\text{Cl}_{12}]^{2+}$ octahedron is compressed along a fourfold axis so as to yield cis Nb—Nb distances from 2.89 to 2.95 Å, and Nb—Cl distances from 2.40 to 2.58 Å.

$\text{Nb}_6\text{Cl}_{14}$ has no free spins, its paramagnetism being of the temperature-independent type ($\chi_{\text{mol}} = 579 \times 10^{-6}$ cgs, corrected for diamagnetism) (665). The heptahydrate, however, has been reported to have an effective moment of 1.48 B.M. as deduced from the Curie-Weiss behavior of the susceptibility (443). Robin and Kuebler (593), however, found this material to have a temperature-independent paramagnetism ($\chi_{\text{mol}} = 850 \times 10^{-6}$ cgs, corrected for diamagnetism) in the temperature range 42°–290°K. In support of a closed-shell ground state configuration for the $[\text{Nb}_6\text{Cl}_{12}]^{2+}$ ion, Mackay and Schneider (471) also find a temperature-independent paramagnetism ($\chi_{\text{mol}} = 456 \times 10^{-6}$ cgs, corrected for diamagnetism) in the double salt $[(\text{C}_2\text{H}_5)_4\text{N}]_4\text{Nb}_6\text{Cl}_{18}$.

Chemically, $[\text{Nb}_6\text{Cl}_{12}]^{2+}$ is rather stable and can be used as a cationic species for the formation of compounds such as $\text{Nb}_6\text{Cl}_{12}(\text{OH})_2 \cdot 8\text{H}_2\text{O}$ and $\text{Nb}_6\text{Cl}_{12}\text{Br}_2 \cdot 7\text{H}_2\text{O}$ (340). The $[\text{Nb}_6\text{Cl}_{12}]^{2+}$ ion has also found use as a "heavy atom" in the X-ray analysis of the structure of wet lysozyme chloride (157). It has been suggested (10) that in alkaline solution the $[\text{Nb}_6\text{Cl}_{12}(\text{OH})_4]^{2-}$ ion forms, and that hydroxyl groups may even be introduced as bridges replacing the chloride ions. The deep green aqueous solution of $\text{Nb}_6\text{Cl}_{14}$ can be oxidized with I_2 in a two-electron step (493), with only the first electron being lost, however, in alcoholic solutions (471).

The oxidized species $[\text{Nb}_6\text{Cl}_{12}]^{3+}$ has been isolated as the double salt $[(\text{C}_2\text{H}_5)_4\text{N}]_3\text{Nb}_6\text{Cl}_{18}$ (471), and has an effective magnetic moment (1.61 B.M.) corresponding closely to that expected for one unpaired electron. The ESR spectrum of the $[\text{Nb}_6\text{Cl}_{12}]^{3+}$ ion shows a symmetrical 49-line pattern, which is that expected if the unpaired electron has the same hyperfine interaction with all six niobium nuclei (spin 9/2). Further oxidation yields $[(\text{C}_2\text{H}_5)_4\text{N}]_2\text{Nb}_6\text{Cl}_{18}$, a compound with an effective moment of 0.47 B.M. Because Mackay and Schneider presume that this compound is, in fact, diamagnetic but contains a large amount of paramagnetic impurity, its true susceptibility is still open to question.

In alcoholic solution, the $[\text{Ta}_6\text{Cl}_{12}]^{2+}$ ion also has the structure shown

in Fig. 23, with the cis Ta—Ta distances amounting to 2.88 Å and the Ta—Cl distances to 2.44 Å (724). The recent crystallographic study of the heptahydrate $\text{Ta}_6\text{Cl}_{14} \cdot 7\text{H}_2\text{O}$ by Burbank (113) shows that the crystal contains one molecule per unit cell (probably $P\bar{3}1m$) with both disorder and stacking faults present. In this material, the $[\text{Ta}_6\text{Cl}_{12}]^{2+}$ ion appears as a distorted octahedron, principally tetragonally extended, with the nonbridging chloride ions coordinated to the tantalums on the tetragonal fourfold axis. The cis Ta—Ta bond distances range from 2.63 to 3.27 Å and the bridging Cl to Ta distances range from 2.28 to 2.72 Å, thereby demonstrating not only a distortion of the $[\text{Ta}_6\text{Cl}_{12}]^{2+}$ ion, which is much larger than that measured (665) for the $[\text{Nb}_6\text{Cl}_{12}]^{2+}$ ion, but which also

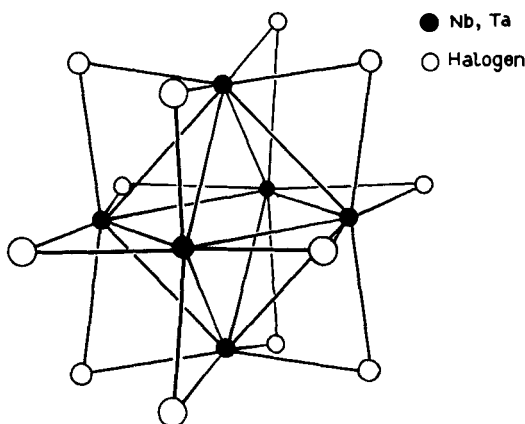


FIG. 23. The idealized geometry of the niobium and tantalum subhalide ions, $[\text{M}_6\text{X}_{12}]^{n+}$, showing the metal atom octahedron and bridging halide ions.

has a different sense to the tetragonality. Careful analytical work on the “heptahydrate” of $\text{Ta}_6\text{Cl}_{14}$ suggests that the true formula is instead $\text{Ta}_6\text{Cl}_{14} \cdot 8\text{H}_2\text{O}$ (630).

As with $\text{Nb}_6\text{Cl}_{14} \cdot 7\text{H}_2\text{O}$, the tantalum analog was first reported to have an effective moment of 1.39 B.M. (443), whereas later work (593) showed that this substance had a zero susceptibility, implying a temperature-independent paramagnetism equal to the diamagnetic correction. The close similarity in properties of the niobium and tantalum subhalides suggests that, like $\text{Nb}_6\text{Cl}_{14} \cdot 7\text{H}_2\text{O}$, $\text{Ta}_6\text{Cl}_{14} \cdot 7\text{H}_2\text{O}$ has a closed-shell ground state.

Reduction of TaCl_5 with aluminum foil in the appropriate temperature gradient yields the greenish brown material $\text{Ta}_6\text{Cl}_{15}$ (447). X-ray (626) and magnetic susceptibility (626, 665) measurements show the presence of the $[\text{Ta}_6\text{Cl}_{12}]^{3+}$ ion having one free spin. The same species is

produced as a stable ion in solution by the oxidation of $[\text{Ta}_6\text{Cl}_{12}]^{2+}$ by either Fe^{3+} or Cl_2 , and probably by O_2 as well (226, 493). Ferric ion can further oxidize the 3+ ion to 4+ in aqueous solution, from which the diamagnetic salt $\text{Ta}_6\text{Cl}_{16} \cdot 9\text{H}_2\text{O}$ can be recovered (226, 494).

Air oxidation of ethanolic solutions of $\text{Nb}_6\text{Cl}_{14} \cdot 8\text{H}_2\text{O}$ results in the formation of $\text{Nb}_6\text{Cl}_{16} \cdot 3\text{C}_2\text{H}_5\text{OH}$, which was demonstrated to contain the $[\text{Nb}_6\text{Cl}_{12}]^{4+}$ ion by the close similarity of its optical spectrum to that of the $[\text{Nb}_6\text{Cl}_{12}]^{2+}$ ion (681). More will be said of this similarity below. Surprisingly, the anhydrous, green niobium subhalide $\text{Nb}_6\text{Cl}_{16}$ does not contain the M_6X_{12} structural unit, but rather has a layered lattice much like that of CdI_2 with only 3/4 of the metal sites filled (733). The Nb—Nb distance within the metal atom layer is 2.78 Å (638), a distance significantly smaller than that in $\text{Nb}_6\text{Cl}_{14}$. The substance, better written as Nb_3Cl_8 , however, may not be metallic as is Ag_2F with the anti- CdI_2 structure (class III-B), for it is reported (638, 666) that the niobiums are grouped into triplets (class III-A), and that the effective magnetic moment amounts to 1.83 B.M., as expected for an isolated Nb_3Cl_8 molecule containing an odd number of *d* electrons. Actually, Nb_3Cl_8 is the end member of a homogeneous mixed valence system of considerable breadth, the other end member being NbCl_4 . This presents the interesting possibility that NbCl_3 is really a mixed valence compound, being composed of equal parts of Nb_3Cl_8 and NbCl_4 (638, 648).

The niobium oxychloride $\text{Nb}_3\text{O}_7\text{Cl}$ presents another possibility as a mixed valence system, for when it is prepared in an oxidizing atmosphere it is colorless, as expected for a $4d^0$ system, but when prepared in the absence of O_2 the product presumably contains lower oxides of niobium and is colored blue. Identical color changes have been observed in the preparation of the $4d^0$ systems Nb_2O_5 and NbOCl_3 (624).

The mixed valence niobium and tantalum subbromides present little that is new and interesting. $\text{Nb}_6\text{Br}_{14} \cdot 7\text{H}_2\text{O}$ possesses a temperature-independent paramagnetism, as does the corresponding tantalum compound (593). Just as was found with the chloride of this composition, $\text{Ta}_6\text{Br}_{15}$ has one free spin (628, 629) and the $[\text{Ta}_6\text{Br}_{12}]^{2+}$ ion in aqueous solution can be oxidized with Fe^{3+} or Br_2 to $[\text{Ta}_6\text{Br}_{12}]^{4+}$ (593). An extensive phase study revealed that, in addition to the $\text{Ta}_6\text{Br}_{14}$ (green) and $\text{Ta}_6\text{Br}_{15}$ (black) compounds, an even higher bromide, $\text{Ta}_6\text{Br}_{17}$, can exist (492), but there is no other information on this substance.

$\alpha\text{-Nb}_3\text{Br}_8$ is isostructural with the chloride, and our comment about “ NbCl_3 ” would apply also to “ NbBr_3 ” (56, 625). Simon and von Schnering (666) report the preparation and properties of a second form of Nb_3Br_8 , the β -form. The black crystals of this substance have a temperature-dependent effective magnetic moment (0.5 B.M. at 90°K, 1.95 B.M.

at 573°K), and a structure composed of Nb_3 triangular units having an irregular octahedron of halide ions about each niobium ion. As with $\text{Nb}_6\text{Br}_{14}$, there appears to be appreciable metal-metal bonding in the $\beta\text{-Nb}_3\text{Br}_8$ system, judging from the 2.88-Å separation between niobium atoms. The system is class III-A.

The preparation and properties of the mixed valence fluoride Nb_6F_{15} have recently been described (629). In this material, the $[\text{Nb}_6\text{F}_{12}]^{3+}$ groups have full octahedral symmetry, with all six of the niobiums of an octahedron being bridged to niobium atoms of other octahedra by fluoride ions. Within an octahedron, the cis Nb—Nb distance is 2.80 Å, and Nb—F equals 2.05 Å. The magnetic properties of Nb_6F_{15} have not yet been reported, but one expects one free spin per Nb_6 , just as has been found for $\text{Ta}_6\text{Cl}_{15}$, $\text{Ta}_6\text{Br}_{15}$, and $[(\text{C}_2\text{H}_5)_4\text{N}]_3\text{Nb}_6\text{Cl}_{18}$. The diamagnetism of the niobium and tantalum tetrahalides $\text{M}^{\text{IV}}\text{X}_4$ has recently been explained as due to a spin-pairing dimer formation, and not to the mixed valence $\text{M}(\text{III}), \text{M}(\text{V})$ configuration suggested earlier (600). However, since NbF_4 does not have the dimer structure and yet has a temperature-independent paramagnetism (299, 629), the mixed valence formulation is a possibility here. As described above for the chlorides, a niobium oxyfluoride $\text{Nb}(\text{O}, \text{F})_3$ also exists as a blue material (629).

The lower iodide of niobium, Nb_6I_{11} , presents an interesting variation of the subhalide structural unit (46, 48, 631, 665). In this material the six niobiums are approximately at the face centers of a cube, with the bridging halogen not at the centers of the cube edges, but instead at the cube corners, each iodide thereby bridging three niobium ions. This ideal structure is in fact distorted in the crystal to symmetry C_i , with an average Nb—Nb distance of 2.85 Å. This is surprisingly close to the Nb—Nb distances found in the $[\text{Nb}_6\text{X}_{12}]^{2+}$ ions. A more regular geometry prevails for the lower tantalum iodide. Ta_6I_{14} , the only lower iodide of tantalum (447, 492, 628), is structurally isotypic with $\text{Nb}_6\text{Cl}_{14}$ and shows a weak temperature-independent paramagnetism (48, 665). The black solid gives a green aqueous solution containing the $[\text{Ta}_6\text{I}_{12}]^{2+}$ ion, which, however, is not as stable as those of the other halides in this series. Whereas it was first thought that Nb_3I_8 might be composed of diamagnetic $[\text{Nb}_6\text{I}_{12}]^{4+}$ units, it is now known to have a trinuclear class III-A structure identical to that of $\beta\text{-Nb}_3\text{Br}_8$ and, like this substance, has a temperature-dependent effective magnetic moment (666).

The $[\text{M}_6\text{X}_{12}]^{2+}$ unit contains 16 metal d electrons in molecular orbitals formed from combinations of the metal atom d orbitals and the halide ligand p orbitals. If all the metal ions are in equivalent sites so as to form a class III-A system, then each metal atom has a formal valence of $2\frac{1}{3}+$. If, however, the $[\text{M}_6\text{X}_{12}]^{2+}$ ion is distorted so as to distinguish

two of the metal atoms from the other four, then these two may be assigned an integral valence of 3+ and the other four an integral valence of 2+, making the system class II. A trapping of the valence could almost be guaranteed in the mixed ion $[\text{Ta}_4\text{Nb}_2\text{X}_{12}]^{2+}$ if it could be made. Schäfer and Spreckelmeyer (632) made a start in this direction, having prepared a substance of the overall composition $\text{Ta}_{3.6}\text{Nb}_{2.4}\text{Br}_{14} \cdot 8\text{H}_2\text{O}$ with an optical spectrum different from that of a simple mixture of $\text{Nb}_6\text{Br}_{14} \cdot 8\text{H}_2\text{O}$ and $\text{Ta}_6\text{Br}_{14} \cdot 8\text{H}_2\text{O}$. To date, the determination of the mixed valence class and valence configurations of the $[\text{M}_6\text{X}_{12}]^{2+}$ polynuclear ions has been attempted using a simplified ligand-field theory analysis of optical spectra and magnetic susceptibility data together with X-ray structure analysis.

Cotton and Haas (159) first derived the molecular orbital ordering appropriate to the $[\text{M}_6\text{X}_{12}]^{2+}$ unit on the assumption that this ordering is determined, with one exception, solely by the various metal-metal interactions. From overlap considerations, they decided that the level ordering depended upon the internuclear separation and the effective nuclear charge, but that, for reasonable values of these parameters, a ground state³ with occupation

$$dxzdyz(t_{1u})^6 dz^2(a_{1g})^2 dxzdyz(t_{2g})^6 dxy(a_{2u})^2$$

was predicted, which is diamagnetic, as observed for the $[\text{M}_6\text{X}_{12}]^{2+}$ ions. The Cotton-Haas orbital diagram (Fig. 24) is derived under the assumption that the orbitals arising from $dx^2 - y^2$ are too high to be of any consequence, due to σ -bonding with the ligands. Kettle (414) concurs with Cotton and Haas as to the symmetries of the occupied levels. A second calculation on this system, which considered not only metal-metal but metal-ligand interactions as well (593), showed that the relative positions of the Cotton-Haas orbitals can depend not only upon the metal-metal interaction, but also upon the metal-ligand interaction. Thus, for example, for the MO's composed of metal atom dxy orbitals only, the level ordering is $a_{2u} < t_{2g} < e_u$, whereas, with the introduction of ligand orbitals into the calculation, an inverted ordering $e_u < t_{2g} < a_{2u}$ can be obtained. The MO's resulting from the "metal d plus ligand orbitals" calculations are shown in Fig. 25, for comparison with the original Cotton-Haas scheme. This second scheme, as proposed

³ Each molecular orbital of the ground state is composed of a linear combination of only certain of the d orbitals of the metal atoms. Thus, for example, taking z as the locally out-of-plane direction, a linear combination of dxz and dyz metal orbitals can be found which transforms like t_{1u} in the octahedral group, and, if it contains six electrons, is written as $dxzdyz(t_{1u})^6$. Similarly, in the ground state the a_{1g} combination of dz^2 orbitals has two electrons in it, etc.

originally, was constructed so as to give a reasonable explanation of the electronic spectra of the $[M_6X_{12}]^{2+}$ ions. In order to do this, it was found that an apparently low-lying $dz^2(a_{1g})$ orbital had to be left unoccupied in the ground state. This undesirable feature arises from the assumption

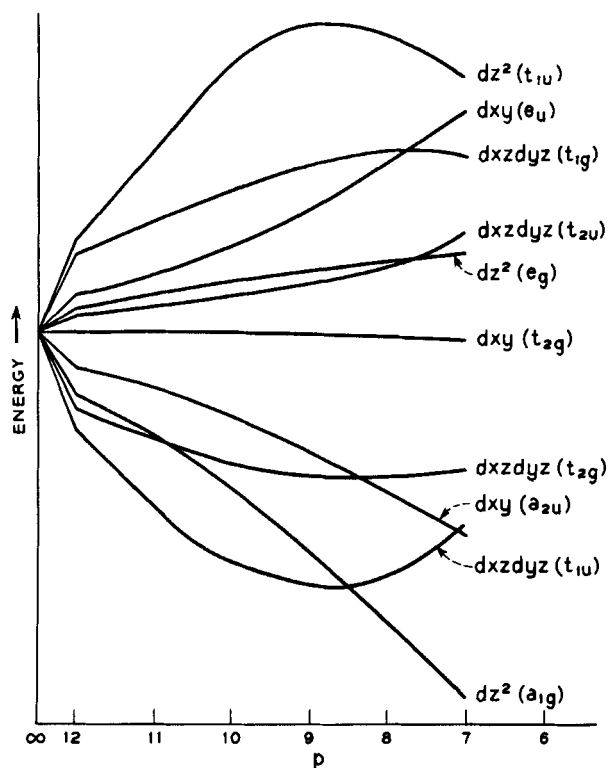


FIG. 24. The molecular orbital scheme for the $[M_6X_{12}]^{2+}$ ion as derived by Cotton and Haas (159). p is a variable equal to the product of the Slater orbital exponent of the metal d orbitals and the metal-metal distance.

that each metal atom is in the plane of the four halide ligands nearest it (local symmetry C_{4h}), when in fact the metal atoms are known to be displaced inward toward each other. As a result, the local symmetry is lowered to C_{4v} , and two of the three p orbitals on each ligand interact with the dz^2 manifold, raising it by an undetermined amount. Thus the closed-shell ground state configuration

$$dxzdyz(t_{1u})^6 dxzdyz(t_{2g})^6 dxy(e_u)^4$$

is attained without occupying $dz^2(a_{1g})$.

On oxidation to $[M_6X_{12}]^{3+}$, both Figs. 24 and 25 predict an ion having one free spin, as observed experimentally. The real test between these two diagrams rests on the prediction for the ion $[M_6X_{12}]^{4+}$. According to

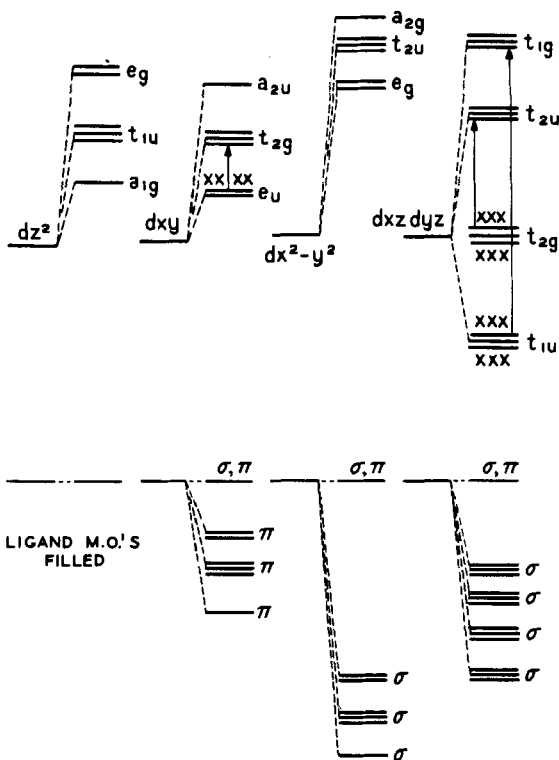


FIG. 25. The molecular orbital scheme for the $[M_6X_{12}]^{2+}$ ion according to Robin and Kuebler (593), as derived from the electronic spectrum.

Fig. 24, for p greater than 8.5, the $[M_6X_{12}]^{4+}$ ion has the closed-shell ground state configuration

$$dxzdyz(t_{1u})^6 dz^2(a_{1g})^2 dxzdyz(t_{2g})^6$$

whereas Fig. 25 predicts a triplet ground state

$$dxzdyz(t_{1u})^6 dxzdyz(t_{2g})^6 dxy(e_u)^2$$

provided that the $4+$ ion is not distorted so that the dxy (e_u) level is split and the electrons paired. Since the $[M_6X_{12}]^{4+}$ ions are claimed to be diamagnetic (471, 494), it would seem that the Cotton-Haas orbital ordering offers more hope for explaining the magnetic properties of these ions, provided that they are not badly distorted.

Electronic spectra of the niobium and tantalum subhalides have been recorded in the $10,000$ – $50,000$ cm^{-1} region by a number of invest-

igators (10, 447, 471, 593), but with only one attempt at interpretation (593). The electronic spectra of polynuclear complexes are complicated by the fact that the metal-metal transitions can be as strong as the

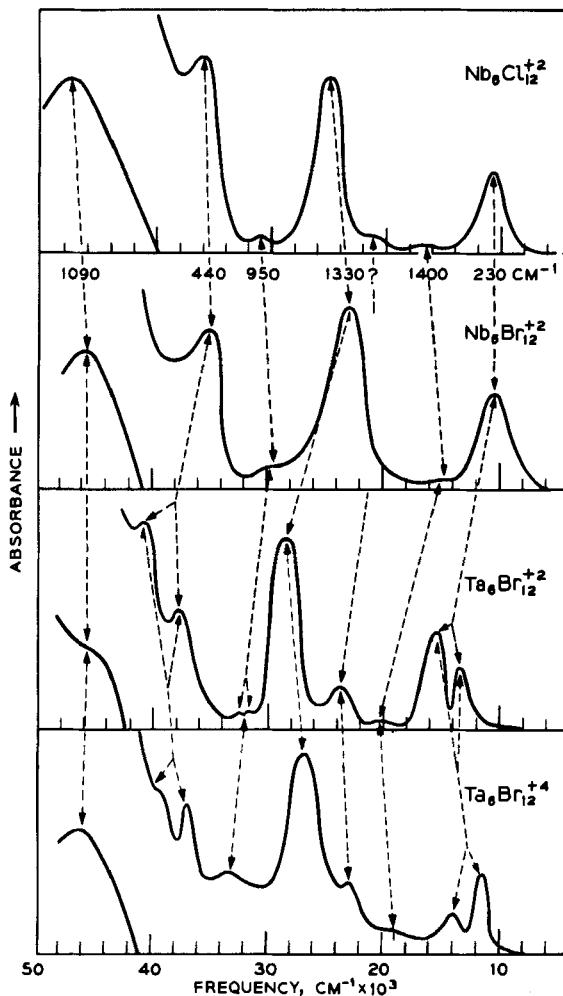


FIG. 26. Correlation of the electronic bands of oxidized and reduced $[M_6X_{12}]^{n+}$ ions in ethanol at -100°C (593).

ligand-metal charge transfer bands, so that a simple intensity argument cannot be used for their identification. In the $[M_6X_{12}]^{2+}$ series, the distinction, however, can be made by changing the ligand from, say, Cl to Br, so that the ligand-metal bands will identify themselves by a larger shift than the metal-metal bands. Figure 26 shows the spectra

of $[\text{Nb}_6\text{Cl}_{12}]^{2+}$ and $[\text{Nb}_6\text{Br}_{12}]^{2+}$ ions in alcohol at -100°C , from which it can be seen that the bands at $11,000\text{ cm}^{-1}$ and $36,000\text{ cm}^{-1}$ are allowed metal-metal transitions ($^1A_{1g} \rightarrow ^1T_{1u}$), all others being ligand \rightarrow metal charge transfer bands, on the basis of their much larger shift. The extinction coefficients of the various bands in aqueous solutions are given by Allen and Sheldon (10).

On comparing the spectra of the $[\text{Nb}_6\text{X}_{12}]^{2+}$ ions with the corresponding $[\text{Ta}_6\text{X}_{12}]^{2+}$ ions (Fig. 26), it is seen that the two metal-metal bands in the tantalum complexes have split into two components, each with intensity ratio 1:2. This splitting was interpreted as that expected of the triply degenerate $^1T_{1u}$ state for $[\text{Ta}_6\text{X}_{12}]^{2+}$ ions having an extended tetragonal distortion in solution. Spectra of the oxidized ions $[\text{Ta}_6\text{X}_{14}]^{4+}$ are very much like those of the reduced species, except that the intensity ratio of the split components is reversed, being 2:1, signaling a tetragonal distortion of the opposite sense (Fig. 26). The spectral similarities of the 2+ and 4+ ions in both the niobium and tantalum subhalides have been explained as the consequence of removing electrons from previously filled, triply degenerate levels on going from 2+ to 4+.

On the basis of this simple interpretation of the optical spectra, Robin and Kuebler concluded that, in ethanol solution, the $[\text{Nb}_6\text{X}_{12}]^{2+}$ ions are class III-A systems with all metal ions of formal charge $2\frac{1}{3}+$, whereas the $[\text{Ta}_6\text{X}_{12}]^{2+}$, $4+$ ions tend to trap integral valences through a tetragonal distortion. One might hope for some verification of these ideas through crystal structure analysis of a number of systems containing the M_6X_{12} ions. Figure 27 shows that there is no obvious regularity in the geometries of these species, except that, wherever a halogen coordinates to an M from outside the M_6X_{12} unit, the result is a displacement of that M atom outward from the symmetrical position. As concluded from the spectral study, it also appears that the distortions are larger in the tantalum complexes than in the niobium ones. The fact that the $[\text{Ta}_6\text{Cl}_{12}]^{2+}$ and $[\text{Ta}_6\text{I}_{12}]^{2+}$ octahedra have tetragonal distortions of the opposite sense demonstrates that these distortions are in large part due to crystal forces and not to any particular preferred electronic configuration of the ions.

An amazingly large number of stable compounds have been found in the niobium-oxygen system within the range $\text{NbO}_{2.50}$ – $\text{NbO}_{2.33}$. As compiled most recently by Gruehn and Schäfer (319, 320) and by Gruehn *et al.* (321), the following mixed valence oxides of niobium have been identified:

$\text{NbO}_{2.489}$ – $\text{NbO}_{2.500}$, $\text{NbO}_{2.482}$, $\text{NbO}_{2.480}$ ($\text{Nb}_{25}\text{O}_{62}$), $\text{NbO}_{2.467}$ – $\text{NbO}_{2.480}$, $\text{NbO}_{2.467}$, $\text{NbO}_{2.474}$ ($\text{Nb}_{19}\text{O}_{47}$?), $\text{NbO}_{2.466}$ – $\text{NbO}_{2.460}$, $\text{NbO}_{2.454}$ ($\text{Nb}_{22}\text{O}_{54}$), $\text{NbO}_{2.417}$ ($\text{Nb}_{12}\text{O}_{29}$), $\text{NbO}_{2.333}$ (Nb_9O_{21})

At present, the structures of only a few of these substances have been solved, yet certain regularities are already apparent.

On the basis of a determination of the crystal structure of the high temperature modification of the single valence material Nb_2O_5 ,

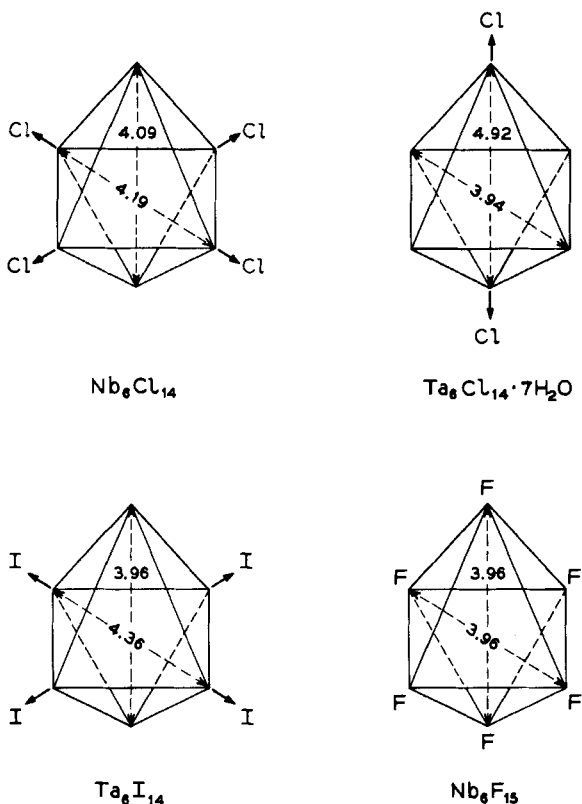


FIG. 27. Distortions of various M_6X_{12} octahedra induced apparently by the placement of halide ions on the fourfold axes of certain M ions, thereby lengthening the trans M-M distance in that direction.

Gatehouse and Wadsley (271) proposed that it is but a member of the general series $\text{Nb}_{3n+1}\text{O}_{8n-2}$, having $n = 9$. This structure consists of ReO_3 -type slabs of edge-sharing octahedra joined at the slab boundaries so as to form tetrahedral holes which are partly, but systematically, occupied by niobium atoms. Of the 28 niobium atoms in the Nb_2O_5 ($\text{Nb}_{28}\text{O}_{70}$) unit cell, 27 are in octahedral sites and one is in a tetrahedral site. It is proposed by them that the $n = 7$ mixed valence compound,

$\text{Nb}_{22}\text{O}_{54}$ ($\text{NbO}_{2.46}$), consists of smaller ReO_3 -type slabs, joined so that 21 of the niobiums are in octahedral sites and one is in a tetrahedral site, and that the $n = 5$ mixed valence compound, $\text{Nb}_{16}\text{O}_{38}$ ($\text{NbO}_{2.375}$), should it exist, would have one tetrahedrally and 15 octahedrally coordinated niobium atoms per unit cell. Although the two compounds $\text{NbO}_{2.48}$ ($\text{Nb}_{25}\text{O}_{62}$) and $\text{NbO}_{2.42}$ ($\text{Nb}_{19}\text{O}_{46}$) fit the formula for $n = 8$ and 6, respectively, Gatehouse and Wadsley point out that the members with even n will have a different crystal structure. Since the proposed $\text{Nb}_{3n+1}\text{O}_{8n-2}$ crystal structures would appear to trap valences readily, one is tempted immediately to try and assign valences to the various sites. The formula $\text{Nb}_{21}^{\text{V}}\text{Nb}^{\text{IV}}\text{O}_{54}$ fits nicely for $\text{Nb}_{22}\text{O}_{54}$, for it is postulated to have two sites in 21 : 1 ratio. However, $\text{Nb}_{16}\text{O}_{38}$ by this reasoning would have to be written as $\text{Nb}_{15}^{\text{V}}\text{Nb}^{\text{I}}\text{O}_{38}$.

A straightforward accounting of electrons in $\text{Nb}_{25}\text{O}_{62}$ shows that it must be written formally as $\text{Nb}^{\text{IV}}\text{Nb}_{24}^{\text{V}}\text{O}_{62}$. Although the structure of this mixed valence oxide has not been determined in detail, it is known to be isostructural with the titanoniobate $\text{Ti}^{\text{IV}}\text{Nb}_{24}^{\text{V}}\text{O}_{62}$ (538). Moreover, although there are 24 octahedral sites to every tetrahedral one in the titanoniobate, the analysis indicates that the structure is partly inverted, in that all the sites appear to be occupied by either niobium or titanium in a random manner. If this is also true for $\text{Nb}_{25}\text{O}_{62}$, then it is a class II or class III system, rather than class I as intimated by the one-to-one correspondence of the numbers of the two types of site available and the numbers of niobium atoms of valency 5+ and 4+. Accepting a class II electronic structure for $\text{Nb}_{25}\text{O}_{62}$, it is reasonable then to postulate that its black color is in large part due to an $\text{Nb}(\text{IV})$ ($4d^1$), $\text{Nb}(\text{V})$ ($4d^0$) mixed valence class II transition, whereas $\text{TiNb}_{24}\text{O}_{62}$ is colorless due to the substitution of $\text{Nb}(\text{IV})$ ($4d^1$) by $\text{Ti}(\text{IV})$ ($3d^0$) and the consequent loss of the optical electrons.

Norin (539) has found monoclinic $\text{Nb}_{12}\text{O}_{29}$ to be an example of a Magneli phase containing corner-sharing blocks of NbO_6 octahedra, as in the ReO_3 -type structure, with edgesharing between blocks. This finding raises the possibility that $\text{Nb}_{12}\text{O}_{29}$ is but one member of a family of mixed valence niobium oxide Magneli phases. The titanoniobate $\text{Ti}_2^{\text{V}}\text{Nb}_{10}^{\text{V}}\text{O}_{29}$ is isostructural with $\text{Nb}_{12}\text{O}_{29}$ (538), and, as with the $\text{Nb}_{25}\text{O}_{62}$, $\text{TiNb}_{24}\text{O}_{62}$ pair mentioned above, $\text{Nb}_{12}\text{O}_{29}$ is black but $\text{Ti}_2\text{Nb}_{10}\text{O}_{29}$ is colorless.

Similarly, Nb_9O_{21} , recognizable as $\text{Nb}_3^{\text{IV}}\text{Nb}_6^{\text{V}}\text{O}_{21}$, is isostructural with $\text{Ti}_3^{\text{IV}}\text{Nb}_6^{\text{V}}\text{O}_{21}$ (740), a substance in which the titanium and niobium sites are both distorted octahedral. Thus, this compound is a class II system, bordering on class III. There are, however, no short metal-metal distances here so the substance may not show metallic conductivity. Although the

oxide $\text{Nb}_{22}\text{O}_{54}$ (537) can be written as $\text{Nb}_2^{\text{IV}}\text{Nb}_{20}^{\text{V}}\text{O}_{54}$, there is no evidence that its valences are trapped. Structural work has yet to be done on the other oxides mentioned above.

An electron diffraction study of oxidized thin films of niobium reveals the existence of Nb_3O_5 , a cubic compound thought to contain the niobium ions in distorted octahedral coordination (424).

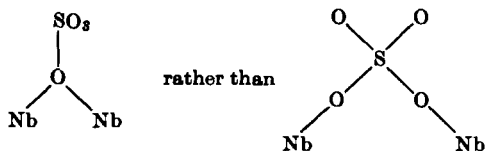
In the tantalum-oxygen system, Schönberg (642) reports a black phase (ϵ) of composition intermediate between TaO_2 and Ta_2O_5 having a complicated crystal structure. The only other compounds in this system of possible mixed valence interest are the metallic lower oxides TaO_x , having x much smaller than 1. Niebuhr has recently presented a critical evaluation of the properties of these substances (532), as well as of the oxides of niobium (533).

The importance of recognizing that such seemingly nonstoichiometric substances as the niobium oxides are, like the titanium, vanadium, molybdenum, and tungsten oxides, stoichiometric mixed valence compounds in disguise, is amply demonstrated by the studies of the electrical conductivity of "nonstoichiometric $\alpha\text{-Nb}_2\text{O}_5$ " [(377) and references cited therein]. Extensive work on materials ranging in composition from $\text{NbO}_{2.4996}$ to $\text{NbO}_{2.4284}$ shows that their resistivity is 0.1–0.01 ohm cm at 1000°C with an average carrier mobility of 0.22 $\text{cm}^2\text{V}^{-1}\text{sec}^{-1}$. These data have been interpreted in detail, using a model which presumes that the materials contain electron pairs trapped in oxygen ion vacancies, and that the electrical conductivity arises from the thermal excitation of electrons from these traps into a narrow 4d conduction band. We can see now that Nb(IV) , Nb(V) compounds were in fact involved here, and that the conductivity might be more properly explained as arising from the thermal ionization of Nb(IV) ions.

Krylov *et al.* (445) report the mixed metal oxide, NbCuO_3 , in which both of the valence isomers can exist as stable phases. Thus, the sintering of Cu_2O with Nb_2O_5 yields diamagnetic $\text{Cu}^{\text{I}}\text{Nb}^{\text{V}}\text{O}_3$, whereas the sintering of CuO with NbO_2 yields paramagnetic $\text{Cu}^{\text{II}}\text{Nb}^{\text{IV}}\text{O}_3$ ($\mu_{\text{eff}} = 1.10$ B.M.). Powder patterns confirm the individuality of these valence isomers as well as those in the corresponding TaCuO_3 system.

The very large number of stable halide complexes built upon the Nb_6 octahedral framework suggests the possibility of formation of Nb_6 polynuclear complexes with other than halide ligands. The red compound $\text{K}_8\text{Nb}_6\text{O}_3(\text{SO}_4)_{12} \cdot 21\text{H}_2\text{O}$ (294, 417, 444) and the corresponding ammonium salt $(\text{NH}_4)_8\text{Nb}_6\text{O}_3(\text{SO}_4)_{12} \cdot 12\text{H}_2\text{O}$ (297, 508) would seem to be examples of just such complexes. Although no structural work has been done on these systems, it seems reasonable to predict that the niobium sulfates contain the Nb_6 octahedron with bridging sulfate

groups, and quite possibly OH^- ions situated on the fourfold axes of the niobium ions. In order to maintain the all-important Nb—Nb direct metal-metal bonding, it is necessary to postulate bridges of the form



The niobium sulfates are soluble in sulfuric acid and in this solvent the red ions migrate to the anode in an electric field, thus demonstrating their negative charge. If the colored ions are indeed M_6X_{12} species, the overall negative charge can result only if X is SO_4^{2-} , and not if X is OH^- .

Krylov and Kalugina (444) have measured the magnetic susceptibility of the crystalline salt $\text{K}_8\text{Nb}_6\text{O}_3(\text{SO}_4)_{12} \cdot 21\text{H}_2\text{O}$ and found an effective moment of 2.0 B.M. per molecule. However, this value is uncorrected for temperature-independent paramagnetism, a factor which seems to be large in the niobium polynuclear complexes (471). Application of a temperature-independent paramagnetism correction, amounting to 600×10^6 cgs, reduces Krylov and Kalugina's effective moment to 1 B.M., a value sufficiently low that it raises doubt as to whether the substance is really paramagnetic or is simply diamagnetic but impure. The latter seems possible for it is known that the substance in question can react further to produce blue substances thought to contain Nb(III) (417).

The hypothetical $[\text{Nb}_6(\text{SO}_4)_{12}]^{2-}$ unit contains eight niobium 4d electrons in metal-metal bonds. According to the scheme of Robin and Kuebler (593) (Fig. 25), the metal-metal electronic configuration for such a system would be

$$dxzdyz(t_{2g})^2 dxzdyz(t_{1u})^6$$

giving a triplet ground state. On the other hand, the Cotton and Haas (159) ground state would be

$$dz^2(a_{1g})^2 dxzdyz(t_{1u})^6$$

which is a spin singlet. Should an X-ray crystallographic study show the presence of *symmetrical* Nb_6X_{12} complexes in the niobium sulfates, an accurate determination of the magnetic susceptibility then would be of great value in deciding between the Robin-Kuebler and Cotton-Haas orbital schemes, although as it stands the Cotton-Haas scheme seems to be the better one.

K. MOLYBDENUM AND TUNGSTEN

With very few exceptions, the mixed valence compounds of molybdenum and tungsten have oxide ion as ligand. The existence of well-defined phases with formulas intermediate between MO_2 and MO_3 has been recognized for many years, but it is primarily as a result of the extensive crystallographic investigations of Hägg, Magneli, Kihlberg, and their collaborators that the structural principles governing their

TABLE IV
MIXED VALENCE MOLYBDENUM OXIDES

MoO_x	Formula	Phase	Structure	Resistivity (ohm cm, 300°K)
3.000	MoO_3	α	MoO_3	$> 10^7$ (419)
2.889	$\text{Mo}_{18}\text{O}_{52}$	ξ	MoO_3	250 (419), 932 (279)
2.889	Mo_9O_{26}	β'	ReO_3	3.7 (419), 3.95 (279)
2.875	Mo_8O_{23}	β	ReO_3	1.2 (419)
2.800	Mo_5O_{14}	θ	Mixed polygonal	< 0.05 (419)
2.765	$\text{Mo}_{17}\text{O}_{47}$	χ	Mixed polygonal	0.2 (419), 0.59 (279)
2.750	Mo_4O_{11}	η	ReO_3	0.25 (419), 1.50 (279)
2.750	Mo_4O_{11}	γ	ReO_3	
2.000	MoO_2	δ	Distorted rutile	

formation are now well established. The most important results of these labors have been several times reviewed (328, 422, 474), and we shall therefore include only a brief outline here.

The seven mixed valence compounds within the composition range $\text{MoO}_{2.75}$ – MoO_3 which have been identified from phase analyses based on X-ray powder (279, 419) and single crystal measurements (422), as well as differential thermal analysis (598), are listed in Table IV. Within this composition range, three basic structure types may be distinguished: ReO_3 , MoO_3 , and what Kihlberg (422) has called the “mixed-polygonal” type. In the “homologous” (476) series with the general formula $\text{M}_n\text{O}_{3n-1}$, based on the ReO_3 lattice, examples having $n = 8$ and 9 have been prepared which contain only molybdenum, but by incorporating increasing concentrations of tungsten it is possible to obtain further members with $n = 10, 11, 12$, and 14. The ReO_3 structure, which can be regarded as built up from MO_6 octahedra linked exclusively at the corners, extends

infinitely along only one axis in the compounds belonging to the M_nO_{3n-1} series, thus forming finite slabs whose width is determined by the value of n . In Fig. 28, the structure of Mo_8O_{23} shows how the slabs are connected through sharing of edges between the octahedra at the slab boundaries. In this way, clusters of four octahedra sharing edges occur throughout the structure, as indicated by the heavy lines. The other structures based on ReO_3 are the two forms of Mo_4O_{11} , in which the slabs of connected octahedra are joined by tetrahedra which share corners with the octahedra of two neighboring slabs. No tetrahedra or octahedra share edges in this structure.

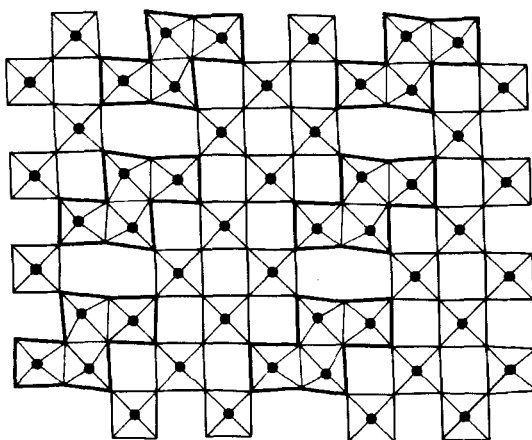


FIG. 28. The crystal structure of Mo_8O_{23} (422). The metal atom clusters are outlined in *bold lines*, while the metal atoms themselves are represented by the *filled circles*, and the oxygen atoms are found above and below the metal atoms and at the apices of the squares.

In the structures based on MoO_3 , e.g., $Mo_{18}O_{52}$, slabs of the basic lattice are once again connected by edgesharing, but, in addition, some of the metal atoms occur in tetrahedral sites. The lattices called "mixed polygonal" are distinguished by a complicated connection of coordination polyhedra in two dimensions, in which not only distorted octahedra but pentagonal bipyramids occur. This class includes mixed valence compounds such as Mo_5O_{14} and $W_{18}O_{49}$ (473), as well as single valence mixed oxides such as $MoW_{11}O_{36}$ and $MoW_{14}O_{45}$ (304). It is also interesting to note the similarity with the tunnel lattices occurring among the tetragonal and hexagonal tungsten bronzes. In the mixed polygonal oxides, the equatorial edges of the pentagonal bipyramids are shared with octahedra so that there exist pronounced metal atom clusters

(Fig. 29), which are still further condensed in $\text{Mo}_{17}\text{O}_{47}$ and $\text{W}_{18}\text{O}_{49}$ by edgesharing between pairs of octahedra attached to neighboring pentagonal clusters. Considerable variations in metal-oxygen and metal-metal distances are needed to accommodate these structural complexities, although it should be noted that they are not necessarily the result of mixed valence interactions, since MoO_2 and WO_2 are themselves distorted from rutile lattices in such a way that the metal atoms appear to form pairs (472).

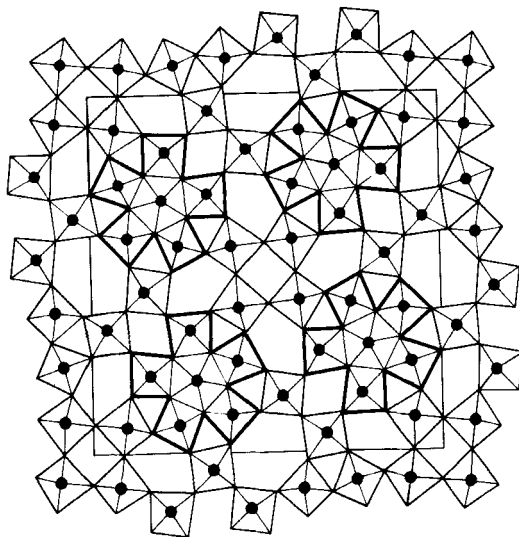


FIG. 29. The crystal structure of Mo_5O_{14} (422). The *filled circles* represent the metal atoms, and oxygen atoms are found above and below the metal atom and at the apices of the squares. The "mixed polygonal" metal clusters are indicated by the *bold lines*.

In contrast to the effort devoted to structure determinations in this series of compounds, very little has been reported which might enable one to rationalize their electronic structures with their complicated stereochemistries and stoichiometries. In closing his most recent review of the structural chemistry of the molybdenum oxides (422), Kihlborg remarks that definite conclusions about the variations in the distortion of the Mo—O coordination with valence state cannot be drawn until reliable measurements of basic physical properties, such as magnetism, have been made. Some of the distortions from regular octahedral coordination may perhaps be accounted for by "rattling" of the small cations, as originally proposed by Orgel (545). Ionic radii of Mo(IV) and Mo(VI) are in the range where this might be expected to occur.

Attempts have been made (422) to fit the observed bond lengths d_n in many of the compounds to a logarithmic relationship with bond number, n , of the kind proposed by Pauling (564)

$$d_n - d_1 = 2k \log n$$

using values for d_1 and k which fit the observed lengths in MoO_3 , and the assumption that $\Sigma n = 2$ for each oxygen atom. The sums Σn_{Mo} for the two modifications of Mo_4O_{11} were taken to suggest that there is a gradual increase in the valence state of the metal atoms from the middle of the basic ReO_3 slab toward the outside, in accord with a previous suggestion (477) that decreasing valency favors the occurrence of higher coordination numbers. However, the tenuous theoretical basis of Pauling's equation makes it difficult to use the "bond number" criterion to decide whether the valences are partly or wholly trapped. From the low resistivities of all except one of the mixed valence oxides (279, 419), one is tempted to conclude that no definite lattice sites or coordination numbers are to be allocated to specific valence states in these compounds, i.e., the compounds are very close to class III-B. Thus in Mo_4O_{11} , for example, 3/4 of the molybdenums are octahedrally coordinated and 1/4 are tetrahedrally coordinated and, furthermore, the formula is compatible with the existence of one Mo(IV) for every three Mo(VI), so at first glance the compound might appear to be a class I mixed valence system. On the other hand, the room temperature resistivity of this compound is less than 1 ohm cm (279, 419) and the bond length arguments of Kihlberg (422) suggest that the tetrahedral sites might be preferentially occupied by Mo(VI). The valence distribution would then be rather like that of an inverse as compared with a normal spinel. Nevertheless, it might prove possible to rationalize the occurrence of blocks of ReO_3 structure, together with regions of metal atom clustering in oxides such as Mo_8O_{23} or Mo_5O_{14} , by deriving bonding schemes similar to those suggested by Cotton (160) for the trinuclear single valence cluster in $\text{Zn}_2\text{Mo}_3\text{O}_8$. If we start from the assumption that the octahedra joined only through their apices contain metal ions trapped as hexavalent, and then apportion the extra electrons corresponding to the Mo(IV) or Mo(V) to the region of the clusters, we find that two d electrons are to be distributed within each cluster of four edgesharing octahedra in the $\text{M}_n\text{O}_{3n-1}$ series. Similarly, four d electrons would have to be assigned to each cluster of six molybdenums in the "mixed polygonal" series. Overlap between d orbitals on adjacent metal atoms in the former case is expected to be greatest for the dxy orbitals, which are nonbonding between metal and oxygen, but which could form σ bonds within the metal cluster. The orbital combination with the phases

shown in Fig. 30 is strongly σ -bonding and nondegenerate, and would therefore accommodate the two "extra" electrons. Unfortunately, the metal-metal distances within the clusters are not notably shorter than that expected for two normally bonded octahedra sharing edges, and there is no evidence that spin pairing of the kind postulated here actually occurs.

All the mixed valence molybdenum oxides are described as blue or blue-violet (422), but no spectra have been reported and care is needed in interpreting their colors as MoO_2 is itself reddish brown. Finally, there

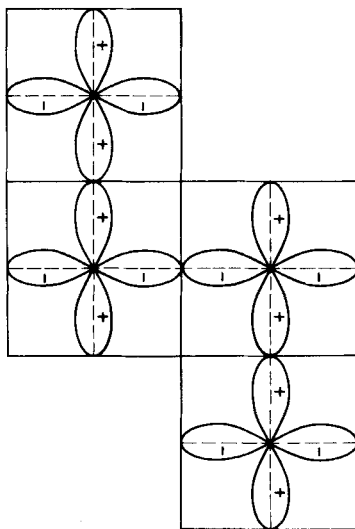


FIG. 30. A possible mode of dxy bonding within the metal atom clusters of Mo_8O_{23} .

is not even conclusive evidence that these systems involve the 4+ and 6+ rather than 5+ and 6+ oxidation states. Once again, unfortunately, our conclusion must be that a great deal more physical evidence will be needed before definite conclusions can be drawn about the electronic structures of these interesting compounds. Magnetic and spectroscopic measurements will be the most profitable lines of attack.

A much more highly reduced mixed valence oxide, Mo_3O , was reported to form when mixtures of Mo and MoO_2 were heated (643), but the preparation could not be repeated (420).

When polymolybdate(VI) and polytungstate(VI) anions are reduced in aqueous solution, the dark blue colors of the products suggest that their electronic structures may be related to those of the mixed valence

molybdenum and tungsten oxides. The photochemical reduction of polymolybdates and tungstates has been studied in connection with photographic processes (132, 789). Molybdenum blue was prepared as long ago as 1805 (110) and since then very many investigations have been reported (289), but little progress could be made in sorting out the variety of products until the structures of the parent iso- and hetero-polyanions had been determined. It was Keggin (408) who first showed that anions with the general formula $[A^{n+} X_{12}O_{40}]^{(8-n)-}$, where A may be a transition or main group element and X is Mo(VI) or W(VI), consisted of compact groups of XO_6 octahedra sharing edges and surrounding the central ion A with a tetrahedron of oxygen atoms. Further members of the series are described and illustrated by Wells (756).

Many of the attempts to characterize solid molybdenum blue compounds have been frustrated by the colloidal nature of the reduction products and the difficulty of isolating them with reproducible amounts of water. Thus Sacconi and Cini (613) claimed to have prepared a continuous series of amorphous blues with Mo(VI):Mo(V) ratios between 3.4 and 6, and Glemser and Lutz (280) showed that not only blue anhydrous oxides, but crystalline hydrates as well, could be prepared by solid phase reactions. However, only the products $Mo_4O_{10}(OH)_2$ and $Mo_8O_{15}(OH)_{16}$ were characterized by X-ray analysis. Both were insoluble in water and stable to alkali, but a range of water-soluble, amorphous products was also prepared. The final reduction product of MoO_3 with zinc in concentrated HCl is a crystalline olive-green Mo(IV) compound, $Mo_5O_5(OH)_{10}$, which when placed in vacuum loses hydrogen to give a red mixed valence compound $Mo_5O_7(OH)_8$ (284). By reducing $WO_3 \cdot H_2O$ and $WO_3 \cdot 2H_2O$ with zinc and HCl, Glemser *et al.* (285) have also succeeded in preparing a series of blue tungsten oxide hydrates which they related to the molybdenum oxides, using X-ray powder diagrams.

In contrast to the variety of solid molybdenum blues, evidence has accumulated that, in homogeneous aqueous solution, reduced species based on the isopolymolybdate structure exist in very limited numbers. When molybdic acid solutions were reduced electrolytically and extracted with butanol, the ratio Mo(VI):Mo(V) in aqueous solutions of the extract was 2.0 (23), a result in accord with the variation in the optical density at $13,300\text{ cm}^{-1}$ as a function of Mo(VI): Mo(V) ratio (675). At higher pH than is needed to form blue solutions, there is also spectrophotometric evidence for a brown hexamolybdate anion with Mo(VI):Mo(V) = 1, which has an absorption maximum at $22,200\text{ cm}^{-1}$ (547), and another having Mo(VI):Mo(V) = 0.5, in which the absorption maximum has shifted even further to the ultraviolet, to $30,800\text{ cm}^{-1}$ (548).

The reduction of 12-heteropolymolybdates and tungstates in aqueous solution has proved rather easier to study than that of the isopolyacids either in solution or in the solid state. It is now quite clear, as a result of polarographic (309–311, 571, 673, 674) and potentiometric (571, 690, 691) work, that these anions can accept limited numbers of electrons, e.g., up to four, without decomposition, and, in a number of instances, salts of the reduced anions have been isolated (331, 332). The values (571) of the reduction potentials for addition of the first electron to $[\text{PW}_{12}\text{O}_{40}]^{3-}$, $[\text{SiW}_{12}\text{O}_{40}]^{4-}$, $[\text{Fe}^{\text{III}}\text{W}_{12}\text{O}_{40}]^{5-}$, and $[\text{Co}^{\text{II}}\text{W}_{12}\text{O}_{40}]^{6-}$ vary with the charges in a way consistent with a model that treats the anion simply as a charged sphere. This suggests that the first electron goes into an orbital whose energy is nearly independent of the central atom. The fact that the spectra of silicomolybdates, to which two and four electrons have been added, remain very similar as to both energy and intensity (676) also suggests that the electrons are entering orbitals that are localized on particular metal atoms. There has been some disagreement about the existence of one- and three- in addition to two- and four-electron reduction products; only the latter have been isolated as solid salts (331, 332), and had been detected by Souchay (673) in his original polarographic work. However, more recently, waves due to the one-electron step have been located by two groups (571, 677). The absorption spectra of various reduced 12-silicomolybdates (676, 677) are shown in Fig. 31.

In one case at least there is clear evidence for the occurrence of Mo(V) in a reduced polymolybdate. By γ -irradiation of polycrystalline ammonium heptamolybdate, $(\text{NH}_4)_6\text{Mo}_7\text{O}_{24} \cdot 6\text{H}_2\text{O}$ (562), paramagnetic centers are formed which, from their ESR spectra, can be identified with NH_3^+ and Mo(V) ions. Irradiation at room temperature gave Mo(V) spectra which were almost isotropic, the major absorption coming from isotopes with $I = 0$, with a smaller contribution from Mo^{95} and Mo^{97} with $I = 5/2$. The most interesting feature, however, is the presence of a further hyperfine interaction between the unpaired electron of the Mo(V) and the $I = 5/2$ isotope of a neighboring Mo(VI). We therefore conclude that this system at least belongs to class II of our classification, and that the first electronic transition will contain an appreciable component of charge transfer. Similar experiments on the crystalline heteropoly-blue salts or their frozen solutions would be extremely interesting. Proton nuclear magnetic resonance spectra of a number of heteropoly-blue acids have recently been measured in the solid state (484), and interpreted as resulting from fast exchange between protons bound to oxygen atoms of the anions and those attached to crystal water molecules. That a nuclear magnetic resonance spectrum can be observed at all in these substances

seems to imply that the anions are diamagnetic. Once again, magnetic measurements would be valuable.

It is not our intention to attempt a review of the very large amount of work carried out on the other class of mixed valence molybdenum and

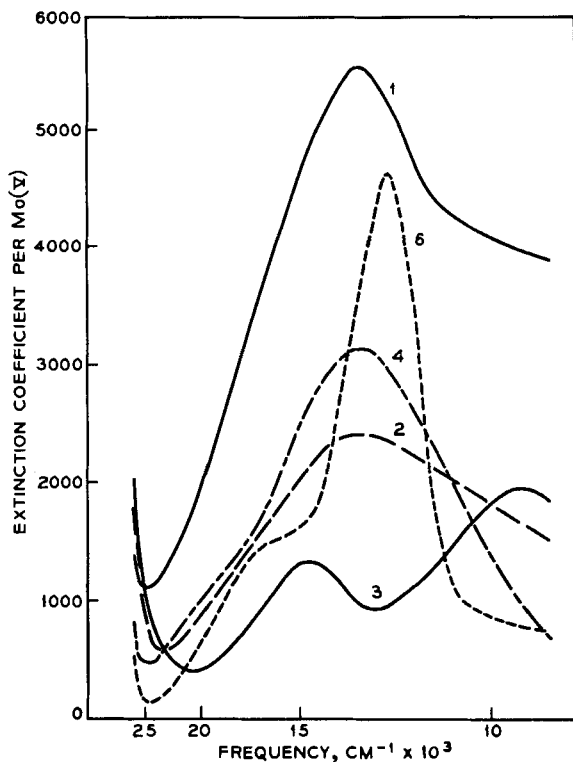


FIG. 31. The electronic spectra of 12-silicomolybdates reduced by 1-6 electrons, as indicated by the labels on the spectral curves (676).

tungsten oxides, the bronzes, since this has recently been done quite thoroughly by others (421, 694). Nevertheless it is worth emphasizing that the volume of physical measurements on these compounds far surpasses that reported for the other reduced group VI-B oxide systems considered here, and that the level of understanding of the electronic properties is correspondingly higher. We will merely record some of the more important conclusions about the crystal and electronic structures of these interesting compounds.

Hägg (326) was the first to show that the bronzes could be given a general formula $A_x\text{WO}_3$, where A was an alkali metal and x varied continuously from about 0.3 to nearly 1.0. At the latter extreme the structure approximates that of a perovskite, while for low values of x the structure goes through various lower symmetry modifications, all based on the lattice of WO_3 . At all A concentrations the tungsten atoms are equivalent and the lattice is a clear example of a class III-B mixed valence system. Ionization of the alkali metal atoms produces electrons which are evenly distributed among all the tungsten atoms. In agreement with this, the sodium bronzes in which x lies between 0.5 and 0.9 behave as metallic conductors between 4° and 800°K (217), with Hall effect coefficients which suggest that each sodium atom contributes one free electron to the conduction band (268). Further evidence that the sodium atoms lose their valence electrons completely into a conduction band that extends only across the tungsten atoms comes from nuclear magnetic resonance experiments (391), which show that the ^{23}Na resonance has an extremely small Knight shift. At high temperatures, the conductivity is nearly proportional to the sodium concentration (217), and the mobility is independent of the electron concentration. The fact that the conductances of lithium, sodium, and potassium tungsten bronzes lie on the same curve when plotted against x (421) also suggests that the alkali metal atoms do not participate directly in the conduction process.

Attempts to prepare molybdenum bronzes by reducing MoO_3 with alkali metal vapors always lead to MoO_2 , and it was only very recently that the first compounds of this type were prepared by electrolyzing fused mixtures of K_2MoO_4 and MoO_3 (789). Two samples have been definitely characterized: $\text{K}_{0.26}\text{MoO}_3$, which formed reddish plates and behaved as a typical semiconductor, and $\text{K}_{0.28}\text{MoO}_3$, a blue compound that conducted like a metal above -100°C . Despite their similarity in composition, the structures of the two compounds were different; the former contained subunits of six and the latter of ten MoO_6 octahedra sharing edges (305, 684). The subunits formed layers by sharing corners and the layers were linked together by the potassium ions. A sodium molybdenum bronze in the same composition range has also been reported (685).

The only other mixed valence molybdenum and tungsten compounds beside the oxides are a small number of halides. When yellow $[\text{W}_6^{\text{VI}}\text{Br}_8]\text{Br}_4$ is reacted with bromine at various temperatures (633, 662), compounds such as W_6Br_{14} , W_6Br_{16} , and W_6Br_{18} can be isolated. These dissolve in ethanol to give intensely red solutions, whose spectra are by no means the superposition of those of W_6Br_{12} and Br_2 . The suggestion is that

$[\text{W}_6\text{Br}_8]^{n+}$ mixed valence ions with structures like $[\text{Nb}_6\text{I}_8]^{3+}$ may be formed. The other mixed valence halide results from reactions between MoF_6 and various main group chlorides, e.g., CCl_4 , and, on the basis of conductance, infrared, and magnetic measurements, has been assigned the formula $[\text{Mo}_3^{\text{IV}}\text{Cl}_9][\text{Mo}^{\text{V}}\text{F}_6]_3$ (543, 686). The trinuclear $[\text{Mo}_3^{\text{IV}}\text{Cl}_9]^{3+}$ cation is assumed to have a similar core structure to that found in $[\text{Re}_3\text{Cl}_{12}]^{3-}$ and $\text{Re}_3\text{Cl}_{12}$. Since the anion is colorless and the cation itself is orange, the reported orange color of the salt suggests that there is no interaction absorption in the visible region and that the salt is a simple class I example.

L. TECHNETIUM AND RHENIUM

No mixed valence compounds of either of these elements appear to have been prepared, with the single exception of $(\text{NH}_4)_3\text{Tc}_2\text{Cl}_8 \cdot 2\text{H}_2\text{O}$ (213). The compound forms shiny black crystals which dissolve in HCl to give a turquoise blue solution having a broad absorption band at $16,300\text{ cm}^{-1}$. Cotton has published a preliminary account of an X-ray diffraction study of this compound (162), which shows the presence of $[\text{Tc}_2\text{Cl}_8]^{3-}$ groups essentially isostructural with $[\text{Re}_2\text{Cl}_8]^{2-}$ (163). Each technetium atom lies at the center of a square of chlorine atoms, and a distorted octahedral coordination is completed by one of the water molecules and the other technetium atom at a distance of 2.13 \AA , a full 0.6 \AA shorter than the $\text{Tc}-\text{Tc}$ distance in the metal. Cotton has described the electronic structure of diamagnetic $[\text{Re}_2\text{Cl}_8]^{2-}$ in terms of a σ bond, two π bonds, and a δ bond between the metal atoms (161), and a comparable description would serve for the technetium analog, which has one more d electron and whose susceptibility is consistent with one unpaired spin per $[\text{Tc}_2\text{Cl}_8]^{3-}$ ion. An ESR measurement on the technetium compound would be exceptionally interesting, as Cotton's bonding scheme for $[\text{Re}_2\text{Cl}_8]^{2-}$ (161) assumes that the relative ordering of the σ , π , and δ orbitals of the metal-metal bond is entirely due to the difference in overlap between the pairs of, respectively, dz^2 , $dxzdyz$, and dxy orbitals on each metal atom. A more detailed consideration of the bonding, taking into account π -bonding between $dxzdyz$ and the chlorine atoms, and σ -bonding between dz^2 and the water molecule, might very easily alter this relative ordering, as we noted in the case of the niobium and tantalum subhalides. It is only fair to say, however, that since the lowest empty orbital, δ^* , is not appreciably antibonding, Cotton's scheme does suggest that the $\sigma^2\pi^4\delta^2$ configuration of $[\text{Re}_2\text{Cl}_8]^{2-}$ might easily add an extra electron, forming a mixed valence system isoelectronic

with $[\text{Tc}_2\text{Cl}_8]^{3-}$. Oxidation and reduction experiments on $[\text{Re}_2\text{Cl}_8]^{2-}$ and the other rhenium halide cluster complexes might lead to other interesting class III-A mixed valence clusters.

M. RUTHENIUM AND OSMIUM

Easily the most famous ruthenium mixed valence compound is the one called "ruthenium red." It is usually prepared by allowing aqueous ruthenium trichloride to react with an excess of ammonia (388), or by exposing solutions of $\text{Ru}(\text{NH}_3)_6\text{Cl}_3$ in aqueous ammonia to air (252). Solutions of the compound have an extremely intense rose color; indeed, it has been said that a $2 \times 10^{-7} M$ solution is clearly pink. The color becomes fixed to silk, although not to wool or cotton, and has been used commercially as a dyestuff. Joly (388) formulated ruthenium red as $\text{Ru}_2\text{Cl}_4(\text{OH})_2 \cdot 7\text{NH}_3 \cdot 3\text{H}_2\text{O}$ and Morgan and Burstall (512), who prepared from it compounds which they thought were monomeric, formulated it as $[\text{Ru}(\text{OH})\text{Cl}(\text{NH}_3)_4]\text{Cl} \cdot \text{H}_2\text{O}$. Gleu and Breuel (286) showed that the latter could not be correct, as $[\text{Ru}(\text{OH})\text{Cl}(\text{NH}_3)_4]^+$ would have an effective magnetic moment of almost 2 B.M. and would be virtually colorless, whereas ruthenium red is only very weakly paramagnetic, if at all, and shows a most intense coloration.

In a very careful investigation, Fletcher *et al.* (252) found that ruthenium red contains no complexed chloride ions, and behaves as a trinuclear cation with a ruthenium: ammonia ratio of 3:14. The average oxidation number of the ruthenium, 10/3, then points to a formula



containing two oxo bridges. The molar extinction coefficient per ruthenium atom is 21,000 at the band maximum, $18,800 \text{ cm}^{-1}$, but in acid solution a reversible oxidation leads to the formation of a brown compound, whose spectrum appears to contain the same band shifted to higher energy ($21,700 \text{ cm}^{-1}$, $\epsilon = 14,100$) (Fig. 32). Ruthenium red has an effective magnetic moment of 0.77 B.M. per metal atom if no diamagnetic correction is made, whereas the moment of the brown compound is 1.13 B.M. per metal atom. The difference, $3(1.13 - 0.77) = 1.1$ B.M., is nearly equivalent to one electron per molecule. The spectra of both the red and brown compounds shift slightly to lower energy with increasing pH, suggesting that in basic solution they were being partly deprotonated.

Jorgensen and Orgel (399) explained the stability of the presumed linear ruthenium red framework as the result of π -bonding between the t_{2g} orbitals of the metal atoms and the $2p \pi$ orbitals of the oxygen atoms.

Aside from the σ -bonding in the linear cation, ten π molecular orbitals can be formed which group themselves as five pairs of doubly degenerate levels, with two pairs bonding, two antibonding, and one nonbonding. As there are 16 π electrons in the system, the π manifold in the ground state is filled up to and including the second highest antibonding pair, so that the net effect is a π -bonding stabilization in addition to the σ bonds. In such a linear system, the first transition is allowed, but the

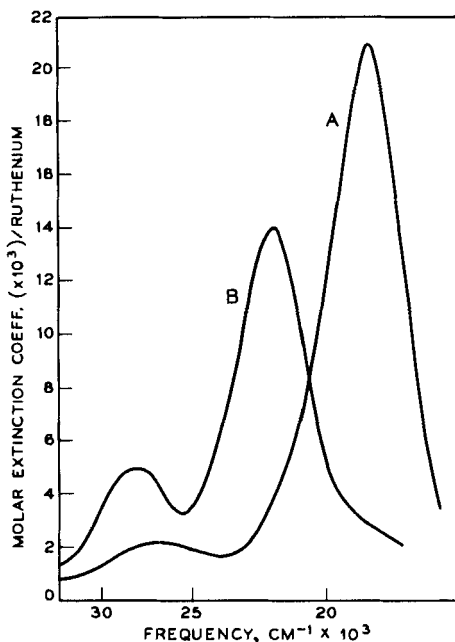
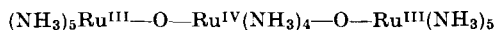


FIG. 32. The electronic spectrum of the ruthenium red cation $[\text{Ru}_3\text{O}_2(\text{NH}_3)_{14}]^{6+}$ in water (A), and the brown cation $[\text{Ru}_3\text{O}_2(\text{NH}_3)_{14}]^{7+}$ in 0.01 *N* HNO_3 (B) (252).

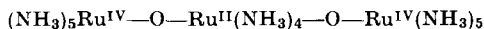
second is forbidden (as observed in Fig. 32, curve A). However, because the intensity of the first band decreases whereas that of the second band increases on bending the molecule, the spectrum of the oxidized ion (curve B) suggests that it is more bent than the reduced ruthenium red.

Regardless of whether ruthenium red is linear or bent, the ion at first appears to be class II, with the terminal ruthenium atoms in principle being clearly distinguishable from the bridging one. However, the unusually high molar extinction coefficient of 61,500 for the first band of ruthenium red in water suggests that α is very large indeed (Eq. 14), and that the delocalization of valences approaches that for

class III-A. This is confirmed by the magnetic susceptibility study, for if ruthenium red were class II with valences trapped as either



or



it would have an effective magnetic moment per ruthenium of 2.2 or 2.3 B.M., whereas 0.77 B.M. is observed, a large part of which may be temperature-independent paramagnetism. The large depression of the effective magnetic moment follows from the strong interaction between the ruthenium atoms via both π and σ bonds.

Other ruthenium mixed valence materials have been suggested as forming when RuO_4 in aqueous solution is reduced in the presence of trifluoroacetic acid (124), and it seems possible that the very dark blue-green precipitate obtained when solutions of $\text{K}_4\text{Ru}(\text{CN})_6$ are acidified after oxidation by chlorine (184, 439) may be the ruthenium analog of Prussian blue, for it analyzes as $\text{Ru}^{\text{II}}\text{Ru}^{\text{III}}(\text{CN})_5 \cdot \text{H}_2\text{O}$.

The literature appears to contain only one reference to a mixed valence compound of osmium, and doubt has been raised as to its constitution. $\text{Os}^{\text{III}}\text{Os}^{\text{IV}}\text{Cl}_7 \cdot 7\text{H}_2\text{O}$ is a red material, said to be possibly a mixture of OsCl_4 and OsOHCl_3 (290).

N. RHODIUM AND IRIDIUM

No rhodium compounds have been shown conclusively to be of mixed valence type. In ice-cold solution, ceric nitrate oxidizes a suspension of Cs_3RhCl_6 to a dark blue-green substance thought to be $\text{Cs}_2\text{Rh}^{\text{IV}}\text{Cl}_6$ (211, 212), but, since it appears that ozone oxidizes $\text{Rh}(\text{III})$ solutions to $\text{Rh}(\text{V})$ in the presence of excess chloride ions (57), the suggestion was therefore made that the Cs_2RhCl_6 salt may contain equimolar proportions of $\text{Rh}(\text{III})$ and $\text{Rh}(\text{V})$, like the isomorphous antimony compound. However, the diffuse reflectance spectrum of the blue-green compound, and its dilution in Cs_2PtCl_6 , sufficiently resemble that of Cs_2IrCl_6 to make it certain that the compound is indeed one of $\text{Rh}(\text{IV})$ (397, 398). Solutions of rhodium perchlorate of average oxidation number 4.5–5.3 (57) were said to exhibit further intense absorption bands in addition to those of $\text{Rh}(\text{III})$ and $\text{Rh}(\text{V})$, which may be taken as indicating the presence of mixed valence species in some of these solutions. The only other rhodium compound which is perhaps a mixed valence system is the dichloride (787) for which, as Kettle (413) pointed out, the original analyses agree much more closely with the formula $\text{Rh}_6\text{Cl}_{14}$. This is thus a potential example of the group of mixed valence compounds based on octahedral metal clusters, such as $[\text{Ta}_6\text{Cl}_{12}]^{2+}$.

Numerous mixed valence iridium compounds are based on a trimeric arrangement of iridium atoms bridged by sulfate groups. Lecoq de Boisbaudran (460) prepared what he thought was an Ir(III) double sulfate, $\text{Ir}_2(\text{SO}_4)_3 \cdot 3\text{K}_2\text{SO}_4$, which, unlike most Ir(III) salts, was not green but blue. His formulation was questioned by Delépine (187), whose analyses agreed better with the formula $\text{K}_{10}\text{Ir}_3(\text{SO}_4)_9$ and who also demonstrated that reducing agents turned the blue solution of the salt green. The original salt therefore apparently contained Ir(IV) as well as Ir(III). Delépine also prepared a green nitrido-iridium sulfate (186), which he showed, 60 years later (188), had the formula $\text{K}_4[\text{N}\{\text{Ir}(\text{H}_2\text{O})(\text{SO}_4)_2\}_3]$, i.e., it contained one Ir(III) atom and two Ir(IV) atoms per anion. Having examined the solution spectrum of the nitrido compound, Jorgensen (396) proposed that the formulas of that and Lecoq's salt were related to those of the trimeric Cr(III) acetates, $[\text{O}\{\text{Cr}(\text{H}_2\text{O})(\text{CH}_3\text{CO}_2)_2\}_3]^+$ (251), in which the oxygen atom and the three chromium atoms are found in a planar triangular arrangement, and octahedral coordination about each metal is completed by bridging acetate groups and the water molecules (Fig. 11). A rationalization of the electronic structures of these unusual compounds can be achieved by considering that, if the t_{2g} orbitals of the iridium atoms and the $2p \pi$ orbital of oxygen were fully occupied, there would be room for twenty electrons, but that one linear combination

$$\frac{1}{\sqrt{3}}[(t_{2g})_1 + (t_{2g})_2 + (t_{2g})_3]$$

forms not only a $d\pi$ - $p\pi$ bonding orbital with the $2p_z$ oxygen orbital, but a strongly antibonding orbital as well. Thus by losing two electrons and becoming mixed valence, an eighteen-electron system results which does not require occupation of the energetically unfavourable antibonding orbital. Delépine's formula (187) for Lecoq's salt becomes analogous to that of the nitrido compound, if one assumes that the three iridium atoms are in that case coordinated to an oxygen atom. If these trinuclear complexes do have the equilateral triangular geometry, then they belong to class III-A, and should be diamagnetic.

Ray and Adhikari (578) report the preparation of $\text{Ir}^{\text{II}}\text{Ir}^{\text{III}}\text{Cl}_5 \cdot 4\text{R}_2\text{S}$, where R_2S is either $\text{S}(\text{CH}_3)_2$ or $\text{S}(\text{C}_2\text{H}_5)_2$, as pale yellow crystals.

O. PALLADIUM AND PLATINUM

These two elements form mixed valence compounds with a wider range of ligands than many others, and intensive studies of their molecular structures and physical properties over many years have provided

us with a clear view of their electronic structures. A few simple compounds such as oxides and halides are known, but the majority of examples contain complex ions or neutral molecules, typically with halide and amine ligands.

Hydrates of the simple oxides Pd_2O_3 and Pt_2O_3 were first prepared by Wöhler and Martin (783, 784). They are reported to be brown-black, but, since PdO_2 and PtO_2 are also black, this fact gives no information about the possibility of an M(II),M(IV) mixed valence interaction. Some controversy has surrounded the formulation and structure of another oxide, Pt_3O_4 . Galloni and Ruffo (265) described the structure as body-centered cubic, with all the platinum ions in equivalent sites (class III-B), and a Pt-Pt spacing of 3.11 Å. An oxide prepared by Waser and McClanahan (745, 746) using the same method, however, contained enough sodium to suggest the formula NaPt_3O_4 . A powder diagram of the latter revealed a simple cubic lattice in which each platinum has four oxygen neighbors and two other platinum ions at 2.85 Å. Since the structure contains infinite chains of platinum atoms, the conductivity was investigated. The volume resistivity at room temperature was about 10^4 ohm cm, but the occurrence of polarization suggested that the conductivity was ionic. The powder pattern of this preparation was quite different than Galloni and Ruffo's, whose results were said to resemble the pattern of PtO_2 . Galloni and Busch (266) reiterated that their product contained no sodium, so one must accept the compromise suggestion (747) that there exists a series of compounds with the general formula $\text{Na}_x\text{Pt}_3\text{O}_4$, based on the platinum and oxygen lattice found by Waser and McClanahan (746). It should perhaps be mentioned that, according to our classification scheme, the high resistivity reported for NaPt_3O_4 is at variance with its proposed class III-B structure.

Oxidation of PdCl_2 with BrF_3 gives black PdF_3 (608, 655), but Pt(II) salts are oxidized to PtF_4 by this reagent. The magnetic moment of PdF_3 was at first interpreted (541) in terms of a Pd(III) ion with a configuration $t_{2g}^6e_g^1$, but Bartlett and Rao (43) have recently shown that the compound is in fact $\text{Pd}^{\text{II}}[\text{Pt}^{\text{IV}}\text{F}_6]$, in which Pd(II) is assigned a high-spin configuration $t_{2g}^6e_g^2$. When Pd(II) salts react with BrF_3 in the presence of quadrivalent oxides, isostructural compounds such as PdGeF_6 and PdSnF_6 are formed. No structural studies of the other simple PtX_3 halides with $\text{X} = \text{Cl}, \text{Br}, \text{or I}$ (784, 788) have been reported, but it seems probable that they are related to the fluoride. However, they cannot be precisely the same since the divalent metal ions in these halides are low-spin (697), and thus, no doubt, in square planar coordination. Mixed valence halides such as K_2PdCl_5 (783) and Cs_2PtCl_5 (785) may perhaps contain $[\text{M}^{\text{II}}\text{Cl}_4]^{2-}$ and $[\text{M}^{\text{III}}\text{Cl}_6]^{2-}$ ions, which, if the

compounds belong to class II, will exhibit their own characteristic absorption bands in addition to any mixed valence absorption. Unfortunately, no information on this point is available, except for the single observation that Cs_2PtCl_5 is green (785).

One of the first mixed valence platinum compounds containing halide and amine ligands to be prepared was the red salt of Wolfram (790):



Its mixed valence character was recognized first from the method of preparation, for mixing solutions of the compounds $[\text{Pt}^{\text{IV}}(\text{EtNH}_2)_4\text{Cl}_2]\text{Cl}_2$ and $[\text{Pt}^{\text{II}}(\text{EtNH}_2)_4]\text{Cl}_2$ (580) precipitates the red salt from the colorless solutions. Propylamine is the only other amine which forms similar salts. Wolfram (790) also has described similar mixed valence materials which apparently did not contain halide, for example, a nitrate, sulfate, and oxalate. The red chloride could be recovered from these salts by adding HCl solution, but no work on them has been described since 1907 (384).

Because they were able to prepare a salt with the formula $\text{Pt}(\text{EtNH}_2)_4\text{Cl}(\text{NCS})_2$, which they thought was a dimer, Drew and Tress (205) thought that Wolfram's red salt was also a dimer rather than a double salt, but a crystal structure determination (165) has confirmed the earlier conclusion. The crystal structure contains chains of platinum atoms with alternately square planar coordinated Pt(II) ions and octahedrally coordinated Pt(IV) ions. Chlorine atoms lie between the platinum atoms, 2.26 Å from the quadrivalent platinum and 3.13 Å from the divalent (as shown in Fig. 33); the compound clearly belongs to class II. The structure could not be fully refined because of the occurrence of stacking faults due to the chains slipping past one another. Craven and Hall (166) recently attempted to resolve this difficulty by determining the structure of the corresponding bromide, but these crystals also proved to be disordered.

Yamada and Tsuchida (800) studied the polarized crystal spectrum of Wolfram's red salt, and also the isomorphous bromide, which is green. Whereas neither $[\text{Pt}^{\text{IV}}(\text{EtNH}_2)_4\text{Cl}_2]\text{Cl}_2$ nor $[\text{Pt}^{\text{II}}(\text{EtNH}_2)_4]\text{Cl}_2$ showed absorption in the visible, the red salt had an absorption band near $17,000\text{ cm}^{-1}$ which was strongly polarized in the direction of the metal atom chain. The first two bands polarized normal to this direction appear to be internal transitions of the quadrivalent complex (Fig. 34), but the $17,000\text{ cm}^{-1}$ band is likely to be the class II mixed valence absorption band due to the transfer of an electron from the highest filled $5d$ orbital of $[\text{Pt}^{\text{II}}(\text{EtNH}_2)_4]^{2+}$ (probably d_{z^2} since the ligands are purely σ -bonding) to the unfilled d_{z^2} orbital of $[\text{Pt}^{\text{IV}}(\text{EtNH}_2)_4\text{Cl}_2]^{2+}$. Since the d_{z^2} orbitals on

the two centers point at one another and can overlap via the $3 p\sigma$ orbital of the intervening chloride ion, the α of Eq. (15) is nonzero and the transition will be electronically allowed (although not necessarily strong), with a polarization along the Pt-Pt chain.

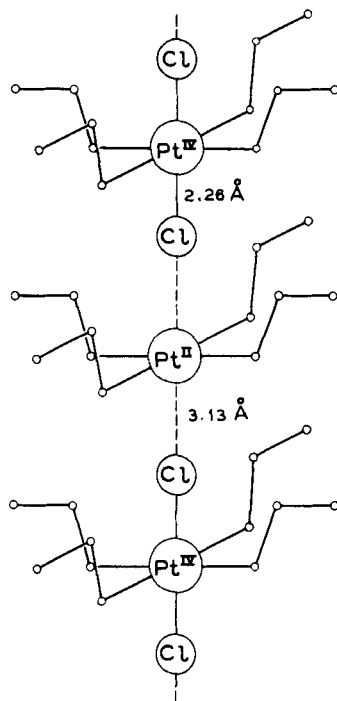
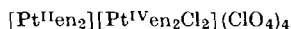


FIG. 33. The platinum atom chain in Wolfram's red salt, $[\text{Pt}^{\text{IV}}(\text{NH}_2\text{C}_2\text{H}_5)_4\text{Cl}_2]^{2+}[\text{Pt}^{\text{II}}(\text{NH}_2\text{C}_2\text{H}_5)_4]^{2-}\text{Cl}_4 \cdot 4\text{H}_2\text{O}$ (165).

A compound which appears to be related to Wolfram's red salt was recently prepared by Kida (416). Chemical analysis suggested the formula



and the compound forms dichroic needles which are red parallel to, and light yellow perpendicular to, the needle axis. A structure determination and polarized spectrum would be of interest.

The other type of mixed valence compound with halide and amine ligands has the general formula $[\text{Ma}_2\text{X}_2][\text{M}'\text{A}_2\text{X}_4]$, where M and M' may be either Pt or Pd, A is an amine, and X a halogen. The palladium salt, with an empirical formula $\text{Pd}(\text{NH}_3)_2\text{Cl}_3$, was first prepared in 1878 (614),

but many others have since been prepared containing palladium or platinum, ammonia or ethylenediamine, and either chloride, bromide, or iodide (202, 204, 205, 314, 708). The compounds are diamagnetic (376, 379, 380, 697) and, as was the case with Wolfram's salt, Drew and his coworkers (203) first thought that they contained metal-metal bonds. However, numerous crystal structure determinations (100, 334, 612, 743) have since shown that the correct formulations are as class II mixed valence compounds. Square planar MA_2X_2 and octahedral $M'A_2X_4$ molecules are stacked in chains with a halogen atom between each pair

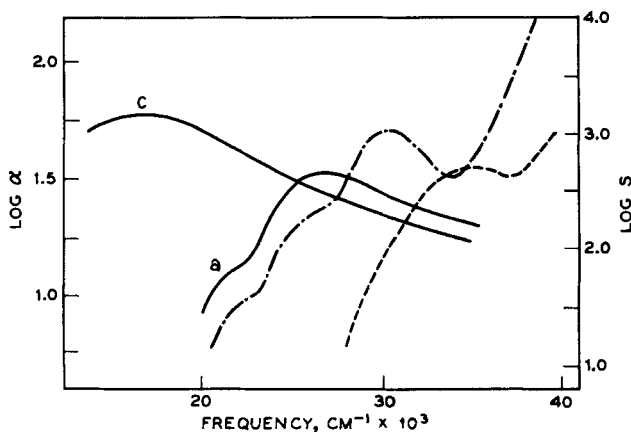


Fig. 34. The polarized absorption spectrum of crystalline $[Pt^{II}(NH_2C_2H_5)_4][Pt^{IV}(NH_2C_2H_5)_4]Cl_6 \cdot 4H_2O$ with the electric vector along the chain direction (c), and perpendicular to it (a). Spectra of the components $[Pt^{II}(NH_2C_2H_5)_4]Cl_2$ (---) and $[Pt^{IV}(NH_2C_2H_5)_4]Cl_2$ (-.-) are also shown for comparison (800).

of metal atoms within the chains (Fig. 35). The most recent determinations (612, 743) agree that the $Pt(II)-Br$ and $Pt(IV)-Br$ bonds at right angles to the chain are slightly longer than the $Pt(IV)-Br$ bond within the chain, and also that the distance between the $Pt(II)$ and the bromine atom attached to $Pt(IV)$ is somewhat smaller than expected from covalent radii. To the degree of approximation obtainable in these determinations, the $Pt(II)-Br$ and $Pt(IV)-Br$ bond lengths appeared identical. Greater precision could not be achieved because of disorder in the crystals resulting from the very weak interactions between neighboring stacks, which enables them to slip past one another. As with Wolfram's salt, the lowest mixed valence absorption in the class II $[MA_2X_2][M'A_2X_4]$ salts should be $dz^2 \rightarrow dz^2$, and allowed with a polarization along the Pt-Pt chain.

In agreement with the formulation of this class of compounds as molecular crystals, the infrared spectrum of PtBr_3 is a superposition of those of PtBr_2 and PtBr_4 (750). In the visible, however, all compounds in the series have intense absorption bands not present in either of their components. Cohen and Davidson (145) reported that $\text{Pd}(\text{NH}_3)_2\text{Cl}_3$ was highly dichroic, being lemon-yellow when the electric vector was perpendicular to the needle axis and black (even for the smallest crystals) when parallel, just as predicted above. When PtBr_3 , reportedly green, is finely ground the powder appears black (750), but

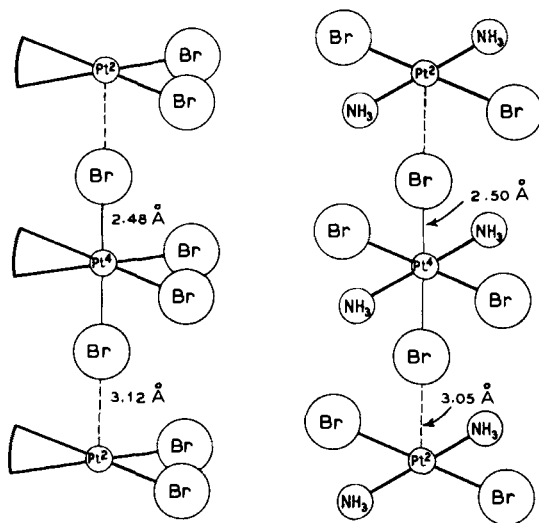
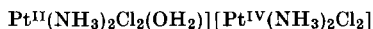


FIG. 35. The alternating $\text{Pt}^{\text{II}}, \text{Pt}^{\text{IV}}$ chains in $[\text{Pt}^{\text{II}}(\text{NH}_2\text{CH}_2\text{CH}_2\text{NH}_2)_2\text{Br}_2][\text{Pt}^{\text{IV}}(\text{NH}_2\text{CH}_2\text{CH}_2\text{NH}_2)_2\text{Br}_4]$, left, and $[\text{Pt}^{\text{II}}(\text{NH}_3)_2\text{Br}_2][\text{Pt}^{\text{IV}}(\text{NH}_3)_2\text{Br}_4]$, right (612).

when viewed in thin sections the transmitted color is purple. The green color is therefore caused by metallic reflection, indicating that the mixed valence absorption is very strong and that therefore α is very large. Attempts to measure the polarized crystal spectra of some of these compounds (798, 799) were not very successful because of the extremely intense absorption, but all the examples studied had a broad absorption band between 15,000 and 20,000 cm^{-1} , polarized in the direction of the metal-metal chains. Like the band in Wolfram's red salt, this transition is probably a mixed valence absorption band involving transfer of an electron from the divalent to the quadrivalent ion, but more refined experimental and theoretical work would be required to make the assignment more precise.

As with Wolfram's red salt, compounds of the type $[\text{MA}_2\text{X}_2][\text{MA}_2\text{X}_4]$ have also been prepared containing X groups other than halogens. For example, the salt

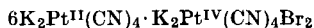


first prepared by Tschugajeff and Tschernjajeff (709) is so strongly dichroic that it has been suggested (78) for use as a polarizer. The dichroism (from black to white in the visible region) is said to extend at least from 12,000 to 29,000 cm^{-1} .

In view of the variety of solid mixed valence halides of palladium and platinum, one might expect that some mixed valence interaction would be detectable in halide-containing solutions. However, Cohen and Davidson (145) were unable to detect a change in the spectrum on mixing solutions of $[\text{Pd}^{\text{II}}\text{Cl}_4]^{2-}$ and $[\text{Pd}^{\text{IV}}\text{Cl}_6]^{2-}$, or $[\text{Pt}^{\text{II}}\text{Cl}_4]^{2-}$ and $[\text{Pt}^{\text{IV}}\text{Cl}_6]^{2-}$. Trivalent platinum has been suggested as an intermediate in the exchange of $[\text{PtCl}_6]^{2-}$ and chloride ions, which proceeds by a chain mechanism (583) but the reaction is catalyzed by $[\text{PtCl}_4]^{2-}$, possibly via a symmetrical transition state. Similarly, electron exchange between PtenBr_2 and PtenBr_4 is catalyzed by bromide ions, which would also allow a symmetrical transition state to be formed (491).

Mixed valence platinum oxalate complexes were first prepared 70 years ago by Werner, who reacted oxalic acid with sodium platinite, and obtained a salt whose copper color contrasted with the yellow color of the normal Pt(II) oxalate (764). This interesting compound has recently been reexamined by Krogmann and his co-workers (441, 442). The crystal structure of $\text{K}_2\text{Pt}(\text{C}_2\text{O}_4)_2 \cdot 2\text{H}_2\text{O}$ contains isolated planar oxalato complexes (489) but, in the compound $\text{K}_{1.6}\text{Pt}(\text{C}_2\text{O}_4)_2 \cdot 2.5\text{H}_2\text{O}$, the complex anions are stacked one above the other so that the Pt—Pt distance is only 2.75 Å. It is not possible to distinguish Pt(II) and Pt(IV) ions in the structure (441) and, on this basis, the compound is a class III-B system. Krogmann suggests that, whereas in $\text{K}_2\text{Pt}(\text{C}_2\text{O}_4)_2 \cdot 2\text{H}_2\text{O}$ the d_{z^2} band is filled, on oxidation electrons are drawn off from that band, and an overall bonding results.

The oxidation of potassium platinocyanide with bromine or nitric acid was first investigated over 100 years ago (430), but there appears to be considerable disagreement about the nature of the products. Knop (430) assigned the formula $\text{K}_2\text{Pt}(\text{CN})_5$ to the metallic-looking coppery crystals, but, according to Levy (461), there are two products of the bromine oxidation, one a Pt(IV) salt $\text{K}_2\text{Pt}(\text{CN})_4\text{Br}_2$ and the other a copper-colored mixed valence salt:



Oxidation by hydrogen peroxide gave another mixed valence salt with a bronze luster, to which analysis assigned the formula $K_{1.5}Pt(CN)_4$. Hydrated lithium cyanoplatinites undergo remarkable color changes when cooled in liquid air (582), which may be related to partial oxidation and formation of a mixed valence chromophore. No work has been done on these interesting compounds since 1912.

P. SILVER

The mixed valence chemistry of silver is limited apparently to its oxides and halides, the latter being mostly mixed compounds with the Au(III) ion. Silver distinguishes itself from its congener element gold in that, whereas the most common valence states of gold are Au(I) and Au(III) and all its mixed valence compounds are formed from these, with silver the most common oxidation states are Ag(I) and Ag(II), yet the mixed valence compounds involve the valence pairs Ag(I)–Ag(0) or Ag(I)–Ag(III). Although we will treat the silver and gold compounds separately, they are closely related in that a large number of Ag(I)–Au(III) complexes have Au(I)–Au(III) counterparts.

Of the silver oxides of potential mixed valence interest, AgO is of prime importance. Reviews of the chemistry of this substance have been presented by McMillan (503) and Dirkse (198). AgO has been prepared in the past in a variety of ways, both chemical and electrochemical, and has been reported to have a variety of conflicting properties. However, AgO preparations made in six different ways by Schwab and Hartmann (646) were shown to have identical X-ray powder patterns. Apparently the purity of the sample varies with its mode of preparation.

The early suggestions that AgO is a peroxide of univalent silver of the form $Ag_2^I O_2$ has been discredited repeatedly by reports of its inability to show reactions thought to be characteristic of peroxides (39, 303). As for AgO being a divalent oxide as its formula implies, one would then expect paramagnetism due to the $4d^9$ Ag(II) ions, yet it is generally agreed that AgO is diamagnetic (425, 528, 622, 651, 696). An obvious suggestion is that AgO should be written as $Ag^I Ag^{III} O_2$, with the $4d^8$ Ag(III) ions in square coordination, thereby making them diamagnetic. Crystal structure analysis demonstrates that this indeed is the case.

It is not entirely clear whether or not AgO can be obtained as a face-centered cubic crystal as well as a monoclinic one, as some have claimed. Although several reports of face-centered cubic AgO have appeared (97, 390, 682), the possibility exists that these are higher or lower oxides

of silver, and not AgO. The monoclinic variety of AgO has been studied extensively by both X-ray and neutron diffraction techniques. Unfortunately, due to the disparity in scattering power of silver and oxygen, the X-ray experiments on powdered AgO do not permit an adequate direct determination of the oxygen positions, but silver positions can be obtained accurately and the oxygen positions then deduced from packing considerations. As determined by Scatturin *et al.* (619, 620), AgO consists of Ag(II) ions in approximately square coordination, forming infinite chains via bridging oxide ions. McMillan (502), on the other hand, finds a distinct difference in the coordination about the silver ions, half of the silver ions being four-coordinated (square) and half two-coordinated (linear). The final word would appear to be that of Scatturin *et al.* (621, 622), who turned to neutron diffraction, wherein silver and oxygen have comparable scattering power, and found that there are indeed two types of silver ion in AgO, one, presumably Ag(III), in square oxygen coordination with Ag—O equal to 2.01–2.05 Å, and the other, presumably Ag(I), in linear coordination having Ag—O equal to 2.18 Å. Monoclinic AgO by this criterion is thus a class I mixed valence system.

Owing no doubt to its importance to the battery industry, there have been a number of studies of electronic conduction in AgO, with some disagreement as to its resistivity. Le Blanc and Sachse (458) found that, whereas the resistivity of Ag₂O is 10⁸ ohm cm, a sample of *approximate* composition AgO had a resistivity of only 10 ohm cm. More recent measurements on pressed pellets of AgO at various pressures yield a resistivity of 0.012 ohm cm (390) when extrapolated to infinite pressure. This material, however, is claimed to be the face-centered cubic variety of AgO. A pellet of monoclinic AgO pressed at 12,000 kg/cm² had a resistivity of 14 ohm cm and the positive temperature coefficient expected for a semiconductor (528). The resistivity of an AgO film formed electrolytically on a metallic silver sheet is 5×10^3 ohm cm (125). These values, although disparate, all indicate a rather high electronic conductivity for AgO, much higher in fact than expected for a class I system. It must be mentioned, however, that pure AgO is a rather unstable compound and the low resistivity reported for it may be due to the presence of impurities.

There are two other compounds which must be mentioned in a discussion of the mixed valence oxides of silver. Unstable, paramagnetic Ag₄O₅, perhaps better written as Ag^IAg^{III}₃O₅, has been described as one of the materials resulting from ozonization of an acidified solution of AgClO₄ (651). It has been claimed, however, that the powder pattern attributed by the original workers to Ag₄O₅ is in fact due to a mixture of Ag₂O₃, AgO, and Ag₂CO₃ (524). A second oxide of presumed composi-

tion Ag_4O_3 has been studied by the analysis of X-ray powder patterns (732), and was said to consist of Ag_4 tetrahedra having three oxide ions bonded symmetrically to each of the silver ions. It remains to be shown if this is a genuine compound, or, as often is the case with silver oxides, simply a mixture of the better known oxides of silver (556).

Electrolysis of an acidic solution of silver nitrate leads to the formation of a black, crystalline substance at the anode having the composition $\text{Ag}_7\text{NO}_{11}$. Although this material has been the subject of a great many studies, its crystal structure only recently has been solved and its electronic structure is still in some doubt. Following the earlier crystallographic work (82, 819), more complete studies by Chou Kung-Du (140) and Naray-Szabo and co-workers (525) finally led to an acceptable structure for $\text{Ag}_7\text{NO}_{11}$. This last study, involving single crystal X-ray work and neutron diffraction on the powdered material, gave a face-centered cubic cell containing polyhedral structural units (as shown in Fig. 36). Each polyhedron (cubo-octadodecahedron) is formed from six square planar AgO_4 units (Fig. 36) and has an NO_3^- ion at its center. The polyhedra themselves are joined by a sharing of the AgO_4 faces, and the smaller cubes formed between polyhedra have Ag(I) ions at their centers. Thus there are two types of silver ion in this structure, one type having eight oxygens about it at the corners of a cube with an Ag—O distance equal to 2.52 Å, and a second type which is in square planar oxygen coordination having Ag—O distances equal to 2.05 Å. The stoichiometry of $[\text{Ag}_7\text{O}_8]^+\text{NO}_3^-$ demands that the ratio $\text{Ag(I)}/\text{Ag(III)}$ be 2/5, whereas the ratio of cubic sites to square planar sites in such a structure is 1/6. Since the cubic sites are occupied only by Ag(I) , and since all the square planar sites are equivalent, the one Ag(I) and the five Ag(III) ions in the square coordination within a polyhedral unit form a two-electron, class III mixed valence system, the metal ions of which are joined by bridging oxygen atoms. Moreover, since each polyhedral unit is joined to twelve similar units by sharing its square AgO_4 faces (Fig. 36), the class III mixed valence system encompasses the entire crystal without involving any of the cubically coordinated silver, and is therefore class III-B.

The mixed valence $[\text{Ag}_7\text{O}_8]^+\text{NO}_3^-$ system involves $4d^8$ and $4d^{10}$ ions in square coordination. Although there is considerable argument as to the ordering of the d levels in square planar systems such as these, there is universal agreement that the uppermost orbital is $dx^2 - y^2$, which thus forms the valence shell of the mixed valence system, together with the $2p\sigma$ orbitals of the bridging oxide ions through which $dx^2 - y^2$ orbitals on adjacent silver ions interact. As was discussed above, the most dramatic properties of a class III-B system are its electrical conductivity and

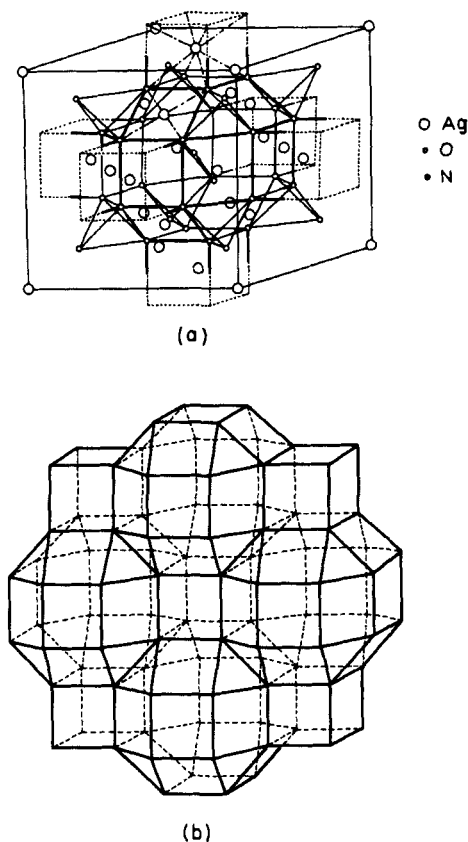


FIG. 36. The unit cell of $\text{Ag}_7\text{O}_8\text{NO}_3$ showing (a) the polyhedral cage with the NO_3^- ion at its center, and (b) the fusion of Ag_8O_8 polyhedra through sharing of the square AgO_4 faces (140, 525).

reflectivity, both of which should be metallic. McMillan (503) first reported that $\text{Ag}_7\text{O}_8\text{NO}_3$ was only semiconducting, but later work on single crystals (594) has shown that it is metallic ($\rho = 2.5 \times 10^{-3}$ ohm cm at 300°K) and is superconducting below 1.04°K . The reflectivity of $\text{Ag}_7\text{O}_8\text{NO}_3$ is also metallic, the crystals being shiny black and quite opaque. The molar susceptibility of $\text{Ag}_7\text{NO}_{11}$ has been reported by various authors as 398×10^{-6} (524), 688×10^{-6} (528), and $6379 \pm 1750 \times 10^{-6}$ (651) cgs, suggesting that the substance as ordinarily synthesized may contain a variable amount of paramagnetic impurity and that the pure substance is only feebly paramagnetic, if at all.

The NO_3^- anion of $\text{Ag}_7\text{NO}_{11}$ apparently can be replaced while keeping

the Ag_7O_8^+ framework intact, for the salts $\text{Ag}_7\text{O}_8\text{F}$ (303, 503), $\text{Ag}_7\text{O}_8\text{ClO}_4$ (503), $\text{Ag}_7\text{O}_8\text{BF}_4$ (594), and $\text{Ag}_7\text{O}_8\text{HSO}_4$ (503, 528) also have been reported, the fluoride, fluoroborate, and bisulfate having unit cell dimensions almost exactly those of the nitrate. Because crystals of the same unit cell dimensions form regardless of the radii of the anions within the polyhedral cages, the systems can be considered as clathrate salts, with mononegative ions as guests within the very rigid Ag_8O_8 cages. Careful analytical work on the fluoride and perchlorate (524) suggests that, unlike the nitrate and bisulfate, these substances may not have a fixed composition. All these substances are metals (594).

Earlier doubts as to the exact composition of Ag_2F and its existence as a stoichiometric compound were settled by the work of Wöhler (786), who showed that there is no oxygen in the substance and that, on dissolution in water, it gives equimolar amounts of AgF and metallic silver, as expected for Ag_2F . Silver subfluoride, Ag_2F , as prepared either electrolytically or by the reaction of silver metal with an AgF solution, is formed as large crystals described as being yellow to yellow-green with a bright metallic, brassy reflex (358).

Bruno and Santoro (109) have performed isotope exchange experiments on Ag_2F in an effort to determine whether or not the silver ions in this substance are equivalent. They found that, following the formation of Ag_2F from inactive AgF and radioactive ^{110}Ag metal and decomposition in H_2O , the resulting Ag metal and AgF had equal activities, indicating the equivalence of the silver atoms. However, a second experiment, in which inactive Ag_2F exchanged heterogeneously with active $^{110}\text{AgNO}_3$ in acetone solution, showed that virtually all the radioactive Ag doped into the compound could be recovered as Ag metal on H_2O decomposition.

X-ray analysis reveals the crystal structure of Ag_2F to be a simple one, having one molecule per hexagonal cell in the anti-cadmium iodide structure (552, 700) (Fig. 37). The structure may be looked upon as consisting of alternate layers of silver and fluoride ions. Within the silver layer, adjacent silver ions are separated by 2.84 Å within the unit cell and 2.989 Å between unit cells, these distances being nearly equal to the Ag-Ag separation of 2.28 Å in metallic silver. All silver atoms are in equivalent sites, and each is coordinated symmetrically by three fluoride ions at a distance of 2.44 Å, equal to the silver-fluoride distance in AgF . Since the Ag_2F stoichiometry demands that half the silver atoms be univalent and half zero-valent, the equivalence of the silver sites and the short repeat distance a lead to a class III-B mixed valence system, which should be an insulator in the c direction and metallic perpendicular thereto.

The resistivity of Ag_2F has been measured, using a four-probe technique at temperatures between 1.4° and 300°K . It increases monotonically from a value of 0.4×10^{-5} to 2.4×10^{-5} ohm cm in this temperature range (359); for comparison, the resistivity of metallic lead is 22×10^{-5} ohm cm at 300°K . Experimental (138) and theoretical (139) studies of the ^{19}F NMR spectra of AgF and Ag_2F show that the spin lattice relaxation time t_1 varies with temperature, as would be expected for relaxation by hyperfine interaction of the ^{19}F nuclei with the conduction electrons. A Knight shift calculated on this assumption is in good agreement with the shift observed between Ag_2F and AgF . The magnetic

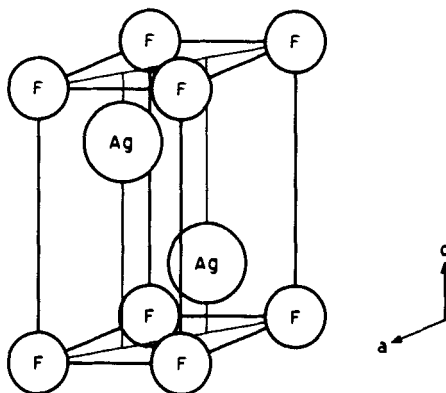


FIG. 37. The hexagonal unit cell of class III-B silver subfluoride, Ag_2F , with $a = 2.989 \text{ \AA}$, $c = 5.710 \text{ \AA}$, and $\text{Ag}-\text{Ag} = 2.84 \text{ \AA}$ (700).

susceptibility of Ag_2F has also been studied (261); the molar susceptibility of -64.3×10^{-6} cgs appears understandable only if the conduction electrons move in an anisotropic potential, in accord with the anisotropic structure of the crystal. Hall measurements (707) on Ag_2F demonstrate that there is one carrier per pair of silver atoms, as one would expect from the $\text{Ag}^0\text{Ag}^{\text{I}}\text{F}$ formulation. Ag_2F is superconducting below 0.058°K (20).

There is a second silver fluoride of interest to us. Fluorination of AgCl results in the formation of a black substance of the composition AgF_2 (609), nominally a divalent silver fluoride. In support of this, it is claimed to be strongly paramagnetic ($\chi_{\text{mol}} = 45 \times 10^{-6}$ cgs at room temperature), as a magnetically dilute divalent silver salt must be. A more detailed study of the magnetic susceptibility of samples of AgF_2 , prepared in three different ways, confirmed the above value of the molar susceptibility and in addition showed that the material is weakly ferromagnetic at 90°K (324). Through the action of fluorine on metallic

silver, a yellow form of AgF_2 is produced (383). The yellow form is poorer in fluoride than the black and has a lower magnetic susceptibility, suggesting perhaps that the black form is contaminated with paramagnetic Ag(III) salts (44). The black form has a face-centred orthorhombic, distorted CaF_2 structure with all the silver ions in equivalent sites (44). The problem as to whether AgF_2 is a salt of Ag(II) or is a mixed valence Ag(I),Ag(III) class III-B system could be clarified perhaps through a study of its resistivity. A similar question exists in regard to the "divalent" black fluoride BaAgF_4 (369).

Solution of the crystal structure of $\text{Ag}_5\text{Pb}_2\text{O}_6$ has revealed it to be a substance containing the Ag_2^+ dimer ion (123). In $\text{Ag}_5\text{Pb}_2\text{O}_6$, the quadrivalent lead ions are surrounded octahedrally by oxygen at 2.19 Å, and three of the five silver ions in the unit cell are univalent and linearly coordinated with oxygen. The two remaining silver atoms form Ag_2^+ dimers having an internuclear separation of 3.04 Å, with each silver of this pair in turn coordinated by three oxygens, much as each silver ion of Ag_2F is coordinated to three fluoride ions. However, unlike the situation in Ag_2F where short Ag-Ag distances imply a very strong interaction between silver ions of adjacent pairs, in the $\text{Ag}_5\text{Pb}_2\text{O}_6$ crystal the Ag_2^+ groups are aligned in chains with 3.39 Å separating the atoms of adjacent pairs. Thus the crystal structure suggests that the system is overall class III-A. Because the Ag_2^+ ion is an odd-electron species, a study of the magnetic susceptibility of $\text{Ag}_5\text{Pb}_2\text{O}_6$ would be of great use in determining just how strongly the Ag_2^+ ions are interacting. If the interaction were strong, then the Ag_2^+ ions form a class III-B system which would be a one-dimensional analog of the two-dimensional silver layer of Ag_2F . There are no data available on the optical, magnetic, or electrical properties of $\text{Ag}_5\text{Pb}_2\text{O}_6$, but the Ag_2^+ ion has been observed by ESR in organic glasses (658).

Q. GOLD

The best known mixed valence gold compounds are the halides of Au(I) and Au(III) and the corresponding compounds having Ag(I) in substitution for the Au(I) ion. Insofar as crystal structures have been determined, these compounds contain the trivalent gold as square coplanar AuX_4 and the univalent gold (silver) as linear bicoordinated AuX_2 (AgX_2) groups, the systems being, in general, class I or class II. The recent report of a genuine, paramagnetic Au(II) complex (749) suggests that one must use some caution in presuming that all nominally divalent gold compounds are univalent-trivalent mixed valence materials.

The AuCl-AuCl_3 system has been studied by Corbett and Druding (150), who conclude that their phase diagram and powder pattern results show no evidence for the formation of the mixed valence compound $\text{Au}^{\text{I}}\text{Au}^{\text{III}}\text{Cl}_4$. However, the silver salt $\text{Ag}^{\text{I}}\text{Au}^{\text{III}}\text{Cl}_4$ (deep red) (355) and the corresponding fluoride $\text{Ag}^{\text{I}}\text{Au}^{\text{III}}\text{F}_4$ (541) have been reported. There also exists a report on the preparation of Au_2I_4 , an unstable, ether-soluble substance (106). Although the double chloride $\text{Au}^{\text{I}}\text{Au}^{\text{III}}\text{Cl}_4$ has not been prepared, salts of $\text{Au}(\text{I}), \text{Au}(\text{III})$ and $\text{Ag}(\text{I}), \text{Au}(\text{III})$ with alkali metal cations abound.

One of the first mixed valence triple salts of gold and silver reported was Pollard's salt (570), originally thought to be $(\text{NH}_4)_8\text{Ag}_3\text{Au}_4\text{Cl}_{23}$, but later revised to $(\text{NH}_4)_6\text{Ag}_2^{\text{I}}\text{Au}_3^{\text{III}}\text{Cl}_{17}$ (760). A rubidium-silver-gold chloride having the same atomic ratios as Pollard's ammonium salt also has been reported (50, 761). The dark red crystals of the ammonium salt show a black-to-red pleochroism, in which the black color is most likely due to the mixed valence absorption between the $[\text{Au}^{\text{III}}\text{Cl}_4]^-$ and $[\text{Ag}^{\text{I}}\text{Cl}_2]^-$ groups. The crystal structure of this material has not been determined, but unit cell parameters are known (245).

The most famous mixed valence double salts of gold are Wells' cesium salt, $\text{Cs}_2\text{Au}^{\text{I}}\text{Au}^{\text{III}}\text{Cl}_6$, and its silver analog, $\text{Cs}_2\text{Ag}^{\text{I}}\text{Au}^{\text{III}}\text{Cl}_6$ (50, 758). The structures of these two isomorphous mixed valence halides have not yet been settled, for there are two different interpretations of the experimental X-ray diffraction data. Elliott and Pauling (219, 220) propose a tetragonal structure containing $[\text{Au}^{\text{III}}\text{Cl}_4]^-$ square planar ions and $[\text{Ag}^{\text{I}}\text{Cl}_2]^-$ or $[\text{Au}^{\text{I}}\text{Cl}_2]^-$ linear ions stacked alternately within columns. One sees from Fig. 38 that each $\text{Au}(\text{III})$ ion is in a nominally octahedral field with a tetragonal extension, whereas each $\text{Ag}(\text{I})$ or $\text{Au}(\text{I})$ ion is nominally octahedral with a tetragonal compression. As is well known, such a tetragonal field about the $5d^8$ $\text{Au}(\text{III})$ ion leads to a singlet ground state, in agreement with the diamagnetism of Wells' salts (219). On the other hand, Ferrari and co-workers (240, 242) propose that the $\text{Au}(\text{III})$ ions in these compounds exist as octahedral $[\text{Au}^{\text{III}}\text{Cl}_6]^{3-}$ ions in a cubic unit cell. That this is inappropriate follows from the fact that the $5d^8$ $\text{Au}(\text{III})$ ion in an octahedral field would have a triplet ground state, in contradiction to the observed diamagnetism of these compounds. In support of the $\text{M}(\text{I}), \text{M}(\text{III})$ formulas of these materials, both the Ag and Au salts are described as "astonishingly" jet black in color (758), as expected for a mixed valence salt containing shared ligands. Related materials have been reported in which the two univalent cations of a double formula are replaced by a single divalent cation (242, 244, 758). Thus the triple salts $\text{Cs}_4\text{M}^{\text{II}}\text{Au}_2^{\text{III}}\text{Cl}_{12}$, wherein M is $\text{Zn}(\text{II}), \text{Pd}(\text{II}), \text{Cd}(\text{II}), \text{Hg}(\text{II}),$ and $\text{Cu}(\text{II})$, have been prepared, but

their colors are little different than the sum of the colors of the $M(II)$ and $Au(III)$ ions.

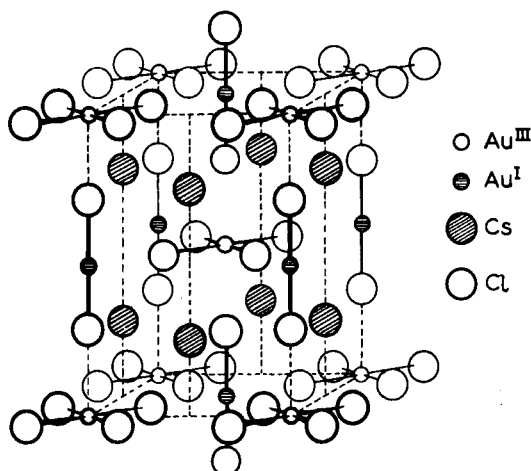
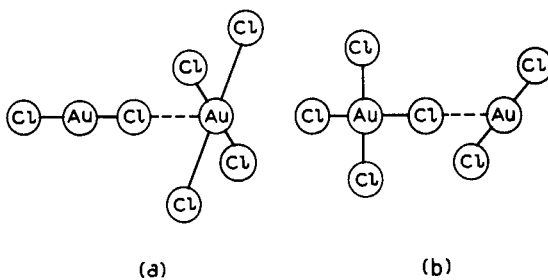


FIG. 38. The tetragonal unit cell proposed by Elliott and Pauling (220) for $Cs_2Au^IAu^{III}Cl_6$.

The black color of $Cs_2Au^IAu^{III}Cl_6$ undoubtedly arises from the class II mixed valence interaction between the $[Au^{III}Cl_4]^-$ and $[Au^ICl_2]^-$ groups. As can be seen from Fig. 38, there are two relative orientations of these groups in the crystal, redrawn below as configurations (a) and (b):



Regardless of the geometric orientations of the groups, the optical electron in the mixed valence transition can safely be regarded as originating in the axially symmetrical dz^2 orbital of the $[Au^ICl_2]^-$ ion and terminating in the $dx^2 - y^2$ orbital of the $[Au^{III}Cl_4]^-$ ion. As explained in Section II, class II mixed valence systems are characterized by a non-zero value of α , which means that the donor and acceptor orbitals must have a nonzero overlap. Inasmuch as this is the case for the chromophore

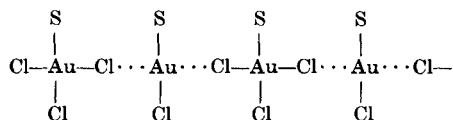
configuration (b), but not for (a), we must assume that it is configuration (b) which is responsible for the mixed valence absorption in $\text{Cs}_2\text{Au}^{\text{I}}\text{Au}^{\text{III}}\text{Cl}_6$, and that this absorption will be polarized in the ab plane.

Preliminary spectra of both $\text{Cs}_2\text{AgAuCl}_6$ and $\text{Cs}_2\text{AuAuCl}_6$ (595) show the mixed valence transition as a rather weak but distinct feature at $15,500\text{ cm}^{-1}$ followed by a stronger absorption centered at $23,500\text{ cm}^{-1}$, having the opposite polarization. The latter band is also found at $23,500\text{ cm}^{-1}$ in the salt $\text{CsAu}^{\text{III}}\text{Cl}_4$ and is due no doubt to the $[\text{Au}^{\text{III}}\text{Cl}_4]^-$ ion. Since Yamada and Tsuchida (798) report that the visible absorption of the triple salts is polarized along the c axis, perpendicular to the planes of the $[\text{Au}^{\text{III}}\text{Cl}_4]^-$ ions, the $23,500\text{ cm}^{-1}$ band must be polarized in the $[\text{Au}^{\text{III}}\text{Cl}_4]^-$ plane. The fact that the absorption spectra are polarized in Wells' salt also argues for the Elliott and Pauling tetragonal unit cell, and against the cubic cell proposed by Ferrari. However, the disagreement between the predicted ab polarization of the first mixed valence absorption band in $\text{Cs}_2\text{Au}^{\text{I}}\text{Au}^{\text{III}}\text{Cl}_6$ and the observed c polarization is still a puzzle requiring further research.

Yamada and Tsuchida (710, 799) also report the polarized crystal spectrum of an ammonium salt of composition $(\text{NH}_4)_3\text{Ag}^{\text{I}}\text{Au}^{\text{III}}\text{Cl}_7$, which has a spectrum much like that mentioned above for $\text{Cs}_2\text{Ag}^{\text{I}}\text{Au}^{\text{III}}\text{Cl}_6$, i.e., two bands, centered at $18,000\text{ cm}^{-1}$ and $23,500\text{ cm}^{-1}$, with opposite polarizations. The spectral similarities suggest that the ammonium salt also contains $[\text{Ag}^{\text{I}}\text{Cl}_2]^-$ and $[\text{Au}^{\text{III}}\text{Cl}_4]^-$ groups sharing halide ions.

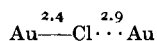
The syntheses of the bromide (241) and iodide (246) salts of the $\text{M}_2(\text{Ag}^{\text{I}}, \text{Au}^{\text{I}})\text{Au}^{\text{III}}\text{X}_6$ mixed valence system have been reported but little is known of them other than that they are black, as expected. According to Ferrari and Cecconi (241), the salt $\text{Cs}_2\text{AgAuBr}_6$ is only an end member in a series of general composition $\text{Cs}_2\text{Ag}_y\text{Au}_{(1-y)/3}\text{AuBr}_6$, as is the corresponding chloride $\text{Cs}_2\text{AgAuCl}_6$.

The properties of an interesting mixed valence compound of gold involving dibenzylsulfide as ligand have been described in detail (84). The compounds $(\text{C}_6\text{H}_5\text{CH}_2)_2\text{SAuCl}_2$ and $(\text{C}_6\text{H}_5\text{CH}_2)_2\text{SAuBr}_2$ are diamagnetic, have molecular weights in bromoform or benzene equal to those of the formulas as written above, and are nonconducting solutes in nitrobenzene. Solution of the crystal structure revealed $(\text{C}_6\text{H}_5\text{CH}_2)_2\text{SAuCl}_2$ to be composed of equal parts of the two neutral species $(\text{C}_6\text{H}_5\text{CH}_2)_2\text{SAu}^{\text{I}}\text{Cl}$ and $(\text{C}_6\text{H}_5\text{CH}_2)_2\text{SAu}^{\text{III}}\text{Cl}_3$, having the mutual orientation:

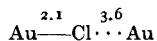


Along the chain direction in this structure, the Au—Cl distance is about 2.1 Å and Au···Cl is about 3.6 Å, but the chains are stacked in such a way in the crystal that the intrachain chloride appears crystallographically to be disordered between Au—Cl and Au···Cl. The structure of the dibromide is closely related, and a dibenzylsulfide gold diiodide has also been prepared (671) but not investigated crystallographically.

As both the component complexes, the monohalo- and the trihalo-gold dibenzylsulfide, can be prepared separately, it is not surprising that the dihalide can be prepared by mixing the components and that the dihalide dissolves to yield the component complexes. There does not appear to be much mixed valence interaction in spite of the bridging chloride ions, for the color of the dihalide is not very different from that of the trihalide, $(\text{C}_6\text{H}_5\text{CH}_2)_2\text{SAuBr}_3$ being ruby red and $(\text{C}_6\text{H}_5\text{CH}_2)_2\text{SAuBr}_2$ being brown. The reason why Wells' salt is black, whereas the dibenzylsulfides have no apparent mixed valence color, may be related to the fact that in Wells' salt the distances (in angstroms) within the chromophoric grouping are



whereas in the dibenzylsulfides they are

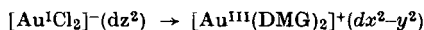


Thus, by comparison, the chlorine is not really bridging in the dibenzylsulfides, and the system is more class I than is Wells' salt.

$[\text{Au}^{\text{III}}(\text{DMG})_2][\text{Au}^{\text{I}}\text{Cl}_2]$, where DMG is the dimethylglyoxime monoanion, is another mixed valence complex of gold containing an organic ligand. This complex, first synthesized by Rundle (611), was found by him to contain linear chains of $\text{Au}(\text{III}) \cdots \text{Au}(\text{I}) \cdots \text{Au}(\text{III})$ ions having the internal structure shown in Fig. 39. The Au(I)-Au(III) separation in the chain is 3.26 Å.

The polarized absorption spectrum of $[\text{Au}^{\text{III}}(\text{DMG})_2][\text{Au}^{\text{I}}\text{Cl}_2]$ has been recorded (798, 801), and it is interesting to compare it with similar spectra of single crystals of $\text{CsAu}^{\text{III}}\text{Cl}_4$ (799). The spectra show what appear to be only minor differences, suggesting that in both cases the spectrum can be attributed to Au(III) ions in square planar coordination, and that there is no visible mixed valence absorption in $[\text{Au}^{\text{III}}(\text{DMG})_2][\text{Au}^{\text{I}}\text{Cl}_2]$. That this is so seems reasonable, considering the very large difference in the ligand fields at the two gold sites, and also from the fact that, given the geometrical arrangement shown above, the highest-energy, filled orbital of $[\text{Au}^{\text{I}}\text{Cl}_2]^-$, d_{z^2} , is orthogonal to the lowest-energy,

unfilled orbital of $[\text{Au}(\text{DMG})_2]^+$, $dx^2 - y^2$, as in configuration (a) of $\text{Cs}_2\text{Au}^{\text{I}}\text{Au}^{\text{III}}\text{Cl}_6$, above. The symmetry of the orbitals thus makes the



optical transition forbidden, and the system belongs to class I, its amber-red color being merely that of the $[\text{Au}^{\text{III}}(\text{DMG})_2]^+$ ion.

There is only one example of a mixed valence gold oxide in the literature. Lux and Niedermaier (469) report that the dissolution of metallic gold in molten KOH in a dry O_2 atmosphere leads to the formation of a deep blue polynuclear complex containing approximately

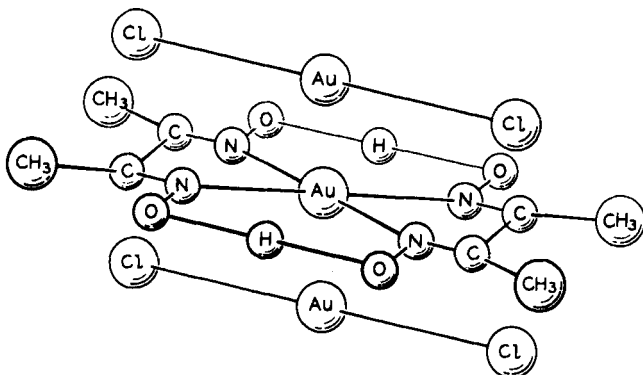


FIG. 39. The class I crystal structure of $[\text{Au}^{\text{III}}(\text{DMG})_2]^+[\text{Au}^{\text{I}}\text{Cl}_2]^-$ (611).

equal amounts of Au(I) and Au(III), as determined spectrophotometrically. Analogous complexes also were said to result in aqueous solution, but there is no evidence for their structure in either case.

R. GALLIUM

Gallium, indium, and thallium are all found in a univalent and a trivalent oxidation state. Although this simple generalization at first appears challenged by the existence of several halides of the composition MX_2 , the possibility that they are $\text{M}(\text{I}), \text{M}(\text{III})$ mixed valence compounds rather than compounds of $\text{M}(\text{II})$ is a good one. The exact constitution of these salts has been a matter of recent interest, and has been approached from a number of directions.

Klemm and Tilk (426) argued that, unlike the diamagnetic $\text{M}^{\text{I}}\text{X}$ and $\text{M}^{\text{III}}\text{X}_3$ salts, $\text{M}^{\text{II}}\text{X}_2$ compounds will be paramagnetic provided the $\text{M}(\text{II})$ ions are not dimerized. Their susceptibility measurements on GaCl_2 and InCl_2 showed that these compounds are diamagnetic and, therefore, are either dimerized like the Hg_2^{2+} ion or are $\text{M}(\text{I}), \text{M}(\text{III})$ mixed valence

compounds. GaI_2 was later shown also to be diamagnetic (148). The first unambiguous structural evidence on the nominally divalent gallium salts was presented by Woodward, Garton, and Roberts, whose Raman spectra of molten GaCl_2 clearly showed the presence of large amounts of the $[\text{Ga}^{\text{III}}\text{Cl}_4]^-$ ion, as recognized from earlier solution work on GaCl_3 in HCl solution (795). On the basis of this, the melt was held to be that of the salt $\text{Ga}^{\text{I}}[\text{Ga}^{\text{III}}\text{Cl}_4]$. This conclusion is also in accord with the high ionic conductivity of the melt (336) and the high resistivity (4.5×10^7 ohm cm) of solid GaCl_2 .

Any doubt still remaining as to the mixed valence nature of GaCl_2 was removed by the determination of the GaCl_2 crystal structure (269).

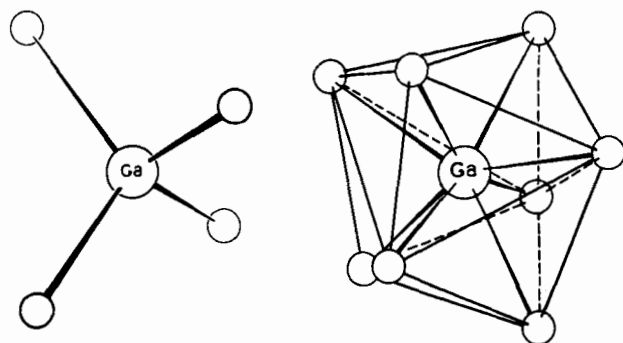


FIG. 40. The coordination about the $\text{Ga}(\text{III})$, *left*, and $\text{Ga}(\text{I})$ ions, *right*, in crystalline $\text{Ga}^{\text{I}}[\text{Ga}^{\text{III}}\text{Cl}_4]$.

In crystalline GaCl_2 , half of the gallium ions are surrounded tetrahedrally by chloride ions with $\text{Ga}-\text{Cl}$ distances equal to 2.19 Å, and are undoubtedly trivalent, whereas the other half of the gallium ions, presumably univalent, are surrounded by an irregular dodecahedron of eight chloride ions with $\text{Ga}-\text{Cl}$ distances equal to 3.2–3.3 Å (Fig. 40). The unusually large $\text{Ga}^{\text{I}}-\text{Cl}$ distance is due perhaps to the $\text{Cl}-\text{Cl}$ repulsions. GaCl_2 is thus an extreme example of class I mixed valence and, as expected, the crystal is a diamagnetic insulator having essentially the color of the constituent ions. Measurement of the vapor pressure above molten Ga_2Cl_4 suggests the presence of large quantities of genuinely divalent $\text{Ga}^{\text{II}}\text{Cl}_2$ (454), as does the optical spectrum of the vapor (751). A colorless substance of the composition Ga_4Cl_9 has been uncovered by a phase study of the $\text{Ga}-\text{GaCl}_3$ system (559); if it is a mixed valence compound it must have $\text{Ga}(\text{III})/\text{Ga}(\text{I})$ equal to 5/3.

Experiments similar to those described for Ga_2Cl_4 have been directed at elucidating the structure of GaBr_2 . Inasmuch as the Raman spectrum

of molten GaBr_2 shows the presence of large amounts of the $[\text{Ga}^{\text{III}}\text{Br}_4]^-$ ion (796), the melt has a conductance typical of a molten salt consisting of a large anion and a small cation (312), and solid GaBr_2 is colorless and diamagnetic, the compound must be formulated as $\text{Ga}^{\text{I}}[\text{Ga}^{\text{III}}\text{Br}_4]$.

Relatively little is known about the mixed valence iodides of gallium. Diamagnetic, yellow GaI_2 was reported by Corbett and McMullan (148) and later by Chadwick *et al.* (131) as being most likely $\text{Ga}^{\text{I}}[\text{Ga}^{\text{III}}\text{I}_4]$, in accord with the formulation of the corresponding chloride and bromide. The electrical conductivities and vapor pressures of the molten iodides of gallium have been studied by Riebling and Erickson (585, 586), who found that, whereas GaI_3 is a low conductance molecular melt, GaI_2 is highly ionic and probably contains the ions $(\text{Ga}^{\text{I}})^+$ and $[\text{Ga}^{\text{III}}\text{I}_4]^-$. Chadwick *et al.* (131) also described the intensely colored, diamagnetic compounds Ga_2I_3 and Ga_3I_5 as being mixed valence materials with formulas $\text{Ga}_3^{\text{I}}\text{Ga}^{\text{III}}\text{I}_6$ and $\text{Ga}_2^{\text{I}}\text{Ga}^{\text{III}}\text{I}_5$, respectively.

There appear to be no lower gallium fluorides (337). In this regard, it is pertinent to note that, unlike the tetrahedral coordination found for the Ga(III) ion in the Ga_2X_4 salts having $\text{X} = \text{Cl}, \text{Br}, \text{or I}$, the complex fluorides of trivalent gallium are octahedrally coordinated (574), as expected from the radius ratio.

Chemically, the salts Ga_2Cl_4 and Ga_2Br_4 are soluble in benzene from which solvent they can be recrystallized as the mixed valence complexes $\text{Ga}_2\text{X}_4 \cdot \text{C}_6\text{H}_6$ (130). Dielectric measurements on solutions of Ga_2Cl_4 in benzene are interpreted as showing the formation of the ion pair $[\text{Ga}^{\text{I}}]^+[\text{Ga}^{\text{III}}\text{Cl}_4]^-$ ($\mu = 8.9$ Debye units) at low concentrations, with aggregation at higher concentrations (504). Addition of basic ligands such as organic amines, ethers, sulfides, selenides, or arsines to the benzene solution of GaCl_2 leads to the immediate precipitation of $[\text{Ga}^{\text{I}}\text{L}_4]^+[\text{Ga}^{\text{III}}\text{Cl}_4]^-$, where L is a monodentate ligand (9, 96, 657). As expected, these mixed valence compounds are all diamagnetic and colorless, except for the 2,2'-dipyridyl complex which is red (9). As the dipyridyl ligands are relatively easily reduced, and Ga(I) is easily oxidized, the red color of the complex may be due to a Ga^{I} -dipyridyl charge transfer absorption. Water immediately hydrolyzes GaCl_2 to a dark brown substance analyzed to be $\text{GaClOH} \cdot \frac{1}{2}\text{H}_2\text{O}$ (97). If this substance indeed is a mixed valence material, it would appear to be one of the few reported which show a Ga(I), Ga(III) mixed valence absorption band in the visible region. Dehydration of this substance gives colorless GaClOH , analogous to the GaClSH formed by addition of H_2S to a GaCl_2 solution in benzene (97).

Although in the case of the nominally divalent gallium halides, GaX_2 , the possibility of spin pairing by dimer formation ($\text{X}_2\text{Ga}-\text{GaX}_2$)

is never realized, it is interesting to note, however, that, in the diamagnetic substances GaS and GaSe, dimer pairs of gallium ions are found, each gallium having three sulfide or selenide ions and one other gallium ion about it in a tetrahedral arrangement (330). Inasmuch as the gallium ions in these structures are equivalent, the systems are technically class III-A mixed valence, although in fact it is just as correct to consider them simply as divalent gallium compounds.

S. INDIUM

Unlike the situation with gallium, almost nothing has been done toward elucidating the structures of the mixed valence compounds of indium. Aside from a few isolated reports of magnetic susceptibility and qualitative reports of color, the only works of mixed valence interest are phase studies showing the existence of certain mixed valence indium halides.

The halides InF_2 (337), InCl_2 (6, 94, 144, 234), InBr_2 (94, 744), and InI_2 (567) have been described briefly. The first three have been shown to be diamagnetic, as would be expected for either $\text{In}^{\text{I}}[\text{In}^{\text{III}}\text{X}_4]$ salts or $\text{X}_2\text{In}-\text{InX}_2$ dimers, but not for $\text{In}^{\text{II}}\text{X}_2$ itself. Although the close analogy with the gallium compounds suggests that the InX_2 compounds are $\text{In}(\text{I}), \text{In}(\text{III})$ mixed valence salts, the possibility that the $\text{In}(\text{II})$ halides are really dimers is worth considering on the basis of the colors of the compounds involved (427). The trihalides InCl_3 and InBr_3 are colorless, whereas the monohalides InCl and InBr are, respectively, yellow-red and carmine red. If the InCl_2 and InBr_2 salts are class I mixed valence compounds, one would expect them to be red, the sum of the colors of their constituent ions. In fact, the dichloride and dibromide of indium are colorless, suggesting either that these compounds contain no $\text{In}(\text{I})$ and are therefore to be taken as dimers, or more probably that the $\text{In}(\text{I})$ in InX is complexed by halide ion and has either a ligand \rightarrow metal charge transfer transition or an atomic $5s^2 \rightarrow 5s^15p^1$ transition in the visible, but is complexed much more weakly in the InX_2 compounds, so that these transitions fall in the ultraviolet. It is to be remembered that, in $\text{Ga}^{\text{I}}[\text{Ga}^{\text{III}}\text{Cl}_4]$, the $\text{Ga}(\text{I})$ cation is essentially uncomplexed. The lack of color in the substance $\text{In}^{\text{I}}[\text{Al}^{\text{III}}\text{Cl}_4]$, however, does make the lack of color in In_2Cl_4 (144) rather less surprising. If InBr_2 is a mixed valence compound, it at first seems likely that the $\text{In}(\text{III})$ would be found in the crystal as $[\text{In}^{\text{III}}\text{Br}_4]^-$, just as is found in GaBr_2 . However, it is to be noted that, unlike the corresponding $\text{Ga}(\text{III})$ salt (794), InBr_3 in concentrated HBr does not form the tetrahedral tetrahalide ion $[\text{InBr}_4]^-$,

although such a species is said to form in an ether extract of the aqueous solution (793). Burns and Hume, on the other hand, have found spectrophotometrically an indium bromide species in aqueous solutions of high Br^- content having $\text{Br}/\text{In} = 4$, which they suggest is the octahedral ion $[\text{InBr}_4(\text{H}_2\text{O})_2]^-$ (114).

The phase diagram of the In-InCl_3 system has been studied rather extensively by a number of investigators, and a large number of mixed valence compounds have been uncovered. To date the list includes InCl_2 (mentioned above), In_4Cl_6 (144, 230, 231, 234, 558), In_4Cl_5 (144), In_4Cl_7 (144, 231), In_5Cl_9 (558), and several other possibilities of undetermined composition. In the In-InBr_3 system, the corresponding bromides In_4Br_6 and In_4Br_7 as well as In_5Br_7 have been found to exist (94, 511, 744). Of the compounds on this list, Clark *et al.* (144) propose that InCl_2 is not a genuine compound, but simply a mixture of In_4Cl_6 and InCl_3 , whereas Chadwick *et al.* (131) claim to have "reestablished the existence" of InCl_2 on the basis of a redetermination of the indium chloride phase diagram. On the other hand, Fedorov and Fadeev (234) can find no evidence for In_4Cl_5 , a compound claimed by Clark *et al.* Surprisingly, In_4Cl_7 exists as such in the gas phase over solid In_4Cl_7 at 450°C , according to the results of a vapor pressure study.

Clark *et al.* (144) present an interesting geometrical argument for the existence of certain but not all indium halides of a given stoichiometry. In_4Cl_6 is formulated as $\text{In}_3^1[\text{In}^{\text{III}}\text{Cl}_6]$, the radius ratio (565) of $\text{In}(\text{III})$ and Cl^- being such as to allow octahedral coordination as well as tetrahedral coordination. Thus, the salt $\text{In}^1[\text{In}^{\text{III}}\text{Cl}_4]$ also forms. In the case of the lower indium iodides, the radii are such that tetrahedral $[\text{In}^{\text{III}}\text{I}_4]^-$ can be realized but octahedral $[\text{In}^{\text{III}}\text{I}_6]^{3-}$ cannot, in agreement with Peretti's (567) finding that In_2I_4 is the only mixed valence lower iodide of indium. As Clark *et al.* point out, both tetrahedral $[\text{In}^{\text{III}}\text{Br}_4]^-$ and octahedral $[\text{In}^{\text{III}}\text{Br}_6]^{3-}$ ions can meet the radius ratio test, so that both InBr_2 and In_4Br_6 should exist, as they do (744). Applying these tests to the In_4X_7 series, it would appear that these substances contain octahedral $[\text{In}^{\text{III}}\text{X}_6]^{3-}$ ions, since they are found as the chloride and bromide, but not the iodide.

There are reports of the synthesis of mixed metal halides having compositions equivalent to several of the mixed valence halides mentioned above. Thus, corresponding to $\text{In}_3^1[\text{In}^{\text{III}}\text{Cl}_6]$, the salts $\text{Ag}_3^1[\text{In}^{\text{III}}\text{Cl}_6]$ and $\text{Tl}_3^1[\text{In}^{\text{III}}\text{Cl}_6]$ have been reported (235), and the salt $\text{In}^1[\text{Al}^{\text{III}}\text{Cl}_4]$ (144) corresponds to $\text{In}^1[\text{In}^{\text{III}}\text{Cl}_4]$.

Both In_2I_4 and In_2Br_4 can be ammoniated to yield the compounds $\text{In}_2\text{X}_4 \cdot 6\text{NH}_3$ and $\text{In}_2\text{X}_4 \cdot 8\text{NH}_3$ (131, 432). The fact that the iodide ammoniates are bright red and the bromides orange-red as compared

with the colorless ammonia-free In_2X_4 compounds is interesting, but perhaps not totally unexpected in view of the red color of the $\text{In}^{\text{I}}\text{X}$ compounds. However, because of the supposed instability of the $[\text{In}^{\text{I}}(\text{NH}_3)_6]^+$ cation, it has been argued that the ammoniates are $\text{In}(\text{II})$ dimers rather than mixed valence materials (431).

There is little evidence about the colors of the indium halides. If the indium dihalides are mixed valence, there is very little tendency toward class II behavior as evidenced by their lack of color. It is important to note that the dihalides of both gallium and indium can appear colored due to trace impurities of the corresponding monohalides. Thus, the report that In-InCl_3 mixtures give dark red to black, transparent crystals in the composition range 50–100 mole % InCl_3 (558) is of questionable importance to our discussion. Inasmuch as, in a class II system, the electron affinity of the oxidized species in the ground state is of consequence to the development of a mixed valence color in the visible region, the lack of color in the GaX_2 and InX_2 systems may be attributable in part to a low electron affinity of the $\text{Ga}(\text{III})$ and $\text{In}(\text{III})$ species. This suggestion is compatible with the very high energy of the ligand-to-metal charge transfer absorption in the $[\text{In}^{\text{III}}\text{Cl}_4]^-$ ($46,500\text{ cm}^{-1}$) (615) and $[\text{In}^{\text{III}}\text{Br}_4]^-$ ($42,600\text{ cm}^{-1}$) (114) ions. Spectra of InCl_2 , InBr_2 , and InI_2 in the gas phase have been reported (762), but the absorbing species are triatomic and most likely are the genuine divalent halides.

The action of H_2 and HCN on indium metal has been found to lead to the formation of $\text{In}(\text{CN})_2$, a white solid formulated as $\text{In}^+[\text{In}(\text{CN})_4]^-$ (293).

T. THALLIUM

In contrast to gallium and indium, a very large number and variety of thallium mixed valence compounds have been synthesized, although no more is known of their constitution than has been determined in the cases of gallium and indium. Crystallographically, the structures of three mixed valence thallium compounds have been solved, with surprising results. TlBr_2 (350) is isostructural with $\text{Ga}^{\text{I}}[\text{Ga}^{\text{III}}\text{Cl}_4]$ (269), discussed above. Thus, in TlBr_2 there are tetrahedral $[\text{Tl}^{\text{III}}\text{Br}_4]^-$ ions having Tl-Br distances equal to 2.51 \AA , and $\text{Tl}(\text{I})$ ions in irregular dodecahedral sites having eight bromines at a mean distance of 3.46 \AA . Surprisingly, in the isostructural diamagnetic compounds TlS and TlSe (329, 412) there are two types of thallium, one determined to be $\text{Tl}(\text{III})$ in tetrahedral coordination with, for example, the Tl-Se distance equal to 2.68 \AA , and one being $\text{Tl}(\text{I})$ having eight Se atoms as nearest neighbors,

with Tl—Se distances equal to 3.42 Å! In fact, in the gallium, indium, thallium group, only four mixed valence compounds have been studied crystallographically, and each has as its structural units the $M^{III}X_4$ tetrahedron and the M^IX_8 dodecahedron. More structures must be solved before one can see how general this combination of coordinations is in the mixed valence compounds of these elements. A preliminary investigation of Tl_2Cl_3 has shown it to have a complex structure with 32 molecules per cell (327).

The thallium halides Tl_2X_3 are probably better written as $Tl_3^I[Tl^{III}X_6]$. That Tl_4Cl_6 is not a class III mixed valence compound is indicated by the radiochemical exchange experiments of McConnell and Davidson (468, 771), which demonstrated that Tl_4Cl_6 , synthesized from radioactive $^{204}TlCl_3$ and inactive $TlCl$ in HCl solution, when decomposed and analyzed, yielded almost all its radioactivity as $Tl(III)$. This result was interpreted as showing that the $Tl(I)$ and $Tl(III)$ ions of crystalline Tl_4Cl_6 are nonequivalent. The same conclusion was reached following similar experiments with Tl_4Br_6 .

A study of the thallium NMR spectra of several thallium compounds including $TlCl_2$ and $TlBr_2$ has been reported (603). It was found that, as expected from the crystal structure of $Tl^I[Tl^{III}Br_4]$, the molten tetrachloride and tetrabromide yield ionic melts which showed two thallium resonances, the one due to $Tl(I)$ being at higher field than that due to $Tl(III)$. As the temperature of the melt was raised, the two lines fused into one, indicating exchange between the two thallium species with an average lifetime of about 10^{-5} sec at 500°K. In similar experiments, crystalline and molten $Tl(I)$ salts showed only one line at all temperatures up to 720°K.

A study of the $TlCl$ – $TlCl_3$ phase diagram by Fadeev and Fedorov (232) demonstrated the existence of only two mixed valence compounds, Tl_2Cl_4 and Tl_4Cl_6 , the first being described by earlier investigators as colorless to yellow, and the second as yellow to red, depending upon the mode of preparation. It is to be noted that $TlCl$ and $TlCl_3$ are colorless and that Tl_4Cl_6 is colorless at the temperature of liquid air. Thus the maximum of the Tl_4Cl_6 mixed valence transition must lie in the ultra-violet region. The corresponding mixed valence bromides, Tl_2Br_4 and Tl_4Br_6 , are respectively yellow and red (54, 55).

Reaction of I_2 with TlI leads to the formation of black Tl_3I_4 (55, 448, 449, 656), a mixed valence iodide having a metal/halogen ratio unlike any reported in the gallium or indium halides. Sharpe (656) proposes $[Tl_2]^+[Tl^{III}I_4]^-$ as the assignment of valences in Tl_3I_4 , but $Tl_5^ITl^{III}I_8$ seems more reasonable. A third possibility exists that it is the iodine that is mixed valence and not the thallium, i.e., Tl_6I_8 is $Tl_6^II_5I_5^-(I_3^-)$.

The deep black color of this substance is certainly consistent with a composition containing triiodide or higher polyiodide ions. This third possibility seems attractive since I^- is known to reduce $Tl(III)$ to $Tl(I)$ with the formation of I_3^- , thus leading one to expect that thallium iodides will not contain $Tl(III)$, but may contain I_3^- or higher polyiodides. Such an explanation is similar to that given by Lawton and Jacobson (456) for some of the antimony halides, which were first thought to be $Sb(III), Sb(V)$ compounds and were later shown by them to be polyhalides of $Sb(V)$.

One finds a similar problem in the assignment of valences in the compound $Tl_3Sb_2Cl_{13}$ (223), which may be taken to be either $Tl_3^I Sb_2^V Cl_{13}$ or $Tl_2^I Tl^{III} Sb^{III} Sb^V Cl_{13}$. The deep black color of this substance argues strongly for the latter formulation, since the mixed valence absorption of $Sb(III), Sb(V)$ halides lies at very low energy (see subsection X on antimony). In the same way, the dark violet compound $Tl_2Sb_2Cl_{10}$ (223) is more likely $Tl_2^I Sb^{III} Sb^V Cl_{10}$ than $Tl^I Tl^{III} Sb_2^{III} Cl_{10}$. Similar problems formally exist in the compounds $InTl_2Cl_5$ (557), $InTl_3Cl_6$ (557), and $TlGaCl_4$ (236) although their reactivity toward water should show immediately which of the ions is univalent and which is trivalent.

Evidence for the mixed valence interaction between $Tl(I)$ and $Tl(III)$ in perchloric acid solution was sought by McConnell and Davidson (495) in the spectral region $33,000\text{--}42,000\text{ cm}^{-1}$, but no mixed valence absorption was found. However, their solution contained no halide ions which might act as bridging groups in a mixed valence complex. In this regard, it is perhaps pertinent to note that the charge exchange between $Tl(I)$ and $Tl(III)$ ions is considerably accelerated by the presence of bridging anions in the solution (104, 105, 339, 774).

Peroxide oxidation of an alkaline thallous salt solution precipitates TlO as an unstable, deep blue material (575, 617), which has been formulated as $Tl_2^I Tl_2^{III} O_4$. Scatturin *et al.* (618) report on various oxides TlO_x , having $x > 1.5$, which were said to contain $Tl(I)$, $Tl(III)$, and $Tl(IV)$, and which had numerous reflection maxima in the $10,000\text{--}25,000\text{ cm}^{-1}$ region.

A fast riffle through the thallium volume of Gmelin's *Handbuch* (291) uncovers the following mixed valence compounds: $TlN_3 \cdot Tl(N_3)_3$ (yellow needles yielding $Tl(I)$ and $Tl(III)$ in solution), $2TlNO_3 \cdot Tl(NO_3)_3$ (colorless prisms blackening in moist air), $Tl_2SO_4 \cdot Tl_2(SO_4)_3$ (colorless crystals), $5Tl_2SO_4 \cdot Tl_2(SO_4)_3$ (pale yellow crystals) and the corresponding selenates $Tl_2SeO_4 \cdot Tl_2(SeO_4)_3$ (colorless crystals) and $5Tl_2SeO_4 \cdot Tl_2(SeO_4)_3$ (yellow crystals), $Tl_2Cl_2SO_4$ and $Tl_2Br_2SO_4$ (both yellow), $Tl_2Cl_2SeO_4$ and $Tl_2Br_2SeO_4$ (both yellow), $TlCN \cdot Tl(CN)_3$ (colorless crystals yielding $Tl(I)$ and $Tl(III)$ in base), $Tl_2C_2O_4 \cdot$

$\text{Ti}_2(\text{C}_2\text{O}_4)_3 \cdot 6\text{H}_2\text{O}$ (colorless crystals), $\text{Ti}_2\text{C}_2\text{O}_4 \cdot \text{Ti}_2(\text{C}_2\text{O}_4)_3 \cdot 4\text{NH}_3$, and $[\text{NH}_4, \text{Ti}(\text{I})]_3\text{Ti}(\text{III})(\text{SO}_4)_3$, a mixed crystal. The compound believed to be $\text{Ti}_2\text{Cl}_4 \cdot 2\text{NOCl}$ (28) is really $\text{TiCl}_3 \cdot \text{NOCl}$ (561).

U. TIN

The interesting work of Davidson and co-workers on the interaction between the $\text{Sb}(\text{III})$ and $\text{Sb}(\text{V})$ ions in concentrated HCl solution was later extended by them to the $\text{Sn}(\text{II}), \text{Sn}(\text{IV})$ system. It was found that mixing $\text{Sn}(\text{II})$ and $\text{Sn}(\text{IV})$ solutions in concentrated HCl results once more in a mixed valence absorption, although much further in the ultraviolet than was found with antimony (770). As before, the intensity of the mixed valence absorption was proportional to the product of the concentrations of $\text{Sn}(\text{II})$ and $\text{Sn}(\text{IV})$, showing that in the ground state, at least, the colored species was an $\text{Sn}(\text{II}), \text{Sn}(\text{IV})$ dimer and not an ion containing $\text{Sn}(\text{III})$. In addition to the composition study, an investigation was made of the thermal isotope exchange rate (103, 771) and the effect on this of irradiation in the region of the mixed valence absorption (164). It was found that the exchange reaction, which was bimolecular, proceeded in the dark at a rate sufficiently slow to demonstrate that the mixed valence dimer was unsymmetrical in the ground state if, indeed, it had anything at all to do with the exchange process. More interestingly, it was found that irradiation of the solution in the region of the mixed valence absorption ($25,000\text{--}30,000 \text{ cm}^{-1}$) at ca. 2°C substantially enhanced the exchange rate, the quantum yield of the photochemically induced exchange being estimated to be 0.2. Since a quantum yield of 0.5 is expected for such a three-level system if the excited state is symmetrical (class III-A), the significantly lower yield may be taken as evidence for an unsymmetrical upper state, as well.

The quantum yield can be interpreted within the framework of the mixed valence model in the following way. Although there is no evidence for the geometry or composition of the unsymmetrical $\text{Sn}(\text{II}), \text{Sn}(\text{IV})$ complex, for the sake of illustration it is represented by configuration A in Fig. 41. The starred atom is radioactive. On excitation in the mixed valence absorption band, an electron is transferred from left to right and both tin atoms become $\text{Sn}(\text{III})$ with a simultaneous rearrangement of ligands being quite probable, but in any case not to a symmetrical geometry (configuration B). On relaxation from the excited state B, either the system can go back to the original ground state A by transfer of an electron from right to left, or a second electron may be transferred again from left to right giving the exchanged configuration C. The

quantum yield of photoinduced exchange is thus seen to be related to the relative probabilities of transitions to the terminal states A and C from the intermediate state B. A relative probability of four to one for the $B \rightarrow A$ and $B \rightarrow C$ transitions would then explain the quantum yield of 0.2 observed for the Sn(II),Sn(IV) exchange. More precisely, the intermediate state B is really two states, one a spin singlet and one a spin triplet, and the quantum yield will depend upon the relative rates of reaching A and C from both of the B surfaces, and also on the rate of excited state singlet-triplet intersystem crossing. By whatever mechanism the relaxation from the intermediate state proceeds, it seems clear that Franck-Condon factors play an important role in determining the relative probabilities involved in the photoinduced exchange

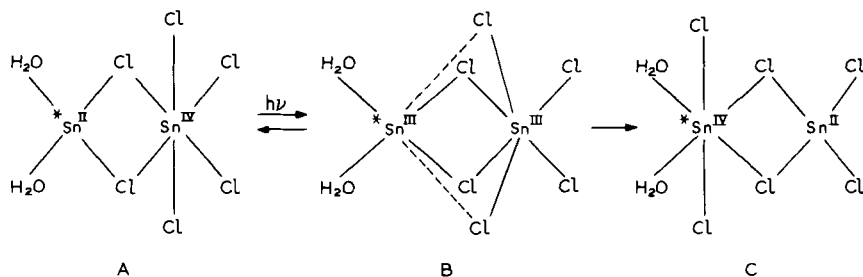


FIG. 41. Configurations involved in photochemical isotope exchange in the three-level system $\text{Sn}_3\text{Cl}_6(\text{H}_2\text{O})_2$.

phenomenon; that terminal state with the larger Franck-Condon overlap with the intermediate state will be favored.

The mixed valence tin oxide Sn_3O_4 has been identified in various thermochemical studies of SnO (678, 679). However, preliminary work on the powder pattern of Sn_3O_4 showed that it could not be indexed as tetragonal (272), this being the crystal system of the analogous lead compound Pb_3O_4 . Similar studies in the Sn-S system (7) indicate the formation of Sn_2S_3 and Sn_3S_4 , mixed valence compounds which may be related to the mixed valence lead oxides of the same stoichiometry. The preparation of the oxide $\text{Sn}^{\text{II}}\text{Sn}^{\text{IV}}\text{O}_6$ by heating SnO at 475°C is described by Decroly and Ghodsi (183).

V. LEAD

The study of the mixed valence oxides of lead is confused by a number of reports on substances thought to be unique compounds, but which may well be mixtures. The mixed valence oxides of lead which

have been authenticated to date have been described most recently by White and Roy (769), who find experimental evidence for Pb_3O_4 , Pb_2O_3 , and $\text{Pb}_{12}\text{O}_{19}$. Byström (121) also discusses the structures and compositions of these compounds and others of less certain stoichiometry.

Pb_3O_4 (red lead) is obtained as transparent scarlet crystals from a solution of PbCO_3 in molten KNO_3 – NaNO_3 flux. According to the X-ray studies of Gross (317) and of Byström and Westgren (118, 122) and the neutron diffraction study of Fayek and Leciejewicz (233), Pb_3O_4 has a class I crystal structure in which lead ions in very different environments

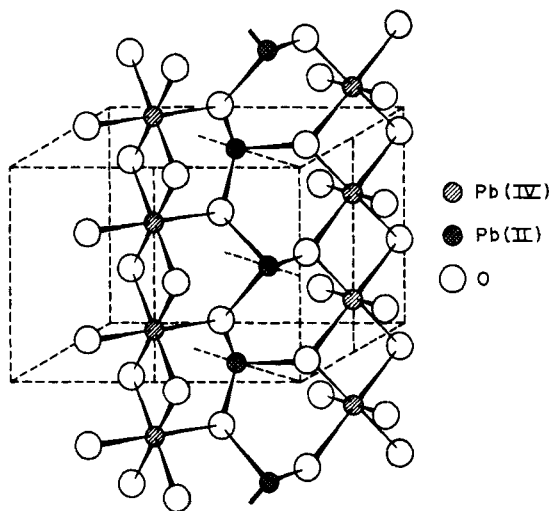


FIG. 42. The class I crystal structure of Pb_3O_4 (756).

share oxide ligands. As shown in Fig. 42, the Pb(IV) ions lie at the centers of oxygen atom octahedra which share edges to form chains and have $\text{Pb(IV)}\text{—O}$ distances equal to 2.15 Å, whereas the Pb(II) are inserted between the $\text{Pb}^{\text{IV}}\text{O}_6$ chains in such a way that each has three oxygen atoms at about 2.2–2.3 Å, the next nearest oxygen neighbor being at 3.0 Å. The O—Pb(II)—O angles are all approximately 90°. Consonant with the class I structure, polycrystalline $\text{Pb}_2^{\text{II}}\text{Pb}^{\text{IV}}\text{O}_4$ has a resistivity of 10^{12} ohm cm (769), and a color (red) which would appear to be just the sum of the colors of $\text{Pb}^{\text{II}}\text{O}$ (red) and $\text{Pb}^{\text{IV}}\text{O}_2$ (red). The bonding and hybridization in Pb_3O_4 have been discussed by Dickens (194).

An anhydrous form of lead sesquioxide, Pb_2O_3 , can be produced by hydrothermal synthesis as large crystals of a lustrous jet black color (143). The striking difference between the colors of Pb_2O_3 and Pb_3O_4 at

first suggests that the lead ion environments are not nearly as dissimilar in Pb_2O_3 as they are in Pb_3O_4 . The structure of Pb_2O_3 has been only partially solved, the all-important positions of the oxygen atoms still being in some doubt (120, 127). It appears that one type of lead atom is at the center of a distorted square with a mean Pb—O distance of 2.1 Å, whereas the second type of lead atom is at the center of a distorted octahedron with four Pb—O distances equal to 2.39 Å, and two additional oxygens at 2.81 Å. If this is so, the two types of lead ion in Pb_2O_3 would seem to form a class I system, judging from our limited experience. On the other hand, the black color of Pb_2O_3 would seem more understandable if it were a class II system. However, the black color may be due to a constituent ion absorption. Because there are two ions of lower valence for every ion of higher valence in Pb_3O_4 , and because the crystal contains twice as many metal ion sites of one type as of the other, the stoichiometry clearly suggests which oxidation states occupy which metal ion sites. Such is not the case in Pb_2O_3 . However, although the question of which oxidation state of lead occupies which type of site in Pb_2O_3 cannot be answered a priori, the bond distances suggest that the Pb(IV) ions are in the distorted square sites and the Pb(II) ions are in the distorted octahedral sites.

The resistivity of Pb_2O_3 is reported as 10^{12} ohm cm, a value which is a composite of bulk resistance, surface resistance, contact resistance, and grain-contact resistance values (769). The fact that the reported resistivities of Pb_2O_3 and class I Pb_3O_4 are of the same order of magnitude demonstrates either the difficulty of divining the significance of resistivities as measured on powders, or that Pb_2O_3 really is a class I system as intimated by its crystal structure. Only further work can decide which is the case.

An experiment widely quoted as refuting the "oscillating valence" concept was preformed by Zintl and Rauch (817) on the mixed valence hydrate $\text{Pb}_2\text{O}_3 \cdot 3\text{H}_2\text{O}$. This yellow-orange material was synthesized, using radioactive Pb(II) and inactive Pb(IV) in a way previously shown not to exchange the Pb(II) and Pb(IV) ions. The solid was irradiated for 3 hours and then decomposed, again without exchange, and the two types of lead were separated and then assayed for radioactivity. It was found that, after irradiation and decomposition, the Pb(IV) was only 1.3% as radioactive as the Pb(II). From this, the conclusion was drawn that in this compound, the valences did not oscillate on irradiation with light and, by analogy, that they did not oscillate in any other mixed valence compound. With the advantage of hindsight, one can point out that, although no structure is available for this hydrated oxide, its lack of an intense, low-energy mixed valence color suggests that the

lead ions are in very different environments in the crystal and that, although it is a three-level system (see tin, subsection U), the excited state reached in a mixed valence absorption will always relax to the no-exchange ground state. This will be especially true in crystals where nuclear rearrangements are difficult. Although the Zintl and Rauch experiment performed on $\text{Pb}_2\text{O}_3 \cdot 3\text{H}_2\text{O}$ therefore sheds no light on the problem of "oscillating valence," the experimental idea has been used with interesting results by Craig and Davidson (164) in the aqueous Sn(II),Sn(IV) system.

A brown-black mixed valence lead oxide, earlier known as $\alpha\text{-PbO}_x$ (122) and now known to have the stoichiometry $\text{Pb}_{12}\text{O}_{19}$, has been briefly described. A crystal structure, deduced both from a single crystal X-ray study (122) and from studies of the lead-oxygen phase equilibria and powder patterns (12, 769), shows that the structure of $\text{Pb}_{12}\text{O}_{19}$ is derived from that of tetragonal PbO by the insertion of a layer of oxygen atoms between the Pb—O—Pb layers. The result is a face-centered, nominally cubic cell having a small monoclinic distortion in which all lead atoms are in nearly equivalent, cubic, eightfold coordination. Because the lead atoms in $\text{Pb}_{12}\text{O}_{19}$ occupy slightly dissimilar sites (class II), its resistivity will not be metallic, but should be considerably lower than those of Pb_3O_4 and Pb_2O_3 . This expectation is fulfilled, for the resistivity of $\text{Pb}_{12}\text{O}_{19}$ is reported to be eight orders of magnitude smaller than that of Pb_3O_4 and Pb_2O_3 (769).

As expected, orthorhombic PbO is an insulator. Strangely, although $\text{Pb}_{12}\text{O}_{19}$ appears to be a relatively good conductor of electricity, it is to be noted that, according to the data of White and Roy (769), the single valence material $\text{Pb}^{\text{IV}}\text{O}_2$ has a resistivity which is three orders of magnitude smaller still than that of $\text{Pb}_{12}\text{O}_{19}$. However, it is pertinent to note that a sample of analytical reagent grade PbO_2 has been analyzed earlier to be of the composition $\text{PbO}_{1.98} \cdot 0.04\text{H}_2\text{O}$ (117), thus demonstrating that " PbO_2 " may well be nonstoichiometrically mixed valence, although nominally it is not. Byström (121) also reports a nonstoichiometric composition for commercial " PbO_2 ." There are many examples of the difficulty of getting oxide crystals of many metals free of interfering, extraneous oxidation states. Because of this, it is difficult to assess the true meaning of powder conductivities in oxides.

Infrared spectra of the mixed valence oxides are given by Roy and co-workers (768) in a paper concerned primarily with their high pressure-high temperature polymorphism.

The addition of a solution of $[\text{M}^{\text{III}}(\text{NH}_3)_6]\text{Cl}_3$ to an HCl solution containing Pb(IV) precipitates a pale colored Pb(IV) salt, which subsequently evolves Cl_2 to form darkly colored mixed valence chloro-

plumbates(II,IV). The salts $[\text{Co}^{\text{III}}(\text{NH}_3)_6]\text{PbCl}_6$ and $[\text{Co}^{\text{III}}(\text{NH}_3)_5\text{H}_2\text{O}]\text{PbCl}_6$ have been investigated by Mori (515), who found them to be diamagnetic. This lack of paramagnetism suggests that, as in the Sb(III),Sb(V) halides, the lead in these compounds is in fact an equimolar mixture of the diamagnetic ions Pb(II) and Pb(IV). The corresponding chromium salts $[\text{Cr}^{\text{III}}(\text{NH}_3)_6]\text{PbCl}_6$ and $[\text{Cr}^{\text{III}}(\text{NH}_3)_5\text{H}_2\text{O}]\text{PbCl}_6$ are strongly paramagnetic owing to the presence of the Cr(III) ion. This series of four salts present an interesting situation in that the two aquopentammines are pale red, as might be expected for a $\text{Pb}^{\text{II}}\text{Cl}_6$ - $\text{Pb}^{\text{IV}}\text{Cl}_6$ system, but the hexammines are reported to be violet-black. The suggestion is that the two types of salt have rather different crystal structures.

The crystal structure of the black-violet $[\text{Co}^{\text{III}}(\text{NH}_3)_6]\text{PbCl}_6$ was investigated by Atoji and Watanabe (34), who found it to be closely related to that of $[\text{Co}^{\text{III}}(\text{NH}_3)_6]\text{TlCl}_6$, a compound studied by them earlier (748). In the latter substance, the $[\text{TlCl}_6]^{3-}$ and $[\text{Co}(\text{NH}_3)_6]^{3+}$ ions form a cubic sodium chloride type lattice with four formula weights per unit cell. Each $[\text{TlCl}_6]^{3-}$ octahedron is surrounded by eight $[\text{Co}(\text{NH}_3)_6]^{3+}$ groups as nearest neighbors and eight $[\text{TlCl}_6]^{3-}$ groups as second nearest neighbors at $2^{1/2}$ times the Co—Tl distance. The powder pattern of the hexachloroplumbate compound was interpreted as showing a cubic cell much like that of the hexachlorothallate, in spite of several lines observed in the former which are not present in the latter. If the hexachloroplumbate is indeed cubic as claimed, then either all lead ions must have the intermediate valence 3+ and be paramagnetic, or the system is metallic. The situation is completely analogous to the dilemma discussed in the case of the M_2SbX_6 salts, where a cubic structure implied a paramagnetic species, yet the compounds are observed to be diamagnetic. And just as the solution to that dilemma rested on showing that the crystals were in fact tetragonal, not cubic, it seems a good guess that a more careful study of $[\text{Co}(\text{NH}_3)_6]\text{PbCl}_6$ will show that it too is tetragonal, with valences trapped as $\text{Pb}^{\text{II}}\text{Cl}_6$ and $\text{Pb}^{\text{IV}}\text{Cl}_6$. Indeed, some of the weak lines in the powder pattern of the lead compound index as reflections not allowed in the cubic space group reported for it (180).

If the valences are really trapped, then the PbCl_6 sublattice of $[\text{Co}(\text{NH}_3)_6]\text{PbCl}_6$ is probably related quite closely to the SbBr_6 superlattice of $(\text{NH}_4)_2\text{SbBr}_6$ (Fig. 46). The analogy between the lead and antimony mixed valence halides can be carried further, since Sb(III) and Sb(V) are isoelectronic with Pb(II) and Pb(IV), except for a difference in principal quantum number, and hence should have quite similar mixed valence spectra. The powder reflection spectrum of $[\text{Co}(\text{NH}_3)_6]\text{PbCl}_6$ (shown in Fig. 43) contains intense bands at lower frequencies

than the absorptions of the component ions, which should probably be assigned as class II mixed valence transitions, although in this case some care is needed to distinguish the mixed valence absorption from absorption due to the $[\text{Co}(\text{NH}_3)_6]^{3+}$ ion.

In this regard, it is of interest that the narrow band at $36,300\text{ cm}^{-1}$ corresponds very closely in energy to the $^1S_0 \rightarrow ^3P_1$ ($6s^2 \rightarrow 6s^16p^1$) transition of the Pb(II) ion in KCl (807). Again, as with the corresponding antimony halides, the frequency and intensity of the mixed valence transition in the chloroplumbates(II, IV) would appear to depend upon

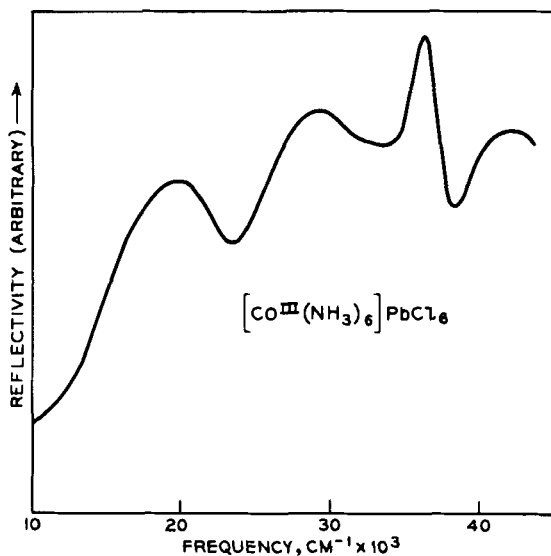


FIG. 43. The diffuse reflectance spectrum of $[\text{Co}^{\text{III}}(\text{NH}_3)_6]\text{PbCl}_6$ (180).

the overlap of halide orbitals on neighboring MX_6 groups transforming the system into class II. Not unexpectedly, the far infrared spectrum of $[\text{Co}(\text{NH}_3)_6]\text{PbCl}_6$ (42) contains a band coincident with that of $[\text{Pb}^{\text{IV}}\text{Cl}_6]^{2-}$, as well as bands at lower frequencies presumably due to $[\text{Pb}^{\text{II}}\text{Cl}_6]^{4-}$.

Arguing by analogy with the Bi_9^{5+} ion characterized by Hershaft and Corbett (356, 357), Britton (98) had proposed that the isoelectronic ion Pb_9^{4-} of Zintl and co-workers (818) also has the tripyramidal structure (Fig. 44). The suggestion of Marsh and Shoemaker (483) that the Pb_9^{4-} ion is formed of three Pb_4 tetrahedra sharing two vertices each is readily seen to be equivalent to Britton's description with allowances for distortion.

A brief note by Gasperin (270) describes the structure of a mixed

valence lead oxychloride of the composition $\text{Pb}_{3.6}\text{Cl}_{1.8}\text{O}_4$, in which 10% of the metal ion sites are empty, 50% of these sites being filled with Pb(II) and 32% with Pb(IV). In the ideal structure, all metal ion sites are equivalent, having as nearest neighbors four oxygen atoms and one chlorine atom in a square bipyramidal arrangement. As the material is reported to be yellow, it appears that the true structure involves considerable distortion from the ideal, such that the lead valences are firmly trapped as in a class I system.

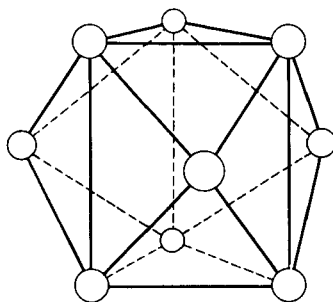


FIG. 44. The structure proposed for the Pb_9^{4-} ion and observed in the iso-electronic Bi_9^{5+} ion in crystalline $\text{Bi}_{12}\text{Cl}_{14}$.

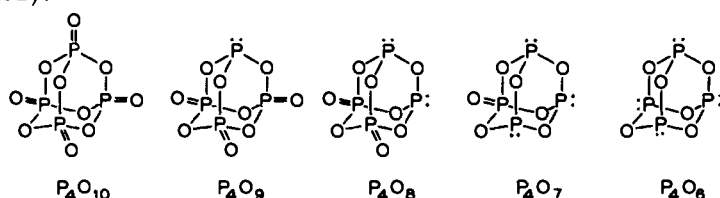
A second compound of apparently nonintegral stoichiometry, $\text{Pb}_3\text{Sb}_2\text{O}_{8.47}$, is discussed by Kuznetsov and Koz'min (452). In this substance, the ratio $\text{Sb(V)}:\text{Pb(IV)}:\text{Pb(II)}$ is equal to 4.0:1:5.0, and the two valences of lead appear trapped, the ions being in different environments. The Pb(IV) is eight-coordinated with six oxygens at 2.19 Å and two at 2.30 Å, whereas the Pb(II) is six-coordinated with oxygens at 2.43 Å. There is no description of the physical properties of $\text{Pb}_3\text{Sb}_2\text{O}_{8.47}$.

A nominally trivalent lead fluoride, PbF_3 , has been mentioned (371), but nothing appears to be known about it.

W. PHOSPHORUS AND ARSENIC

Between the two phosphorus oxides, $\text{P}_4^{\text{V}}\text{O}_{10}$ and $\text{P}_4^{\text{III}}\text{O}_6$, there exist three intermediate oxides, P_4O_9 , P_4O_8 , and P_4O_7 , each of which contains P(III) and P(V) oxidation states in the same molecule. As can be seen from the structures given below, the valences in these molecules are

firmly trapped as P(III) and P(V), and so the crystals are class I (353, 400, 401):



These mixed valence oxides are colorless and diamagnetic, as expected. Similar mixed valence oxides are reported in the arsenic oxide (466) and the phosphorus sulfide (199) systems. As might be expected from the lack of color in the solid mixed valence arsenic oxides, a concentrated HCl solution containing As(III) and As(V) failed to give a mixed valence absorption band in the 14,000–31,000 cm^{-1} region (772).

X. ANTIMONY

There are two general types of mixed valence system thought to contain Sb(III) and Sb(V) ions. The double halides of Sb(III) and Sb(V) are, with one exception, of a very dark violet, blue, or black color and all present interesting problems in electronic structure, color, magnetism, and molecular structure. The mixed valence antimony oxides, on the other hand, are colorless, and, in the light of the deeply colored halides, present yet another problem in the study of color and constitution.

Salts of antimony of the kind Cs_2SbX_6 were long ago regarded as examples of the 4+ oxidation state of antimony. Although the possibility of the presence of Sb(IV) in such halide salts now appears quite remote, there still remains considerable confusion as to the molecular and electronic structures of the component ions, in spite of recent efforts to rationalize seemingly contradictory experimental results. Setterberg (654) first synthesized the intensely blue salt Cs_2SbCl_6 from the colorless components CsCl , SbCl_3 , and SbCl_5 , and raised the question as to whether it was a salt of Sb(IV) or was to be formulated as the mixed valence compound $\text{Cs}_4\text{Sb}^{\text{III}}\text{Sb}^{\text{V}}\text{Cl}_{12}$. For comparison, the salts $\text{Rb}_3\text{Sb}^{\text{III}}\text{Cl}_6$ and $\text{RbSb}^{\text{V}}\text{Cl}_6$ are colorless and pale yellow-green, respectively. The first indication that Cs_2SbCl_6 was a salt of Sb(IV) came from the work of Wells and Metzger (757), who showed that it was isostructural with $\text{Cs}_2\text{Pb}^{\text{IV}}\text{Cl}_6$, forming mixed crystals with it having a pale to dark green color depending upon the Sb/Pb ratio. Following this, black Rb_2SbCl_6 was found to give violet-colored mixed crystals with $\text{Rb}_2\text{Pt}^{\text{IV}}\text{Cl}_6$, as did the corresponding potassium salts, and the unstable $(\text{NH}_4)_2\text{SbCl}_6$ was

obtained readily as a deeply colored mixed crystal with either $(\text{NH}_4)_2\text{Pt}^{\text{IV}}\text{Cl}_6$ or $(\text{NH}_4)_2\text{Sn}^{\text{IV}}\text{Cl}_6$ (752). That these salts contain Sb(IV) was apparently confirmed by X-ray powder diffraction work on $(\text{NH}_4)_2\text{SbBr}_6$, Rb_2SbBr_6 , and Rb_2SbCl_6 , in which consideration of extinctions and intensities led to the conclusion that each of the salts is face-centered cubic (381), having the anti-fluorite structure of the $\text{M}_2\text{Pt}^{\text{IV}}\text{Cl}_6$ salts. Thus, in these salts all antimony ions appeared to be crystallographically equivalent, and the unusual colors were therefore ascribed to the Sb(IV) ion in octahedral coordination.

The Sb(IV) ion has the outer electronic configuration $5s^1$ and as such should show the paramagnetism characteristic of a 2S state, whereas the ions Sb(III) and Sb(V), being $5s^2$ and $5s^0$, respectively, are diamagnetic. Repeated magnetic susceptibility measurements on the M_2SbX_6 salts and on $(\text{NH}_4)_2(\text{Sb},\text{Sn})\text{Cl}_6$ have shown them in every case to be diamagnetic with $\chi_d \sim 0.3 \times 10^{-6}$ cgs (28, 29, 218, 381, 382). Although demonstrating that these substances do not contain magnetically dilute Sb(IV) ions, the observed diamagnetism may not rule out a strongly antiferromagnetic aggregation of Sb(IV). The latter possibility, however, is a remote one, for the crystal structure determination shows that neither direct Sb—Sb interactions nor bridged configurations of the type Sb—X—Sb are present, but, instead, only $\text{SbX}_6\text{—X}_6\text{Sb}$ contacts with a center-to-center distance of about 7 Å, a grouping which has never been found to give antiferromagnetic ordering at 300°K. On the other hand, the observed diamagnetism of these compounds agrees with the Sb(III),-Sb(V) formulation.

The high resistivity of the salts (29, 382) demonstrates that, if they are indeed mixed valence, the valences are firmly trapped, although it should be marked that thermally activated electron transfer remains a possibility in class II mixed valence systems. Indeed, $(\text{NH}_4)_2(\text{Sb}_x\text{Sn}_{1-x})\text{Cl}_6$ mixed crystals behave as high resistance semiconductors (33), with a room temperature resistivity which drops sharply with increasing antimony concentration. On the other hand, the thermal activation energy for conductivity is almost independent of composition, suggesting that it is dominated by the energy of mobility rather than production of charge carriers, as in mixed valence hopping semiconductors like $\text{Li}_x\text{Ni}_{1-x}\text{O}$ (Section III, G).

In an interesting application of the continuous variation technique to the problem of the valences in the solid state, Brauer and Schnell (91) attempted to refute the presence of Sb(IV) in these complexes. In this experiment, the intensity of light reflected from powdered samples was measured as the concentration of $(\text{NH}_4)_2\text{SbBr}_6$ was increased in the host crystal $(\text{NH}_4)_2\text{SnBr}_6$. Here, as in the solution work (*vide infra*), it

was found that, at low antimony concentrations, the reflectivity varied as the square root of the $(\text{NH}_4)_2\text{SbBr}_6$ concentration and not linearly as would be expected if the chromophoric grouping were $[\text{Sb}^{\text{IV}}\text{Br}_6]^{2-}$. At higher antimony concentrations, the variation of the reflected light intensity with antimony concentration was not so marked. Such solid state spectrophotometry can sometimes yield useful results when

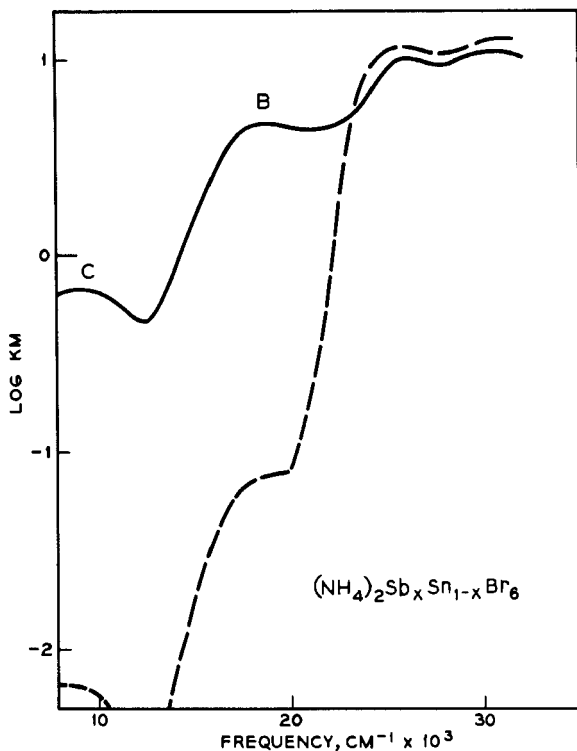


FIG. 45. The diffuse reflectance spectrum of solid solutions of $(\text{NH}_4)_2\text{SbBr}_6$ in $(\text{NH}_4)_2\text{SnBr}_6$ at high (—), and low (---) concentrations. The bands B and C are mixed valence transitions.

comparisons are made between sets of very similar samples and precautions are taken to ensure uniform particle sizes. However, it is not clear whether such precautions were taken in this case, and since the frequency at which measurements were made ($21,300\text{ cm}^{-1}$) does not correspond to the interaction absorption frequency (Fig. 45), it is difficult to draw conclusions from the experiment.

Further evidence of the mixed valence nature of the hexahaloantimonates was provided by Turco and co-workers (711-714), who have shown in a series of studies that the introduction of radioactive

Sb(III) into these salts does not yield equal amounts of radioactive Sb(III) and Sb(V) on decomposition, as would be expected if all the antimony ions in the crystal were equivalent. They also report that Rb_2SbCl_6 can be made with Sb(V)/Sb(III) ratios as large as 1.6, while still maintaining the color and external form of the 1:1 substance. Even larger deviations of the Sb(V)/Sb(III) ratio from 1.0 were reported for the mixed crystals of $(\text{NH}_4)_2\text{SbCl}_6$ in $(\text{NH}_4)_2\text{SnCl}_6$, but a recent study of this system (33) did not confirm this result.

The major objection to the Sb(III),Sb(V) mixed valence model of the M_2SbX_6 crystals was removed by Tovborg Jensen and Rasmussen (705), who found that the crystals reported as cubic by Jensen (381) are in fact tetragonal with $c/a = 1.43$, whereas this ratio is 1.414 for a cubic cell. In particular, it was found that $(\text{NH}_4)_2\text{SbBr}_6$, Rb_2SbBr_6 , and Cs_2SbBr_6 are tetragonal and that Rb_2SbCl_6 is strictly cubic but has an anomalous X-ray intensity distribution, which suggests disorder among the Sb(III) and Sb(V) ions. Recent confirmation of Tovborg Jensen and Rasmussen's powder measurements has come from single crystal X-ray work by Lawton and Jacobson (456) on $(\text{NH}_4)_2\text{SbBr}_6$. They found a small tetragonal distortion of the cubic cell resulting from ordering of the $[\text{Sb}^{\text{V}}\text{Br}_6]^-$ and $[\text{Sb}^{\text{III}}\text{Br}_6]^{3-}$ units, as shown in Fig. 46. In this structure, each $[\text{SbBr}_6]^{3-}$ is surrounded by eight $[\text{SbBr}_6]^-$ and four $[\text{SbBr}_6]^{3-}$ ions, and vice versa. The average Sb(III)—Br and Sb(V)—Br bond lengths were 2.795 Å and 2.564 Å, respectively. Thus, the sites of the two types of antimony ion are quite similar, which, when taken with the mixed valence absorption in the visible, strongly suggests that the system is class II. However, it is not immediately obvious how this can be, since there do not appear to be any shared ligands.

Experimentally, the only spectra available are those obtained by diffuse reflection by Day (178) in the systems $\text{M}_2[\text{Sb},\text{Sn}]\text{X}_6$, where $\text{M} = \text{K}, \text{NH}_4, \text{N}(\text{CH}_3)_4, \text{N}(\text{C}_2\text{H}_5)_4, \text{Rb},$ or Cs , and X is Cl or Br (Figs. 45 and 47). The latter was recorded as the difference spectrum between samples of differing dilutions and thus accentuates the visible absorption. In these spectra, the host lattice absorptions are assigned as those bands which do not lose intensity on lowering the concentration of antimony in the solid solution. In the cesium stannic chloride mixed crystal, the sharp band at $31,000\text{ cm}^{-1}$ (marked A) is most probably the $^1\text{S}_0 \rightarrow ^3\text{P}_1$ component of the $5s^2 \rightarrow 5s^15p^1$ transition in Sb(III), which occurs at $29,000\text{ cm}^{-1}$ in $[\text{Co}(\text{NH}_3)_6][\text{Sb}^{\text{III}}\text{Cl}_6]$. The first absorption band of $[\text{Sb}^{\text{V}}\text{Cl}_6]^-$, which occurs at $37,000\text{ cm}^{-1}$ in solution (772), is hidden under the host lattice absorption. The lower frequency bands (marked B and C in Figs. 45 and 47) are clearly the interaction bands responsible for the mixed valence color in M_2SbX_6 systems.

Day (178) suggested that the two mixed valence transitions B and C are the singlet and triplet components of the lowest symmetry-allowed excitation, but it does not now seem likely that an exchange interaction

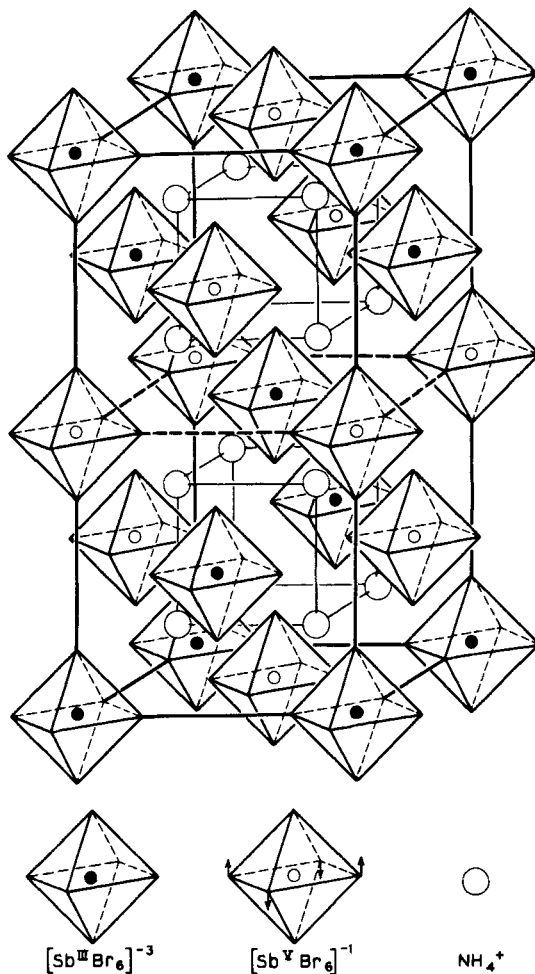


FIG. 46. The class II tetragonal unit cell of $(\text{NH}_4)_4\text{Sb}^{\text{III}}\text{Sb}^{\text{V}}\text{Br}_{12}$, showing the relative disposition of $\text{Sb}^{\text{V}}\text{Br}_6$ and $\text{Sb}^{\text{III}}\text{Br}_6$ octahedra. The distortion of the $\text{Sb}^{\text{V}}\text{Br}_6$ octahedron is as indicated at the bottom (456).

between two $5s$ orbitals separated by about 7 \AA could produce a singlet-triplet separation of 9000 cm^{-1} . Two other explanations present themselves. As can be seen from Fig. 46, each $\text{Sb}(\text{III})$ ion in $(\text{NH}_4)_2\text{SbBr}_6$ is surrounded by four $\text{Sb}(\text{V})$ ions in a plane, and by four $\text{Sb}(\text{V})$ ions at the

vertices of a tetrahedron. If the salts that Day investigated also have this structure and are sufficiently tetragonal, then two symmetry-allowed mixed valence absorption bands would be expected, one, a doubly degenerate, in-plane-polarized transition involving the Sb(III) ion and the planar array of Sb(V) ions, and the second a nearly triply degenerate, weakly polarized transition involving the Sb(III) ion and the tetrahedral array of Sb(V) ions. Another explanation for the second band is that electron transfer occurs to higher orbitals on the Sb(V). The transition

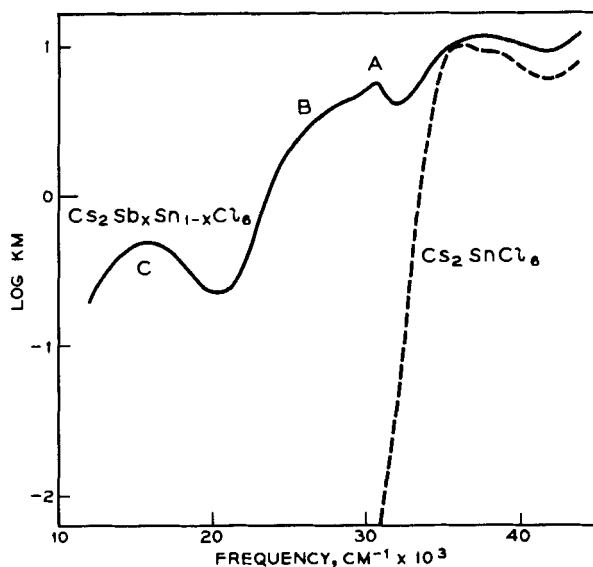


FIG. 47. The diffuse reflectance spectra of Cs_2SnCl_6 (---), and of Cs_2SbCl_6 doped into Cs_2SnCl_6 (—) (180).

$\psi_A 5s^2 \psi_B 5s^0 \rightarrow \psi_A 5s^1 \psi_B 5p^1$ is expected to lie above $\psi_A 5s^2 \psi_B 5s^0 \rightarrow \psi_A 5s^1 \psi_B 5s^1$ by an amount corresponding to the excitation $\psi_B 5s^1 \rightarrow \psi_B 5p^1$, which is about $86,000 \text{ cm}^{-1}$ in the Sb(IV) free ion (510), but could be considerably less when the Sb(IV) is imbedded in a crystal as a hexahalogen anion.

As was seen in Section II, for a mixed valence transition in the trapped valence case, the transition moment cannot be large unless there is overlap between the functions,

$$\Psi_A(5s) \text{ and } \sum C_i \Psi_{B_i}(5s)$$

The former function is that of the $5s$ orbital on the central antimony ion, and the sum is taken over the $5s$ orbitals of the surrounding antimony

ions, with the signs of the coefficients C_i taken so as to give a function which has a single nodal plane. Thus the qualitative reports, which describe the M_2SbX_6 mixed valence colors as very intense, necessitate a significant overlap between the antimony ion wave functions of neighboring $Sb^{III}X_6$ and Sb^VX_6 groups. This is rather unexpected since the Sb—Sb distance is approximately 7 Å in all cases. The required overlap between the antimony could be imagined to arise from delocalization of the $5s$ orbitals through σ -bond formation with the halide $p\sigma$ orbitals. If the halide ions on adjacent $[SbX_6]^-$ and $[SbX_6]^{3-}$ ions have a nonzero overlap, there is then formed a path over which an electron could be transferred from Sb(III) to Sb(V). That such an SbX_6-X_6Sb overlap may exist was first suggested by Jensen (382), but Lawton and Jacobson state specifically that there is nothing in the least unusual about the $SbBr_6-SbBr_6$ distances in $(NH_4)_2SbBr_6$ (456). Since it is notoriously difficult to assess absorption intensities in solids from visual depth of color, it may well be that the transition moment of the mixed valence absorption and the associated overlap are really quite small, and that it is this small ligand-ligand overlap which turns the formally class I system into a class II system with a visible mixed valence absorption. Charge transfer from halide to metal in adjacent hexahalogen anions has been proposed already by Owen to explain the antiferromagnetic interaction between the Ir(IV) ions in the lattice of K_2IrCl_6 (553).

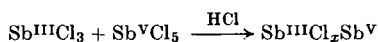
As might be expected, the substitution of the Sb(III) in $M_4Sb^{III}Sb^VCl_{12}$ by the ions Fe(III) or In(III) changes the color from black to pale yellow, since all metal ions are then fully oxidized and there is no electron readily available for low-energy transfer. Day (178) reports the intermolecular charge transfer transition of $Cs_4In^{III}Sb^VCl_{12}$ to fall at $30,800\text{ cm}^{-1}$, and that of the Tl(III) analog to fall at $29,600\text{ cm}^{-1}$. The corresponding Bi(III) compound has a deep red color with a maximum at $24,000\text{ cm}^{-1}$ in the diffuse reflectance spectrum.

Many other halide salts have been described as containing Sb(III) and Sb(V). Brauer and Schnell (89) have prepared black $Rb_3Sb_2Br_{11}$ and also mention the salt $TlSbCl_5$. Since this latter substance is reported to have only a pale color, and in view of the fact that the mixed valence thallium chloride compounds are never deeply colored, it may be more reasonable to consider it as being $Tl^ITl^{III}Sb_2^{III}Cl_{10}$ rather than $Tl_2Sb^{III}Sb^VCl_{10}$. The materials $Rb_8Sb_3Cl_{18}$, $(NH_4)_5Sb_2Cl_{12}$, $(pyH)_5Sb_3Cl_{18}$, and $(pyH)_{11}Sb_5Cl_{30}$ (752) are all brown-black crystalline solids of apparent mixed valence constitution, but a recent X-ray study of $[N(CH_3)_4]_3Sb_2Br_{11}$ (455) reveals that the compound is not an example of antimony mixed valence, for $[Sb_2^{III}Br_9]^{3-}$ groups alternate with

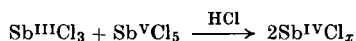
bromine molecules in the lattice. The only mixed valence antimony fluorides reported to date have the compositions $\text{Sb}_2^{\text{III}}\text{Sb}^{\text{V}}\text{F}_{11}$ and $\text{Sb}_5^{\text{III}}\text{Sb}^{\text{V}}\text{F}_{20}$ (607), and are low melting, colorless solids.

Ephraim and Weinberg (224) report a thermochromic effect in an Sb(III), Sb(V) halide system which certainly deserves more exploration, both crystallographically and spectroscopically. Addition of NH_4Cl in sufficient quantity to a molten mixture of SbCl_3 and SbCl_5 leads to the formation of a black mass which on cooling becomes colorless. Heating then restores the black color, and the white-black cycle can be repeated indefinitely. Clearly, more crystallographic and spectroscopic work will be needed before a clear picture emerges of the relationship between the color and constitution of the many mixed valence antimony halides.

The "interaction color" of concentrated HCl solutions containing both SbCl_3 and SbCl_5 , first observed by Weinland and Schmid (752), has since been studied by a very large number of workers. Hydrochloric acid solutions of SbCl_3 and SbCl_5 are colorless and pale yellow, respectively, and both obey Beer's law, showing that there are no Sb(III)-Sb(III) or Sb(V)-Sb(V) interactions in the solutions. However, the HCl solution containing both Sb(III) and Sb(V) is a deep lemon-yellow to brown color, and continuous variation studies show that the concentration of the species responsible for the mixed valence absorption, as measured by the optical density of the solutions at frequencies where the components are only weakly absorbing, is a maximum for $[\text{Sb(III)}]/[\text{Sb(V)}] = 1$. Moreover, the concentration of this colored species varies as the product $[\text{Sb(III)}][\text{Sb(V)}]$ (177, 215, 770, 772). These facts are consistent with a color-producing reaction of the sort



but inconsistent with the reaction



It is to be noted, however, that, since the two antimony atoms in a mixed valence dimer complex in solution might very well have identical ligand fields, the spectrophotometric studies do not rule out the formation of $\text{Sb}^{\text{IV}}\text{Cl}_x\text{Sb}^{\text{IV}}$ in these solutions. The susceptibilities of the Sb(III), Sb(V) solutions have not been measured.

Studies of electrochemical redox reactions (101, 102) as well as radiochemical exchange experiments (79, 434, 529) also point to the formation of an Sb(III), Sb(V) dimer in concentrated HCl solutions. Bonner and Goishi (79) made a careful study of the rate of electron exchange in HCl solutions, using ^{124}Sb as a tracer. The exchange rate increased steadily

with increasing HCl concentration, reaching a maximum at approximately 9.3 *M* HCl and decreasing again in 12 *M* HCl. Up to 8 *M* HCl, complex exchange curves were observed and explained by slow inter-conversion among two complexes of Sb(V) which exchange at different rates with Sb(III). To discover whether the interaction absorption complex in solution was also the reaction intermediate for exchange, they made qualitative observations on the interaction absorption in non-equilibrium solutions. Their conclusion was that the interaction absorption, which occurs only between $[\text{Sb}^{\text{III}}\text{Cl}_4]^-$ and $[\text{Sb}^{\text{V}}\text{Cl}_6]^-$ ions, does not result from a symmetrical dimer, nor does it lead to a symmetrical excited state, because there is no correlation with the rate of electron exchange. Transition states such as $[\text{Cl}_5\text{Sb}^{\text{III}}\text{ClSb}^{\text{V}}\text{Cl}_5]^{3-}$, $[\text{Cl}_4\text{Sb}^{\text{III}}\text{Cl}_2\text{Sb}^{\text{V}}\text{Cl}_4]^{2-}$, and $[\text{Cl}_4\text{Sb}^{\text{III}}\text{Cl}_2\text{Sb}^{\text{V}}\text{Cl}_3]^-$ have been suggested for the thermochemical electron exchange (434, 529), but no unequivocal choice has been made between them. However, the fact that the mixed valence dimer has a class II absorption suggests that the coordinations about the two antimony ions are very similar.

Under the influence of an electric field, the colored Sb(III),Sb(V) species in 12 *M* HCl was found to migrate to the positive electrode (215), showing that it had a negative charge. Thus, there are more than eight chloride ions in the mixed valence complex $[\text{Sb}^{\text{III}}\text{Sb}^{\text{V}}\text{Cl}_x]^{n-}$. Although a high formal concentration of HCl is required to form the complex, a brown color is also reported to form on heating a mixture of pure SbCl_3 and SbCl_5 ⁴ (224). Usanovitch *et al.* (715) studied this system and concluded that the components reacted to form the ion pair $[\text{SbCl}_4]^-[\text{SbCl}_4]^+$.

Solution of metallic antimony in the molten halides SbX_3 might be expected to lead to the formation of reduced species in the presence of the oxidized SbX_3 , and thence to mixed valence compounds. However, Corbett and students (107, 151) have studied the product of dissolution of antimony in SbI_3 and found it to be diamagnetic Sb_2I_4 .

The oxides of antimony present a most interesting contrast, for although the mixed valence halides are black, the mixed valence oxides are colorless! The difference is even more striking when one realizes that

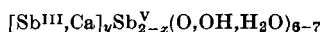
⁴ Whitney and Davidson (772) report that there is no perceptible color change on cooling the concentrated HCl solution of SbCl_3 and SbCl_5 to -80°C , and conclude that the reaction forming the colored species has a very low heat. An alternate explanation rests on the fact that, in any case, one sees only the band edge as the source of color and the intensity of absorption in the band edge will decrease rapidly with a decrease in temperature. The experimental result is then understandable as the simultaneous decrease of visible absorption intensity per absorbing molecule, and increase of the number of absorbing species as the temperature is decreased. According to such an explanation, the heat of dimer formation could be appreciable.

the oxides contain anions bridging the mixed valence antimony whereas, formally, the halides do not. As expected, the difference in color of the oxides and halides can be traced directly to differences in structure.

The primary product formed on heating hydrated Sb_2O_5 is $\text{Sb}_3\text{O}_6\text{OH}$, which contains two gram ions of Sb(V) and one gram ion of Sb(III) per formula weight, and is reported to be colorless to pale yellow, suggesting a class I crystal structure. After a few near misses (185, 527), the crystal structure of $\text{Sb}_3\text{O}_6\text{OH}$ was finally deduced by Dihlström and Westgren (196) from the powder pattern. They found a face-centered, cubic cell in which all the Sb(V) ions lie at the centers of oxide ion octahedra having an Sb(V)—O distance of 2.02 Å, whereas each of the Sb(III) ions is surrounded by six oxide ions at a distance of 2.48 Å and two OH^- ions at 2.23 Å. Since a normal Sb(III)—O distance is 2.02–2.1 Å, the Sb(III) is in effect only two-coordinated and the other six oxygens, which simultaneously surround the Sb(III) ion and form octahedra with the Sb(V) ions, have only a very weak interaction with the former. Thus it appears possible to rationalize the lack of color in this compound as the consequence of a class I crystal structure.

On further dehydration of $\text{Sb}_3\text{O}_6\text{OH}$ by prolonged heating at 900°C, the colorless, diamagnetic, insulating, mixed valence oxide $\alpha\text{-Sb}_2\text{O}_4$ is formed. Although a structure had been advanced for $\alpha\text{-Sb}_2\text{O}_4$ in which both the Sb(III) and Sb(V) ions were octahedrally coordinated (197), Wells (756) has criticized it, pointing out that the four shortest Sb(III)—O distances were 0.5 Å longer than the 2.0 Å expected. The validity of this criticism is now apparent from the work of Skapski and Rogers (599, 670), who solved the crystal structures of $\alpha\text{-Sb}_2\text{O}_4$ and of a second polymorph $\beta\text{-Sb}_2\text{O}_4$. In both the α and β forms of Sb_2O_4 the Sb(V) ions are found in layers, each Sb(V) being at the center of a slightly deformed octahedron with Sb—O distances ranging from 1.956 to 1.990 Å. On the other hand, the Sb(III) ions form columns between the layers with each Sb(III) ion having two oxide ions at 2.032 Å and two at 2.218 Å (as shown in Fig. 48). Although the color of $\beta\text{-Sb}_2\text{O}_4$ is not given, one presumes that it is colorless, like the $\alpha\text{-Sb}_2\text{O}_4$ from which it is made, and that both are class I systems. Titration of solutions of Sb_2O_4 in mineral acids is said to show that the antimony in such solutions is present as Sb(III) and Sb(V) in equal amounts (435).

There is a naturally occurring mixed valence mineral, stibiconite, which has the general formula



in which x varies from zero to almost one, and y is approximately one (486). Because this yellow mineral has been shown to be isostructural

with the pyrochlore minerals (5, 389, 810), it no doubt has a structure closely related to that of $\text{Sb}_3\text{O}_6\text{OH}$, described above, with Sb(III) and Sb(V) ions in distinctly different environments.

Thus, in the mixed valence antimony oxides, the Sb(V) ion prefers a sixfold, octahedral coordination, whereas the Sb(III) ion has only four

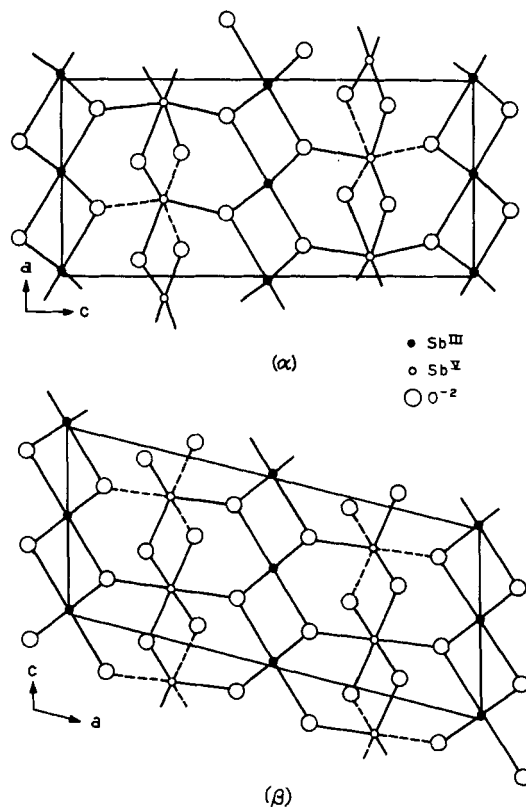


FIG. 48. The class I crystal structures of $\alpha\text{-Sb}_2\text{O}_4$, upper, and $\beta\text{-Sb}_2\text{O}_4$, lower (599, 670).

near neighbors. The fact that no mixed valence optical transition is observed in the visible region in these compounds, even though there are Sb(III)-O-Sb(V) bridges, may result not only from the difference in site symmetries, but also from the very high stability of the Sb(III) ion in fourfold coordination and its consequent resistance to thermal or photochemical oxidation. The mixed valence oxide $\beta\text{-Sb}_2\text{O}_4$ can be heated to over 1000°C in oxygen without oxidation of the Sb(III).

Y. BISMUTH

Metallic bismuth has long been known to dissolve in molten bismuth trichloride, forming lower halides of debatable composition (149). Although BiCl is a predominant species in the gas phase reaction, the condensed phase reaction has been shown by a single crystal X-ray study to yield a compound of the stoichiometry $\text{Bi}_{12}\text{Cl}_{14}$ (356, 357). The compound was shown to consist of two $[\text{BiCl}_5]^{2-}$, one-half $[\text{Bi}_2\text{Cl}_8]^{2-}$, and one mole of the mixed valence cation Bi_9^{5+} per formula weight. This latter cation is a tripyramid of nominal symmetry D_{3h} , having six bismuth atoms at the vertices of a trigonal prism and a bismuth atom placed symmetrically above each of the three rectangular faces of the prism (Fig. 44). Although the observed structure of Bi_9^{5+} is of a symmetry lower than D_{3h} , it approximates the ideal arrangement wherein all nine bismuth atoms are equidistant from a central point. As there are two types of bismuth atom in the complex (the six prism atoms and the three equatorial ones), one might at first attempt to assign integral valences in accord with the trapped valence model. However, this is not possible if the overall charge is to be $5+$. Thus the ion is a class III-A system in spite of certain inequivalences between atoms, and is best considered by using molecular orbital theory. This has been done by Corbett and Rundle (153), who found that the MO theory, using $6p$ orbitals only, predicts a diamagnetic ground state, as observed, and that the equatorial atoms are much less positive than the prism atoms.

Spectroscopically, there are no quantitative data for $\text{Bi}_{12}\text{Cl}_{14}$, but it is reported to form shiny black prisms, the color being due no doubt to the Bi_9^{5+} cation. Because the mixed valence Bi_9^{5+} units are separated by essentially insulating material, the $\text{Bi}_{12}\text{Cl}_{14}$ crystals will probably be found to be insulators, unless, however, there is an additional mixed valence interaction between the reduced Bi_9^{5+} and oxidized $[\text{Bi}^{\text{III}}\text{Cl}_5]^{2-}$ groups.

Spectra of Bi-BiCl_3 melts recorded by Boston and Smith (81) in the visible region show a large absorption tail in the $20,000\text{--}25,000\text{ cm}^{-1}$ region due to hot BiCl_3 (BiCl_3 in a KCl matrix shows a transition centered at $30,500\text{ cm}^{-1}$) (277) and a broad band centered at $17,860\text{ cm}^{-1}$ with a weak shoulder claimed at $16,400\text{ cm}^{-1}$, the combination of the three acting to make the melt black. The large deviation from Beer's law observed by them in the visible region was felt to be due to the presence of two species of unknown structure, each absorbing in the same spectral region. It is to be remembered, however, that, although the black substance $\text{Bi}_{12}\text{Cl}_{14}$ is a solid recovered from a solution of bismuth in BiCl_3 , there is in fact no evidence for the Bi_9^{5+} ion in the melt. In a later spectral

study, Bjerrum *et al.* (71) found that solution of metallic bismuth in dilute solutions of BiCl_3 in liquid $\text{AlCl}_3\text{--NaCl}$ and $\text{ZnCl}_2\text{--KCl}$ eutectics resulted in the formation of Bi^+ ions with three bands in the 10,000–16,000 cm^{-1} region, and Bi_5^{3+} ions with major bands at 12,000 and 25,000 cm^{-1} . This latter mixed valence species may be further coordinated by halide ions.

The magnetic susceptibility of Bi--BiCl_3 solutions has been measured by Nachtrieb (523). In accord with the observed lack of electronic conduction in the dilute melts (30, 31), the Bi--BiCl_3 solutions are diamagnetic, indicating that there are neither metallic conduction electrons nor neutral ground state Bi atoms ($^4S_{3/2}$) in the melt. Thus the dissolved metallic bismuth is associated with itself and/or the BiCl_3 solvent. The susceptibilities and conductivities of solutions of bismuth metal in molten BiBr_3 (308) and BiI_3 (307, 576, 704) have also been studied recently.

There are a few bismuth oxides about which little can be said, but which may later prove to be of mixed valence interest. Zemann (811) has described the preparation and results of a crystal structure study of an orange-red "bismuth acid," thought to contain Bi(III) and Bi(IV) in a structure like that of "antimony acid," $\text{Sb}^{\text{III}}\text{Sb}_2^{\text{V}}\text{O}_6\text{OH}$. In addition to the red and brown-black forms of $\text{Bi}_2\text{O}_4 \cdot x\text{H}_2\text{O}$ (639), anhydrous BiO has been reported (809). BiO has a slightly distorted sphalerite structure and probably contains equal numbers of Bi(I) and Bi(III) ions.

Z. LANTHANIDES

The reduction of $\text{Ce}^{\text{IV}}\text{O}_2$ by H_2 at high temperatures results in the formation of lower oxides of cerium having a deep blue-black color, which fades to pale yellow-green as the reduction proceeds to $\text{Ce}_2^{\text{III}}\text{O}_3$ (64, 65, 86, 92, 587). Similar lower mixed valence oxides can be produced by firing mixtures of $\text{Ce}^{\text{IV}}\text{O}_2$ and $\text{Ce}_2^{\text{III}}\text{O}_3$ (88, 108). Studies of the phase diagram in the region $\text{CeO}_2\text{--CeO}_{1.50}$ show the presence of three stoichiometric intermediate phases, $\text{Ce}_{11}\text{O}_{20}$, Ce_9O_{16} , and Ce_7O_{12} , and two other regions of composition $\text{CeO}_{1.70}\text{--CeO}_{1.67}$ and $\text{CeO}_{1.67}\text{--CeO}_{1.50}$ (64, 65, 88). There is no evidence for the earlier reported compound Ce_4O_7 . The stoichiometric intermediate phases have rhombohedral structures based on that of fluorite with an extension along a cube diagonal. In these structures, the cation lattice is complete, but there is presumed to be an ordering of vacancies in the anion lattice. The other two regions of lower oxide homogeneity have the type-C and type-A rare earth oxide structures, respectively (64). The lower cerium oxides are most likely

class II systems, but no other physical measurements on them have been reported as yet.

Numerous mixed valence oxides of the other lanthanide elements known to exist in oxidation states higher than 3+, i.e., praseodymium and terbium, have also been widely studied. The best known praseodymium oxide is Pr_6O_{11} , which is formed when any other praseodymium oxide or oxy-salt is strongly heated in air. There was once speculation (573) that praseodymium could be oxidized beyond 4+ in the presence of other trivalent rare earths, and, on this basis, Pr_6O_{11} was given the formula $2\text{Pr}_2^{\text{III}}\text{O}_3 \cdot \text{Pr}_2^{\text{V}}\text{O}_5$, and $\text{Pr}^{\text{IV}}\text{O}_2$ was thought to be $\text{Pr}_2^{\text{III}}\text{O}_3 \cdot \text{Pr}_2^{\text{V}}\text{O}_5$. Marsh (482), however, was able to oxidize praseodymium only to the 4+ oxidation state, a conclusion many times reconfirmed (229, 485, 500, 501). The major features of the phase diagram between $\text{PrO}_{1.5}$ and PrO_2 were mapped by Martin (485), who found two types of phase, one cubic, with essentially the fluorite lattice of PrO_2 systematically deficient in oxygen, and the other hexagonal, based on the A-type Pr_2O_3 lattice. Since 1950 many structural investigations of the PrO_x system have been made by Brauer (88) and by Eyring and his associates, whose results have recently been reviewed (229). We shall not go into details here, except to say that, for carefully annealed samples, it now seems likely that the entire range of composition between $\text{PrO}_{1.5}$ and PrO_2 will be resolved into definite compounds with narrow composition ranges separated by two-phase regions. The existence of a homologous series $\text{M}_n\text{O}_{2n-1}$ has been proposed (229), with slabs of MO_2 joined by facesharing of their coordination polyhedra, as in A-type M_2O_3 .

Similar conclusions would apply to the terbium oxides, of which Tb_4O_7 and Tb_6O_{11} were characterized by Prandtl and Rieder (573) and confirmed by Gruen *et al.* (322), and may also be relevant to the so-called solid solutions of La_2O_3 , Nd_2O_3 , and Sm_2O_3 in CeO_2 and PrO_2 . The latter were said (167, 168) to show a region of homogeneity from MO_2 to about 60% M_2O_3 , but closer examination might reveal details of ordering comparable to that found with the mixed valence transition metal oxides (compare $\text{Ti}_n\text{O}_{2n-1}$ and $\text{Cr}_2^{\text{III}}\text{Ti}_{n-2}^{\text{IV}}\text{O}_{2n-1}$, for example).

Measurements of the physical properties of the lanthanide(III,IV) oxides began with the observation of Foëx (255) that Pr_6O_{11} had a conductivity at 500°C at least 10^7 times greater than that of Pr_2O_3 , and further careful work on all the trivalent lanthanide oxides (535, 536), as well as Pr_6O_{11} and Tb_4O_7 , showed that the latter two compounds were very much more conducting than any of the others. It was also concluded that the conductivity was electronic and not ionic. In his work on the PrO_x phase diagram, Martin (485) used thermoelectric measurements to show that, while type-A Pr_2O_3 is a *p*-type semiconductor, indicating

that the Pr_2O_3 lattice can accommodate small amounts of additional oxygen, Pr_6O_{11} is n -type, suggesting that it is effectively PrO_2 with an oxygen deficiency, rather than Pr_2O_3 with excess oxygen. Eyring and his collaborators (228) as well as Honig [quoted in Eyring and Baenziger (228)] have begun to make electrical measurements on the praseodymium oxides as a function of temperature and oxygen pressure, but their results as reported up to the present add little to the earlier qualitative conclusions, except that the transition from n -type conduction in PrO_x occurs when x is between 1.65 and 1.83.

All the praseodymium(III,IV) oxides are reported as black (229) and those of terbium as dark brown, but, in the oxides closest in composition to Pr_2O_3 , f - f transitions of Pr(III) are clearly seen (734) against a background of absorption steadily increasing into the ultraviolet. There is also an extremely broad absorption in the near infrared, beginning at about $12,000\text{ cm}^{-1}$. In the terbium(III,IV) oxides, there is a very broad absorption centered near $15,000\text{ cm}^{-1}$, extending into the near infrared and as far as the ultraviolet cut-off of Tb_2O_3 . From the available structural and physical evidence it therefore appears that all these oxides are class II systems.

Mixed valence oxides of those lanthanides which form stable divalent states have been much less investigated than the quadrivalent ones. One of the best characterized compounds of this type is Eu_3O_4 (2), which, with the isomorphous compound SrEu_2O_4 (40), is related structurally to CaFe_2O_4 . A recent structure analysis (577) showed that each Eu(III) was surrounded by six oxide ions and each Eu(II) by eight, so the compound, which is dark red by transmitted light (577), belongs to class I. Nothing has been reported about its electrical properties. Another mixed valence europium oxide, LiEu_3O_4 (41), has been described as isomorphous with $\text{LiSr}_2\text{Eu}^{\text{III}}\text{O}_4$.

By melting some lanthanide metals with their respective sesquioxides, compounds LnO_x with $1.450 < x < 1.500$ were prepared for Gd, Y, Er, and Lu (507), and their dark colors were attributed to the presence of high concentrations of color centers. Whether this is the case, or whether the excess electrons are trapped on metal ions, forming Ln(II) , Ln(III) mixed valence systems, remains to be seen.

Although a mixed valence cerium chloride and fluoride have been mentioned in the literature, it appears that, to the moment, the only genuine mixed valence cerium halide is an iodide. Asker and Wylie (27) mention the double fluoride $(\text{NH}_4)_2\text{Ce}^{\text{III}}\text{Ce}^{\text{IV}}\text{F}_9$, but give no details or references about it; it may well exist only as a misprint. On the basis of e.m.f. studies, Senderoff and Mellors (653) have suggested that the dissolution of Ce metal in molten CeCl_3 results in the formation of

$\text{Ce}^{\text{I}}[\text{Ce}^{\text{III}}\text{Cl}_4]$, analogous to the $\text{Ga}^{\text{I}}[\text{Ga}^{\text{III}}\text{X}_4]$ compounds. On quenching the Ce/CeCl₃ melt, an intensely black solid phase resulted which analyzed for large amounts of both metallic cerium and CeCl₃ (170). Later work (99), however, convincingly refutes the conclusions of the e.m.f. study, and so it would appear that there is no evidence for a mixed valence cerium chloride.

A phase study of the Ce–CeI₃ system by Corbett *et al.* (152) shows that, in addition to CeI₂, a lower iodide of composition CeI_{2.4} can be made. The compound is isomorphous with PrI_{2.5} and can be formulated as $\text{Ce}_2^{\text{III}}\text{Ce}_3^{\text{II}}\text{I}_{12}$. Although nothing more is known of this material, it may well be a metallic conductor, for CeI₂ itself is metallic (152) due to the fact that the Ce(II) ion prefers to put its second 4*f* electron into a conduction band of the solid, thereby becoming Ce(III). According to Sallach and Corbett (616), there are no intermediate mixed valence cerium bromides.

There are a number of lower-valent halides of the other lanthanides which may be of mixed valence interest. By dissolving lanthanide metals in the appropriate molten trihalides, the following “nonstoichiometric” phases have been detected (152, 206–208, 505, 616): NdCl_{2.37}, NdI_{1.95}, PrCl_{2.31}, PrBr_{2.38}, PrI_{2.50}, and GdCl_{1.58}. Scandium (154), yttrium, and erbium (155) do not form such compounds. Like cerium, the diiodides of praseodymium and neodymium are metals, so the corresponding mixed valence compounds may be class III-B systems with partly filled conduction bands based on 5*d* orbitals. In contrast, the other mixed valence halides have very low electrical conductivities including, surprisingly, GdCl_{1.6}, which has a magnetic moment of 7.89 ± 0.03 B.M. per gadolinium (313), very close to that expected if all the gadoliniums had effective 4*f*⁷ configurations (7.94 B.M.). What has happened to the “extra” 1.4 electrons per metal atom has by no means been determined, but the close proximity of the configurations 4*f*⁷5*d*¹ and 4*f*⁸ for Gd(II) suggests that spin pairing might have occurred through the formation of metal-metal bonds using 5*d* orbitals. The compound would then be a member of our class III-A.

AA. ACTINIDES

Stimulated in large part by their potential use as nuclear fuels, large areas of the complicated uranium oxide phase diagram have been studied, revealing many mixed valence materials. Makarov (478) attempted to bring some order to the wealth of data collected by 1961, by suggesting that the uranium oxides form a related series of compounds,

just as was found with the titanium, vanadium, molybdenum, and niobium oxides. In the case of uranium, the general formula U_nO_{2n+2} accounts for a number, but not all the reported oxides. The most studied region of the uranium oxide phase diagram (70, 72, 362, 364, 481, 589, 590) lies between UO_3 ($n = 2$) and UO_2 ($n = \infty$), wherein five members of the series with mixed valence stoichiometry have been located so far.

UO_2 , the end member of the series, is a readily oxidizable material which, at low temperature, can incorporate oxygen into its fluorite lattice up to a composition of $UO_{2.3}$ (24, 316, 568). On annealing, this oxide decomposes to a mixture of UO_2 and U_4O_9 (25, 316, 438, 481, 589). Further oxidation leads to the formation of U_7O_{16} (568), U_6O_{14} (189, 191, 364, 387, 636, 637), U_5O_{12} (636, 637), U_4O_{10} (361, 481, 610), and U_3O_8 (191, 316, 481). In addition to these compounds, the compositions $UO_{2.90}$ (51, 363, 689), U_5O_{13} (72, 637), U_3O_4 (806), $UO_{2.61}$ (589), and U_8O_{17} (481) have been reported. Many of these phases listed above have polymorphic forms and are of appreciable breadth.

In the UO_{2+x} phase, in the region $0 < x < 0.3$, the excess oxygen ions occupy interstitial sites in the host UO_2 fluorite-type lattice in a random manner (24, 781). The contraction of the UO_2 unit cell as oxygen is added to it was interpreted by Anderson *et al.* (11) to result from the partial oxidation of U(IV) to the smaller U(V) ions. Because the interstitial oxide ions form part of the uranium ions' coordination sphere, these ions effectively trap the uranium valence, turning UO_{2+x} into a class II system. Over wide variations of x , the systems all seem to have a resistivity of approximately 10^5 ohm cm at 300° K (521). The color of " UO_2 " has been reported variously as all shades between green and black, due no doubt to the ease with which UO_{2+x} is formed even at room temperature.

U_4O_9 has a structure much like that of the UO_{2+x} phase, except that the interstitial positions are filled in an orderly way (52, 782). Like UO_{2+x} , U_4O_9 is a semiconductor ($E_{act} = 0.46$ eV) (521) and is paramagnetic from 1.4° to 500° K with a maximum susceptibility at 6.4° K (301, 457). The effective magnetic moment of U_4O_9 is 2.06 B.M. per uranium, to be compared with 2.83 B.M. in pure UO_2 . Gotoo *et al.* (301) have computed the effective magnetic moment of U_4O_9 on the assumption that the valences are trapped as either $U_2^{IV}U_2^V O_9$ or $U_3^{IV}U^VI O_9$, and find 2.10 B.M. for the former and 1.42 B.M. for the latter. Although appearing to support a U(IV), U(V) configuration for U_4O_9 , it must be said that the calculation is based upon a simplified model of the structure. The compound CaU_3O_9 also has a face-centered cubic structure and very nearly the resistivity of U_4O_9 (804).

The application of X-ray (315) and neutron diffraction (467)

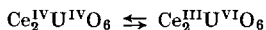
techniques to the problem of the structure of U_3O_8 was successful in showing the positions of both the uranium and oxygen atoms in the unit cell. There are two types of uranium site in U_3O_8 (467), the first having six oxygens at 2.07–2.23 Å and a seventh at 2.44 Å, and a second with six oxygens at 2.07–2.23 Å and a seventh at 2.71 Å, there being twice as many of the latter as the former. Such a structure allows one to assign the valences in U_3O_8 as either $U^{VI}U^{IV}_2O_8$ or $U^{VI}_2U^{IV}O_8$. Whereas the U(VI),U(V) formulation is suggested by Loopstra (467), the U(VI),U(IV) formula is compatible with the general formula $U^{VI}_2U^{IV}_{n-2}O_{2n+2}$ for the uranium oxide series. The green color of U_3O_8 is also that expected for a material containing the U(IV) ion. A radiochemical exchange experiment on U_3O_8 , using first radioactive UO_2 and then radioactive UO_3 in the preparation of U_3O_8 , yielded equal amounts of uranium radioactivity in both oxidation states, suggesting at first that all the uranium atoms were equivalent in the structure (73). The authors admit, however, that it is more likely that an isotopic exchange occurred on formation of the U_3O_8 . Reported resistivity measurements on U_3O_8 differ by a factor of 10^6 , due no doubt to the fact that U_3O_8 and UO_3 readily form solid solutions which upset the stoichiometry. The resistivity of stoichiometric α - U_3O_8 would seem to be 10^5 ohm cm at 300°K, with a semi-conduction activation energy of 0.6–0.7 eV (274, 521). U_3O_8 is paramagnetic with a susceptibility anomaly at 4.2°K (457), and an effective magnetic moment per mole of 1.39 B.M. (338). Assuming that the electron spin is the only source of paramagnetism, $U^{VI}U^{IV}_2O_8$ has an expected moment of 1.41 B.M., and $U^{VI}_2U^{IV}O_8$ has one of 1.63 B.M., both in acceptable agreement with the experimental value.

The α - and β -forms of U_3O_7 have structures much like that of UO_2 , except that they are tetragonally deformed. As with many of the other mixed valence uranium oxides, the material is paramagnetic with a maximum susceptibility at 6.4°K (457), and, as with the others, the resistivity has been reported to be as low as 3×10^2 (780) and as high as 3×10^6 ohm cm (521) for different samples at 300°K.

There are indications that spectral studies on the uranium oxides might be of value in understanding their molecular and electronic structures, particularly as regards the distribution of valence. Thus, Narbutt and Laputina (526) have studied the X-ray fluorescence M spectra of UO_2 , U_3O_8 , and UO_3 , and find small but distinct differences between UO_2 and UO_3 , with U_3O_8 occupying an intermediate position. Gruen's study of the optical spectrum of UO_2 in ThO_2 (323) clearly shows the presence of the U(IV) ion, and his technique might be of value in determining the presence of this valence state in other class II oxides. Finally, Hoekstra and Siegel (363) report that the infrared spectra of

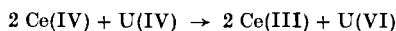
U_3O_8 and $\text{UO}_{2.9}$ show that neither of these substances contains the isolated $[\text{U}^{\text{VI}}\text{O}_2]^{2+}$ group.

Hofmann and Höschle (366) first reported the preparation of the deep blue materials "cerium-uranium blue," having the approximate composition $2\text{CeO}_2 \cdot \text{UO}_2$, and a dihydrate having the same Ce/U ratio. Because $\text{U}^{\text{IV}}\text{O}_2$ is brown and $\text{Ce}^{\text{IV}}\text{O}_2$ is colorless, these authors ascribed the blue color of the mixed oxides as due to an oscillation of valence:

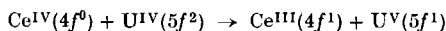


Later investigators (87, 372, 475, 604, 606) have since shown that, because both CeO_2 and UO_2 have the fluorite lattice with only a very small difference in their lattice parameters, mixed crystals of UO_2 and CeO_2 are to be expected over a wide range of composition, and that the Ce_2UO_6 composition is but one unexceptional example of these solid solutions. In addition to the Ce/U ratio, the water content of the cerium-uranium blue "dihydrate" is also variable continuously (87). In spite of extensive X-ray work on the CeO_2 - UO_2 system, a disagreement still remains as to the upper limit of UO_2 solubility in CeO_2 , Hund *et al.* (372) claiming that a solid solution forms only in the range 0-63% UO_2 , while Magneli and Kihlberg (475) and Rüdorff and Valet (604, 606) find unlimited UO_2 solubility, with the Vegard law very nearly obeyed.

In HClO_4 - NaClO_4 solutions, the Ce(IV) ion rapidly oxidizes the U(IV) ion, according to the reaction (36a):



If such a redox reaction were to occur during the formation of cerium-uranium blue, then, depending upon whether the Ce(IV) or U(IV) ions were in excess in the crystal, there would arise the possibility of either Ce(III),Ce(IV) or U(IV),U(VI) mixed valence optical transitions. However, at the $2\text{Ce(IV)}:1\text{U(IV)}$ stoichiometry there would be no excess ions for mixed valence interaction and the blue color should fade at this composition. In fact, the intensity of the blue color is maximal at approximately the 2:1 composition (87), showing that the blue color is instead due to a Ce-U interaction. Now the U(VI) ion when in eightfold oxygen coordination, as it would be in the fluorite lattice of cerium-uranium blue, is known to always draw two of the oxygens toward itself so as to form the $[\text{UO}_2]^{2+}$ ion (756). However, were such to happen in cerium-uranium blue, the lattice would no longer be that of fluorite. Thus it appears that the blue color is due to the transfer of an electron between Ce(IV) and U(IV):



Solution of UO_2 in the not easily reduced host ThO_2 results in brownish solids, as expected (87). Pressed pellets of cerium-uranium blue of

various Ce/U ratios show a minimum resistivity of 1.6×10^2 ohm cm at about 40% CeO₂ with maximal resistivity at pure CeO₂ and UO₂ (606).

Oxidation of cerium-uranium blue leads to the formation of CeO₂-U₃O₈ mixed crystals containing up to 45 mole % U₃O₈ while still maintaining the fluorite structure. As determined from density measurements, the excess oxygen ions in CeO₂-U₃O₈ mixed crystals occupy both interstitial and cation sites. The CeO₂-U₃O₈ crystals are described as being dark green to black (606).

The mixed valence halides of uranium have been investigated but very little. There are two chlorides of possible mixed valence interest, $2\text{U}^{\text{IV}}\text{Cl}_4 \cdot \text{U}^{\text{VI}}\text{Cl}_6 \cdot 6\text{POCl}_3$, described as dark green crystals (560), and the dark brown prismatic crystals formed by the action of CCl₄ on U₃O₈, formulated as either $2\text{U}^{\text{IV}}\text{Cl}_4 \cdot \text{U}^{\text{VI}}\text{O}_2\text{Cl}_2$, or $3\text{U}^{\text{IV}}\text{Cl}_4 \cdot \text{U}^{\text{IV}}\text{OCl}_2 \cdot 2\text{U}^{\text{VI}}\text{O}_2\text{Cl}_2$ (375).

Uranium enneafluoride, U₂F₉, is a black substance formed in varying yield in many fluorination reactions (4, 531, 534). According to Zachariasen (808), U₂F₉ has a class III-B crystal structure with all uranium atoms in structurally equivalent positions. The unit cell is body-centered cubic with the uranium in ninefold coordination, the average U-F distance of 2.30 Å being intermediate between the U(IV)-F and U(V)-F distances of UF₄ and UF₅. However, the same cannot be said for the black color of U₂F₉, for UF₄ is green and UF₅ is colorless. An effective magnetic moment of 2.11 B.M. per uranium atom has been measured for U₂F₉ (595). The resistance of U₂F₉ has not been measured, but would be very interesting as it might suggest whether the system is really class III-B or class II. A second black mixed valence uranium fluoride, U₄F₁₇, has a structure described as "distorted UF₄," and a specific susceptibility of 8.8×10^{-6} cgs at 22°C (4, 531).

The physical and chemical properties of many of the uranium halides and oxides have been described in detail in reference works (406) and (649). Of the other actinide elements, there are only a few oxides whose stoichiometry suggests that they are mixed valence (649). Protactinium forms the oxide Pa₄O₉ which is cubic, as is U₄O₉, but which is white, whereas U₄O₉ is black. The lower oxides PaO_{2.25}-PaO_{2.20} (cubic), Pa₅O₁₁ (tetragonal), and PaO_{2.20}-PaO_{2.00} (cubic) are all black, however. Neptunium forms a chocolate-brown oxide Np₃O₈ isomorphous with U₃O₈ (405), and plutonium forms an oxide phase PuO_{1.50}-PuO_{1.75} isomorphous with Mn₂O₃.

BB. MISCELLANEOUS

Those elements which have as yet only a scant mixed valence chemistry are brought together in this section. The most surprising of

these is xenon, which forms a stable yellow oxide of the apparent composition $K_4Xe^{VIII}Xe_2^{VI}O_{12}$, which by its color is most likely class I (21, 680). A possible mixed valence compound of aluminum, $Al_4B[N(CH_3)_2]_3(CH_3)_6$, has been reported as a yellow solid having an average aluminum oxidation number of 1.5+ (644). Solutions of cadmium metal in molten $CdCl_2$ have been shown repeatedly to contain species formed from one cadmium atom and from one to three $Cd(II)$ ions (520), but no mixed valence compounds have yet been isolated.

Considerably more can be said about the mixed valence polyhalides; however, we shall limit our remarks to the triiodide ion, and refer the interested reader to the review by Wiebenga *et al.* (773) for information on the other polyhalides. The triiodide ion, I_3^- , is a nominally linear species with ends which are more or less equivalent, depending upon the environment in which it finds itself. Its bonding has been investigated and its electronic spectrum in water explained on the basis of a slightly bent, class III-A system (91). The blue starch-iodine complex has been described as both a class III-A (592) and class III-B (62) polymer of the triiodide ion.

IV. Conclusions

At this point, a survey study of mixed valence chemistry is rather frustrating, because the data for virtually every substance are too meager to allow the deduction and testing of firm conclusions. The reason for this lies in the fact that mixed valence compounds up to now seem to have been studied only by chance, without a real appreciation of their uniqueness and the complementary nature of their various properties. The future is bright, however, in that papers on mixed valence chemistry are presently appearing at the healthy rate of about 60 per year and could easily double, once mixed valence chemistry becomes fashionable. As it stands now, though, the dearth of information is not only in a way frustrating, but also stimulating, we think, and it is our hope that this article will prompt the work in the near future needed to build a proper understanding of this phenomenon. Moreover, the thermodynamic, kinetic, and mechanistic aspects of mixed valence are all important ones which we have not mentioned, along with mixed metal mixed valence, covalent materials, and intermetallics.

It appears that until the properties of mixed valence substances have been more completely investigated, the classification scheme presented here can be used profitably to predict the properties of a substance, given any one of them. One imagines that, in the future, as mixed valence

becomes more and more understandable, it will prove as rewarding to inorganic chemistry as the concept of resonance has been to organic chemistry.

ACKNOWLEDGMENT

P.D. is very grateful to Bell Telephone Laboratories, Inc., for their hospitality during the summer of 1966, when most of this review was written. We both wish to acknowledge the assistance of Mr. N. A. Kuebler with the clerical work, and to thank Dr. H. Basch for performing the H_3^+ calculation for us.

REFERENCES

1. Abe, R., *J. Phys. Soc. Japan* **6**, 345 (1951).
- 1a. Abrahams, S. C., and Bernstein, J. L., *J. Chem. Phys.* **46**, 3776 (1967).
2. Achard, J. C., *Compt. Rend.* **250**, 3025 (1960).
3. Aebi, F., *Helv. Chim. Acta* **31**, 8 (1948).
4. Agron, P., Grenall, A., Kunin, R., and Weller, S., *U.S. At. Energy Comm. Rept. MDDC-1588* (1948).
5. Aia, M. A., Mooney, R. W., and Hoffman, C. W. W., *J. Electrochem. Soc.* **110**, 1048 (1963).
6. Aiken, J. K., Haley, J. B., and Terrey, H., *Trans. Faraday Soc.* **32**, 1617 (1936).
7. Albers, W., and Schol, K., *Philips Res. Rept.* **16**, 329 (1961).
8. Albrecht, W. H., and Wedekind, E., *Z. Anorg. Allgem. Chem.* **210**, 105 (1933).
9. Ali, S. M., Brewer, F. M., Chadwick, J. L., and Garton, G., *J. Inorg. & Nucl. Chem.* **9**, 124 (1959).
10. Allen, R. J., and Sheldon, J. C., *Australian J. Chem.* **18**, 277 (1965).
11. Anderson, J. S., Edgington, D. N., Roberts, L. E. J., and Wait, E., *J. Chem. Soc.* p. 3324 (1954).
12. Anderson, J. S., and Sterns, M., *J. Inorg. & Nucl. Chem.* **11**, 272 (1959).
13. Andersson, G., *Acta Chem. Scand.* **8**, 1599 (1954).
14. Andersson, G., *Acta Chem. Scand.* **10**, 623 (1956).
15. Andersson, S., Collén, B., Kuylenstierna, V., and Magneli, A., *Acta Chem. Scand.* **11**, 1641 (1957).
16. Andersson, S., Sundholm, A., and Magneli, A., *Acta Chem. Scand.* **13**, 989 (1959).
17. Andersson, S., and Wadsley, A. D., *Acta Cryst.* **15**, 201 (1962).
18. Andersson, S., and Jahnberg, L., *Arkiv Kemi* **21**, 413 (1963).
19. Andes, M. T. N. S., *Z. Astrobot.* **17A**, 612 (1939).
20. Andres, K., Kuebler, N. A., and Robin, M. B., *J. Phys. Chem. Solids* **27**, 1747 (1966).
21. Appelman, E. H., and Malm, J. G., *J. Am. Chem. Soc.* **86**, 2141 (1964).
22. Ariya, S. M., Shehukarev, S. A., and Glushkova, V. B., *Zh. Obshch. Khim.* **23**, 1241 (1953).
23. Arnold, R., and Walker, S. M., *J. S. African Chem. Inst.* **9**, 80 (1956).
24. Aronson, S., and Belle, J., *J. Chem. Phys.* **29**, 151 (1958).
25. Aronson, S., and Clayton, J. C., *J. Inorg. & Nucl. Chem.* **7**, 384 (1958).
26. Asbrink, S., and Magneli, A., *Acta Cryst.* **12**, 575 (1959).

27. Asker, W. J., and Wylie, A. W., *Australian J. Chem.* **18**, 959 (1965).
28. Asmussen, R. W., *Z. Anorg. Allgem. Chem.* **243**, 127 (1939).
29. Asmussen, R. W., *Z. Elektrochem.* **45**, 698 (1939).
30. Aten, A. H. W., *Z. Physik. Chem.* **66**, 641 (1909).
31. Aten, A. H. W., *Z. Physik. Chem.* **73**, 578 (1910).
32. Aten, A. H. W., Jr., Steinberg, H., Heymann, D., and Fontijn, A., *Rec. Trav. Chim.* **72**, 94 (1953).
33. Atkinson, L., and Day, P., unpublished results (1966).
34. Atoji, M., and Watanabe, T., *J. Chem. Phys.* **20**, 1045 (1952).
35. Austin, I. G., *Phil. Mag.* [8] **7**, 961 (1962).
36. Bachmann, H. G., Ahmed, F. R., and Barnes, W. H., *Z. Krist.* **115**, 110 (1961).
- 36a. Baker, F. B., Newton, T. W., and Kahn, M., *J. Phys. Chem.* **64**, 109 (1960).
37. Baker, L. C. W., and McCutcheon, T. P., *J. Am. Chem. Soc.* **78**, 4503 (1956).
38. Baker, L. C. W., Baker, V. S., Eriks, K., Pope, M. T., Shibata, M., Rollins, O. W., Fang, J. H., and Koh, L. L., *J. Am. Chem. Soc.* **88**, 2329 (1966).
39. Barbieri, G. A., *Ber. Deut. Chem. Ges.* **60**, 2424 (1927).
40. Bärnighausen, H., and Brauer, G., *Acta Cryst.* **15**, 1059 (1962).
41. Bärnighausen, H., *Angew. Chem.* **77**, 1014 (1965).
42. Barrowcliffe, C., Beattie, I. R., Day, P., and Livingstone, K., *J. Chem. Soc.* (1967) (to be published).
43. Bartlett, N., and Rao, P. R., *Proc. Chem. Soc.* p. 393 (1964).
44. Bartlett, N., private communication (1966).
45. Bashilova, N. I., *Dokl. Akad. Nauk SSSR* **141**, 1083 (1961).
46. Bateman, L. R., Blount, J. F., and Dahl, L. F., *J. Am. Chem. Soc.* **88**, 1082 (1966).
47. Baudisch, O., and Welo, L. A., *J. Biol. Chem.* **61**, 261 (1924).
48. Bauer, D., Schnering, H. G., and Schäfer, H., *J. Less-Common Metals* **8**, 388 (1965).
49. Bauminger, R., Cohen, S. G., Marinov, A., Ofer, S., and Segal, E., *Phys. Rev.* **122**, 1447 (1961).
50. Bayer, E., *Monatsh. Chem.* **41**, 223 (1920).
51. Beketov, A. R., Strekalovskii, V. N., and Vlasov, V. G., *J. Struct. Chem. (USSR) (English Transl.)* **6**, 64 (1965).
52. Belbeoch, B., Piekarski, C., and Pério, P., *Acta Cryst.* **14**, 837 (1961).
53. Belov, N. V., and Mokeeva, V. I., *Tr. Inst. Kristallogr., Akad. Nauk SSSR* **9**, 47 (1954).
54. Benrath, A., *Z. Anorg. Allgem. Chem.* **93**, 161 (1915).
55. Benrath, A., *Z. Anorg. Allgem. Chem.* **136**, 358 (1924).
56. Berdonosov, S. S., and Lapitskii, A. V., *Zh. Neorgan. Khim.* **10**, 2812 (1965).
57. Berecki-Biedermann, C., *Arkiv. Kemi* **19**, 35 (1962).
- 57a. Berglund, E., *Ber. Deut. Chem. Ges.* **7**, 470 (1874).
58. Bernal, I., Ebsworth, E. A. V., and Weil, J. A., *Proc. Chem. Soc.* p. 57 (1959).
59. Bernard, J., and Theobald, F., *Compt. Rend.* **256**, 4916 (1963).
60. Bernard, J., Theobald, F., and Theobald, J. G., *Compt. Rend.* **260**, 873 (1965).
61. Berry, L. G., *Am. Mineralogist* **39**, 504 (1954).
62. Bersohn, R., and Isenberg, I., *J. Chem. Phys.* **35**, 1640 (1961).
63. Berzelius, J. J., "*Lehrbuch*", 5th ed., Vol. 4, p. 422 (1847); quoted in Biltz (69).
64. Bevan, D. J. M., *J. Inorg. & Nucl. Chem.* **1**, 49 (1955).
65. Bevan, D. J. M., and Kordis, J., *J. Inorg. & Nucl. Chem.* **26**, 1509 (1964).
66. Bhattacharya, A. K., and Dhar, N. R. Z., *Z. Anorg. Allgem. Chem.* **213**, 240 (1933).

67. Bhattacharya, A. K., *J. Indian Chem. Soc.* **12**, 143 (1935).
68. Bhattacharya, A. K., *J. Indian Chem. Soc.* **18**, 85 (1941).
69. Biltz, W., *Z. Anorg. Allgem. Chem.* **127**, 169 (1923).
70. Biltz, W., and Müller, H., *Z. Anorg. Allgem. Chem.* **163**, 257 (1927).
71. Bjerrum, N. J., Boston, C. R., Smith, G. P., and Davis, H. L., *Inorg. Nucl. Chem. Letters* **1**, 141 (1965).
72. Blackburn, P. E., *J. Phys. Chem.* **62**, 897 (1958).
73. Blinova, N. I., and Tolmachev, Yu. M., *Radiokhimiya* **4**, 447 (1962).
74. Blomstrom, D. C., Knight, E., Jr., Phillips, W. D., and Weiher, J. F., *Proc. Natl. Acad. Sci. U.S.* **51**, 1085 (1964).
75. Blumberg, W. E., Eisinger, J., Aisen, P., Morell, A. G., and Scheinberg, I. H., *J. Biol. Chem.* **238**, 1675 (1963).
76. Blumenthal, R. N., Coburn, J., Baukus, J., and Hirthe, W. M., *J. Phys. Chem. Solids* **27**, 643 (1966).
77. Bogackij, D. P., *Zh. Obshch. Khim.* **21**, 3 (1951).
78. Bokii, G. B., and Distler, G. I., *Dokl. Akad. Nauk. SSSR* **56**, 923 (1947).
79. Bonner, N. A., and Goishi, W., *J. Am. Chem. Soc.* **83**, 85 (1961).
80. Bosman, A. J., and Crevecoeur, C., *Phys. Rev.* **144**, 763 (1966).
81. Boston, C. R., and Smith, G. P., *J. Phys. Chem.* **66**, 1178 (1962).
82. Braekken, H., *Kgl. Norske Videnskab. Selskabs, Forh.* **7**, 143 (1935).
83. Bragg, W. L., "Atomic Structure of Minerals." Cornell Univ. Press, Ithaca, New York, 1937.
84. Brain, F. H., Gibson, C. S., Jarvis, J. A. J., Phillips, R. F., Powell, H. M., and Tyabji, A., *J. Chem. Soc.* p. 3686 (1952).
85. Braterman, P. S., *J. Chem. Soc. A. Inorg., Phys., Theoret.* p. 1471 (1966).
86. Brauer, G., and Holtzschmidt, U., *Z. Anorg. Allgem. Chem.* **265**, 105 (1951).
87. Brauer, G., and Tiessler, R., *Z. Anorg. Allgem. Chem.* **271**, 273 (1953).
88. Brauer, G., and Gradinger, H., *Z. Anorg. Allgem. Chem.* **277**, 89 (1954).
89. Brauer, G., and Schnell, W. -D., *Z. Anorg. Allgem. Chem.* **283**, 49 (1956).
90. Brauer, G., and Eichner, M., *Z. Anorg. Allgem. Chem.* **285**, 118 (1956).
91. Brauer, G., and Schnell, W. -D., *Z. Anorg. Allgem. Chem.* **287**, 87 (1956).
- 91a. Brauer, G., and Eichner, M., *Z. Anorg. Allgem. Chem.* **287**, 95 (1956).
92. Brauer, G., and Gingerich, K., *Angew. Chem.* **69**, 480 (1957).
93. Brauer, G., and Eichner, M., *Z. Anorg. Allgem. Chem.* **296**, 13 (1958).
94. Brauer, G., and Morawietz, H., *Z. Anorg. Allgem. Chem.* **340**, 133 (1965).
95. Braun, P. B., *Nature* **170**, 708 (1952).
96. Brewer, F. M., Chadwick, J. R., and Garton, G., *J. Inorg. & Nucl. Chem.* **23**, 45 (1961).
97. Brewer, F. M., Chadwick, J. R., and Garton, G., *J. Inorg. & Nucl. Chem.* **25**, 322 (1963).
98. Britton, D., *Inorg. Chem.* **3**, 305 (1964).
99. Bronstein, H. R., Dworkin, A. S., and Bredig, M. A., *J. Phys. Chem.* **64**, 1344 (1960).
100. Brosset, C., *Arkiv Kemi, Mineral. Geol.* **25A**, No. 19 (1948).
101. Brown, R. A., and Swift, E. H., *J. Am. Chem. Soc.* **71**, 2717 (1949).
102. Brown, R. A., and Swift, E. H., *J. Am. Chem. Soc.* **71**, 2719 (1949).
103. Browne, C. I., Craig, R. P., and Davidson, N., *J. Am. Chem. Soc.* **73**, 1946 (1951).
104. Brubaker, C. H., Jr., Groves, K. O., Mickel, J. P., and Knop, C. P., *J. Am. Chem. Soc.* **79**, 4641 (1957).
105. Brubaker, C. H., Jr., and Mickel, J. P., *J. Inorg. & Nucl. Chem.* **4**, 55 (1957).

106. Brüll, L., and Griffl, F., *Ann. Chim. Appl.* **28**, 536 (1938).
107. Bruner, B. L., and Corbett, J. D., *J. Inorg. & Nucl. Chem.* **20**, 62 (1961).
108. Bruno, M., *Ric. Sci.* **20**, 645 (1950).
109. Bruno, M., and Santoro, V., *Gazz. Chim. Ital.* **86**, 1095 (1956).
110. Bucholz, C. F., *Gehlen J.* **4**, 626 (1805).
111. Buckel, W., and Hilsch, R., *Z. Physik* **128**, 324 (1950).
112. Buerger, M. J., *Z. Krist.* **95**, 163 (1936).
113. Burbank, R. D., *Inorg. Chem.* **5**, 1491 (1966).
114. Burns, E. A., and Hume, D. N., *J. Am. Chem. Soc.* **79**, 2704 (1957).
115. Burrows, G. J., and Sandford, E. P., *J. Proc. Roy. Soc. N. S. Wales* **69**, 182 (1936).
116. Bury, C. R., *J. Am. Chem. Soc.* **57**, 2115 (1935).
117. Butler, G., and Copp, J. L., *J. Chem. Soc.* p. 725 (1956).
118. Byström, A., and Westgren, A., *Arkiv Kemi. Mineral. Geol.* **16B**, No. 14 (1943).
119. Byström, A., and Mason, B., *Arkiv. Kemi, Mineral. Geol.* **16B**, No. 15 (1943).
120. Byström, A., *Arkiv Kemi, Mineral. Geol.* **18A**, No. 23 (1944).
121. Byström, A., *Arkiv Kemi, Mineral. Geol.* **20A**, No. 11 (1945).
122. Byström, A., *Arkiv Kemi, Mineral. Geol.* **25A**, No. 13 (1947).
123. Byström, A., and Evers, L., *Acta Chem. Scand.* **4**, 613 (1950).
124. Cady, H. H., Ph.D. Thesis, University of California, Berkeley, California (1957).
125. Cahan, B. D., Ockerman, J. B., Amlie, R. F., and Ruetschi, P., *J. Electrochem. Soc.* **107**, 725 (1960).
126. Calhoun, B. A., *Phys. Rev.* **94**, 1577 (1954).
127. Cambi, L., *Rend. Ist. Lombardo Sci. Lettere* **A68**, 182 (1935).
128. Cambi, L., *Gazz. Chim. Ital.* **77**, 575 (1947).
129. Campion, R. J., Conocchioli, T. J., and Sutin, N., *J. Am. Chem. Soc.* **86**, 4591 (1964).
130. Carlston, R. C., Griswold, E., and Kleinberg, J., *J. Am. Chem. Soc.* **80**, 1532 (1958).
131. Chadwick, J. R., Atkinson, A. W., and Huckstepp, B. G., *J. Inorg. & Nucl. Chem.* **28**, 1021 (1966).
132. Chalkley, L., *J. Opt. Soc. Am.* **44**, 699 (1954).
133. Chapin, D. S., Kafalas, J. A., and Honig, J. M., *J. Phys. Chem.* **69**, 1402 (1965).
134. Chapin, W. H., *J. Am. Chem. Soc.* **32**, 323 (1910).
135. Chester, P. F., *J. Appl. Phys.* **32**, 866 (1961).
136. Chester, P. F., *J. Appl. Phys.* **32**, 2233 (1961).
137. Chevreul, M., *Ann. Chim. (Paris)* [1] **83**, 181 (1812).
138. Choi, Q. W., *J. Am. Chem. Soc.* **82**, 2686 (1960).
139. Choi, Q. W., and Clark, W. G., *J. Chem. Phys.* **34**, 1584 (1961).
140. Chou Kung-du, *Sci. Sinica (Peking)* **12**, 139 (1963).
141. Chretien, A., and Lous, E., *Bull. Soc. Chim. France* **11**, 446 (1944).
142. Christensen, V. J., Kleinberg, J., and Davidson, A. W., *J. Am. Chem. Soc.* **75**, 2495 (1953).
143. Clark, G. L., Schieltz, N. C., and Quirke, T. T., *J. Am. Chem. Soc.* **59**, 2305 (1937).
144. Clark, R. J., Griswold, E., and Kleinberg, J., *J. Am. Chem. Soc.* **80**, 4764 (1958).
145. Cohen, A. J., and Davidson, N., *J. Am. Chem. Soc.* **73**, 1955 (1951).
146. Cooper, D., and Plane, R. A., *Inorg. Chem.* **5**, 1677 (1966).

147. Conroy, H., *J. Chem. Phys.* **41**, 1341 (1964).
148. Corbett, J. D., and McMullan, R. K., *J. Am. Chem. Soc.* **77**, 4217 (1955).
149. Corbett, J. D., *J. Am. Chem. Soc.* **80**, 4757 (1958).
150. Corbett, J. D., and Druding, L. F., *J. Inorg. & Nucl. Chem.* **11**, 20 (1959).
151. Corbett, J. D., and Albers, F. C., *J. Am. Chem. Soc.* **82**, 533 (1960).
152. Corbett, J. D., Druding, L. F., Burkhard, W. J., and Lindahl, C. B., *Discussions Faraday Soc.* **32**, 79 (1961).
153. Corbett, J. D., and Rundle, R. E., *Inorg. Chem.* **3**, 1408 (1964).
154. Corbett, J. D., and Ramsey, B. N., *Inorg. Chem.* **4**, 260 (1965).
155. Corbett, J. D., Pollard, D. L., and Mee, J. E., *Inorg. Chem.* **5**, 761 (1966).
156. Cordite, B. A. M., and Phires, G. L. O., *Heat Combust* **17**, 123 (1946).
157. Corey, R. B., Stanford, R. H., Marsh, R. E., Leung, Y. C., and Kay, L. M., *Acta Cryst.* **15**, 1157 (1962).
158. Cossee, P., *J. Inorg. & Nucl. Chem.* **8**, 483 (1958).
159. Cotton, F. A., and Haas, T. E., *Inorg. Chem.* **3**, 10 (1964).
160. Cotton, F. A., *Inorg. Chem.* **3**, 1217 (1964).
161. Cotton, F. A., *Inorg. Chem.* **4**, 334 (1965).
162. Cotton, F. A., and Bratton, W. K., *J. Am. Chem. Soc.* **87**, 921 (1965).
163. Cotton, F. A., and Harris, C. B., *Inorg. Chem.* **4**, 330 (1965).
164. Craig, R. P., and Davidson, N., *J. Am. Chem. Soc.* **73**, 1951 (1951).
165. Craven, B. M., and Hall, D., *Acta Cryst.* **14**, 475 (1961).
166. Craven, B. M., and Hall, D., *Acta Cryst.* **21**, 177 (1966).
167. Croatto, U., and Bruno, M., *Gazz. Chim. Ital.* **78**, 83 (1948) (and references cited therein).
168. Croatto, U., and Bruno, M., *Gazz. Chim. Ital.* **78**, 95 (1948).
169. Cronmeyer, D. C., *Phys. Rev.* **113**, 1222 (1959).
170. Cubicciotti, D., *J. Am. Chem. Soc.* **71**, 4119 (1949).
171. Culpin, D., Day, P., Edwards, P. R., and Williams, R. J. P., *Chem. Commun.* No. 19, p. 450 (1965).
172. Dana, E. S., and Ford, W. E., "A Textbook of Mineralogy." Wiley, New York, 1958.
173. Dasent, V. E., and Morrison, D., *J. Inorg. & Nucl. Chem.* **26**, 1122 (1964).
174. Dasgupta, D. R., and Mackay, A. L., *J. Phys. Soc. Japan* **14**, 932 (1959).
175. Davidson, A. W., and Kleinberg, J., *J. Phys. Chem.* **57**, 571 (1953).
176. Davidson, D., and Welo, L. A., *J. Phys. Chem.* **32**, 1191 (1928).
177. Davidson, N., *J. Am. Chem. Soc.* **73**, 2361 (1951).
178. Day, P., *Inorg. Chem.* **2**, 452 (1963).
179. Day, P., Ph.D. Thesis, Oxford University (1965).
180. Day, P., unpublished observations (1966).
181. de Boer, J. H., and Verwey, E. J. W., *Rec. Trav. Chim.* **55**, 541 (1936).
182. de Boer, J. H., and Verwey, E. J. W., *Proc. Phys. Soc.* **49**, Suppl., 59 (1937).
183. Decroly, C., and Ghodsi, M., *Compt. Rend.* **261**, 2659 (1965).
184. DeFord, D. D., and Davidson, A. W., *J. Am. Chem. Soc.* **73**, 1469 (1961).
185. Dehlinger, U., *Z. Krist.* **66**, 108 (1928).
186. Delépine, M., *Compt. Rend.* **120**, 152 (1895).
187. Delépine, M., *Compt. Rend.* **142**, 1525 (1906).
188. Delépine, M., *Ann. Chim. (Paris)* [13] **4**, 1115 (1959).
189. DeMarco, R. E., Heller, H. A., Abbott, R. C., and Burkhardt, W., *Am. Ceram. Soc. Bull.* **38**, 360 (1959).

190. Derbyshire, S. W., Fraker, A. C., and Stadelmaier, H. H., *Acta Cryst.* **14**, 1293 (1961).
191. Deshpande, V. V., Saxena, R. P., Daroowalla, S. H., and Karkhanavala, M. D., *Indian J. Chem.* **1**, 511 (1963).
192. Deussen, E. *Monatsh. Chem.* **28**, 163 (1907).
193. de Wet, J. F., and Rolle, R., *Z. Anorg. Allgem. Chem.* **336**, 96 (1965).
194. Dickens, B., *J. Inorg. & Nucl. Chem.* **27**, 1509 (1965).
195. Diehl, H., Carlson, P. A., Christian, D., Dewel, E. H., Emerson, M. R., Heumann, F. K., and Standage, H. W., *Proc. Iowa Acad. Sci.* **55**, 241 (1948).
196. Dohlström, K., and Westgren, A., *Z. Anorg. Allgem. Chem.* **235**, 153 (1937).
197. Dohlström, K., *Z. Anorg. Allgem. Chem.* **239**, 57 (1938).
198. Dirkse, T. P., *J. Electrochem. Soc.* **106**, 453 (1959).
199. Dixon, D. T., Einstein, F. W. B., and Penfold, B. R., *Acta Cryst.* **18**, 221 (1965).
200. Doehlemann, E., and Fromherz, H., *Z. Physik. Chem.* **A171**, 353 (1934).
201. Drago, R. S., and Sisler, H. H., *J. Am. Chem. Soc.* **79**, 1811 (1957).
202. Drew, H. D. K., Pinkard, F. W., Wardlaw, W., and Cox, E. G., *J. Chem. Soc.* p. 1004 (1932).
203. Drew, H. D. K., Pinkard, F. W., Preston, G. H., and Wardlaw, W., *J. Chem. Soc.* p. 1895 (1932).
204. Drew, H. D. K., and Tress, H. J., *J. Chem. Soc.* p. 1335 (1933).
205. Drew, H. D. K., and Tress, H. J., *J. Chem. Soc.* p. 1244 (1935).
206. Druding, L. F., and Corbett, J. D., *J. Am. Chem. Soc.* **81**, 5512 (1959).
207. Druding, L. F., and Corbett, J. D., *J. Am. Chem. Soc.* **83**, 2462 (1961).
208. Druding, L. F., Corbett, J. D., and Ramsey, B. N., *Inorg. Chem.* **2**, 869 (1963).
- 208a. Dubois, P., *Ann. Chim. (Paris)* **5**, 411 (1936).
209. Duncan, J. F., and Wigley, P. W. R., *J. Chem. Soc.* p. 1120 (1963).
210. Dunitz, J. D., and Orgel, L. E., *J. Chem. Soc.* p. 2594 (1953).
211. Dwyer, F. P. J., and Nyholm, R. S., *Nature* **160**, 502 (1947).
212. Dwyer, F. P. J., Nyholm, R. S., and Rogers, L. E., *J. Proc. Roy. Soc. N.S. Wales* **81**, 267 (1947).
213. Eakins, J. D., Humphreys, D. G., and Mellish, C. E., *J. Chem. Soc.* p. 6012 (1963).
214. Ebsworth, E. A. V., and Weil, J. A., *J. Phys. Chem.* **63**, 1890 (1959).
215. Edwards, F. C., Voigt, A. F., and Diehl, H., *Proc. Iowa Acad. Sci.* **55**, 247 (1948).
216. Ehrlich, P., *Z. Elektrochem.* **45**, 362 (1939).
217. Ellerbeck, L. D., Shanks, H. R., Sidles, P. H., and Danielson, G. C., *J. Chem. Phys.* **35**, 298 (1961).
218. Elliott, N., *J. Chem. Phys.* **2**, 298 (1934).
219. Elliott, N., *J. Chem. Phys.* **2**, 419 (1934).
220. Elliott, N., and Pauling, L., *J. Am. Chem. Soc.* **60**, 1846 (1938).
221. Emeleus, H. J., and Anderson, J. S., "Modern Aspects of Inorganic Chemistry." Routledge, London, 1938.
222. Emschwiller, G., *Compt. Rend.* **238**, 1414 (1954).
223. Ephraim, F., and Barteczko, P., *Z. Anorg. Allgem. Chem.* **61**, 238 (1909).
224. Ephraim, F., and Weinberg, S., *Ber. Deut. Chem. Ges.* **42**, 4447 (1909).
225. Epstein, L. M., *J. Chem. Phys.* **36**, 2731 (1962).
226. Espenson, J. H., and McCarley, R. E., *J. Am. Chem. Soc.* **88**, 1063 (1966).
227. Evans, H. T., Jr., *Inorg. Chem.* **5**, 967 (1966).
228. Eyring, L., and Baenziger, N. C., *J. Appl. Phys.* **33**, 428 (1962).

229. Eyring, L., and Holmberg, B., *Advan. Chem. Ser.* **39**, 46 (1963).
230. Fadeev, V. N., and Fedorov, P. I., *Russ. J. Inorg. Chem. (English Transl.)* **8**, 1046 (1963).
231. Fadeev, V. N., and Fedorov, P. I., *Russ. J. Inorg. Chem. (English Transl.)* **9**, 209 (1964).
232. Fadeev, V. N., and Fedorov, P. I., *Russ. J. Inorg. Chem. (English Transl.)* **9**, 1094 (1964).
233. Fayek, M. K., and Leciejewicz, J., *Z. Anorg. Allgem. Chem.* **336**, 104 (1965).
234. Fedorov, P. I., and Fadeev, V. N., *Russ. J. Inorg. Chem. (English Transl.)* **9**, 207 (1964).
235. Fedorov, P. I., and Il'ina, N. I., *Russ. J. Inorg. Chem. (English Transl.)* **9**, 659 (1964).
236. Fedorov, P. I., and Tsimbalist, V. V., *Russ. J. Inorg. Chem. (English Transl.)* **9**, 908 (1964).
237. Feitknecht, W., and Marti, W., *Helv. Chim. Acta* **28**, 129 (1945).
238. Feitknecht, W., and Keller, G., *Z. Anorg. Allgem. Chem.* **262**, 61 (1950).
239. Fensham, P. J., *J. Am. Chem. Soc.* **76**, 969 (1954).
240. Ferrari, A., *Gazz. Chim. Ital.* **67**, 94 (1937).
241. Ferrari, A., and Cecconi, R., *Gazz. Chim. Ital.* **72**, 170 (1942).
242. Ferrari, A., Cecconi, R., and Cavalca, L., *Gazz. Chim. Ital.* **73**, 23 (1943).
243. Ferrari, A., Cavalca, L., and Coghi, L., *Gazz. Chim. Ital.* **82**, 385 (1952).
244. Ferrari, A., Cavalca, L., and Nardelli, M., *Gazz. Chim. Ital.* **85**, 137 (1955).
245. Ferrari, A., Cavalca, L., and Nardelli, M., *Gazz. Chim. Ital.* **85**, 1551 (1955).
246. Ferrari, A., and Tani, M. E., *Gazz. Chim. Ital.* **89**, 502 (1959).
247. Ferrari, A., Tani, M. E., and Magnano, G., *Gazz. Chim. Ital.* **89**, 2512 (1959).
248. Ferrari, A., Braibanti, A., and Tiripicchio, A., *Acta Cryst.* **21**, 605 (1966).
249. Fielding, P. E., *J. Chem. Phys.* **22**, 1153 (1954).
250. Fielding, P. E., and Mellor, D. P., *J. Chem. Phys.* **22**, 1155 (1954).
251. Figgis, B. N., and Robertson, G. B., *Nature* **205**, 694 (1965).
252. Fletcher, J. M., Greenfield, B. F., Hardy, C. J., Scargill, D., and Woodhead, J. L., *J. Chem. Soc.* p. 2000 (1961).
253. Flood, H., Krog, T., and Sorum, H., *Tidsskr. Kjemi, Bergvesen Met.* **3**, 32 (1946).
254. Fluck, E., Kerler, W., and Neuwirth, W., *Angew. Chem. Intern. Ed. English* **2**, 277 (1963).
255. Foëx, M., *Compt. Rend.* **220**, 359 (1945).
256. Ford, W. F., and Rees, W. J., *Trans. Brit. Ceram. Soc.* **47**, 207 (1948).
257. Ford, W. F., and Rees, W. J., *Trans. Brit. Ceram. Soc.* **48**, 291 (1949).
258. Ford, W. F., and White, J., *Trans. Brit. Ceram. Soc.* **48**, 417 (1949).
259. Fraker, A. C., *J. Phys. Chem.* **69**, 4395 (1965).
260. Frederikse, H. P. R., *J. Appl. Phys.* **32**, Suppl., 2211 (1961).
261. Freed, S., Sugarman, N., and Metcalf, R. P., *J. Chem. Phys.* **8**, 225 (1940).
262. Freym, E., *Ann. Chem.* **83**, 240 (1852).
263. Fry, T. K., Lazzarini, R. A., and San Pietro, A., *Proc. Natl. Acad. Sci. U.S.* **50**, 652 (1963).
264. Fyfe, W. S., *Nature* **164**, 790 (1949).
265. Galloni, E. E., and Roffo, A. E., Jr., *J. Chem. Phys.* **9**, 875 (1941).
266. Galloni, E. E., and Busch, R. H., *J. Chem. Phys.* **20**, 198 (1952).
267. Galy, J., and Hardy, A., *Acta Cryst.* **19**, 432 (1965).
268. Gardner, W. R., and Danielson, G. C., *Phys. Rev.* **93**, 46 (1964).
269. Garton, G., and Powell, H. M., *J. Inorg. & Nucl. Chem.* **4**, 84 (1957).

270. Gasperin, M., *Bull. Soc. Franc. Mineral. Crist.* **87**, 278 (1964).
271. Gatehouse, B. M., and Wadsley, A. D., *Acta Cryst.* **17**, 1545 (1964).
272. Gauzzi, F., *Ann. Chim. (Rome)* **53**, 1503 (1963).
273. Gendell, J., Cotts, R., and Sienko, M. J., *J. Chem. Phys.* **37**, 220 (1962).
274. George, A. M., and Karkhanavala, M. D., *J. Phys. Chem. Solids* **24**, 1207 (1963).
275. Gibb, T. C., and Greenwood, N. N., *Trans. Faraday Soc.* **61**, 1317 (1965).
276. Gillis, E., *Compt. Rend.* **258**, 4765 (1964).
277. Glasner, A., and Reisfeld, R., *J. Chem. Phys.* **32**, 956 (1960).
278. Glasser, F. P., and Osborn, E. F., *J. Am. Ceram. Soc.* **41**, 358 (1958).
279. Glemser, O., and Lutz, G., *Z. Anorg. Allgem. Chem.* **263**, 2 (1950).
280. Glemser, O., and Lutz, G., *Z. Anorg. Allgem. Chem.* **264**, 17 (1951).
281. Glemser, O., Hauschild, U., and Trüpel, F., *Naturwissenschaften* **40**, 317 (1953).
282. Glemser, O., Hauschild, U., and Trüpel, F., *Z. Anorg. Allgem. Chem.* **277**, 113 (1954).
283. Glemser, O., and Schwarzmann, E., *Z. Anorg. Allgem. Chem.* **278**, 249 (1955).
284. Glemser, O., Lutz, G., and Meyer, G., *Z. Anorg. Allgem. Chem.* **285**, 173 (1956).
285. Glemser, O., Weidelt, J., and Freund, F., *Z. Anorg. Allgem. Chem.* **332**, 299 (1964).
286. Gleu, K., and Breuel, W., *Z. Anorg. Allgem. Chem.* **237**, 350 (1937).
287. Gleu, K., and Rehm, K., *Z. Anorg. Allgem. Chem.* **237**, 79 (1938).
288. "Gmelins Handbuch der Anorganischen Chemie," Iron, Part 59B, 8th ed. Verlag Chemie, Weinheim, 1932.
289. "Gmelins Handbuch der Anorganischen Chemie," Molybdenum, Part 53, 8th ed. Verlag Chemie, Weinheim, 1935.
290. "Gmelins Handbuch der Anorganischen Chemie," Osmium, Part 66, 8th ed. Verlag Chemie, Weinheim, 1939.
291. "Gmelins Handbuch der Anorganischen Chemie," Thallium, Part 38, 8th ed. Verlag Chemie, Weinheim, 1940.
292. "Gmelins Handbuch der Anorganischen Chemie," Chromium, Part 52, 8th ed. Verlag Chemie, Weinheim, 1962.
293. Goggin, P. L., and McColm, I. J., *J. Less-Common Metals* **11**, 292 (1966).
294. Golibersuch, E. W., and Young, R. C., *J. Am. Chem. Soc.* **71**, 2402 (1949).
295. Goodenough, J. B., *Phys. Rev.* **100**, 564 (1957).
296. Goodenough, J. B., Wickham, D. G., and Croft, W. J., *Phys. Chem. Solids* **5**, 107 (1958).
297. Goroshchenko, Ya. G., Andreeva, M. I., and Babkin, A. G., *Zh. Prikl. Khim.* **32**, 1664 (1959).
298. Goroshchenko, Ya. G., and Godneva, M. M., *Russ. J. Inorg. Chem. (English Transl.)* **6**, 744 (1961).
299. Gortsema, F. P., and Didchenko, R., *Inorg. Chem.* **4**, 182 (1965).
300. Gossner, B., and Arm, M., *Z. Krist.* **72**, 202 (1929).
301. Gotoo, K., Nomura, S., and Naito, K., *J. Phys. Chem. Solids* **26**, 1679 (1965).
302. Graff, H., and Wilmarth, W. K., *Proc. Symp. Co-ord. Chem., Tihany, Hungary, 1963* p. 255 (1964).
303. Graff, W. S., and Stadelmaier, H. H., *J. Electrochem. Soc.* **105**, 446 (1958).
304. Graham, J., and Wadsley, A. D., *Acta Cryst.* **14**, 379 (1961).
305. Graham, J., and Wadsley, A. D., *Acta Cryst.* **20**, 93 (1966).
306. Grant, F. A., *Rev. Mod. Phys.* **31**, 646 (1959).
307. Grantham, L. F., and Yosim, S. J., *J. Chem. Phys.* **38**, 1671 (1963).
308. Grantham, L. F., *J. Chem. Phys.* **43**, 1415 (1965).

309. Grasshoff, K., and Hahn, H., *Z. Anal. Chem.* **168**, 247 (1959).
310. Grasshoff, K., and Hahn, H., *Z. Anal. Chem.* **180**, 18 (1961).
311. Grasshoff, K., and Hahn, H., *Z. Anal. Chem.* **187**, 328 (1962).
312. Greenwood, N. N., and Worrall, I. J., *J. Chem. Soc.* p. 1680 (1958).
313. Greiner, J. D., Smith, J. F., Corbett, J. D., and Jelinek, F. J., *J. Inorg. & Nucl. Chem.* **28**, 971 (1966).
314. Grinberg, A. A., and Filinov, F. M., *Bull. Acad. Sci. URSS, Classe Sci. Math., Ser. Chim.* p. 1245 (1937).
315. Gronvold, F., *Nature* **162**, 70 (1948).
316. Gronvold, F., *J. Inorg. & Nucl. Chem.* **1**, 357 (1955).
317. Gross, S. T., *J. Am. Chem. Soc.* **65**, 1107 (1943).
318. Grossmann, G., Proskurenko, O. W., and Ariya, S. M., *Z. Anorg. Allgem. Chem.* **305**, 121 (1960).
319. Gruehn, R., and Schäfer, H., *Naturwissenschaften* **50**, 642 (1963).
320. Gruehn, R., and Schäfer, H., *J. Less-Common Metals* **10**, 152 (1965).
321. Gruehn, R., Bergner, D., and Schäfer, H., *Angew. Chem.* **77**, 1082 (1965).
322. Gruen, D. M., Koehler, W. C., and Katz, J. J., *J. Am. Chem. Soc.* **73**, 1475 (1951).
323. Gruen, D. M., *J. Am. Chem. Soc.* **76**, 2117 (1954).
324. Gruner, E., and Klemm, W., *Naturwissenschaften* **22**, 59 (1937).
325. Guillaud, E., Michel, A., Bénard, J., and Fallot, M., *Compt. Rend.* **219**, 58 (1944).
326. Hägg, G., *Z. Physik. Chem.* **29B**, 192 (1935).
327. Hägg, G., and Jerslev, B., *Experientia* **2**, 495 (1946).
328. Hägg, G., and Magneli, A., *Rev. Pure Appl. Chem.* **4**, 235 (1955).
329. Hahn, H., and Klinger, W., *Z. Anorg. Allgem. Chem.* **260**, 110 (1949).
330. Hahn, H., and Frank, G., *Z. Anorg. Allgem. Chem.* **278**, 340 (1955).
331. Hahn, H., and Schmidt, G., *Naturwissenschaften* **49**, 513 (1962).
332. Hahn, H., and Becker, W., *Naturwissenschaften* **50**, 402 (1963).
333. Haim, A., and Wilmarth, W. K. J., *J. Am. Chem. Soc.* **83**, 509 (1961).
334. Hall, D., and Williams, P. P., *Acta Cryst.* **11**, 624 (1958).
335. Hamilton, W. C., *Phys. Rev.* **110**, 1050 (1958).
336. Hampe, W., *Jahresber.* Part I, p. 388 (1888).
337. Hannebohn, O., and Klemm, W., *Z. Anorg. Allgem. Chem.* **229**, 337 (1936).
338. Haraldsen, H., and Bakken, R., *Naturwissenschaften* **28**, 127 (1940).
339. Harbottle, G., and Dodson, R. W., *J. Am. Chem. Soc.* **73**, 2442 (1951).
340. Harned, H. S., *J. Am. Chem. Soc.* **35**, 1078 (1913).
341. Harris, C. M., *J. Proc. Roy. Soc. N. S. Wales* **82**, 218 (1948).
342. Harris, C. M., *J. Proc. Roy. Soc. N. S. Wales* **84**, 111 (1950).
343. Harris, C. M., *J. Proc. Roy. Soc. N. S. Wales* **85**, 138 (1952).
344. Harris, C. M., *J. Proc. Roy. Soc. N. S. Wales* **85**, 142 (1952).
345. Harris, C. M., and Schafer, H. N. S., *J. Proc. Roy. Soc. N. S. Wales* **85**, 145 (1952).
346. Harris, C. M., and Schafer, H. N. S., *J. Proc. Roy. Soc. N. S. Wales* **85**, 148 (1952).
347. Hathaway, B. J., and Holah, D. G., *J. Chem. Soc.* p. 2408 (1964).
348. Hauffe, K., and Block, J., *Z. Physik. Chem. (Leipzig)* **196**, 438 (1950).
349. Hauffe, K., "Reactionen in und am festen Stoffen." Springer, Berlin, 1955.
350. Hazell, A. C., *J. Chem. Soc.* p. 3459 (1963).
351. Heikes, R. R., and Johnston, W. D., *J. Chem. Phys.* **26**, 582 (1957).
352. Hein, F., and Pauling, H., *Z. Anorg. Allgem. Chem.* **273**, 209 (1953).

353. Heinz, D., *Z. Anorg. Allgem. Chem.* **336**, 137 (1965).
354. Hendricks, S. B., *Am. Mineralogist* **24**, 529 (1939).
355. Herrmann, F., *Ber. Deut. Chem. Ges.* **27**, 596 (1894).
356. Hershaf, A., and Corbett, J. D., *J. Chem. Phys.* **36**, 551 (1962).
357. Hershaf, A., and Corbett, J. D., *Inorg. Chem.* **2**, 979 (1963).
358. Hettich, A., *Z. Anorg. Allgem. Chem.* **167**, 67 (1927).
359. Hilsch, R., von Minnigerode, G., and von Wartenberg, H., *Naturwissenschaften* **44**, 463 (1957).
360. Hilpert, R. S., Hoffmann, A., and Schacht, R., *Ber. Deut. Chem. Ges.* **71**, 82 (1938).
361. Hoekstra, H. R., Siegel, S., Fuchs, L. H., and Katz, J. J., *J. Phys. Chem.* **59**, 136 (1955).
362. Hoekstra, H. R., and Siegel, S., *Proc. Intern. Conf. Peaceful Uses At. Energy, Geneva, 1955* Vol. 7, p. 394. Columbia Univ. Press (I.D.S.), New York, 1955.
363. Hoekstra, H. R., and Siegel, S., *J. Inorg. & Nucl. Chem.* **18**, 154 (1961).
364. Hoekstra, H. R., Santoro, A., and Siegel, S., *J. Inorg. & Nucl. Chem.* **18**, 166 (1961).
365. Hofmann, K. A., and Resenscheck, F., *Ann. Chem.* **342**, 364 (1905).
366. Hofmann, K. A., and Höschele, K., *Ber. Deut. Chem. Ges.* **48**, 20 (1915).
367. Holden, A. N.; Matthias, B. T., Anderson, P. W., and Lewis, H. W., *Phys. Rev.* **102**, 1463 (1956).
368. Holtzman, H., *Ind. Eng. Chem.* **37**, 855 (1945).
369. Hoppe, R., *Z. Anorg. Allgem. Chem.* **292**, 28 (1957).
370. Hoschek, E., and Klemm, W., *Z. Anorg. Allgem. Chem.* **242**, 63 (1939).
371. Huckel, W., *Nachr. Akad. Wiss. Goettingen, IIa. Math.-Physik.-Chem. Abt. Math.-Phys. Kl.*, No. 1, p. 36 (1946).
372. Hund, F., Wagner, R., and Peetz, U., *Z. Elektrochem.* **56**, 61 (1952).
373. Ibers, J. A., and Davidson, N., *J. Am. Chem. Soc.* **73**, 476 (1951).
374. Ipatiew, W., and Nikolajew, W., *Ber. Deut. Chem. Ges.* **59**, 1423 (1926).
375. Iwase, E., Nishiyama, S., Kobayashi, I., and Matsuda, K., *Rika Gaku Kenkyusho Hokoku* **36**, 714 (1960).
376. Janes, R. B., *J. Am. Chem. Soc.* **57**, 471 (1935).
377. Janninck, R. F., and Whitmore, D. H., *J. Chem. Phys.* **37**, 2750 (1962).
378. Janusz, T. P., Heikes, R. R., and Johnston, W. D., *J. Chem. Phys.* **26**, 973 (1957).
379. Jensen, K. A., *Z. Anorg. Allgem. Chem.* **229**, 252 (1936).
380. Jensen, K. A., *Z. Anorg. Allgem. Chem.* **229**, 261 (1936).
381. Jensen, K. A., *Z. Anorg. Allgem. Chem.* **232**, 193 (1937).
382. Jensen, K. A., *Z. Anorg. Allgem. Chem.* **252**, 317 (1944).
383. Jockusch, H., *Naturwissenschaften* **22**, 561 (1934).
384. Johnsen, A., *Neues Jahrb. Mineral.* **1**, 89 (1907).
385. Johnson, G., and Weyl, W. A., *J. Am. Ceram. Soc.* **32**, 398 (1949).
386. Johnston, W. D., and Heikes, R. R., *J. Am. Chem. Soc.* **78**, 3255 (1956).
387. Jolibois, P., *Compt. Rend.* **224**, 1395 (1947).
388. Joly, M. A., *Compt. Rend.* **115**, 1299 (1892).
389. Jona, F., Shirane, G., and Pepinsky, R., *Phys. Rev.* **98**, 903 (1955).
390. Jones, P., and Thirsk, H. R., *Trans. Faraday Soc.* **50**, 732 (1954).
391. Jones, W. H., Garbaty, E. A., and Barnes, R. G., *J. Chem. Phys.* **36**, 494 (1962).
392. Jonker, G. H., and van Santen, J. H., *Physica* **16**, 337 (1950).
393. Jonker, G. H., and van Santen, J. H., *Physica* **16**, 599 (1950).
394. Jonker, G. H., and van Santen, J. H., *Physica* **19**, 120 (1953).

395. Jorgensen, C. K., *Acta Chem. Scand.* **11**, 73 (1957).
396. Jorgensen, C. K., *Acta Chem. Scand.* **13**, 196 (1959).
397. Jorgensen, C. K., *Mol. Phys.* **4**, 231 (1961).
398. Jorgensen, C. K., *Mol. Phys.* **4**, 235 (1961).
399. Jorgensen, C. K., and Orgel, L. E., *Mol. Phys.* **4**, 215 (1961).
400. Jost, K.-H., *Acta Cryst.* **21**, 34 (1966).
401. Jost, K.-H., *Acta Cryst.* **17**, 1593 (1964).
402. Kachi, S., Takada, T., and Kosuge, K., *J. Phys. Soc. Japan* **18**, 1839 (1963).
403. Kamimura, H., *J. Phys. Soc. Japan*, **21**, 484 (1966).
404. Kasper, J. S., *Bull. Am. Phys. Soc.* [2] **4**, 178 (1959).
405. Katz, J. J., and Gruen, D. M., *J. Am. Chem. Soc.* **71**, 2106 (1949).
406. Katz, J. J., and Rabinowitch, E., "The Chemistry of Uranium." McGraw-Hill, New York, 1951.
407. Katz, L., and Lipscomb, W. N., *Acta Cryst.* **4**, 345 (1951).
408. Keggins, J. F., *Proc. Roy. Soc. A* **144**, 75 (1934).
409. Keggins, J. F., and Miles, F. D., *Nature* **137**, 577 (1936).
410. Kerler, W., Neuwirth, W., Fluck, E., Kuhn, P., and Zimmermann, B., *Z. Physik* **173**, 321 (1963).
411. Kestigian, M., and Ward, R., *J. Am. Chem. Soc.* **77**, 6199 (1955).
412. Ketelaar, J. A. A., t'Hart, W. H., Moerel, M., and Polder, D., *Z. Krist.* **101**, 396 (1939).
413. Kettle, S. F. A., *Nature* **207**, 1384 (1965).
414. Kettle, S. F. A., *Theoret. Chim. Acta* **3**, 211 (1965).
415. Khakhan, I. B., and Reibel, I. M., *Tr. Kishinevsk. Sel'skokhoz. Inst.* **11**, 159 (1956).
416. Kida, S., *Bull. Chem. Soc. Japan* **38**, 1804 (1965).
417. Kiehl, S. J., Fox, R. L., and Hardt, H. B., *J. Am. Chem. Soc.* **59**, 2395 (1937).
418. Kierkegaard, P., and Nyborg, B., *Acta Chem. Scand.* **19**, 2189 (1965).
419. Kihlberg, L., *Acta Chem. Scand.* **13**, 954 (1959).
420. Kihlberg, L., *Acta Chem. Scand.* **16**, 2458 (1962).
421. Kihlberg, L., *Advan. Chem. Ser.* **39**, 37 (1963).
422. Kihlberg, L., *Arkiv Kemi* **21**, 471 (1964).
423. King, E. L., and Neptune, J. A., *J. Am. Chem. Soc.* **77**, 3186 (1955).
424. Klechkovskaya, V. V., Troitskaya, N. V., and Pinsker, Z. G., *Soviet Phys.-Cryst. (English Transl.)* **10**, 28 (1965).
425. Klemm, W., *Z. Anorg. Allgem. Chem.* **201**, 32 (1931).
426. Klemm, W., and Tilk, W., *Z. Anorg. Allgem. Chem.* **207**, 175 (1932).
427. Klemm, W., and von Vogel, H. U., *Z. Anorg. Allgem. Chem.* **219**, 45 (1934).
428. Klemm, W., *Z. Anorg. Allgem. Chem.* **301**, 323 (1959).
429. Klotz, I. M., Czerlinski, G. H., and Fiess, H. A., *J. Am. Chem. Soc.* **80**, 2920 (1958).
430. Knop, W., *Ann. Chem.* **43**, 111 (1842).
431. Kochetkova, A. P., Tronev, V. G., and Gilyarov, O. N., *Dokl. Akad. Nauk SSSR* **147**, 1373 (1962).
432. Kochetkova, A. P., and Gilyarov, O. N., *Zh. Neorgan. Khim.* **11**, 1239 (1966).
433. Koide, S., and Takei, H., *J. Phys. Soc. Japan* **18**, 319 (1963).
434. Kolditz, L., and Rochusch, W., *Z. Anorg. Allgem. Chem.* **318**, 17 (1962).
435. Konopik, N., and Zwiauer, J., *Monatsh. Chem.* **83**, 189 (1952).
436. Korshunov, I. A., and Lebedeva, Z. M., *Zh. Neorgan. Khim.* **1**, 1912 (1956).
437. Kosuge, K., Takada, T., and Kachi, S., *J. Phys. Soc. Japan* **18**, 318 (1963).

438. Kovba, L. M., Kuz'micheva, E. U., and Ippolitova, E. A., *Vestn. Mosk. Univ., Ser. II: Khim.* **19**, 34 (1964).
439. Krauss, F., and Schrader, G., *Z. Anorg. Allgem. Chem.* **165**, 59 (1927).
440. Krauss, H. L., and Gnatz, G., *Chem. Ber.* **92**, 2110 (1959).
441. Krogmann, K., *Angew. Chem. Intern. Ed. English* **3**, 147 (1964).
442. Krogmann, K., Dodel, P., and Hansen, H. D., *Proc. 8th Intern. Conf. Coord. Chem., Vienna, 1964* p. 157.
443. Krylov, E. I., *Nauchn. Dokl. Vysshei Shkoly, Khim. i Khim. Tekhnol.* p. 676 (1958).
444. Krylov, E. I., and Kalugina, N. N., *Zh. Neorgan. Khim.* **4**, 2476 (1959).
445. Krylov, E. I., Samarina, V. A., and Shtol'ts, A. K., *Dokl. Akad. Nauk SSSR* **130**, 556 (1960).
446. Kubota, B., *J. Am. Ceram. Soc.* **44**, 239 (1961).
447. Kuhn, P. J., and McCarley, R. E., *Inorg. Chem.* **4**, 1482 (1965).
448. Kul'ba, F. Ya., and Mironov, V. E., *Zh. Neorgan. Khim.* **2**, 19 (1957).
449. Kul'ba, F. Ya., and Mironov, V. E., *Zh. Neorgan. Khim.* **2**, 46 (1957).
450. Kunze, J., *Chem. Tech. (Berlin)* **5**, 392 (1953).
451. Kurkjian, C. R., and Lefort, J., *Compt. Rend.* **69**, 169 (1869).
452. Kuznetsov, V. G., and Koz'min, P. A., *Russ. J. Inorg. Chem. (English Transl.)* **3**, 182 (1958).
453. Lander, J. J., and Wooten, L. A., *J. Am. Chem. Soc.* **73**, 2452 (1951).
454. Laubengayer, A. W., and Schirmer, F. B., *J. Am. Chem. Soc.* **62**, 1578 (1940).
455. Lawton, S. L., personal communication (1966).
456. Lawton, S. L., and Jacobson, R. A., *Inorg. Chem.* **5**, 743 (1966).
457. Leask, M. J. M., Roberts, L. E. J., Walter, A. J., and Wolf, W. P., *J. Chem. Soc.* p. 4788 (1963).
458. Le Blanc, M., and Sachse, H., *Physik. Z.* **32**, 887 (1931).
459. Lecerf, A., Rault, M., and Villers, G., *Compt. Rend.* **261**, 749 (1965).
460. Lecoq de Boisbaudran, P. E., *Compt. Rend.* **96**, 1406 (1883).
461. Levy, L. A., *J. Chem. Soc.* **101**, 1081 (1912).
462. Lindberg, M. L., and Christ, C. L., *Acta Cryst.* **12**, 695 (1959).
463. Linhard, M., and Weigel, M., *Z. Physik. Chem. (Frankfurt)* [N.S.] **11**, 312 (1957).
464. Linhard, M., and Weigel, M., *Z. Anorg. Allgem. Chem.* **308**, 254 (1961).
465. Littler, J. G. F., and Williams, R. J. P., *J. Chem. Soc.* p. 6368 (1965).
466. Long, L. H., and Sackman, J. F., *J. Inorg. & Nucl. Chem.* **25**, 79 (1963).
467. Loopstra, B. O., *Acta Cryst.* **17**, 651 (1964).
468. Lorthioir, G., and Michel, A., *Compt. Rend.* **258**, 4560 (1964).
469. Lux, H., and Niedermaier, T., *Z. Naturforsch.* **11a**, 613 (1956).
470. MacCarthy, G. R., *Am. J. Sci.* **12**, 16 (1926).
471. Mackay, R. A., and Schneider, R. F., *Inorg. Chem.* **6**, 549 (1967).
472. Magneli, A., *Arkiv Kemi, Mineral. Geol.* **24A**, No. 2 (1946).
473. Magneli, A., *Arkiv Kemi* **1**, 223 (1949).
474. Magneli, A., *Nova Acta Regiae Soc. Sci. Upsaliensis* **14**, 8 (1950).
475. Magneli, A., and Kihlberg, L., *Acta Chem. Scand.* **5**, 578 (1951).
476. Magneli, A., *Acta Cryst.* **6**, 495 (1953).
477. Magneli, A., *J. Inorg. & Nucl. Chem.* **2**, 330 (1956).
478. Makarov, E. S., *Proc. Acad. Sci. USSR, Chem. Sect. (English Transl.)* **139**, 720 (1961).
479. Makarov, S. Z., and Vakrushev, A. A. *Izv. Akad. Nauk SSSR, Otd. Khim. Nauk* No. 10, p. 1731 (1960).

480. Malatesta, L., *Gazz. Chim. Ital.* **72**, 287 (1942).
481. Margotin, P., Stuckens, W., and Durand, R., *Compt. Rend.* **252**, 4005 (1961).
482. Marsh, J. K., *J. Chem. Soc.* p. 15 (1946).
483. Marsh, R. E., and Shoemaker, D. P., *Acta Cryst.* **6**, 197 (1953).
484. Marsmann, H., and Hahn, H., *Z. Naturforsch.* **21b**, 188 (1966).
485. Martin, R. L., *Nature* **165**, 202 (1950).
486. Mason, B., and Vitaliano, C. J., *Mineral. Mag.* **30**, 100 (1953).
487. Mason, H. S., *Biochem. Biophys. Res. Commun.* **10**, 11 (1963).
488. Mathieu, J. P., *Bull. Soc. Chim. France* **5**, 105 (1938).
489. Mattes, R., and Krogmann, K., *Z. Anorg. Allgem. Chem.* **332**, 247 (1964).
490. Mazzi, F., and Rossi, G., *Z. Krist.* **121**, 243 (1955).
491. McCarley, R. E., Martin, D. J., Jr., and Cox, L. T., *J. Inorg. & Nucl. Chem.* **7**, 113 (1958).
492. McCarley, R. E., and Boatman, J. C., *Inorg. Chem.* **4**, 1486 (1965).
493. McCarley, R. E., Hughes, B. G., Cotton, F. A., and Zimmerman, R., *Inorg. Chem.* **4**, 1491 (1965).
494. McCarley, R. E., quoted in MacKay and Schneider (471).
495. McConnell, H. M., and Davidson, N., *J. Am. Chem. Soc.* **71**, 3845 (1949).
496. McConnell, H. M., and Davidson, N., *J. Am. Chem. Soc.* **72**, 3168 (1950).
497. McConnell, H. M., and Davidson, N., *J. Am. Chem. Soc.* **72**, 5557 (1950).
498. McConnell, H. M., and Weaver, H. E., Jr., *J. Chem. Phys.* **25**, 307 (1956).
499. McConnell, H. M., and Berger, S. B., *J. Chem. Phys.* **27**, 230 (1957).
500. McCullough, J. D., *J. Am. Chem. Soc.* **72**, 1386 (1950).
501. McCullough, J. D., and Britton, J. D., *J. Am. Chem. Soc.* **74**, 5225 (1952).
502. McMillan, J. A., *J. Inorg. & Nucl. Chem.* **13**, 28 (1960).
503. McMillan, J. A., *Chem. Rev.* **62**, 65 (1962).
504. McMullan, R. K., and Corbett, J. D., *J. Am. Chem. Soc.* **80**, 4761 (1958).
505. Mee, J. E., and Corbett, J. D., *Inorg. Chem.* **4**, 88 (1965).
506. Mikhalevich, K. N., and Litvinchuk, V. M., *Zh. Neorgan. Khim.* **9**, 2391 (1964).
507. Miller, A. E., and Daane, A. H., *J. Inorg. & Nucl. Chem.* **27**, 1955 (1965).
508. Milyutina, M. I., and Sharova, A. K., *Tr. Inst. Khim. Akad. Nauk SSSR, Ural'sk. Filial* p. 85 (1963).
509. Miyatani, K., Kohn, K., Kamimura, H., and Iida, S., *J. Phys. Soc. Japan* **21**, 464 (1966).
510. Moore, C. E., *Nat. Bur. Std. (U.S.), Circ.* **467**, 94.
511. Morawietz, W., Morawietz, H., and Brauer, G., *Z. Anorg. Allgem. Chem.* **316**, 220 (1962).
512. Morgan, G. T., and Burstall, F. H., *J. Chem. Soc.* p. 41 (1936).
513. Morgan, G. T., and Burstall, F. H., *J. Chem. Soc.* p. 2018 (1926).
514. Mori, H., and Ito, T., *Acta Cryst.* **3**, 1 (1950).
515. Mori, M., *Bull. Chem. Soc. Japan* **24**, 285 (1951).
516. Mori, M., *Bull. Chem. Soc. Japan* **33**, 985 (1960).
517. Mori, M., Saito, Y., and Watanabe, T., *Bull. Chem. Soc. Japan* **34**, 295 (1961).
518. Mori, M., *Bull. Chem. Soc. Japan* **34**, 1249 (1961).
519. Mott, N. F., *Nuovo Cimento* [10] **7**, Suppl., 312 (1958).
520. Munday, T. C. F., and Corbett, J. D., *Inorg. Chem.* **5**, 1263 (1966).
521. Murat, M., Chevreton, M., Berodias, G., and Eyraud, C., *J. Chim. Phys.* **61**, 812 (1964).
522. Murray-Rust, P., Day, P., and Prout, C. K., *Chem. Commun.*, p. 277 (1966).
523. Nachtrieb, N. H., *J. Phys. Chem.* **66**, 1163 (1962).
524. Naray-Szabo, I., and Popp, K., *Z. Anorg. Allgem. Chem.* **322**, 286 (1963).

525. Naray-Szabo, I., Argay, G., and Szabo, P., *Acta Cryst.* **19**, 180 (1965).
526. Narbutt, K. I., and Laputina, I. P., *Bull. Acad. Sci. USSR, Phys. Ser. (English Transl.)* **26**, 410 (1962).
527. Natta, G., and Baccaredda, M., *Z. Krist.* **85**, 271 (1933).
528. Neiding, A. B., and Kazarnovskii, I. A., *Dokl. Akad. Nauk. SSSR* **78**, 713 (1951).
529. Neumann, H. M., and Brown, H., *J. Am. Chem. Soc.* **78**, 1843 (1956).
530. Newton, T. W., and Baker, F. B., *Inorg. Chem.* **3**, 569 (1964).
531. Nguyen-Nghi, H., Plurien, P., Mme. Baggioni-Escoubes, and Eyraud, C., *Bull. Soc. Chim. France* p. 72 (1963).
532. Niebuhr, J., *J. Less-Common Metals* **10**, 312 (1966).
533. Niebuhr, J., *J. Less-Common Metals* **11**, 191 (1966).
534. Nikolaev, N. S., and Shishkov, Yu. D., *Proc. Acad. Sci. USSR, Chem. Sect. (English Transl.)* **143**, 168 (1962).
535. Noddack, W., and Walsh, H., *Z. Physik. Chem. (Leipzig)* **211**, 194 (1959).
536. Noddack, W., and Walsh, H., *Z. Elektrochem.* **63**, 269 (1959).
537. Norin, R., and Magneli, A., *Naturwissenschaften* **47**, 354 (1960).
538. Norin, R., *Naturwissenschaften* **52**, 300 (1965).
539. Norin, R., *Acta Chem. Scand.* **20**, 871 (1966).
540. Nyholm, R. S., *J. Chem. Soc.* p. 1767 (1951).
541. Nyholm, R. S., and Sharpe, A. G., *J. Chem. Soc.* p. 3579 (1952).
542. Oberhauser, F., and Schormuller, J., *Ber. Deut. Chem. Ges.* **62**, 1482 (1929).
543. O'Donnell, T. A., and Stewart, D. F., *Inorg. Chem.* **5**, 1434 (1966).
544. Ohyagi, Y., *Bull. Chem. Soc. Japan* **15**, 186 (1940).
545. Orgel, L. E., *Discussions Faraday Soc.* **26**, 138 (1958).
546. Osmond, W. P., *Proc. Phys. Soc. (London)* **87**, 767 (1966).
547. Ostrowetsky, S., and Souchay, P., *Compt. Rend.* **251**, 373 (1960).
548. Ostrowetsky, S., *Compt. Rend.* **251**, 1068 (1960).
549. Ostrowetsky, S., *Bull. Soc. Chim. France* No. 5, p. 1012 (1964).
550. Ostrowetsky, S., *Bull. Soc. Chim. France* No. 5, p. 1018 (1964).
551. Oswald, H. R., Feitknecht, W., and Wampetich, M. J., *Nature* **207**, 72 (1965).
552. Ott, H., and Seyfarth, H., *Z. Krist.* **67**, 430 (1928).
553. Owen, J., *Discussions Faraday Soc.* **26**, 53 (1958).
554. Ozerov, R. P., *Soviet Phys.-Cryst. (English Transl.)* **2**, 219 (1957).
555. Paglia, E., and Sironi, C., *Gazz. Chim. Ital.* **88**, 541 (1958).
556. Palagyi, T., and Naray-Szabo, I., *Acta Chim. Acad. Sci. Hung.* **30**, 1 (1962).
557. Palkin, A. P., Vigutova, T. N., and Glotova, L. I., *Russ. J. Inorg. Chem. (English Transl.)* **8**, 128 (1963).
558. Palkin, A. P., Ostrikova, N. V., and Vigutova, T. N., *Russ. J. Inorg. Chem. (English Transl.)* **8**, 1344 (1963).
559. Paklin, A. P., and Ostrikova, N. V., *Russ. J. Inorg. Chem. (English Transl.)* **9**, 1104 (1964).
560. Panzer, R. E., and Suttle, J. F., *J. Inorg. & Nucl. Chem.* **20**, 229 (1961).
561. Partington, J. R., and Whynes, A. L., *J. Chem. Soc.* p. 1952 (1948).
562. Pascari, I., Constantinescu, O., Constantinescu, M., and Arizan, D., *J. Chim. Phys.* **62**, 1283 (1965).
563. Pauling, L., and Shappell, M. D., *Z. Krist.* **75**, 128 (1930).
564. Pauling, L., *J. Am. Chem. Soc.* **69**, 542 (1947).
565. Pauling, L., "The Nature of the Chemical Bond." 3rd ed. Cornell Univ. Press, Ithaca, New York, 1960.

566. Perakis, N., Serres, A., Parravano, G., and Wucher, J., *Compt. Rend.* **242**, 1275 (1956).
567. Peretti, E. A., *J. Am. Chem. Soc.* **78**, 5745 (1956).
568. Péro, P., *Bull. Soc. Chim. France*, p. 256 (1953).
569. Perthiel, R., and Jahn, H., *Phys. Status Solidi* **5**, 563 (1964).
570. Pollard, W. B., *J. Chem. Soc.* **117**, 99 (1920).
571. Pope, M. T., and Varga, G. M., Jr., *Inorg. Chem.* **5**, 1249 (1966).
572. Powell, H. M., *Proc. Chem. Soc.* p. 73 (1959).
573. Prandl, W., and Rieder, G., *Z. Anorg. Allgem. Chem.* **238**, 225 (1938).
574. Pugh, W., *J. Chem. Soc.* p. 1959 (1937).
575. Rabe, O., *Z. Anorg. Allgem. Chem.* **58**, 23 (1908).
576. Raleigh, D. O., *J. Chem. Phys.* **38**, 1677 (1963).
577. Rau, R. C., *Acta Cryst.* **20**, 716 (1966).
578. Ray, P. C., and Adhikari, N., *J. Indian Chem. Soc.* **9**, 254 (1932).
579. Recoura, A., *Bull. Soc. Chim. France* **17**, 934 (1897).
580. Reihlen, H., and Flohr, E., *Ber. Deut. Chem. Ges.* **67**, 2010 (1934).
581. Reuter, B., Jaskowsky, J., and Riedel, E., *Z. Elektrochem.* **63**, 937 (1959).
582. Reynolds, J. E., *Proc. Roy. Soc. A* **82**, 380 (1909).
583. Rich, R. L., and Taube, H., *J. Am. Chem. Soc.* **76**, 2608 (1954).
584. Richardson, J., and Elliott, N., *J. Am. Chem. Soc.* **62**, 3182 (1940).
585. Riebling, E. F., and Erickson, C. E., *J. Phys. Chem.* **67**, 307 (1963).
586. Riebling, E. F., and Erickson, C. E., *J. Phys. Chem.* **67**, 509 (1963).
587. Rienäcker, G., and Birkenstaedt, M., *Z. Anorg. Allgem. Chem.* **265**, 99 (1951).
588. Rigamonti, R., *Gazz. Chim. Ital.* **67**, 137 (1937).
589. Roberts, L. E. J., and Walter, A. J., *J. Inorg. & Nucl. Chem.* **22**, 213 (1961).
590. Roberts, L. E. J., *Advan. Chem. Ser.* **39**, 66 (1963).
591. Robin, M. B., *Inorg. Chem.* **1**, 337 (1962).
592. Robin, M. B., *J. Chem. Phys.* **40**, 3369 (1964).
593. Robin, M. B., and Kuebler, N. A., *Inorg. Chem.* **4**, 978 (1965).
594. Robin, M. B., Andres, K., Geballe, T. H., Kuebler, N. A., and McWhan, D. B., *Phys. Rev. Letters* **17**, 917 (1966).
595. Robin, M. B., unpublished results (1962).
596. Rode, T. V., Kazanskii, V. B., and Pecherskaya, Yu. I., *Russ. J. Phys. Chem. (English Transl.)* **35**, 1170 (1961).
597. Rode, T. V., and Rode, V. E., *Russ. J. Phys. Chem. (English Transl.)* **35**, 1225 (1961).
598. Rode, E. Ya., and Lysanova, G. V., *Dokl. Akad. Nauk SSSR* **145**, 351 (1962).
599. Rogers, D., and Skapski, A. C., *Proc. Chem. Soc.* p. 400 (1964).
600. Rolsten, R. F., *J. Am. Chem. Soc.* **80**, 2952 (1958).
601. Ross, M., *Am. Mineralogist* **44**, 322 (1959).
602. Roth, W. L., *J. Phys. Chem. Solids* **25**, 1 (1964).
603. Rowland, T. J., and Bromberg, J. P., *J. Chem. Phys.* **29**, 626 (1958).
604. Rüdorff, W., and Valet, G., *Z. Naturforsch.* **7b**, 57 (1952).
605. Rüdorff, W., Schwarz, H. G., and Walter, M., *Z. Anorg. Allgem. Chem.* **269**, 141 (1952).
606. Rüdorff, W., and Valet, G., *Z. Anorg. Allgem. Chem.* **271**, 257 (1953).
607. Ruff, O., and Plato, W., *Ber. Deut. Chem. Ges.* **37**, 673 (1904).
608. Ruff, O., and Ascher, E., *Z. Anorg. Allgem. Chem.* **183**, 193 (1929).
609. Ruff, O., and Giese, M., *Z. Anorg. Allgem. Chem.* **219**, 143 (1934).
610. Rundle, R. E., Baenziger, N. C., Wilson, A. S., and McDonald, R. A., *J. Am. Chem. Soc.* **70**, 99 (1948).

611. Rundle, R. E., *J. Am. Chem. Soc.* **76**, 3101 (1954).
612. Ryan, T. D., and Rundle, R. E., *J. Am. Chem. Soc.* **83**, 2814 (1961).
613. Sacconi, L., and Cini, R., *J. Chem. Phys.* **18**, 1124 (1950).
614. Sainte-Claire Deville, H., and Debray, H., *Compt. Rend.* **86**, 927 (1878).
615. Sakellariadis, P., and Coromanzou, M., *Bull. Soc. Chim. France* p. 769 (1962).
616. Sallach, R. A., and Corbett, J. D., *Inorg. Chem.* **2**, 457 (1963).
617. Scatturin, V., *Atti, Ist. Veneto Sci., Lettere Arti, Classe Sci. Mat. Nat.* **109**, 109 (1951).
618. Scatturin, V., Zannetti, R., and Censolo, G., *Ric. Sci.* **26**, 3108 (1956).
619. Scatturin, V., Bellon, P. L., and Zannetti, R., *Ric. Sci.* **27**, 2163 (1957).
620. Scatturin, V., Bellon, P. L., and Zannetti, R., *J. Inorg. & Nucl. Chem.* **8**, 462 (1958).
621. Scatturin, V., Bellon, P. L., and Salkind, A. J., *Ric. Sci.* **30**, 1034 (1960).
622. Scatturin, V., Bellon, P. L., and Salkind, A. J., *J. Electrochem. Soc.* **108**, 819 (1961).
623. Schaefer, W. P., and Marsh, R. E., *J. Am. Chem. Soc.* **88**, 178 (1966).
624. Schäfer, H., Sibbing, E., and Gerken, R., *Z. Anorg. Allgem. Chem.* **307**, 163 (1961).
625. Schäfer, H., and Dohmann, K.-D., *Z. Anorg. Allgem. Chem.* **311**, 134 (1961).
626. Schäfer, H., Scholz, H., and Gerken, R., *Z. Anorg. Allgem. Chem.* **331**, 154 (1964).
627. Schäfer, H., and Schnering, H. G., *Angew. Chem.* **76**, 833 (1964).
628. Schäfer, H., Gerken, R., and Scholz, H., *Z. Anorg. Allgem. Chem.* **335**, 96 (1965).
629. Schäfer, H., von Schnering, H. G., Niehues, K.-J., and Nieder-Vahrenholz, H. G., *J. Less-Common Metals* **9**, 95 (1965).
630. Schäfer, H., and Bauer, D., *Z. Anorg. Allgem. Chem.* **340**, 62 (1965).
631. Schäfer, H., von Schnering, H. G., Siepmann, R., Simon, A., Giegling, D., Bauer, D., and Spreckelmeyer, B., *J. Less-Common Metals* **10**, 154 (1966).
632. Schäfer, H., and Spreckelmeyer, B., *J. Less-Common Metals* **11**, 73 (1966).
633. Schäfer, H. S., and Siepmann, R., *J. Less-Common Metals* **11**, 76 (1966).
634. Scharizer, R., *Z. Krist.* **37**, 530 (1903).
635. Scharizer, R., *Z. Krist.* **43**, 113 (1907).
636. Scheibe, H., and Ermischer, W., *Kernenergie* **6**, 178 (1963).
637. Scheibe, H., and Ermischer, W., *Kernenergie* **7**, 95 (1964).
638. Schnering, H. G., and Wöhrle, H., *Angew. Chem. Intern. Ed. English* **2**, 558 (1963).
639. Scholder, R., and Stobbe, H., *Z. Anorg. Allgem. Chem.* **247**, 392 (1941).
640. Scholder, R., and Klemm, W., *Angew. Chem.* **66**, 461 (1954).
641. Schönberg, N., *Acta Chem. Scand.* **8**, 221 (1954).
642. Schönberg, N., *Acta Chem. Scand.* **8**, 240 (1954).
643. Schönberg, N., *Acta Chem. Scand.* **8**, 617 (1954).
644. Schramm, E. P., *Inorg. Chem.* **5**, 1291 (1966).
645. Schultz, C., *J. Prakt. Chem.* **68**, 257 (1856).
646. Schwab, G.-M., and Hartmann, G., *Z. Anorg. Allgem. Chem.* **281**, 183 (1955).
647. Schwartz, R. S., Fankuchen, I., and Ward, R., *J. Am. Chem. Soc.* **74**, 1676 (1952).
648. Seabough, P. W., and Corbett, J. D., *Inorg. Chem.* **4**, 176 (1965).
649. Seaborg, G. T., and Katz, J. J., "The Actinide Elements." McGraw-Hill, New York, 1954.
650. Seifer, G. B., *Russ. J. Inorg. Chem. (English Transl.)* **7**, 621 (1962).

651. Selbin, J., and Usategui, M., *J. Inorg. & Nucl. Chem.* **20**, 91 (1961).
652. Selwood, P. W., "Magnetochemistry," Wiley (Interscience), New York, 1956.
653. Senderoff, S., and Mellors, A. S., *J. Electrochem. Soc.* **105**, 224 (1958).
654. Setterberg, C., *Oefversigt K. Vetensk. Akad. Forhandl.* No. 6, p. 23 (1882).
655. Sharpe, A. G., *J. Chem. Soc.* p. 3444 (1950).
656. Sharpe, A. G., *J. Chem. Soc.* p. 2165 (1952).
657. Sheka, I. A., Chaus, I. S., and Mityureva, T. T., "The Chemistry of Gallium." Elsevier, Amsterdam, 1966.
658. Shields, L., and Symons, M. C. R., *Mol. Phys.* **11**, 57 (1966).
659. Shively, R. R., Jr., and Weyl, W. A., *J. Phys. Chem.* **55**, 512 (1951).
660. Shull, C. G., Wollan, E. O., and Koehler, W. C., *Phys. Rev.* **84**, 912 (1951).
661. Sienko, M. J., *Advan. Chem. Ser.* **39**, 224 (1963).
662. Siepmann, R., and Schäfer, H., *Naturwissenschaften* **52**, 344 (1965).
663. Sil'nichenko, V. G., *Uch. Zapisk. Mosk. Obl. Ped. Inst.* **84**, 119 (1959).
664. Simon, A., and Schmidt, T., *Z. Anorg. Allgem. Chem.* **153**, 191 (1926).
665. Simon, A., Schnering, H. G., Wöhrle, H., and Schäfer, H., *Z. Anorg. Allgem. Chem.* **339**, 155 (1965).
666. Simon, A., and von Schnering, H. G., *J. Less-Common Metals* **11**, 31 (1966).
667. Sinha, A. P. B., Sanjana, N. R., and Biswas, B. A., *J. Phys. Chem.* **62**, 191 (1958).
668. Sinha, S. C., and Nigam, H. L., *Current Sci. (India)* **35**, 63 (1966).
669. Sisler, H. H., and Jirik, F. E., *J. Am. Chem. Soc.* **66**, 1344 (1944).
670. Skapski, A. C., and Rogers, D., *Chem. Commun.* p. 611 (1965).
671. Smith, G. MCP., *J. Am. Chem. Soc.* **44**, 1769 (1922).
672. Souchay, P., *Bull. Soc. Chim. France* **7**, 875 (1940).
673. Souchay, P., *Ann. Chim. (Paris)* [12] **18**, 73 (1943).
674. Souchay, P., *Ann. Chim. (Paris)* [12] **18**, 169 (1943).
675. Souchay, P., and Ostrowetsky, S., *Compt. Rend.* **250**, 4168 (1960).
676. Souchay, P., and Massart, R., *Compt. Rend.* **253**, 1699 (1961).
677. Souchay, P., and Herve, G., *Compt. Rend.* **261**, 2486 (1965).
678. Spandau, H., and Kohlmeyer, E. J., *Z. Anorg. Allgem. Chem.* **254**, 65 (1947).
679. Spinedi, P., and Gauzzi, F., *Ann. Chim. (Rome)* **47**, 1305 (1957).
680. Spittler, T. M., and Jaselskis, B., *J. Am. Chem. Soc.* **88**, 2942 (1966).
681. Spreckelmeyer, B., and Schäfer, H., *J. Less-Common Metals* **11**, 74 (1966).
682. Stehlik, B., and Weidenthaler, P., *Collection Czech. Chem. Commun.* **24**, 1416 (1959).
683. Steinfink, H., and Burns, J. H., *Acta Cryst.* **17**, 823 (1964).
684. Stephenson, N. C., and Wadsley, A. D., *Acta Cryst.* **19**, 241 (1965).
685. Stephenson, N. C., *Acta Cryst.* **20**, 59 (1966).
686. Stewart, D. F., and O'Donnell, T. A., *Nature* **210**, 836 (1966).
687. Stieglitz, J., *Proc. Natl. Acad. Sci. U.S.* **9**, 308 (1923).
688. Streintz, F., in "Sammlung elektrotechnischer Vorträge," Vol. 4, Stuttgart, Enke, 1903; quoted in Biltz (69).
689. Strekalovskii, V. N., Beketov, A. R., and Vlasov, V. G., *Russ. J. Inorg. Chem. (English Transl.)* **9**, 1347 (1964).
690. Strickland, J. D. H., *J. Am. Chem. Soc.* **74**, 862 (1952).
691. Strickland, J. D. H., *J. Am. Chem. Soc.* **74**, 868 (1952).
692. Stringer, J., *J. Less-Common Metals* **8**, 1 (1954).
693. Sturm, B. J., *Inorg. Chem.* **1**, 665 (1962).
694. Subbarao, E. C., in "Non-Stoichiometric Compounds" (L. Mandelcorn, ed.), p. 268. Academic Press, New York, 1964.

695. Suchow, L., Fankuchen, I., and Ward, R., *J. Am. Chem. Soc.* **74**, 1678 (1952).
696. Sugden, S., *J. Chem. Soc.* p. 161 (1932).
697. Syrkin, Ya. K., and Belova, V. I., *Zh. Fiz. Khim.* **23**, 664 (1949).
698. Takéuchi, Y., Watanabé, T., and Ito, T., *Acta Cryst.* **3**, 98 (1950).
699. Tammann, G., and von Samson-Himmelstjerna, H. O., *Z. Anorg. Allgem. Chem.* **207**, 319 (1932).
700. Terrey, H., and Diamond, H., *J. Chem. Soc.* p. 2820 (1928).
701. Theobald, J. G., *Compt. Rend.* **261**, 2185 (1965).
702. Thompson, L. R., and Wilmarth, W. K., *J. Phys. Chem.* **56**, 5 (1952).
703. Thompson, R. C., *J. Am. Chem. Soc.* **70**, 1045 (1948).
704. Topol, L. E., and Ransom, L. D., *J. Chem. Phys.* **38**, 1663 (1963).
705. Tovborg Jensen, A., and Rasmussen, S. E., *Acta Chem. Scand.* **9**, 708 (1955).
706. Treadwell, F. P., and von Girsowald, C., *Z. Anorg. Allgem. Chem.* **39**, 84 (1904).
707. Trzebiatowski, W., and Rozyczka, J., *Roczniki Chem.* **32**, 183 (1958).
708. Tschugajeff, L., Chlopin, W., and Fritzmann, E., *Z. Anorg. Allgem. Chem.* **151**, 253 (1926).
709. Tschugajeff, L., and Tschernjajeff, J., *Z. Anorg. Allgem. Chem.* **182**, 159 (1929).
710. Tsuchida, R., and Yamada, S., *Nature* **174**, 1064 (1954).
711. Turco, A., and Mazzon, L., *Ann. Chim. (Rome)* **43**, 853 (1953).
712. Turco, A., and Sordillo, G., *Ann. Chim. (Rome)* **43**, 865 (1953).
713. Turco, A., and Sordillo, G., *Ric. Sci.* **24**, 831 (1954).
714. Turco, A., and Sordillo, G., *Ann. Chim. (Rome)* **45**, 614 (1955).
715. Usanovitch, M. I., Sumarokova, T. N., and Beketov, M. B., *Izv. Akad. Nauk Kaz. SSR, Ser. Khim.* **123**, 3 (1953).
716. Vaciago, A., and Mugnoli, A., *Atti. Accad. Nazl. Lincei, Rend., Classe Sci. Fis., Mat. Nat.* [8] **25**, 531 (1958).
717. Vaciago, A., and Mugnoli, A., *Atti. Accad. Nazl. Lincei, Rend., Classe Sci. Fis., Mat. Nat.* [8] **26**, 517 (1959).
718. Van Bever, A. K., *Rec. Trav. Chim.* **57**, 1259 (1939).
719. Van Houten, S., *Phys. Chem. Solids* **17**, 7 (1960).
720. Vannerberg, N.-G., *Acta Cryst.* **18**, 449 (1965).
721. Vannerberg, N.-G., and C. Brosset, *Acta Cryst.* **16**, 247 (1963).
722. van Santen, J. H., and Jonker, G. H., *Physica* **16**, 599 (1950).
723. Vasenin, F. I., *Zh. Prikl. Khim.* **21**, 429 (1948).
724. Vaughan, P. A., Sturdivant, J. H., and Pauling, L., *J. Am. Chem. Soc.* **72**, 5477 (1950).
725. Verwey, E. J. W., and de Boer, J. H., *Rec. Trav. Chim.* **55**, 531 (1936).
726. Verwey, E. J. W., and Haayman, P. W., *Physica* **8**, 979 (1941).
727. Verwey, E. J. W., *Phillips Tech. Rev.* **9**, 46 (1947).
728. Verwey, E. J. W., and Heilmann, E. L., *J. Chem. Phys.* **15**, 174 (1947).
729. Verwey, E. J., Haayman, P. W., and Romeijn, F. C., *J. Chem. Phys.* **15**, 181 (1947).
730. Verwey, E. J. W., Haaijman, P. W., Romeijn, F. C., and van Oosterhout, G. W., *Philips Res. Rept.* **5**, 173 (1950).
731. Viel, S., *Ann. Chem.* **6**, 136 (1925).
732. Vlach, J., and Stehlik, B., *Collection Czech. Chem. Commun.* **25**, 676 (1960).
733. von Schnering, H.-G., Wöhrle, H., and Schäfer, H., *Naturwissenschaften* **48**, 159, (1961).
734. Vratny, F., Tsai, M., and Honig, J. M., *J. Inorg. & Nucl. Chem.* **16**, 263 (1961).
735. Vratny, F., and Micalc, F., *Trans. Faraday Soc.* **59**, 2739 (1963).

736. Wadsley, A. D., *Acta Cryst.* **8**, 695 (1955).
737. Wadsley, A. D., *Acta Cryst.* **10**, 261 (1957).
738. Wadsley, A. D., *J. Proc. Roy. Soc. N. S. Wales* **92**, 25 (1958).
739. Wadsley, A. D., and Andersson, S., *Nature* **192**, 551 (1961).
740. Wadsley, A. D., *Acta Cryst.* **14**, 660 (1961).
741. Wagner, C., and Koch, E., *Z. Physik. Chem.* **B32**, 439 (1936).
742. Walden, P. T., *Am. J. Sci.* **48**, 283 (1894).
743. Wallen, J., Brosset, C., and Vannerberg, N.-G., *Arkiv Kemi* **18**, 541 (1962).
744. Walter, P. H. L., Kleinberg, J., and Griswold, E., *J. Inorg. & Nucl. Chem.* **19**, 223 (1961).
745. Waser, J., and McClanahan, E. D., *Experientia* **6**, 379 (1950).
746. Waser, J., and McClanahan, E. D., Jr., *J. Chem. Phys.* **19**, 413 (1951).
747. Waser, J., and McClanahan, E. D., Jr., *J. Chem. Phys.* **20**, 199 (1952).
748. Watanabe, T., Atoji, M., and Okazaki, C., *Acta Cryst.* **3**, 405 (1950).
749. Waters, J. H., and Gray, H. B., *J. Am. Chem. Soc.* **87**, 3534 (1965).
750. Watt, G. W., and McCarley, R. E., *J. Am. Chem. Soc.* **79**, 4585 (1957).
751. Wehrli, M., and Wenk, W., *Helv. Phys. Acta* **12**, 559 (1939).
752. Weinland, R. F., and Schmid, H., *Ber. Deut. Chem. Ges.* **38**, 1080 (1905).
753. Weiser, H. B., Milligan, W. O., and Bates, J. B., *J. Phys. Chem.* **45**, 701 (1941).
754. Weiser, H. B., Milligan, W. O., and Bates, J. B., *J. Phys. Chem.* **46**, 99 (1942).
755. Weiss, J., *Proc. Roy. Soc.* **A222**, 128 (1954).
756. Wells, A. F., "Structural Inorganic Chemistry," 3rd ed. Oxford Univ. Press (Clarendon), London and New York, 1962.
757. Wells, H. L., and Metzger, F. J., *Am. Chem. J.* **26**, 268 (1901).
758. Wells, H. L., *Am. J. Sci.* **3**, 315 (1922).
759. Wells, H. L., *Am. J. Sci.* **3**, 417 (1922).
760. Wells, H. L., *Am. J. Sci.* **4**, 257 (1922).
761. Wells, H. L., *Am. J. Sci.* **4**, 476 (1922).
762. Wenk, W., *Helv. Phys. Acta* **14**, 355 (1941).
763. Went, J. J., Rathenau, G. W., Gorter, E. W., and van Oosterhout, G. W., *Philips Tech. Rev.* **13**, 194 (1952).
764. Werner, A., *Z. Anorg. Allgem. Chem.* **12**, 46 (1896).
765. Werner, A., *Ber. Deut. Chem. Ges.* **40**, 4605 (1907).
766. Werner, A., *Ann. Chem.* **375**, 1 (1910).
767. Weyl, W. A., *J. Soc. Glass Technol.* **27**, 265 (1943).
768. White, W. B., Dachtler, F., and Roy, R., *J. Am. Ceram. Soc.* **44**, 170 (1961).
769. White, W. B., and Roy, R., *J. Am. Ceram. Soc.* **47**, 242 (1964).
770. Whitney, J. E., and Davidson, N., *J. Am. Chem. Soc.* **69**, 2076 (1947).
771. Whitney, J. E., Browne, C. I., McConnell, H. M., and Davidson, N., *Brookhaven Conf. Rept.* **2**, 196 (1948).
772. Whitney, J. E., and Davidson, N., *J. Am. Chem. Soc.* **71**, 3809 (1949).
773. Wiebenga, E. H., Havinga, E. E., and Boswijk, K. N., *Advan. Inorg. Chem. Radiochem.* **3**, 133 (1961).
774. Wiles, D. R., *Can. J. Chem.* **36**, 167 (1958).
775. Wilhelmi, K.-A., *Naturwissenschaften* **44**, 580 (1957).
776. Wilhelmi, K.-A., and Jonsson, O., *Acta Chem. Scand.* **12**, 1532 (1958).
777. Wilhelmi, K.-A., *Acta Chem. Scand.* **12**, 1965 (1958).
778. Wilhelmi, K.-A., *Acta Chem. Scand.* **19**, 165 (1965).
779. Wilhelmi, K.-A., *Chem. Commun.* p. 437 (1966).
780. Willardson, R. K., Moody, J. W., and Goering, H. L., *J. Inorg. & Nucl. Chem.* **6**, 19 (1958).

781. Willis, B. T. M., *Nature* **197**, 755 (1963).
782. Willis, B. T. M., *J. Phys. Radium* **25**, 431 (1964).
783. Wöhler, L., and Martin, F., *Z. Anorg. Chem.* **57**, 398 (1908).
784. Wöhler, L., and Martin, F., *Ber. Deut. Chem. Ges.* **42**, 3958 (1909).
785. Wöhler, L., and Martin, F., *Ber. Deut. Chem. Ges.* **42**, 4100 (1909).
786. Wöhler, L., *Z. Anorg. Chem.* **78**, 239 (1912).
787. Wöhler, L., and Müller, W., *Z. Anorg. Allgem. Chem.* **149**, 125 (1925).
788. Wöhler, L., and Muller, F., *Z. Anorg. Allgem. Chem.* **149**, 377 (1925).
789. Wold, A., Kunnmann, W., Arnott, R. J., and Ferretti, A., *Inorg. Chem.* **3**, 545 (1964).
790. Wolfram, H., Dissertation, Königsberg (1900).
791. Wollan, E. O., and Koehler, W. C., *Phys. Rev.* **100**, 545 (1957).
792. Wood, D. L., and Remeika, J. P., *J. Appl. Phys.* **37**, 1232 (1966).
793. Woodward, L. A., and Bill, P. T., *J. Chem. Soc.* p. 1699 (1955).
794. Woodward, L. A., and Nord, A. A., *J. Chem. Soc.* p. 2655 (1955).
795. Woodward, L. A., Garton, G., and Roberts, H. L., *J. Chem. Soc.* p. 3723 (1956).
796. Woodward, L. A., Greenwood, N. N., Hall, J. R., and Worrall, I. J., *J. Chem. Soc.* p. 1505 (1958).
797. Yamada, S., Shimura, Y., and Tsuchida, R., *Bull. Chem. Soc. Japan* **26**, 72 (1953).
798. Yamada, S., and Tsuchida, R., *Ann. Rept. Sci. Works, Fac. Sci., Osaka Univ.* **4**, 79 (1956).
799. Yamada, S., and Tsuchida, R., *Bull. Chem. Soc. Japan* **29**, 421 (1956).
800. Yamada, S., and Tsuchida, R., *Bull. Chem. Soc. Japan* **29**, 894 (1956).
801. Yamada, S., and Tsuchida, R., *Bull. Chem. Soc. Japan* **30**, 715 (1957).
802. Yamashita, J., and Kurosawa, T., *Phys. Chem. Solids* **5**, 34 (1958).
803. Yoshioka, H., *J. Phys. Soc. Japan* **4**, 270 (1949).
804. Young, A. P., and Schwartz, C. M., *J. Inorg. & Nucl. Chem.* **25**, 1133 (1963).
805. Young, C. G., Shuskus, A. J., Gilliam, O. R., and Levy, P. W., *Bull. Am. Phys. Soc.* [2] **6**, 248 (1961).
806. Young, R. C., *J. Inorg. & Nucl. Chem.* **7**, 418 (1958).
807. Yuster, P., and Delbecq, C., *J. Phys. Chem.* **21**, 892 (1953).
808. Zachariasen, W. H., *Acta Cryst.* **2**, 390 (1949).
809. Zav'yalova, A. A., Imamov, R. M., and Pinsker, Z. G., *Soviet Phys.-Cryst. (English Transl.)* **10**, 401 (1966).
810. Zedlitz, O., *Z. Krist.* **81**, 253 (1932).
811. Zemann, J., *Mineral. Petrog. Mitt.* **1**, 361 (1950).
812. Zener, C., *Phys. Rev.* **81**, 440 (1951).
813. Zener, C., *Phys. Rev.* **82**, 403 (1951).
814. Zener, C., and Heikes, R. R., *Rev. Mod. Phys.* **25**, 191 (1953).
815. Zhdanov, G. S., and Rusakov, A. A., *Tr. Inst. Kristallogr., Akad. Nauk SSSR* **9**, 165 (1954).
816. Zhuze, V. P., and Shelykh, A. I., *Soviet Phys.-Solid State (English Transl.)* **5**, 1278 (1963).
817. Zintl, E., and Rauch, A., *Ber. Deut. Chem. Ges.* **57**, 1739 (1924).
818. Zintl, E., and Harder, A., *Z. Physik. Chem.* **154**, 47 (1931).
819. Zvonkova, Z. V., and Zhdanov, G. S., *Zh. Fiz. Khim.* **22**, 1284 (1948).
820. Zvonkova, Z. V., *Zh. Fiz. Khim.* **28**, 453 (1954).